



**UNIVERSIDADE ESTADUAL DE CAMPINAS
FACULDADE DE ODONTOLOGIA DE PIRACICABA**

RAPHAEL CAVALCANTE COSTA

**BIOMATERIAIS PARA O CONTROLE DAS INFECÇÕES EM IMPLANTES
DENTÁRIOS: MECANISMOS BIOLÓGICOS, FATORES MODULADORES E
NOVAS ESTRATÉGIAS DE TRATAMENTO**

**BIOMATERIALS FOR CONTROLLING DENTAL IMPLANT INFECTIONS:
BIOLOGICAL MECHANISMS, MODULATING FACTORS AND NEW
TREATMENT STRATEGIES**

Piracicaba/SP

2023

RAPHAEL CAVALCANTE COSTA

**BIOMATERIAIS PARA O CONTROLE DAS INFECÇÕES EM IMPLANTES
DENTÁRIOS: MECANISMOS BIOLÓGICOS, FATORES MODULADORES E
NOVAS ESTRATÉGIAS DE TRATAMENTO**

**BIOMATERIALS FOR CONTROLLING DENTAL IMPLANT INFECTIONS:
BIOLOGICAL MECHANISMS, MODULATING FACTORS AND NEW
TREATMENT STRATEGIES**

Tese apresentada à Faculdade de Odontologia de Piracicaba da Universidade Estadual de Campinas como parte dos requisitos exigidos para a obtenção do título de Doutor em Clínica Odontológica, na Área de Prótese Dental.

Thesis presented to the Piracicaba Dental School of the University of Campinas in partial fulfillment of the requirements for the degree of Doctor in Dental Clinic, in Prosthodontics area.

Orientador: Prof. Dr. Valentim Adelino Ricardo Barão

Coorientador: Prof. Dr. João Gabriel Silva Souza

ESTE EXEMPLAR CORRESPONDE À VERSÃO FINAL DA TESE DEFENDIDA PELO ALUNO RAPHAEL CAVALCANTE COSTA, E ORIENTADA PELO Prof. Dr. VALENTIM ADELINO RICARDO BARÃO.

Piracicaba/SP

2023

Ficha catalográfica
Universidade Estadual de Campinas
Biblioteca da Faculdade de Odontologia de Piracicaba
Marilene Girello - CRB 8/6159

C823b Costa, Raphael Cavalcante, 1994-
Biomateriais para o controle das infecções em implantes dentários :
mecanismos biológicos, fatores moduladores e novas estratégias de
tratamento / Raphael Cavalcante Costa. – Piracicaba, SP : [s.n.], 2023.

Orientador: Valentim Adelino Ricardo Barão.
Coorientador: João Gabriel Silva Souza.
Tese (doutorado) – Universidade Estadual de Campinas, Faculdade de
Odontologia de Piracicaba.

1. Implantes dentários. 2. Biofilmes. 3. Infecção. 4. Biomateriais. I. Barão,
Valentim Adelino Ricardo, 1983-. II. Souza, João Gabriel Silva, 1991-. III.
Universidade Estadual de Campinas. Faculdade de Odontologia de Piracicaba.
IV. Título.

Informações Complementares

Título em outro idioma: Biomaterials for controlling dental implant infections : biological mechanisms, modulating factors, and new treatment strategies

Palavras-chave em inglês:

Dental implants

Biofilms

Infection

Biomaterials

Área de concentração: Prótese Dental

Titulação: Doutor em Clínica Odontológica

Banca examinadora:

Valentim Adelino Ricardo Barão [Orientador]

Karina Gonçalves Silverio Ruiz

Marlise Inês Klein Furlan

Érica Dorigatti de Avila

Diana Gabriela Soares dos Passos

Data de defesa: 16-06-2023

Programa de Pós-Graduação: Clínica Odontológica

Identificação e informações acadêmicas do(a) aluno(a)

- ORCID do autor: <https://orcid.org/0000-0002-2684-5488>

- Currículo Lattes do autor: <http://lattes.cnpq.br/5227412843129808>



UNIVERSIDADE ESTADUAL DE CAMPINAS
Faculdade de Odontologia de Piracicaba

A Comissão Julgadora dos trabalhos de Defesa de Tese de Doutorado, em sessão pública realizada em 16 de junho de 2023, considerou o candidato RAPHAEL CAVALCANTE COSTA aprovado.

PROF. DR. VALENTIM ADELINO RICARDO BARÃO

PROF^a. DR^a. DIANA GABRIELA SOARES DOS PASSOS

PROF^a. DR^a. ÉRICA DORIGATTI DE AVILA

PROF^a. DR^a. KARINA GONZALES SILVERIO RUIZ

PROF^a. DR^a. MARLISE INÊZ KLEIN FURLAN

A Ata da defesa, assinada pelos membros da Comissão Examinadora, consta no SIGA/Sistema de Fluxo de Dissertação/Tese e na Secretaria do Programa da Unidade.

Dedicatória

A **Deus**, por guiar diariamente meus caminhos e permitir a realização dos meus maiores sonhos.

Aos meus pais, **Ednaldo de Sousa Costa (Dinda)** e **Maria das Graças Cavalcante Araújo de Sousa (Galega)**, por me darem “asas para voar” e buscarem a concretização dos meus sonhos. Vocês me ensinaram a ter coragem e ser independente. Mesmo distantes, sempre se fizeram presentes transmitindo todo amor. Obrigada por possibilitarem que eu seguisse este caminho e por apoiarem todas as minhas escolhas. A vocês eu devo tudo que sou e que serei.

Aos meus irmãos **Ricardo Cavalcante Costa** e **Renata Cavalcante Costa**, e meus sobrinhos **Guilherme** e **Heloísa** pela amizade, lealdade e experiências compartilhadas.

Agradeço por todo apoio e amor incondicional

Esta tese eu dedico a vocês.

Agradecimento especial

Ao meu orientador, **Prof. Dr^a Valentim Adelino Ricardo Barão**, agradeço pela confiança depositada ao longo de todos esses anos. Se hoje me sinto preparado para obter o título de doutor, foi por todas as oportunidades que o senhor me deu. Agradeço pelos ensinamentos e por permitir o desenvolvimento de cada trabalho sem criar barreiras, pelo contrário, sempre incentivando e orientado cada passo. Acima de tudo, agradeço por me ajudar a construir um pensamento crítico, por toda disponibilidade, paciência e por me motivar a seguir em frente mesmo diante de tantas adversidades. O senhor é um grande exemplo de dedicação e competência. Tenho um prazer imenso em dizer que fui seu orientado de mestrado e doutorado, e o quanto aprendi na FOP/UNICAMP. Muito obrigado!

Ao meu coorientador, **Prof. Dr^a João Gabriel Silva Sousa**, por ter me acolhido como seu primeiro orientado de doutorado. Agradeço imensamente pela orientação na condução desta tese, assim como demais estudos, e pelo incentivo na carreira científica, me permitindo pensar, executar e desenvolver as minhas habilidades e ideias. Sem sua parceria o caminho teria sido muito mais difícil, obrigada pela dedicação, comprometimento e compreensão em vários momentos difíceis na pós-graduação. Nos méritos desta conquista, há muito de você. Por toda sua amizade e companheirismo, minha gratidão.

Agradecimentos

À Universidade Estadual de Campinas, por meio do seu Magnífico Reitor, **Prof. Dr. Antonio José de Almeida Meirelles**.

À Faculdade de Odontologia de Piracicaba (FOP/UNICAMP), nas pessoas do diretor **Prof. Dr. Flávio Henrique Baggio Aguiar** e da vice-diretora **Profª. Drª. Karina Gonzales Silvério Ruiz**.

Ao Coordenador dos Cursos de Pós-Graduação e do Programa de Pós-Graduação em Clínica Odontológica da Faculdade de Odontologia de Piracicaba, **Prof. Dr. Valentim Adelino Ricardo Barão**.

À **Coordenação de Aperfeiçoamento de Pessoal de Nível Superior – Brasil (CAPES)** pela concessão inicial da bolsa de doutorado (Código de Financiamento 001), e à **Fundação de Amparo à Pesquisa do Estado de São Paulo (FAPESP)**, pela concessão da bolsa de doutorado (2020/10436-4).

Aos laboratório de Bioquímica Oral e Periodontia, em nome da **Profª. Drª. Cíntia Pereira Machado Tabchoury** and **Profª. Drª. Karina Gonzales Silvério Ruiz**, por todo apoio, confiança e disponibilidade para utilização da infra-estrutura dos laboratórios.

Aos docentes da área de Prótese Total da Faculdade de Odontologia de Piracicaba, **Prof. Dr. Marcelo Ferraz Mesquita** e **Prof. Dr. Rafael Leonardo Xediek Consani**, e aos professores da área de Prótese Parcial Removível, **Profa. Dra. Altair Del Bel Cury**, **Profa. Dra. Renata Cunha Matheus Rodrigues Garcia**, **Prof. Dr. Wander José da Silva**, agradeço à disponibilidade, inspiração e conhecimento transmitido ao longo destes anos.

Aos **demais docentes** da Faculdade de Odontologia de Piracicaba, que de alguma forma contribuíram para meu aprendizado e crescimento profissional.

Aos professores colaboradores, **Dra. Martinna Bertolini, Dra. Magda Feres, Dr. Jamil Shibli, Dr. Leonardo Perez Faverani, Dra. Erica Dorigatti de Avila, Dra. Maria del Pilar Taboaba Sotoyamor, Dr. Javier Villa, Dr. Nilson Cristino da Cruz, Dra. Elidiane Cipriano Rangel, e Dra. Bruna Benso**, pela parceria no desenvolvimento destes trabalhos e ensinamentos compartilhados.

Aos grandes amigos que fiz desde o mestrado e levarei para vida, **Jairo Matozinho Cordeiro, Rodrigo Barros Estevão Lins, Bruna Egumi Nagay, Caroline Dini e Guilherme Almeida Borges**, agradeço o apoio, paciência, amizade, disponibilidade em ajudar, boas risadas, conversas profundas (ou nem tanto), e pela parceria que vai além da esfera acadêmica. Melhor que evoluir, é ver o crescimento de quem amamos. Vocês têm toda minha admiração, carinho e torcida, tenho certeza que conquistarão todos seus sonhos. Ter amigos como vocês é algo precioso!

À **Fábio Furlan Oliveira**, cujo apoio foi fundamental durante esse período de pós-graduação. Agradeço, principalmente, pela convivência diária e por ser minha família em Piracicaba, me ajudando em diversos momentos difíceis e partilhando bons momentos juntos.

Aos demais “baronetes”, **Maria Helena, Luís Fernando, João Pedro, Cátia, e Samuel** por tamanha amizade e companheirismo, por cada conversa, ajuda, parcerias e por tornarem os dias mais leves no laboratório e fora dele.

Aos meu primeiros co-orientados, **Thaís Terumi, Júlia Teodoro e João Vitor**, por me permitirem participar de sua formação acadêmica e proporcionar um grande momento de aprendizado para mim enquanto futuro docente. Muito obrigado por toda dedicação e empenho.

Aos amigos do Laboratório de Prótese Total, **Thais Barbin, Letícia Del Rio, Daniele Valente, Luana Matias, Licínia Pignaton, Juliana Andrade e Ana Larisse**, agradeço pela amizade e convívio harmonioso em nosso ambiente de trabalho.

Aos velhos e novos amigos feitos durante os quase seis anos de pós-graduação, em especial, **Mariana Marinho, Loyse Martorano, Mariana Barbosa, Olivia Figueiredo, Heloisa Pantaroto, Deborah Rocha, Catharina Sacramento, Tamires Dutra, Thayane**

Businari, Talita Malini, Elis Lira, Ingrid Andrade, Mayara Abreu, Matheus Kury, Matheus Gonçalves, Bruno Cazotti, Natalia Reiche. por toda parceria, amizade e aprendizado compartilhado durante esses anos. Sentirei saudades de todos!

Aos funcionários da Faculdade de Odontologia de Piracicaba, em especial à **Sr. Eduardo (Du), Sr^a. Eliete, Sr. Adriano, Sr^a. Gislaine, e Sr. Alfredo (*in memoriam*)**, pela dedicação ao realizar suas funções, pelo carinho, cuidado e amizade.

À **Prof^a. Dr^a. Ana Maria Gondim Valença**, da Universidade Federal da Paraíba, por toda orientação e ensinamentos desde a graduação. Obrigada por todo apoio, confiança, amizade, e por ser esse exemplo de pessoa, professora e pesquisadora.

Aos professores **Dr^a. Bianca Marques Santiago, Dr^a. Leopoldina de Fátima Dantas Almeida, e Dr. Yuri Wanderley Cavalcanti**, da Universidade Federal da Paraíba, por serem grandes exemplos de professores, pesquisadores e, especialmente, seres humanos. Sou muito grata por todos os ensinamentos acadêmicos e pessoais durante a graduação, e por todo incentivo para iniciar nessa jornada da pós-graduação.

As amigas de longa data, **Karla Lorene e Priscila Sarmiento**, que torceram por mim a cada nova conquista e me encorajaram a persistir este sonho. Os laços que nos unem são impossíveis de se explicar, nos reconhecemos uns nos outros e cativamos uma amizade verdadeira que perdura por anos. Muito obrigado pelo companheirismo e carinho constantes.

Aos **voluntários das pesquisas** desenvolvidas durante todo período de pós-graduação, sempre dispostos a ajudar e fundamentais para a construção da ciência.

A **minha família**, , representada pelas minhas queridas tias, **Carminha, Nenzinha, Salete, Inácia, Sônia** e alguns primos **Sylvanna, Suzanna, Vivianny, Daniel, Victor, Johann, François e Paulo**. Somos muitos e nosso amor não cabe em palavras e folhas! Obrigada por tudo sempre.

A todos que estiveram ao meu lado nesta jornada, meus sinceros agradecimentos.

“Coragem! Eu venci o mundo.” (Jo 16,33)

RESUMO

As infecções peri-implantares são doenças inflamatórias crônicas associadas a uma comunidade microbiana patogênica que afeta progressivamente a integridade dos tecidos de suporte. As terapias clínicas atuais visam remover o biofilme de forma mecânica e ocasionalmente com abordagens antimicrobianas adjuvantes sem considerar o papel das superfícies e da inflamação. Desta forma, esta abordagem nem sempre é eficaz, principalmente para reverter a disbiose do biofilme e controlar a inflamação. Neste contexto, estratégias terapêuticas estão sendo desenvolvidas para prevenir as infecções peri-implantares e aumentar as taxas de sucesso das reabilitações com implantes. Este trabalho de Tese objetiva descrever o estado da arte e pesquisas emergentes sobre o uso de biomateriais para o controle das infecções/inflamação em implantes dentários. Uma revisão crítica baseada em evidências foi inicialmente desenvolvida para resumir estudos pré-clínicos e clínicos sobre as superfícies antimicrobianas emergentes propostas para implantes à base de titânio (Ti) [Estudo 1]. Os achados desta revisão sugerem que não existe superfície de Ti disponível capaz de reduzir o acúmulo bacteriano oral e prevenir infecções polimicrobianas. Além das superfícies de implantes, pesquisa futuras devem se concentrar em entender a etiopatogenia e os fatores moduladores do biofilme no Ti como estratégia para aprimorar as terapias anti-biofilmes, como a matriz extracelular (ME) do biofilme. ME é amplamente discutida em superfície dentárias, mas seu efeito na patogênese de infecções de implantes tem sido negligenciado. Portanto, uma revisão do estado da arte sobre o papel da ME em superfícies de Ti foi desenvolvido [Estudo 2]. Os resultados sumarizados indicam que a ME é um importante fator de virulência, contribuindo para a colonização bacteriana, resistência antimicrobiana e patogênese e deve ser considerado no desenvolvimento de novas terapias. Motivados por estas revisões e pela ausência de um protocolo clínico de tratamento baseado na degradação da ME, uma pesquisa *in vitro* e *in situ* foi conduzido [Estudo 3]. Um protocolo de descontaminação em 3 etapas para superfícies de Ti usando iodopovidine (0,2%) como um agente de degradação de ME mostrou-se eficaz e seguro, eliminando biofilmes sem danificar a superfície do implante ou afetar a adesão celular. Além a associação de terapias antimicrobianas com imunomodulares ainda são escassos na implantodontia. Portanto, desenvolvemos um novo biomaterial para liberação de folato visando aprimorar estratégia antimicrobiana via modulação da inflamação tecidual [Estudo 4]. Em síntese, o polímero molecularmente impresso carregado com folato mostrou ser uma estratégia promissora para o controle da inflamação *in vitro* e *in vivo*. Os resultados desta Tese suportam a indicação de uma nova terapia não cirúrgica que deve ser testado clinicamente para o controle das infecções de implantes dentários.

Palavras-chave: Implante Dentário. Biofilme. Infecção. Biomaterial.

ABSTRACT

Peri-implant infections are chronic inflammatory diseases associated with a pathogenic microbial community that progressively affects the integrity of supporting tissues. Current clinical therapies aim to remove biofilm mechanically and occasionally with adjuvant antimicrobial approaches without considering the role of surfaces and inflammation. Thus, this approach is not always effective, especially for reversing biofilm dysbiosis and controlling inflammation. In this context, therapeutic strategies are being developed to prevent peri-implant infections and increase the success rates of rehabilitations with implants. This thesis work aims to describe the state of the art and emerging research on the use of biomaterials to control infections/inflammation in dental implants. An evidence-based critical review was initially developed to summarize preclinical and clinical studies on proposed emerging antimicrobial surfaces for titanium (Ti)-based implants [Study 1]. The findings of this review suggest that there is no available Ti surface capable of reducing oral bacterial accumulation and preventing polymicrobial infections. In addition to implant surfaces, future research should focus on understanding the etiopathogenesis and modulating factors of biofilm on Ti as a strategy to improve anti-biofilm therapies, such as biofilm extracellular matrix (EM). ME is widely discussed on tooth surfaces, but its effect on the pathogenesis of implant infections has been neglected. Therefore, a review of the state of the art on the role of ME on Ti surfaces was developed [Study 2]. The summarized results indicate that ME is an important virulence factor, contributing to bacterial colonization, antimicrobial resistance and pathogenesis and should be considered in the development of new therapies. Motivated by these reviews and the absence of a clinical treatment protocol based on ME degradation, an *in vitro* and *in situ* research was conducted [Study 3]. A 3-step decontamination protocol for Ti surfaces using povidone-iodine (0.2%) as an ME degradation agent was shown to be effective and safe, eliminating biofilms without damaging the implant surface or affecting cell adhesion. In addition, the association of antimicrobial therapies with immunomodulators is still scarce in implant dentistry. Therefore, we developed a new biomaterial for folate release aiming to improve antimicrobial strategy via modulation of tissue inflammation [Study 4]. In summary, the molecularly imprinted polymer loaded with folate proved to be a promising strategy for controlling inflammation *in vitro* and *in vivo*. The results of this Thesis support the indication of a new non-surgical therapy that should be clinically tested for the control of dental implant infections.

Keywords: Dental Implant. Biofilm. Infection. Biomaterial.

SUMÁRIO

1 INTRODUÇÃO.....	14
2 ARTIGOS.....	18
2.1. Fitting pieces into the puzzle: The impact of titanium-based dental implant surface modifications on bacterial accumulation and polymicrobial infections.....	19
2.2. Polymicrobial biofilms related to dental implant diseases: unravelling the critical role of extracellular biofilm matrix.....	96
2.3. Novel 3-step nonsurgical decontamination protocol for titanium-based dental implants: An <i>in vitro</i> and <i>in situ</i> study	134
2.4 Pathogenesis-guided engineering: pH-responsive imprinted polymer co-delivering folate for inflammation-resolving as immunotherapy in implant infections.....	163
3 DISCUSSÃO	192
4 CONCLUSÃO.....	195
REFERENCIAS	196
ANEXOS	
Anexo 1. Certificado de aprovação no Cômite de Ética em Pesquisa da FOP/UNICAMP..	201
Anexo 2. Certificado de aprovação no Cômite de Ética em Pesquisa da FOP/UNICAMP..	202
Anexo 3. Certificado de aprovação no Comitê de Ética no Uso de Animais (CEUA).....	203
Anexo 4. Autorização de re-utilização na Tese (Artigo 1)	204
Anexo 5. Autorização de re-utilização na Tese (Artigo 2)	205
Anexo 6. Relatório de similaridade.....	206

1 INTRODUÇÃO

Desde a sua introdução na década de 1960, os implantes dentários à base de titânio (Ti) tornaram-se a principal opção terapêutica para pacientes que necessitam de suporte para próteses unitárias, parciais ou totais (Brånemark et al., 1977; Chiapasco; Gatti, 2003). Após a inserção cirúrgica dos implantes, o Ti propicia a osseointegração fornecendo ancoragem suficiente (adesão osso-implante) para a reconstrução dentária funcional (Barão et al., 2022). Diante disto, as reabilitações implanto-suportadas promovem ganhos na função mastigatória, nas condições estéticas e na qualidade de vida tornando-se um tratamento de primeira escolha na prática clínica (Cardoso et al., 2016; Lam Vo et al., 2019). Estudos de metanálises com ensaios clínicos de longos períodos de acompanhamento evidenciam que os implantes dentários são previsíveis, altamente confiáveis e com prognóstico favorável em cenários clínicos desafiadores (Chen et al., 2019; Gallardo et al., 2019; Hu et al., 2019). No Brasil, projeta-se um aumento na instalação de implantes dentários tendo em vista a alta taxa de edentulismo na população demonstrado nos dados preliminares do último levantamento nacional de saúde bucal (SBBrazil 2020; Ministério da Saúde, 2023).

Embora os implantes dentários apresentem alta taxa de sucesso (~95% em 10 anos)(Adell et al., 1981; Howe; Keys; Richards, 2019), estes dispositivos não são isentos de insucesso e podem ser acometidos por complicações mecânicas e/ou biológicas. As falhas iniciais são geralmente mecânicas e técnicas relacionadas à fraturas de implantes e componentes, delaminações da cerâmica e afrouxamento de parafusos protéticos (Chochlidakis et al., 2020). Dentro das complicações biológicas, as doenças peri-implantares são as principais causas de falhas tardias das reabilitações com implantes (Lee et al., 2017). O biofilme oral aderido à superfície do implante é o principal fator etiológico das doenças peri-implantares (Daubert; Weinstein, 2019; Mombelli; Décaillot, 2011). As doenças peri-implantares continuam a aumentar em todo o mundo devido à popularidade dos implantes dentários, podendo requerer a remoção do implante, gerando sérios problemas à saúde bucal e à qualidade de vida dos pacientes (Costa et al., 2021).

A etiopatogenia das doenças peri-implantares envolve um processo inflamatório crônico imunomediado por uma comunidade polimicrobiana patogênica que afeta progressivamente a integridade dos tecidos moles (mucosite peri-implantar) e duros (peri-implantite)(Araujo; Lindhe, 2018; Berglundh et al., 2018). Conceitualmente, a mucosite peri-

implantar é a reação inflamatória restrita aos tecidos moles ao redor dos implantes dentários (Heitz-Mayfield; Salvi, 2018), enquanto a peri-implantite caracteriza-se pela inflamação dos tecidos moles e a perda progressiva do osso de suporte (Schwarz et al., 2021). O último “*World Workshop on the Classification of Peri-implant Diseases and Conditions*” determinou que a mucosite peri-implantar é como uma condição precursora para a peri-implantite (Berglundh et al., 2018). A peri-implantite é uma condição patológica prevalente, podendo afetar 12% a 24% dos pacientes 5 a 10 anos após a colocação do implante (Derks; Tomasi, 2015; Lee et al., 2017). Embora a periodontite e a peri-implantite compartilhem fenótipos inflamatórios aparentemente semelhantes, os mecanismos patogénéticos desta doenças são diferentes, necessitando de abordagens direcionadas para tal condição (Bertolini et al., 2022; Kotsakis; Olmedo, 2021).

Considerando o problema emergente das infecções peri-implantares, o controle do biofilme oral tem sido alvo de inúmeras pesquisas na implantodontia (Ananth et al., 2015). As modificações de superfícies representam a abordagem clássica e mais investigada nos últimos 30 anos para aprimorar o processo de osseointegração e garantir o sucesso e a sobrevivência do implante em situações desafiadoras (Lee et al., 2021). Além disso, superfícies de implantes que podem também apresentar potencial antimicrobiano estão em desenvolvimento (Barão et al., 2022; Souza et al., 2021). Para isso, diversas técnicas visam funcionalizar as superfícies com elementos bioativos, nanopartículas, agentes antimicrobianos e medicamentos (Alipal et al., 2021; Ferraris et al., 2014). O maior desafio destas superfícies emergente encontra-se no equilíbrio entre a obtenção de propriedades físico-químicas favoráveis à osseointegração aliado aos atributos antimicrobianos necessários para controlar infecções (Malheiros et al., 2023). Ademais, é importante considerar a etiopatogênese das infecções peri-implantares baseada no processo de formação de biofilmes e da resposta imune-inflamatória no delineamento de novas superfícies e biomateriais.

Os biofilmes peri-implantares são comunidades polibacterianas inseridas em uma matriz extra-celular polimérica tridimensional (Flemming; Wingender, 2010; Karygianni et al., 2020). Esta matriz é produzida por microrganismos através da síntese de α -glucanos por exoenzimas (denominadas glicosiltransferases), atuando na síntese de polissacarídeos extracelular [EPS, do inglês] que é o principal componente da matriz do biofilme (Koo;

Falsetta; Klein, 2013; Oliveira; Cury; Filho, 2017). Os polissacarídeos extracelulares compreendem um dos principais componentes do biofilme oral, contribuindo para a colonização bacteriana, resistência antimicrobiana e patogênese (Branda et al., 2005; Guggenheim, 1970). A presença da matrix extracelular é crucial para a criação de um ambiente ecológico favorável que permite o crescimento de patógenos facultativos e anaeróbicos, levando a disbiose microbiológica (Costa et al., 2020). Ainda, o substrato de formação do biofilme, incluindo superfícies de Ti, modula a quantidade e o conteúdo de matriz sintetizada (Souza et al., 2020b). Embora o papel da matriz extracelular de biofilmes crescendo em superfícies bióticas, especialmente superfícies dentárias, é amplamente desvendado (Aires et al., 2011; Klein et al., 2015; Xiao et al., 2012), o estado da arte existente sobre a relação entre a matriz do biofilme em superfícies de implante e o seu papel nas infecções peri-implantares ainda é limitado. Sendo assim, é válido incorporar o estudo desse fator de virulência em biofilmes formados nas superfícies de implantes e também no contexto de novas terapias.

Na prática clínica, a descontaminação não cirúrgica da superfície do implante é a primeira abordagem utilizada para erradicar o biofilme peri-implantar e, conseqüentemente, controlar clinicamente a inflamação tecidual (Lafaurie et al., 2017). Atualmente, os métodos físicos de descontaminação envolvem o polimento de superfícies de implantes usando diversas curetas manuais, escovas de polimento, dispositivos ultra-sônicos, sistemas de pó abrasivos ou laserterapia (Louropoulou; Slot; Van Der Weijden, 2014). Diversos antimicrobianos tópicos e sistêmicos também são utilizados como adjuvantes da terapia convencional de remoção mecânica do biofilme (Dostie et al., 2017). Entretanto, revisões sistemáticas (Heitz-Mayfield; Mombelli, 2014; Louropoulou; Slot; Van Der Weijden, 2014, 2012) têm demonstrando não existir um consenso sobre o melhor método não cirúrgico para descontaminação de superfícies de implantes e controle da peri-implantite. Nesse contexto, estratégias para interromper/degradar a matriz extracelular polimérica, aumentando a capacidade de remoção e morte do biofilme, têm sido sugeridas para superar a limitação terapêutica do tratamento da peri-implantite (Costa et al., 2020; Souza et al., 2022; Yang et al., 2023).

Por fim, embora na ciência de materiais o principal foco no desenvolvimento de biomateriais seja o controle da infecção por controle da colonização bacteriana (Costa et al.,

2021), em infecções crônicas como doenças peri-implantares, o processo imune-inflamatório representa um fator crucial para o designer racional de novos biomateriais (Corrêa et al., 2019). Nas infecções relacionados aos implantes dentários, o sucesso das terapias aplicadas acontece por meio da remoção efetiva do biofilme aliado ao controle clínico da inflamação (Heitz-Mayfield; Mombelli, 2014). Desta forma, novos biomateriais com propriedades imuno-moduladoras estão sendo indicados para doenças inflamatórias crônicas devem ser testadas também no contexto das aplicações dentárias.

Com base no exposto, esta Tese tem como objetivos avaliar:

- (1) Avaliar criticamente os estudos pré-clínicos e clínicos sobre as superfícies antimicrobianas emergentes desenvolvidas para implantes à base de titânio (Ti);
- (2) Determinar o estado da arte sobre o papel da matriz extracelular do biofilme em superfícies de implantes dentários como fator de virulência para infecções peri-implantares;
- (3) Validar, *in vitro* e *in situ*, um protocolo mecânico/químico combinado com uma estratégia prévia de degradação da matriz do biofilme, visando potencializar a morte e remoção bacteriana de superfícies de implantes dentários.
- (4) Desenvolver um novo biomaterial por meio da técnica de impressão molecular para liberação controlada/sustentada de folato (imunomodulador) via mecanismo de variação de pH, visando potencializar terapias convencionais de tratamento das doenças peri-implantares por meio do controle da inflamação tecidual.

2 ARTIGOS

Este trabalho foi realizado no formato alternativo, conforme a Informação CCPG/001/2015, da Comissão Central de Pós-Graduação (CCPG) da Universidade Estadual de Campinas.

O artigo 1, intitulado “*Fitting pieces into the puzzle: The impact of titanium-based dental implant surface modifications on bacterial accumulation and polymicrobial infections*”, encontra-se publicado no periódico *Advances in Colloid and Interface Science* (<https://doi.org/10.1016/j.cis.2021.102551>).

O artigo 2, intitulado “*Polymicrobial biofilms related to dental implant diseases: unravelling the critical role of extracellular biofilm matrix*”, encontra-se publicado no periódico *Critical Reviews in Microbiology* (<https://doi.org/10.1080/1040841X.2022.2062219>).

O artigo 3, intitulado “*Novel 3-step nonsurgical decontamination protocol for titanium-based dental implants: An in vitro and in situ study*”, encontra-se submetido no periódico *Clinical Oral Implant Research* (under review - COIR-Apr-23-OGA-10049).

O artigo 4, intitulado “*Pathogenesis-guided engineering: pH-responsive imprinted polymer co-delivering folate for inflammation-resolving as immunotherapy in implant infections*”, será submetido no periódico *Advances Healthcare Materials* (IF=11.092).

.

2.1 Fitting pieces into the puzzle: the impact of titanium implant surface modifications on bacterial accumulation and polymicrobial infections

Running title: Effects of titanium implant surface modifications on bacterial accumulation

Raphael C. Costa¹ | Bruna E. Nagay¹ | Martinna M. Bertolini² | Bárbara E. Costa-Oliveira^{1,3} | Aline A. Sampaio⁴ | Belén Retamal-Valdes⁵ | Jamil A. Shibli⁵ | Magda Feres⁵ | Valentim A. R. Barão^{1*} | João Gabriel S. Souza^{1,5,6*}

¹ Department of Prosthodontics and Periodontology, Piracicaba Dental School, University of Campinas (UNICAMP), 901 Limeira Ave, Piracicaba, São Paulo, 13414-903, Brazil.

² Department of Oral Health and Diagnostic Sciences, University of Connecticut Health Center, 263 Farmington Ave, Farmington, CT, 06030, USA.

³ Graduate Program in Dentistry, University Ceuma (UNICEUMA), 01 Josué Montello St, Renascença II, São Luis, Maranhão, 65075-120, Brazil.

⁴ Department of Clinic, Pathology and Dental Surgery, Federal University of Minas Gerais (UFMG), 6627 Antônio Carlos Ave, Belo Horizonte, Minas Gerais, 31270-901, Brazil.

⁵ Dental Research Division, Guarulhos University, Guarulhos, São Paulo, 07023-070, Brazil.

⁶ Dental Science School (Faculdade de Ciências Odontológicas - FCO), 20 Waldomiro Marcondes Oliveira Ave, Montes Claros, Minas Gerais, 39401-303, Brazil.

Valentim Adelino R. Barão and João Gabriel S. Souza should be considered joint senior author.

*Corresponding authors

1. João G. S. Souza, Department of Prosthodontics and Periodontology, Piracicaba Dental School, University of Campinas (UNICAMP), Av. Limeira, 901, Piracicaba, São Paulo 13414-903, Brazil. E-mail: jgabriel.ssouza@yahoo.com.br

2. Valentim A.R. Barão, Department of Prosthodontics and Periodontology, Piracicaba Dental School, University of Campinas (UNICAMP), Av. Limeira, 901, Piracicaba, São Paulo 13414-903, Brazil. E-mail: vbarao@unicamp.br

#Costa RC, Nagay BE, Bertolini M, Costa-Oliveira BE, Sampaio AA, Retamal-Valdes B, Shibli JA, Feres M, Barão VAR, Souza JGS. Fitting pieces into the puzzle: The impact of titanium-based dental implant surface modifications on bacterial accumulation and polymicrobial infections. *Adv Colloid Interface Sci.* 2021 Dec;298:102551. doi: 10.1016/j.cis.2021.102551.

ABSTRACT

Polymicrobial infection is the main cause of dental implant failure. Although numerous studies have reported the ability of titanium (Ti) surface modifications to inhibit microbial adhesion and biofilm accumulation, the majority of solutions for the utilization of Ti antibacterial surfaces have been tested in *in vitro* and animal models, with only a few developed surfaces progressing into clinical research. Motivated by this huge gap, we critically reviewed the scientific literature on the existing antibacterial Ti surfaces to help understand these surfaces' impact on the “*puzzle*” of undesirable dental implant-related infection. This manuscript comprises three main sections: (i) a narrative review on topics related to oral biofilm formation, bacterial-implant surface interactions, and on how implant-surface modifications can influence microbial accumulation; (ii) a critical evidence-based review to summarize pre-clinical and clinical studies in an attempt to “*fit pieces into the puzzle*” to unveil the best way to reduce microbial loads and control polymicrobial infection around dental implants showed by the current *in vivo* evidence; and (iii) discussion and recommendations for future research testing emerging antibacterial implant surfaces, connecting basic science and the requirements for future clinical translation. The findings of the present review suggest no consensus regarding the best available Ti surface to reduce bacterial colonization on dental implants. Smart release or on-demand activation surface coatings are a “*new piece of the puzzle*”, which may be the most effective alternative for reducing microbial colonization on Ti surfaces, and future studies should focus on these technologies.

Keywords:

Dental implant

Titanium

Surface modification

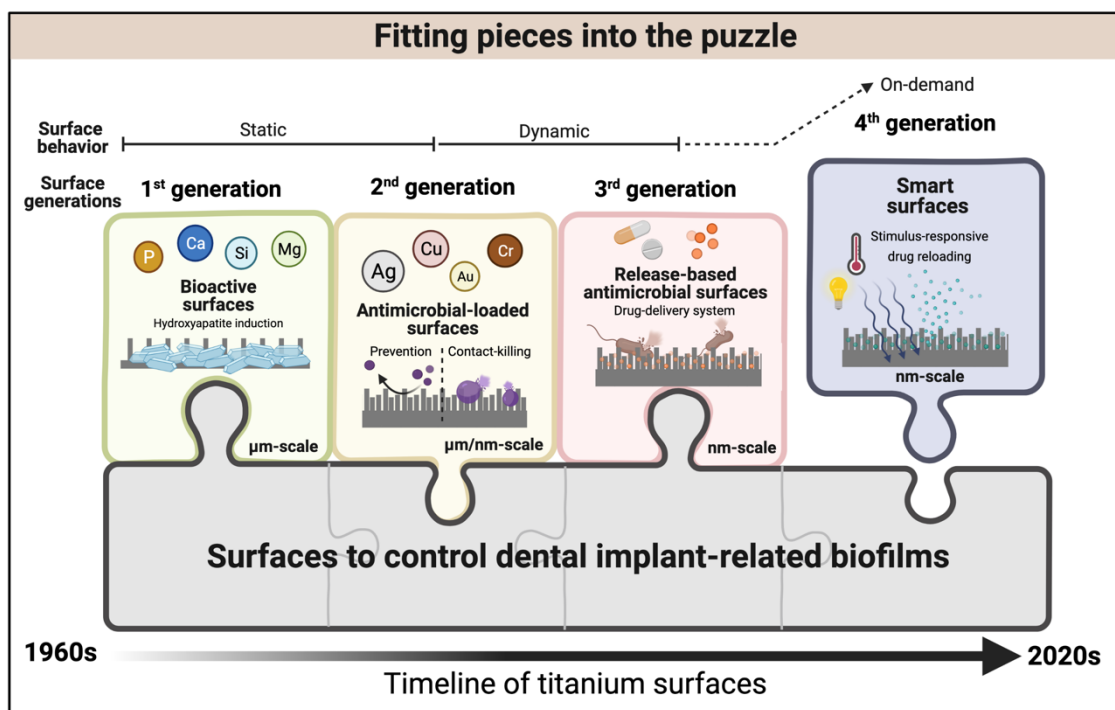
Biofilm

Microbial infection

Highlights

1. The role of titanium surface modifications on bacterial accumulation was critically reviewed.
2. No consensus was revealed on the best available surface to prevent dental implant contamination.
3. Pre-clinical and clinical research on clinically relevant oral bacteria is scarce.
4. Smart release or on-demand activation coatings may provide solutions for the “puzzle” issues.

Graphical abstract



1. Introduction

Titanium (Ti) and its alloys are the main biomedical materials used for the manufacturing of dental implants due to their good biocompatibility, suitable mechanical properties, and adequate corrosion resistance [1]. Nevertheless, Ti biomaterial is a substrate that allows for bacterial-surface interactions and microbial accumulation over time [2–4]. Once a microbial biofilm forms on the Ti surface, the host immune-mediated responses and inflammatory processes are activated, and the environmental conditions surrounding the implant may change [5]. If a deleterious shift in the balance of the healthy-associated endogenous microbiome occurs, an overgrowth of pathogenic species within the biofilm leads to progressive destruction of the peri-implant bone [6]. Thus, biofilm-related infections can lead to the failure of the implant and its associated prosthetic devices, which may require implant removal, generating severe problems to the patients' oral health and quality of life [7,8].

Implant surface modifications designed to fight microbial infections and enhance implant survival rates have been a major focus of biomedical research in the last 30 years [9,10]. In this context, many surface modification techniques have been proposed, with countless variations in Ti surfaces in terms of bioactivity, functionalization, and antibacterial activity [11–13]. For instance, the application of coatings that contain bioactive elements, anti-infective agents, therapeutic nanoparticles, or antimicrobial drugs became popular for the prevention of microbial colonization of implants, but these lacked long-term effect options [14]. Recently, a new generation of antibacterial surfaces, combining methods to create on-demand activation antimicrobial coatings, has been proposed to solve the increasing burden of peri-implant infections [1,15]. However, the influence of clinically available Ti-surface modifications and these emerging coatings on bacterial accumulation remains clinically relevant.

Despite numerous literature reviews on implant surface topography and biofilm control [9,11,12,14,16], there are still “*missing pieces of the puzzle*” that would explain why the *in vitro* options proven to create antibacterial Ti surfaces have not yet entered clinical use. Furthermore, the

antibacterial potential of these surfaces has only been partially portrayed on those reviews, and the assessment of microbial contamination for all developed implant surfaces has not been systematically reviewed. Importantly, the focus on antibacterial surfaces is an ever-prevalent issue, especially when considering the current rise in antibiotic resistance, widely considered to be the next global pandemic [17], and the need for alternative solutions.

This review aims to provide a critical appraisal of the existing literature assessing the effects of antibacterial Ti surfaces for controlling bacterial accumulation. This manuscript was divided into three main sessions. (i) In order to create a background on the important topics to be considered, we first generated a narrative review to detail topics related to biofilm formation, bacterial-implant-surface interactions, and how implant-surface modifications can influence oral biofilm formation on Ti biomaterial. (ii) Next, will systematically summarize pre-clinical and clinical studies in an attempt to *"fit pieces into the puzzle"* to unveil the best way to reduce microbial loads and control polymicrobial infection around dental implants. (iii) Finally, a perspective on the current literature regarding expanding the applicability of Ti surfaces as antibacterial materials will be discussed.

2. Biofilm formation vs. Surface modifications: A narrative review

2.1 Dental implant-related infections: a disease of the century

Since their introduction in the 1960s, dental implants have revolutionized dental medicine allowing the replacement of missing teeth by using Ti screws directly osseointegrated into patients' bone [18]. Notably, the use of dental implants has grown rapidly in recent decades, accompanied, unfortunately, by a steady increase in implant failures caused by microbial infections [8]. Such infections may also have harmful consequences to general health, causing significant morbidity and considerably increasing healthcare costs [19]. In this regard, more than 40% of implants can be affected by infection when affecting soft tissues, and over 22% can also affect anchoring bone within 5-10 years after placement [20]. Thus, microbial accumulation control is essential for the long-term

survival of implants [21]. These facts emphasize the need for discussion of topics critical to the understanding of microbial accumulation on dental implant devices and how surface changes can affect this process and control or prevent the infection.

2.1.1. Mechanism of biofilm formation on implant surfaces

Biofilms consist of highly organized microbial communities embedded in a self-produced extracellular polymer matrix adhered on the surface [22–24], which contribute to the unique attributes of biofilm lifestyle and virulence [25], forming a protected community on implant surface [26]. In fact, oral biofilms are complex systems that have high microbial cell densities and typically represent 5–35% of the biofilm volume, while the remaining volume is composed of the biofilm matrix [27]. The biofilm matrix is formed by biomolecules such as exopolysaccharides (EPS), nucleic acids (eDNA and eRNA), proteins, lipids, and other biomolecules responsible for the structural and biochemical properties of biofilms [25]. This complex architecture of biofilms is a survival mechanism that provides a protected mode of growth, allowing cells to survive in hostile environments and providing growth conditions better than those of planktonic cells [28]. The classic model of microbial biofilm formation includes several stages: protein adsorption, microbial adhesion, biofilm formation, maturation, and dispersal [3,16], which can be modulated by different factors (i.e., carbohydrate exposure) promoting or suppressing microbial growth (Figure 1).

Microbial biofilm formation relies on the interaction among bacterial cells, adhesion to substrates, and the availability of nutrients [22,29]. Cell-surface interactions allow for the accumulation of certain microbial species on exposed surfaces, and they pave the way for the colonization of the implant surface [30]. Biofilms can show microbial composition in a symbiotic state related to health; however, different factors can trigger the microbiological shift increasing the levels of putative pathogens [31]. Despite the considerable progress that has been made over the past few decades in attempts to understand the etiology of biofilm formation and maturation on dental implants, it is important to appreciate that this field is still an area of ongoing research. Targeted

approaches to biofilm eradication can be applied to different steps of biofilm formation, which should be considered a ‘chronic process’ of formation onto implant surfaces. Therefore, therapeutic strategies that reduce initial microbial adhesion may do not control the chronic microbial accumulation and disease progression.

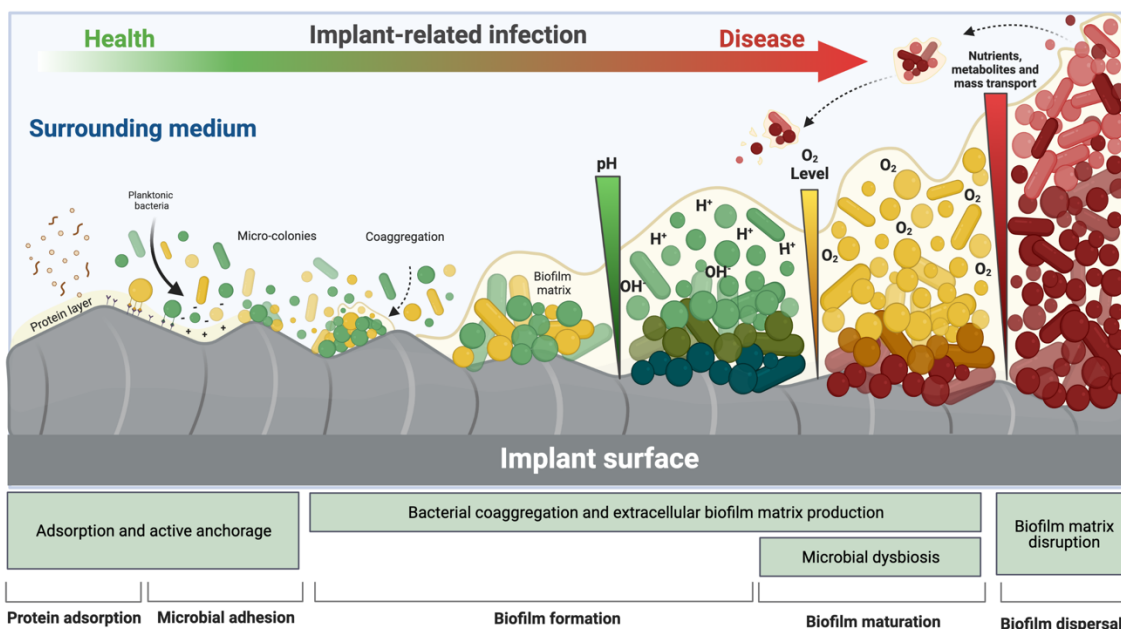


Fig. 1. An overview of the temporal sequence of polymicrobial biofilm formation on a dental implant. Immediately after implant insertion, the titanium surface is coated by proteins from saliva (supra-mucosal segment) and plasma (sub-mucosal segment). Stable anchorage of initial bacterial colonizers is generally followed by the formation of an early biofilm. Subsequently, intercellular interactions mediated by proteins on the surface and cell-wall proteins lead bacteria to cluster together, forming microcolonies, and this interaction also promotes bacterial co-aggregation and biofilm accumulation. These microbial communities are gradually embedded into the extracellular matrix as part of the oral biofilm maturation process. Environmental conditions such as pH, oxygen level, nutrients, metabolites, and mass transport mechanisms can lead to microbial dysbiosis. Consequently, the transition process from health to disease occurs. Finally, proteases and nucleases are involved in biofilm dispersal, whereby cells leave the biofilm to re-enter the planktonic phase. Overall, this biofilm environment (structure) provides the emergent properties of biofilms, including surface adhesion, spatial and chemical heterogeneities, synergistic/competitive polymicrobial interactions, antimicrobial recalcitrance, and biofilm virulence. Created with BioRender.com (Licence number: FH22YOWKFD).

2.1.2. Bacteria-surface interactions and peri-implant tissue damage

Bacteria-surface interactions may be influenced by several factors, such as implant characteristics, peri-implant environment, site-specific microbiota, nutrient availability, and host response [6]. Indigenous microbial species can reach all implant surfaces *via* saliva or blood plasma, but peri-implant environmental factors determine which species are able to remain and colonize successfully [31]. Transmucosal surfaces support a distinctive oral microbiota (supragingival biofilm) dominated by facultative Gram-positive cocci, rods, and bacilli, while implant screws harbor a submucosal microbiota, with an abundance of anaerobic Gram-negative species (subgingival biofilm) [29]. Nonetheless, the factors that influence the transition from a health-associated to a disease-associated oral microbiome are still not fully understood. Until now, it was believed that the inflammatory process [29], poor oral hygiene [32], lack of regular dental implant maintenance [33], frequency of sucrose consumption [34], products released by implant degradation [35], and nature of the EPS-enriched environment [36] are conditions indicated as potential players in the microbiological shift of oral biofilms inducing overgrowth of putative species with pathogenic potential. Likewise, each individual displays unique biological factors that influence disease initiation, activity, and progression [37].

In health, the soft tissues surrounding dental implants are characterized by the absence of erythema, bleeding on probing, swelling, and suppuration, with stable bone levels around the implant platform [38,39]. In contrast, if patient compliance is not fully obtained and proper oral hygiene is not performed, microbial accumulation will certainly induce inflammatory changes in the peri-implant sites [6]. Peri-implant mucositis is characterized by inflammation in the mucosa around dental implants, with local bleeding and/or suppuration, but its progression and the subsequent progressive loss of supporting bone are known as peri-implantitis [7]. Both conditions are considered “biofilm-associated pathological conditions”, strengthening the evidence that biofilm is the etiological factor in dental implant-related infections [38].

As suggested for dental caries and periodontal disease [3,31], an adaptation of the “ecological plaque hypothesis” on tooth surfaces may be applied to describe a transition from a healthy state to a disease state in the peri-implant mucosa and bone structures (Figure 2). In this adapted hypothesis, suggested by Souza *et al.* (2021) [16], increased biofilm accumulation acts as a “stress” factor triggering an inflammatory process that leads to changes in the local microenvironment, favoring proteolytic and anaerobic Gram-negative bacterial overgrowth [16]. This microbiological shift favors disease progression, which can be affected by different factors that either lead to tissue damage or reverse the process [31]. Although oral biofilm formation and factors affecting this accumulation have been widely explored in the literature, research has focused mainly on dental surfaces, but the knowledge we have gained about biofilm formation on oral surfaces cannot be simply transferred to implant surfaces [16]. Therefore, to control and prevent biofilm accumulation on implant devices, we must first understand these chronic processes and the factors that modulate them and use this information to develop suitable therapeutic strategies [40]. Unfortunately, there is no consensus regarding the best therapeutic protocol to treat dental implant-related infections [41], and this may be due to the lack of knowledge regarding biofilm accumulation, pathogenesis process, and irregular implant topography, which hamper biofilm removal.

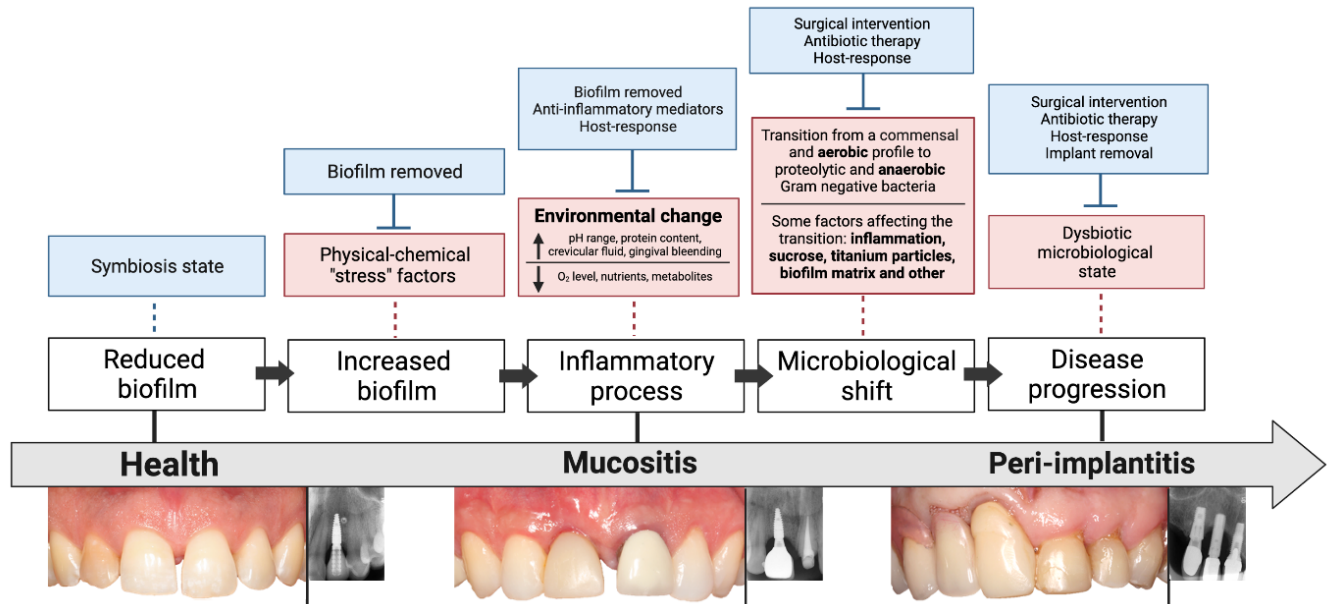


Fig. 2. Schematic representation of the “ecological plaque hypothesis” in relation to peri-implant disease, adapted from Souza *et al.* (2021) [16]. Increased biofilm accumulation on the implant surface triggers an inflammatory process that changes the environment, leading to a microbiological shift and disease progression (red boxes). Other host and environmental factors can also favor the microbiological shift on biofilms growing on titanium surfaces. However, some factors can control biofilm accumulation and inflammatory responses (blue boxes), such as surgical and antimicrobial intervention and host responses. Consequently, the clinical transition from peri-implant mucositis to peri-implantitis occurs (please see the clinical photographs).

2.2. Microbial responses to implant surfaces: design and engineering concepts for dental implants

One way to interfere with microbial adhesion and biofilm formation is by modifying the characteristics of implant surfaces [40]. Notably, a plethora of surface modification techniques has been investigated, aimed at altering the interfacial properties of implanted devices without disrupting the bulk properties of the Ti biomaterial [1,11]. For the purposes of this review, it is worth dividing surface treatments into two broad categories: surface modifications and multifunctional coatings (Figure 3). Conceptually, it is often quite difficult to categorize some of these novel techniques, since most are still in the preliminary stage of development and some fall into both categories. Depending

on how they are applied, a method could be used to coat Ti with biocompatible elements, and, equally, the same method may be used to develop an antimicrobial coating. Here, we summarize the arsenal of strategies that have been deployed to overcome the harmful effects resulting from microbial accumulation on Ti surfaces.

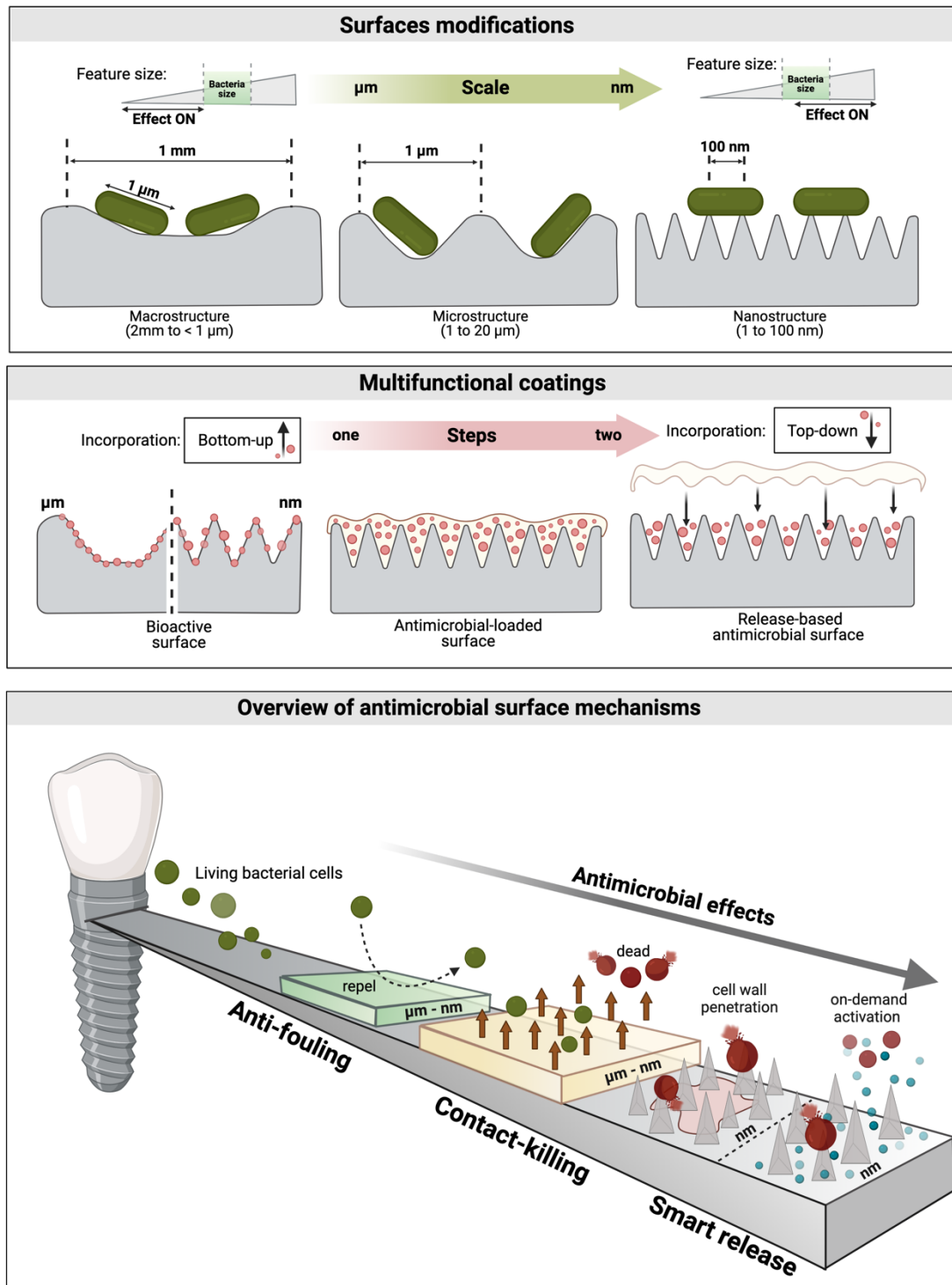


Fig. 3. Schematic diagram of surface treatments applied to a Ti substrate divided into surface modifications (macro-, micro-, and nanostructured) and multifunctional coatings (bioactive and antimicrobial) and possible antimicrobial surface mechanisms, adapted from Linklater *et al.* (2021) [15]. For micro- and nanostructured surfaces (top panel), there is a relationship between the length

scale of the bacteria (green) and the characteristic dimensions of the surface topography (gray), which may impart antifouling or antimicrobial capabilities. Nanostructured surfaces have been demonstrated to be more efficient at reducing bacterial attachment and preventing biofilm accumulation than surfaces exhibiting modifications in only macro or micro scale. For the Ti coating developed (middle panel), the incorporation of antimicrobial agents (red) can be in both molecular and particle forms, including one- or two-step with bottom-up (direct antimicrobial incorporation during the deposition process) or up-down (secondary antimicrobial deposition after surface treatment) approaches to functionalize the surface. In general, bioactive, antimicrobial, and release-based antimicrobial coatings have been investigated to control microbial biofilms. In terms of antimicrobial mechanisms (bottom panel), antifouling, contact-killing, and smart release with on-demand activation have been proposed as promising surface mechanisms. Created with BioRender.com (Licence number: WL22YP56T8).

2.2.1. Ti surface modifications

Surface modification implies that the micro- or nanostructure of Ti is modified [42,43]. This can be performed at the atomic, molecular, or textural level to determine the overall topography of the surface [9]. In terms of dental implants, the vast majority of commercial surface treatments focus on changes in the surface layer of titanium's roughness, mostly focused on improving the osseointegration process [1]. Nonetheless, the remarkable properties of micro- and nanostructured materials go far beyond this. Based on current evidence, the topographical modification of the material may also include bioactive, antifouling, or antimicrobial capabilities [15]. In addition to the micro-nanostructuring of Ti biomaterial, changes in the physicochemical properties of the substrate can also be achieved to promote anti-biofilm effects by killing bacteria upon direct contact [15,44]. Moreover, the bactericidal and/or bacteriostatic effect does not lead to the eradication of biofilms, since dead cells still attached to the substrate can act as binding sites for other microorganisms, promoting colonization by live pathogens [45].

2.2.2. Ti coatings developed

Antimicrobial/bioactive coatings are formed by the apposition or spreading of an antimicrobial agent or bioactive element onto a substrate, or by changes on physical-chemical surface properties focusing

on aspects that reduce microbial adhesion, such as wettability [1]. Hence, an additional layer is formed on the existing surface to enhance biomechanical behavior or even to reduce bacterial adherence to the Ti biomaterial [9]. A critical issue in the development of new coatings is how the coating will be applied to and stabilized on the biomaterial to be stable over time or possibly recharged, mainly considering that proteins and even microorganisms will immediately cover the surface after the insertion [46]. This can be achieved by various techniques, which may be physical, chemical, mechanical, or a combination of these [47]. Additionally, to avoid introducing an external coating, Ti-based alloys containing heavy metal elements can also endow the implants with self-antibacterial ability [42]. Ti coatings involved the incorporation of antimicrobials, such as metallic ions, antibiotics, drugs, antimicrobial peptides (AMP), and biopolymers, which can be incorporated in bulk or by the coating of a Ti biomaterial based on chemical compatibility [1,9,14]. They are incorporated onto the surfaces by many different techniques, such as immersion in Ti substrate, covalent binding to functionalized polymeric coatings, and incorporation into self-assembling mono/multilayer organic coatings [47]. The incorporation can be in either molecular or particle forms, including one- or two-step, with bottom-up or up-down approaches for surface functionalization [9]. In this framework, because coating synthesis methods allow for the incorporation of a broad range of compounds, researchers have undertaken the development of biomedical coatings that do not rely solely on one target property, but instead seek to couple multiple approaches that likely present antimicrobial mechanisms with no additive cytotoxicity to surrounding tissues [48,49]. This opens up a broader array of promising approaches and deposition techniques for designing coatings with controlled multifunctional capabilities that can remain on biomaterial surfaces for long periods. Although most experimental antimicrobial coatings are designed for non-dental systems, some have the potential to be used in implant dentistry and, therefore, could be considered from a dental implant standpoint in future studies.

3. Evidence-based review findings

3.1. Systematic search outcomes: state-of-the-art in surface science

To summarize the current *in vivo* evidence of Ti surfaces developed to prevent or control microbial accumulation on implant surfaces, we conducted a systematic search. For complete details about the searching method, see Supplementary Methods (Supplemental materials and methods; Table S1). From an initial pool of 4,155 relevant search titles collected from all databases, 2,793 were included after the elimination of duplicate studies (Supplemental results; Figure S1). From a total of 128 articles thoroughly assessed in full text, 59 were considered not eligible according to the inclusion/exclusion criteria (Supplemental results; Table S2). Consequently, 69 studies were included in this critical evidence-based review, comprising 61 pre-clinical studies (51 animal models; 10 *in situ* models) and 8 human clinical studies.

Although Ti implants have progressively evolved and completely revolutionized the biomedical field, with several attempts to reduce biofilm formation on Ti surfaces, thus far, no evidence-based review has comprehensively covered this engaging research area. Here, we noted that in the first 20 years following initial publications about Ti surface modifications (1990–2010), only 13 articles were published, for a mean of 1.6 articles per year. These studies were initiated by research groups in the USA, with a focus on hydroxyapatite-coated assessment in animals [50] and humans [51]. Within the past five years (2015–2020), the field grew rapidly, with 56 published articles dominated by research groups in China and in the USA, testing surface modifications and emerging coatings on Ti implants (Supplemental results; Figure S2).

3.2. Current pre-clinical and clinical models to test antimicrobial effects of implant surfaces

To explore differences between and among the study designs, data from animal model (Table 1), *in situ* model (Table 2), and human clinical studies (Table 3) were outlined. Regarding animal models, the vast majority of the 51 studies were conducted with rodents (rats, $n = 32$; mice, $n = 5$) or in small animals (rabbits, $n = 13$; dogs, $n = 1$). For biomaterials research, these rodent and small-

animal models have predominated, since they are cost-effective in the majority of research laboratories around the world, allow for ideal sample size, standardized age, diet, and behavior, as well as requiring limited implant samples that can be fabricated or processed to a size appropriate for small surgical sites [52]. Meanwhile, large animals like sheep, goats, pigs, and dogs have extra housing requirements with a high cost of feeding, surgery, and post-operative care, and raise complex ethical issues [53].

In terms of surgical site, implants were commonly located in the femoral shaft ($n = 22$), tibial shaft ($n = 15$), or subcutaneous sites ($n = 12$), which do not ideally represent the environmental conditions and healing processes that occur in the oral cavity. Moreover, this different environment may modulate microbiological accumulation and composition and the results found may not be applied for oral conditions, but it may suggest promising results to be further tested by models resembling the oral environment. The antimicrobial activity and infection rate were evaluated in a broad range of follow-up times, varying from 2 h [54] up to 8 weeks [55,56] after implant insertion at different time points. In the current review, the long-term effects of antimicrobial coatings were analyzed based on the longest follow-up time reported in each study.

For *in situ* models, 10 eligible articles were fully reviewed. This study design has been commonly used in dental research to evaluate polymicrobial biofilm formation on Ti surfaces [36] and dental surfaces [57] inserted in the oral environment. For this, samples are positioned in intra-oral appliances that are maintained in the volunteer's mouth throughout the experimental period. As a result, biofilm grows in the mouth, mimicking real conditions that allow biofilm to form, with the expected oral bacterial interactions. In this case, *in situ* studies can mimic the *in vivo* biofilm formation when the implant is placed in a patient's mouth, but with better control of outcomes. All 75 volunteers described in the selected articles wore intra-oral appliances containing Ti samples to allow for biofilm accumulation. The follow-up times in the included articles ranged from 30 min [58] up to 21 days [59] after early biofilm formation. Although *in situ* models represent an interesting and

ethically acceptable research approach, the extrapolation of results to dental implant condition should be carefully done, since host–bacterial interactions cannot be fully reproduced with this model, because the Ti samples are in contact not with oral mucosa, but with acrylic appliances only and may not mimic sub-gingival environment.

Different from pre-clinical studies, only 8 human studies met the inclusion and exclusion criteria for assessment of the effects of available implant coatings on microbial accumulation. Importantly, many human studies were excluded, since they did not evaluate the antimicrobial effect of the Ti surface by any microbiological method. Therefore, this represents a significant scientific barrier to be overcome in the implant dentistry field. Altogether, approximately 104 participants of both genders and a range of ages were treated with 300 dental implants for tooth replacement. Prosthetic and patient factors could not be summarized due to the lack of information. For the included studies, the minimum and maximum follow-up periods were 14 days [60] and 12 years [61], respectively.

3.3. Outlining deposition technologies applied to promote surface modifications and antimicrobial agents' functionalization

The implant materials used in all eligible studies were medical-grade pure titanium, titanium-aluminum-vanadium (Ti-Al-V), and titanium-aluminum-niobium (TiAlNb) alloys. Only in the animal model studies were the most common anchoring implant designs screw-type (threaded), cylindrical (without thread), and wires (rod-shaped). Screw-type implants have been most used because of their excellent initial stability, whereas the stability of cylindrical and wire implants depends on an exact fit within the bone [62]. Conversely, Ti discs (various shapes and diameters) were commonly tested in *in situ* models, while human studies have used real dental implants with different macrogeometric shapes/designs. In terms of microbiological assessment, both surface topography and design of implants can influence biofilm accumulation [10,59], and these factors

should also be considered in pre-clinical studies for translation of these findings into clinical situations.

Since the implant surface is involved, surface properties and chemical composition play a crucial role in the predictability of the implant-to-bone response [12]. Among the physical-chemical modifications that have been proposed so far to alter Ti surface properties, the most important are surface-free energy, wettability, charge, and topography, to limit microbial adhesion [16]. Clearly, the combination of suitable rough topography ($R_a = 0.51\text{-}1.36\ \mu\text{m}$; $S_a = 0.66\text{-}2.91\ \mu\text{m}$) [63] and higher surface energy/hydrophilicity [64] may synergistically induce a suitable microenvironment to modulate macrophage polarization and host-cell migration and proliferation, thus reducing healing time and accelerating osseointegration [47]. This principle is used in sandblasted and acid-etched (SLA) surfaces, which are commonly available surface treatments in dental implants [65]. Although SLA surfaces have a strong track record of clinical success in dentistry, they lack antibacterial capabilities, and their effects against biofilm infections are limited. In line with clinical demands, several antibacterial Ti surfaces modifications have frequently been proposed over the years (Figure 4). The mechano-bactericidal mechanisms have been well-defined in material science and surface engineering in recent decades, including the creation of biomimetic surfaces bioinspired in nature [66–68], which offers various physical ways to reduce microbial adhesion [15]. In addition to the micro-nanostructuring of Ti biomaterial, changes in the physicochemical properties of the substrate can also be achieved to promote anti-biofilm effects by killing bacteria upon direct contact[69–71].

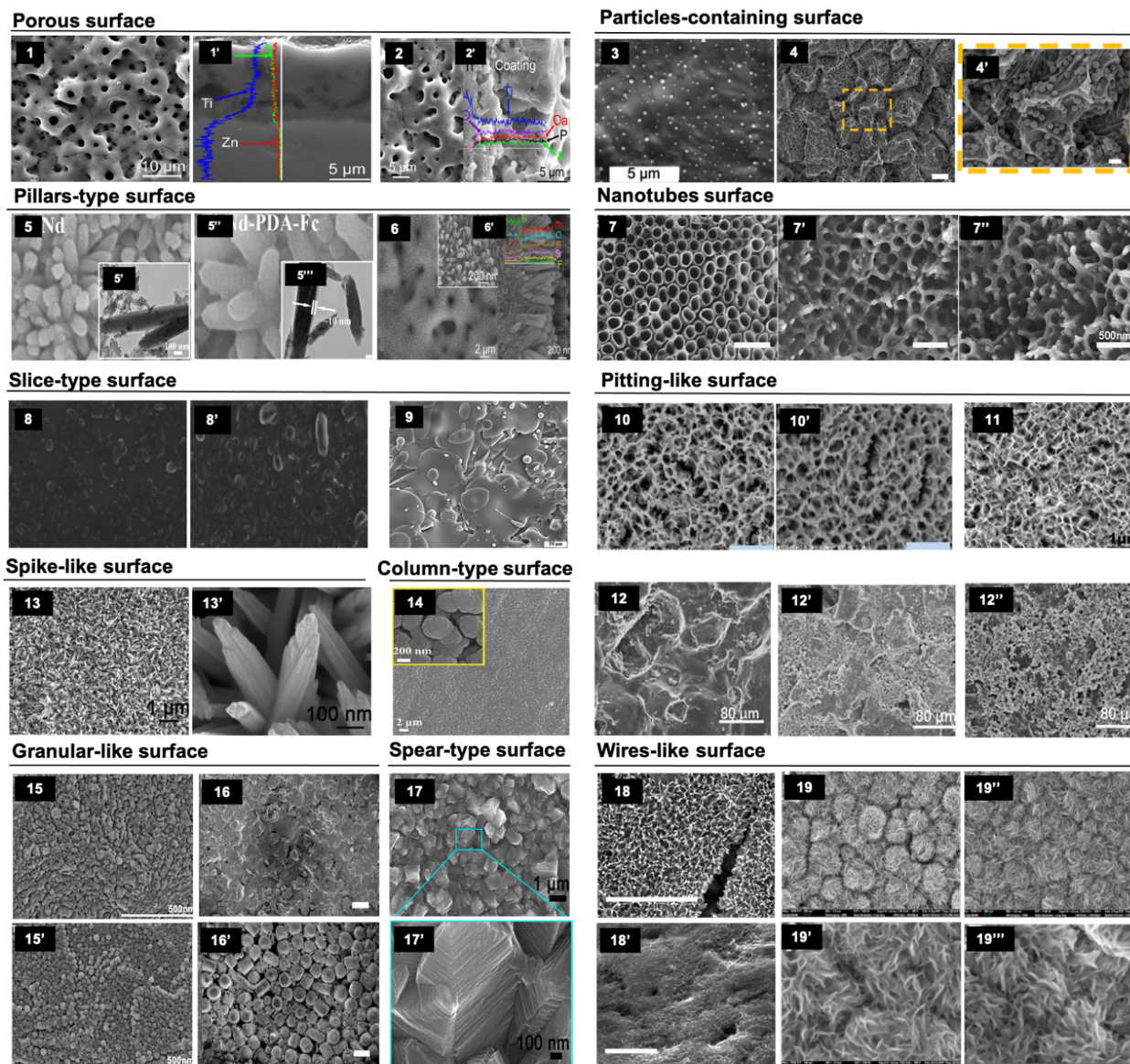


Fig. 4. Overview of available titanium surface modifications. The physical, chemical, and physical-chemical methods were used to produce Ti surface modifications, as follows: porous surface (1[72] and 2[55]), particles-containing surface (3[73] and 4[49]), pillars-type surface (5[74] and 6[56]), nanotubes surface (7[69]), slice-type surface (8[75] and 9[76]), pitting-like surface (10[71], 11[77] and 12[78]), spike-like surface (13[66]), column-type surface (14[79]), granular-like surface (15[80] and 16[81]), spear-type surface (17[82]), wires-like surface (18[83] and 19[68]). Each number (black square) represents the study and its respective micrograph of the surface. Different scale bars were considered based on study's description, showing μm - and nano-scale surfaces changes. Reprinted (adapted) with permission from Elsevier (License Numbers: 5155910020417; 515591036048; 5155910766325; 5155911132061; 5155920044862; 5155920350790; 5155920489184; 5158220465489; 5158220682404; 5158220945204; 5158230390889),

Springer Nature, American Chemical Society, and John Wiley and Sons in terms of Creative Commons CC BY license.

Regarding surface treatment applied in bulk Ti material, the majority of the studies used machined ($n = 30$), titanium dioxide (TiO₂) nanotubes ($n = 7$), hydroxyapatite-coated ($n = 6$), or porous-coated ($n = 3$) implant surfaces. Mostly, these surfaces were evaluated either isolated or associated with antimicrobial components incorporated into the coatings. For the development of emerging antimicrobial coatings, plasma treatment ($n = 13$) and the immersion method ($n = 10$) were the most used coating technologies (Figure 5). The antimicrobial agents were functionalized directly into the material surface (one-step reaction) or under pre-formed surface treatment (two-step reactions), by either several physical and chemical methods or both. Generally, a one-step reaction was directly applied to implant surfaces to change their topography (μm and nm scales), while two-step reactions under pre-formed surface treatments were used as cross-linker substrates to functionalize therapeutic nanoparticles [49,66] or drug immobilization [84,85].

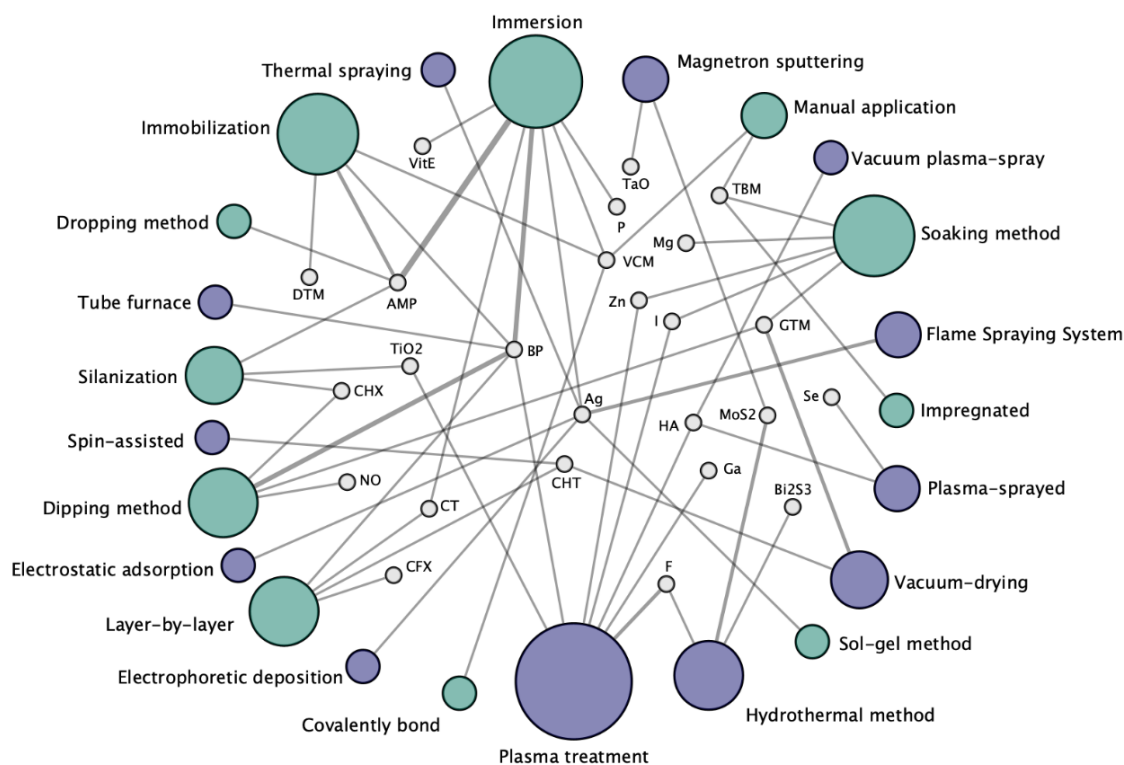


Fig. 5. The spider-web-like graph presents the network of antimicrobial subgroups functionalized on a Ti surface by different deposition methods. Green nodes represent the chemical deposition methods and purple nodes the physical deposition methods. The size of the node is proportional to the number of animal studies included. Gray lines represent the direct comparisons of each antimicrobial deposition method, and the line thickness is directly proportional to the number of incorporations. The antibacterial polymers, biological peptides, silver ions, and vancomycin were the agents most functionalized in implant surfaces. Abbreviations: AMP = antimicrobial peptides; BP = biopolymers; VitE = Vitamin E; DTM = Daptomycin; CHX = Chlorhexidine; NO = nitric oxide; CT = catechol; CFX = Ciprofloxacin; CHT = Chitosan; F = Fluoride ion; Ga = Gallium ion; HA = Hydroxyapatite; MoS₂ = Molybdenum disulfide; Bi₂S₃ = Bismuth sulfide; Se = Selenium ion; GTM = Gentamycin; TBM = Tobramycin; TaO = Tantalum oxide; P = Red Phosphorus; VCM = Vancomycin; Zn = Zinc ion; I = Iodine ion; Ag = Silver ion; and TiO₂ = Titanium dioxide. Of note, biopolymer (BP) and antimicrobial peptide (AMP) classes were created to match biological agents with similar biocompatible behavior. (Created by Cytoscape®).

Based on antimicrobial incorporation, biopolymers ($n = 7$), AMP ($n = 7$), silver ions ($n = 7$), and vancomycin ($n = 7$) were the agents most functionalized on implant surfaces. Also, it was possible to observe that the same agent could be incorporated into the substrate either alone or in combination with others, by physical or chemical methods. Interestingly, chemical methods were more often applied to immobilize organic elements, because long-term adsorption may not be successful due to possible detachment when physical methods are used [9]. Meanwhile, physical and physical-chemical methods have been widely used to dope metallic ions onto Ti surfaces by a one-step reaction. Each deposition method has pros and cons as a route to synthesis Ti modifications, as previously revised [9]. Physical methods (e.g., plasma treatment, hydrothermal method, magnetron sputtering, thermal spraying, tube furnace, spin-assisted, electrostatic adsorption, vacuum-drying, plasma-sprayed, and flame spraying system) are cheaper and generally performed in a shorter time, while chemical methods (e.g., immersion, soaking method, manual application, impregnation, sol-gel method, covalently bond, layer-by-layer, dipping method, silanization, dropping method, and immobilization) are more expensive and often involve several steps for coating synthesis [12]. Conceptually, the ideal

method should be low-cost, structurally reliable, reproducible, and environmentally friendly, thus being a critical industrial challenge [86]. Obviously, it was not possible to strictly delimit physical from chemical coatings for the current study analysis since some techniques combined multiple physical and chemical processes. However, we relied mostly on the main idea behind each process. The main features of surface modifications and deposition methods were described individually for direct comparison among the studies (Table 1, 2 and 3).

Another relevant point is that antimicrobial concentrations on the surfaces should be suitable to promote the dose-response effect without affecting biocompatibility or creating a lower dose that could allow for the selection and overgrowth of bacteria-resistant strains. Moreover, it is essential that the drug delivery system release the antimicrobial agent in a minimum concentration for a long period to achieve the antimicrobial effect for a chronic process, such as implant-related infections. We found a wide range in the antimicrobial concentrations tested among the animal studies, in which either concentrations were standardized based on *in vitro* screening tests or this information was not reported. Furthermore, only a few studies ($n = 11$) evaluated sustained drug release in long-term follow-ups (e.g., weeks or months). Overall, drug-release methods were observed in almost half of the experiments ($n = 21$), with antibacterial effects reported in only early biofilm development (Supplemental results; Table S3). Importantly, drug-release kinetics is dependent on the type of deposition method applied [87], and the same drugs [54,88] can show different chemical and release behavior when immobilized on the surface by physical or chemical methods. Thus, the choice of deposition method, the drug type, and establishment of the desired concentration to be released are essential steps toward the production of a sustainable drug delivery system in the physiological environment.

Based on the available scientific literature, we have confirmed that there is a huge discrepancy in the surfaces investigated between pre-clinical and clinical studies. In animal studies, many experimental antimicrobial coatings have been tested ($n = 50$; $\sim 98\%$). However, even when promising laboratory results were demonstrated, these surfaces have barely progressed to be tested in

in situ models ($n = 4$; $\sim 40\%$), non-randomized clinical trials (N-RCTs; $n = 2$; $\sim 40\%$), and a randomized clinical trial (RCT; $n = 1$; $\sim 30\%$). As expected, almost all current clinical studies in implant dentistry have used commercial implant surfaces such as SLA[®][21,60,89], TiUnite[®] [58,90], Turned[®] / Bioblast[®][61,90], and PerioApatite[®] [51,91]. This can be partially attributed to the fact that all papers retrieved in our literature search were focused on the interrelationship between surface treatments and osseointegration, and, therefore, microbiological outcomes were not their main purpose. Surprisingly, a small number of clinical research papers ($n = 8$) addressed relevant oral microorganisms and conducted biofilm characterizations.

Among the antibacterial coatings tested in humans, only chlorhexidine [92], silver [93], and titanium dioxide (anatase phase) [94] were compared with either machined or commercial surfaces. To date, no Ti surface modifications or antimicrobial coatings have shown a good clinical effect in controlling dental implant-related infections. Another current limitation is that some studies [60,93,94] used the screw-type implant component known as the healing abutment (located in the transmucosal area, not in contact with the bone) as a clinical substrate for testing the impact of antibacterial coatings on microbial accumulation. This research approach can be interesting for evaluation of the treatment for the abutment itself but not for coatings proposed to be applied to the implant screw body. Moreover, distinct oral microbiomes, expected on different implant sites (supragingival and subgingival environments) [95] are not considered in this experimental design, thereby demonstrating the need for careful evaluation of the microbiological effect found and the experimental design used.

3.4. From animals to humans: bacterial profiles and microbial assessments on titanium-based implants

Aside from the previous findings, the evaluation of bacterial profiles also differed between pre-clinical and clinical studies (Figure 6). *Staphylococcus aureus*, the main bacterium related to bone infection in orthopedic implants [96], is the preferred pathogen used in animal models (where tested

implants are usually in extra-oral sites) ($n = 47$). Importantly, since dental implant-related infections feature polymicrobial communities [29], it is necessary to consider infection models with relevant bacteria for peri-implant diseases and the microbial diversity of oral biofilms. In this way, a single study [50] used bacterial strains from clinical isolates, including *Porphyromonas gingivalis*, *Prevotella intermedia*, and *Aggregatibacter actinomycetemcomitans*. From animal data, it is possible to observe that a majority of experimental coatings were developed exclusively for orthopedic applications. Consequently, these results should be interpreted with caution, since the antibacterial effects in clinically important oral bacterial strains were not investigated. A more diverse pool of bacteria has been considered in *in situ* and clinical studies ($n = 45$); however, only 5 *in situ* and 3 human studies investigated the total load of polymicrobial communities formed over antimicrobially treated Ti surfaces. Therefore, these findings are also limited, due to the different bacterial species and surface treatments evaluated in each study, not allowing for direct comparison among all studies. Furthermore, it is relevant to highlight the need for a study model that reproduces mature biofilm, since implant-related infections are chronic diseases.

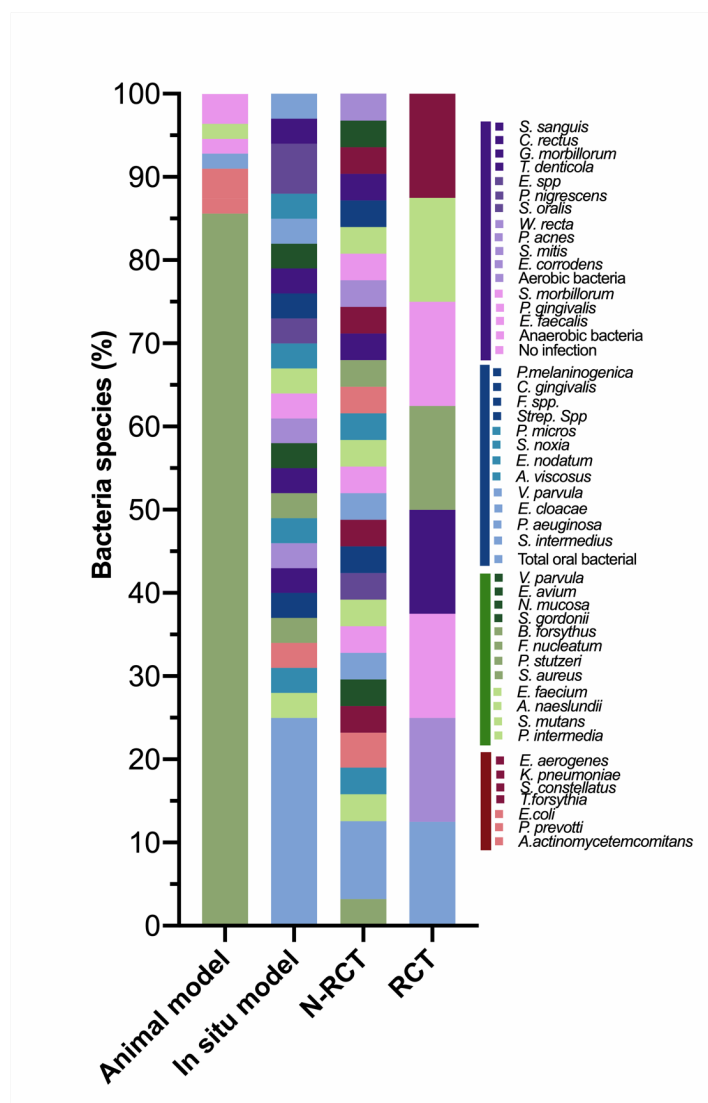


Fig. 6. Bacterial species assessment in each study design. The bacterial abundance (%) was calculated based on the main pathogen used in the infection model for all included studies. Total oral bacteria, anaerobic bacteria, and aerobic bacteria were generally reported as described by the authors. Altogether, 45 bacterial species were used, with different frequencies among the studies. The *in situ* model and the N-RCT showed more extensive diversity of the bacterial species evaluated.

Nearly all included animal studies reported contamination of the surgical site immediately after implant insertion by a wide range of bacterial inoculum sizes (ranging from 10^2 up to 10^9 CFU [colony-forming units]). Conversely, only 2 studies [97,98] did not induce infection exogenously. It is important to mention that for an implant infection model to be established, a sublethal microbial infection is required — that is, the bacterial concentration must be high enough to generate a self-

sustaining infection but low enough to maintain the localized condition, not resulting in systemic disease or sepsis in the animal [53]. For this purpose, optimal bacterial inoculum concentrations and vehicles (media or pre-formed biofilm) must be evaluated in a pilot study for better standardization of microbial concentrations [52,96], not reported in most of the included studies. To check the effects of Ti-surface modifications on the underlying mechanisms of infection, some animal studies ($n = 42$) have evaluated hard and soft tissues surrounding the implants by radiologic, histologic, immunohistochemical, and biomechanical tests (Supplemental results; Table S4). Overall, the bacterial reduction on Ti surfaces had a direct impact on better control of implant-related infections.

In biofilm analyses, bacterial load was measured by destructive methods leading to disorganization of the three-dimensional biofilm structure, not allowing for qualitative and architecture biofilm analyses in animal models. Some studies ($n = 11$) evaluated biofilm morphology by scanning electron microscopy (SEM) and confocal images. In transition from the laboratory to the clinic, the techniques most performed for biofilm harvesting included the use of paper-point instruments in the peri-implant sulcus or microbiota removal with a curette. In contrast to animal models, no microscopy analyses for the evaluation of biofilm morphology have been conducted in humans, which would be expected since samples cannot be removed. As previously mentioned, the extracellular biofilm matrix, which is an important virulence factor of pathogenic biofilms [36], and their morphology, biovolume, and distribution in implants remain to be investigated. Understanding the biofilm morphology and 3D arrangement can guide new mechanical approaches to disrupt pathogenic biofilms, including the use of sonic instruments [82] and a dual strategy whereby biofilm matrix is first degraded followed by antimicrobial use, as recently described for Ti surfaces [36]. Only microbial accumulation on healing abutments has been measured by photographs used to determine the percentage of biofilm area coverage [60,93]. Thus, information about the spatial organization of naturally grown biofilm associated with a human peri-implant disease is currently unavailable.

Another methodological issue is that several analytical methods have been used to determine implant contamination. Generally, in pre-clinical and clinical studies, microbial load has been

determined by CFU counts. For the animal model, an infected implant sample is harvested, and microorganisms are removed, placed in a medium (often by homogenization or sonication), and plated after serial dilution [96]. Interestingly, two studies with mice [81,99] used *in vivo* imaging of bacteria with a bioluminescence-labeled strain to track the progression of microbial infection in real-time. Since rodents are small, it is somewhat less challenging, since light penetration depth is shorter than in larger animals, thus being a relevant strategy for the evaluation of release-based antimicrobial coatings [100]. Additionally, in some studies ($n = 4$), contaminated implants were rolled out on agar plates only, for the determination of infection rates. As a result, the infection rates in the experimental groups were lower (close to 0%) compared with those on control surfaces (Table 1).

Polymicrobial biofilms have been exclusively evaluated in human studies (*in situ* and clinical) by the Checkerboard DNA-DNA Hybridization technique and/or PCR analysis to determine individual or total bacterial levels, or both (Tables 2 and 3). Biofilm composition is a crucial factor for further studies, since a high bacterial load with an unknown profile does not represent a microbiological composition related to infection. Classic animal studies have used biofilm-retaining ligatures around the implant to initiate tissue damage and lead to biofilm accumulation [101]. Nevertheless, alveolar bone loss in the ligature model is dependent on pathogenic bacterial abundance on the ligature, not necessarily on the implant surface [6,29]. Additionally, some aspects of the animal model — such as dietary habits, oral microbiota, stability of immune responses, and specific dento-alveolar anatomy — are also significantly different from those of humans [102]. With those limitations, these models cannot fully address specific questions related to the disease-associated human oral microbiome and require further and detailed investigation for findings to be determined appropriately.

Tables 1, 2, and 3 summarize the bacterial loads (control and test groups) based on the microbiological test used, taking into account the longest follow-up time for each study. To facilitate reporting, included studies were also ‘lumped’ into each study design, and then the percentages (%) of biofilm reduction were calculated (Figure 7). Although various Ti implant-surface modifications

and experimental coatings have been considered, it is essential to highlight the considerable gap between pre-clinical and clinical findings. Regardless of the study design, there is a highly variable % of biofilm reduction, ranging from -25% to > 95%. In terms of study design, the animal model shows % of biofilm reduction higher than that of other study designs in all follow-up periods (~ 3-fold increase), which may be due to greater control of the experimental models and conditions. Indeed, we also found a trend toward reduced antibacterial effects in long-term periods (~ 28% of reduction). Importantly, *in situ* models were used only in short-term periods, showing a more extensive range of effects between 1 and 2 days (from 65% to 5% reduction). In a clinical scenario, the effects of Ti implant surfaces in long-term periods were limited (< 25% of reduction), also showing an absence of effect (from -10% to -25% of reduction) at some time points. From a careful evaluation of all these contrasting studies, it seems that the anti-biofilm effects of these experimental surfaces are often transient or subject to "species bias".

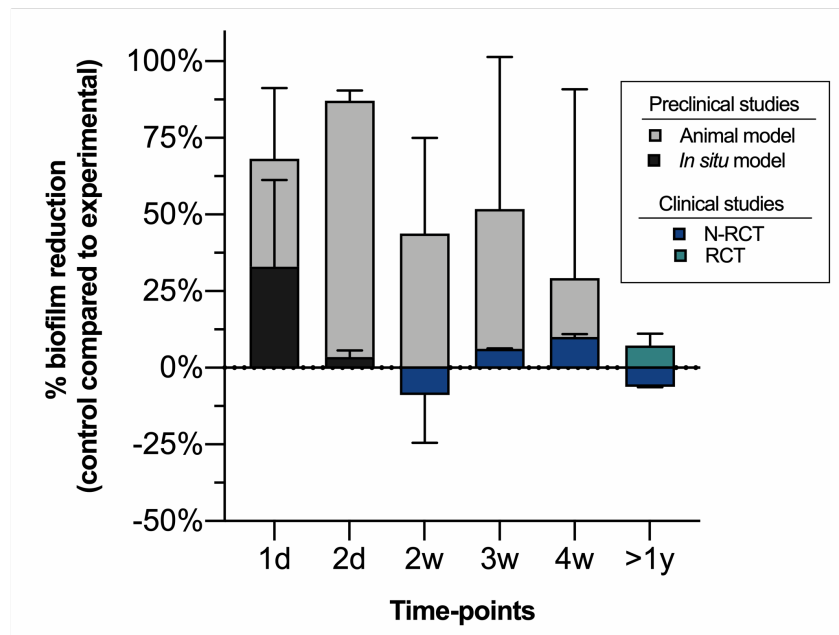


Fig. 7. Percentage of reduction in the bacterial load on different titanium implant modifications and developed coatings (compared with their control groups) according to the study results included in this systematic review. For this analysis, only studies with the same end-point follow-up were considered from the total number of studies. The animal model showed a higher % of biofilm reduction at all periods of follow-up. *In situ* models had a large range of antibacterial effects between

1 and 2 days. There were no clinically relevant effects of the Ti implant surface in preventing bacterial accumulation over long periods.

3.5. Methodological weaknesses and strategies to enhance the weight of evidence in antimicrobial implant surfaces research

To provide a better critical appraisal of the pre-clinical and clinical studies included in this critical evidence-based review, we performed a risk-of-bias assessment in animal, N-RCT, and RCT studies (Figure 8). For this analysis, *in situ* studies were not considered because of the current lack of availability of quality assessment methods. For animal models (Figure 8A), we have demonstrated that all studies failed to report whether caregivers and outcome assessors were blinded to knowledge regarding the intervention to which each animal was assigned, as well as sample size calculation to determine the numbers of samples and animals required to achieve statistical significance without alpha or beta errors, and other bias. Consequently, most animal studies were classified as having unclear risk-of-bias. We have provided a full list of risk-of-bias assessments for each included animal study (Supplemental results; Figure S3).

Regarding the quality assessment of N-RCTs (Figure 8B), the included articles exhibited a serious or moderate overall risk-of-bias. Generally, problems were related to confounders in either the participant selection process or inequality among participants. In addition, potential biases associated with the measured outcomes arose for all clinical trials, since blinding of outcome assessors was not possible, and the inclusion of an examiner outside the trial context was not done. Overall, risk-of-bias in RCTs (Figure 8C) revealed some concerns as a final classification, mainly because of insufficient information about randomization, selection of patients, and measurement outcomes domains. In cases where participants were selected into studies by a randomization process, these were biased by the selection of participants based on characteristics observed after the start of intervention and the absence of accordance between methodology and reported results. Individually, the included human studies were also fully described (Supplemental results; Figures S4 and S5).

From the risk-of-bias assessments, it is not surprising, therefore, why several antimicrobial implant coatings have been developed over time with promising laboratory results but have not progressed to clinical use. This creates the need to revisit the basic science models and methodological principles for biomedical research, especially for animal models. Furthermore, animal studies must provide more comprehensive and complete reports for an adequate risk-of-bias assessment, since the prevalence of “unclear” judgment was noted, which is not surprising, since numerous unclear risk-of-bias items are often observed in animal experiments in the implant field [103]. By careful evaluation and reporting of these unclear issues, an optimization of the design and conduct of animal studies may be achieved [103]. Thus, since animals are vulnerable, models should be carefully planned, and sample sizes clearly justified. Clinically, well-designed randomized clinical studies comparing emerging antimicrobial coatings and control surfaces (i.e., commercial or without the incorporation of antimicrobial factors) with well-defined inclusion and exclusion criteria, adequate sample size, experienced and blinded surgeons, standardization of implant and prosthesis types, sites of implant placement, and suitable microbiological assessments are required to validate current laboratory findings.

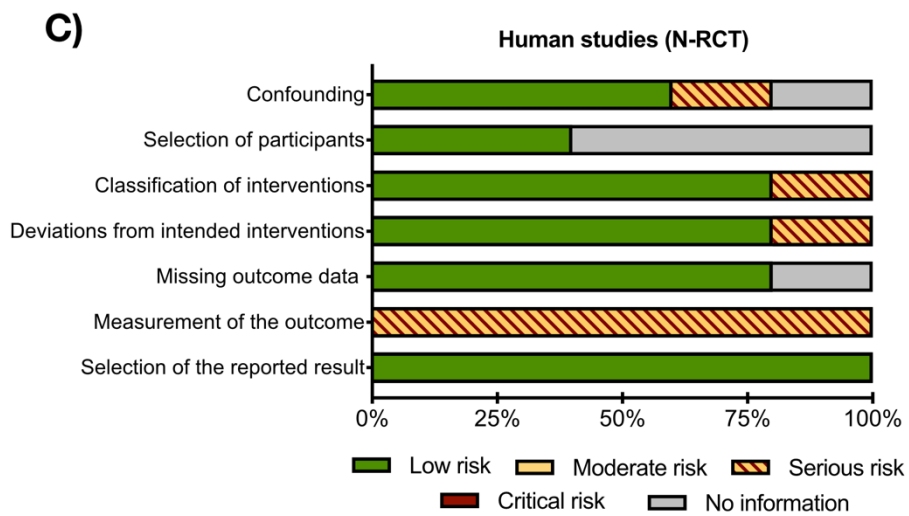
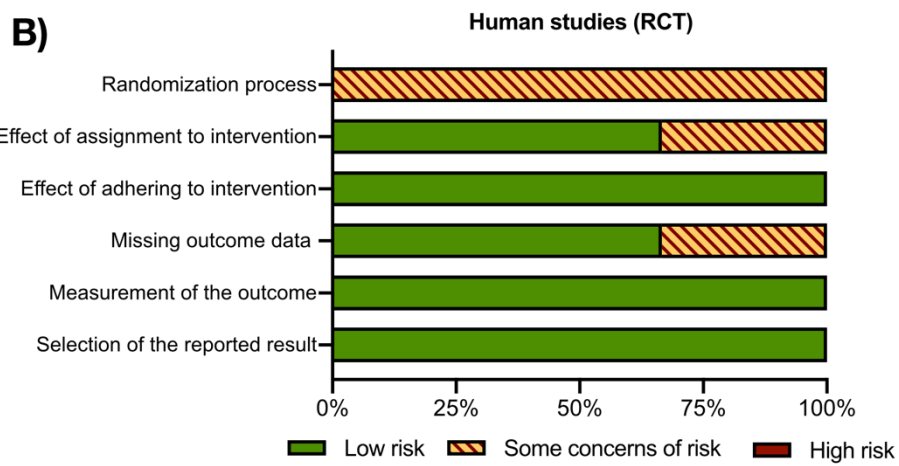
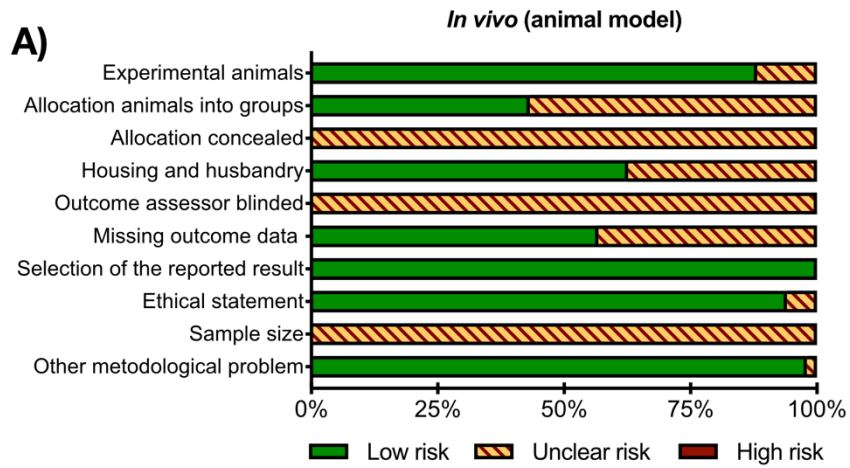


Fig. 8. The risk-of-bias graphs review the authors' overall judgments about each risk-of-bias item as a percentage of the total number of studies. **(A)** Quality assessment for animal studies based on the Systematic Review Centre for Laboratory Animal Experimentation (SYRCLE). **(B)** Quality assessment for non-randomized studies based on the ROBINS-I tool (Risk Of Bias In Non-randomized Studies - of Interventions). **(C)** Quality assessment for randomized studies based on the Revised Cochrane risk-of-bias tool for randomized trials (RoB 2). Overall, some methodological problems were found in each study design.

4. Discussion and suggestions for future research in surface science

The pursuit of Ti surface modifications is a research area that has received substantial attention in recent years due to the possibility of preventing microbial infections. In this regard, we conducted this narrative and critical evidence-based review about the potential of various available surface-modification methods as well as emerging coatings to combat oral bacterial accumulation investigated in pre-clinical and clinical studies. Our main strength was in showing, systematically, that there is no current consensus regarding the optimal Ti surface for reducing oral microbial accumulation and preventing dental implant-related infections. There is a huge gap between animal and human studies related to the limitations of methodological issues and clinical expectations. Thus, because dental implant-related infection remains a major clinical challenge, new smart-release approaches to improve current surfaces have been strongly recommended to control and treat dysbiotic biofilms and allow for the re-establishment of a health-associated microbiome.

According to the regulatory requirements of the ISO (International Organization for Standardization) and the FDA (U.S. Food & Drug Administration), animal experimentation in dental research is an essential step toward the conduct of clinical trials [104]. The animal studies in our review varied in methodological quality and sample sizes rather than providing a single, definitive high-quality experiment for each emerging Ti implant modification and coating tested. Furthermore, there are many critical variables to be considered in selection of a model of dental implant-related infections. Pathogen species (type of inoculum), amount of pathogen (concentration of inoculum),

inoculation vehicle, and the course of infection/inflammation should be monitored and validated [53,96]. These issues need to be taken into consideration for future research to improve quality and reduce heterogeneity among studies [103]. In general, the goal should not be to define the most similar model to humans, but rather to investigate how various models can be used to provide insights into the mechanisms of implant-related infections [101]. It is well-established that the etiology of peri-implant diseases is multifactorial, more specifically polymicrobial, and host-specific. However, the pathogenesis of peri-implant disease is inflammatory [38]. Thus, we are now in a position to deepen and improve the classic animal models with a focus on the expression of virulence factors and host responses. In this way, the aim is to induce deleterious microbial dysbiosis and hence the inflammation process to establish a cause-effect inference by using different implant surfaces.

From the implant surface standpoint, future challenges include the newly proposed biomimetic surfaces inspired by nature, with micro- or nanoscale modifications, which could constitute a dynamic behavior pattern for the prevention of bacterial re-colonization [11]. Although nanopattern topography can lead to bacterial killing by bacteria-surface interactions (without drug incorporation), the increased accumulation of dead bacteria over time might also promote new attachment of live bacteria and development of a multi-structured biofilm [15]. To overcome this current limitation, flexible nanopatterns (bioinspired in the cilia of epithelial cells) have been suggested to ensure more effective mechano-bactericidal actions regulated by an electromagnetic field [105]. Additionally, other emergent and promising strategies for biofilm removal on Ti surfaces, such as electron transfer between the bacteria and the implant interface, or electrical modulation of the implant have been proposed in recent years [106,107]. Both methods are able to disrupt bacterial viability on implant surface based on electron-transfer-induced reactive oxygen species mechanism, either by using wave-driven triboelectric nanogenerator and two nanobrush electrodes made of Ag-nanoparticles integrated ZnO-nanowires or by using Ti embedded with silver nanoparticles (Ag-NPs@Ti) that after electron transfer between the Ag-NPs and Ti substrate produce bursts of reactive oxygen species leading to bacteria death by inducing intracellular oxidation. As a result, both

treatments create strong antibiofilm mechanisms, which can facilitate the control of titanium-associated microbial infections, as also reported by others [15,105]. Another interesting idea would be to combine these antimicrobial nanostructures with bioactive compounds, biomolecules, growth factors, and immunomodulators for future multi-targeting strategies based on the modulation of the local immune responses of the host [1,9].

In terms of antimicrobial load on and release-based coatings of Ti biomaterials, there are three main barriers to the design of these surfaces: (i) long-term and sustained antibacterial effects; (ii) ability to reload the surface; and, primarily, (iii) maintenance of an effective local bacteriostatic or bactericidal effect at the implant surface without affecting the host response, causing cytotoxicity to the implant-surrounding tissues or allowing increased antimicrobial-resistant strains at the site [87,100]. Based on the revised scientific literature, we show that designing an implant coating to overcome these current barriers, regardless of deposition technology, is still an unfulfilled promise. Clinically, until now, only chlorhexidine, silver, and titanium dioxide antimicrobial coatings for dental implants have been tested in humans [92–94]. Despite the efforts made by the scientific community to create and test new antimicrobial coatings, most of them are still under development and, for this reason, have only been tested *in vitro*, thus with yet unknown long-term clinical benefits. In the near future, we hope that some of the currently emergent surfaces can show promising results under *in vivo* conditions. For this, it is imperative that future studies use standardized and widely accepted validation methodologies for antibacterial coatings in the setting of specifically structured dental research that is consistent with its intended oral-clinical applications [16]. Furthermore, investigators undertaking the development of new surfaces should consider basic sciences, including the biologic and microbiological aspects of the oral environment and factors modulating biofilm formation, which affect bacterial growth. As we showed recently [108], a surface coating may not reduce late biofilm growth, but can affect the process and modulate the microbial composition, driving toward an increased level of host-related microorganisms favoring a symbiotic state. Since most of the studies evaluated only initial biofilm formation, it should not be considered to control

peri-implantitis infections — a chronic disease triggered by mature biofilms [29] — and the developed surface may act only during the healing process of the implant device.

The accumulated knowledge in material and surface engineering for the last 30 years has facilitated the consolidation of the new generation of activated biomedical surfaces, denominated as ‘functional self-regulating’ or ‘smart’ surfaces (Figure 9) [109,110]. Although many of these surfaces are still under development in the laboratory, some are advancing rapidly and certainly represent a powerful and valuable option to prevent implant-related infections in the near future [111]. Conceptually, smart surfaces are substrates that respond to distinct physical, chemical, or biochemical stimuli, to start the drug release process whenever infections are present [110]. The key issue is the prospect of forming smart surfaces activated only during an infection period to control the release of antimicrobial drugs with suitable concentrations to fight the disease without causing tissue toxicity or bacterial resistance [40]. In other words, smart surfaces provide ideal concentrations of an antimicrobial agent at the precise moment and local of the infection occurrence. These smart surfaces can be activated exogenously (ultrasound, temperature, light, magnetic field, and electrical pulses) or endogenously (potential redox, enzymatic activity, O₂ level, and pH) [112,113]. Among these stimuli-responsive smart systems, recent researches suggest that pH-responsive polymeric coatings as drug carriers [114,115], temperature-responsive coatings [116], and light-responsive surfaces [48] can better adapt to different biological status and may accomplish better and faster both prevention and treatment clinical stages of dental implants therapy. Although these smart surfaces, designed for interface sciences, have a promising future in dental implant applications, their mechanical stability, corrosion/wear behavior, and biological properties have rarely been tested or disclosed. However, we believe that such advances are possible because of the variety of methods available for modifying the Ti substrate and the wide array of strategies used to build it, as shown here.

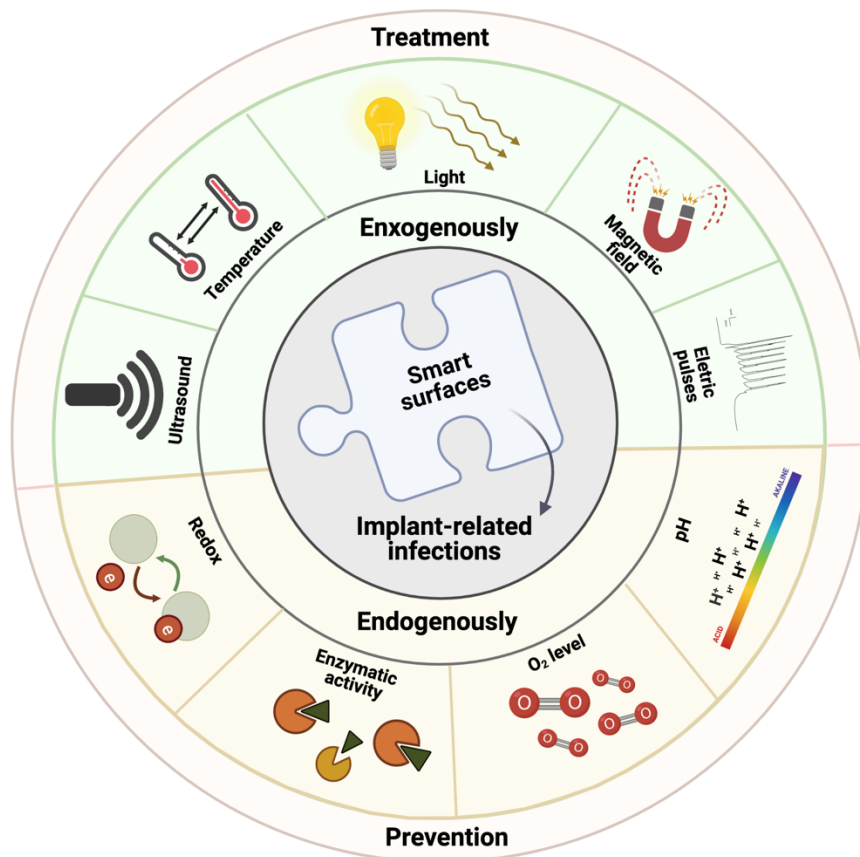


Fig. 9. *Fitting pieces into the puzzle:* Overview of emergent smart surfaces and their mechanisms to improve implant-related infection management. Created with BioRender.com (Licence number: KS22ZBDZ12).

5. Concluding remarks and future perspectives

Emerging implant surface modifications and coatings have been proposed to hold great promise for enhancing Ti-based dental implant survival. Some pieces of the “big puzzle” of implant infections have been added over the years with progress in deposition technologies to create antimicrobial surfaces for preventing implant-related infections. Nevertheless, there is no consensus regarding the best available Ti surface for reduced oral bacterial accumulation and the prevention of microbial infections. While additional well-defined studies are necessary to further elucidate the effects of Ti surfaces, several future perspectives could be identified from the present review. Notably, many antibacterial surfaces often have their potential well-demonstrated in pre-clinical studies. However,

the real weakness of the process lies in the methodological issues, which are crucial for clinical translatability. Self-regulating and smart surfaces activated by biological stimuli have been recently investigated as possible ways to overcome the current limitations of implant surfaces. Finally, we may not yet have “*all the pieces of the puzzle*”, and we certainly need to learn much more about how to assemble them in future studies to produce cutting-edge applications in dentistry. However, we have established that smart-release or on-demand activation coatings can help solve the “*puzzle*” issues, as long as the correct models and primary outcomes are considered to generate insights for clinical studies.

Conflict of interest: The authors declare that the research was conducted in the absence of any commercial or financial relationships that could be construed as a potential conflict of interest.

Acknowledgments: This study was funded by São Paulo Research Foundation (FAPESP) grant number 2020/10436-4 and Coordenação de Aperfeiçoamento de Pessoal de Nível Superior (Grant/Award Number: 001) to R.C.C., and Conselho Nacional de Desenvolvimento Científico e Tecnológico (CNPq) grant number 304853/2018-6 and São Paulo Research Foundation (FAPESP) grant number 2020/05231-4 to V.A.R.B. Graphical abstract and figures were designed using the web interface BioRender[®].

Authors contribution: Conceptualization: J.G.S.S.; Methodology: R.C.C., B.E.N. and J.G.S.S.; Investigation: B.E.C.O., A.A.S., R.C.C. and B.E.N.; Writing-Original Draft: R.C.C.; Writing-Review & Editing: M.B., J.A.S., M.F., V.A.R.B., J.G.S.S., B.R.V.; Supervision: V.A.R.B., J.G.S.S.; Funding acquisition: V.A.R.B.

8. References

- [1] Spriano S, Yamaguchi S, Bairo F, Ferraris S. A critical review of multifunctional titanium surfaces: New frontiers for improving osseointegration and host response, avoiding bacteria contamination. *Acta Biomater* 2018;79:1–22. <https://doi.org/10.1016/j.actbio.2018.08.013>.
- [2] Lang NP, Brägger U, Walther D, Beamer B, Kornman KS. Ligature-induced peri-implant infection in cynomolgus monkeys. I. Clinical and radiographic findings. *Clin Oral Implants Res* 1993;4:2–11. <https://doi.org/10.1034/j.1600-0501.1993.040101.x>.
- [3] Marsh PD, Moter A, Devine DA. Dental plaque biofilms: communities, conflict and control. *Periodontol* 2000 2011;55:16–35. <https://doi.org/10.1111/j.1600-0757.2009.00339.x>.

- [4] Costa RC, Abdo VL, Mendes PHC, Mota-Veloso I, Bertolini M, Mathew MT, et al. Microbial Corrosion in Titanium-Based Dental Implants: How Tiny Bacteria Can Create a Big Problem? *J Bio Tribo Corros* 2021;7:136. <https://doi.org/10.1007/s40735-021-00575-8>.
- [5] Schwarz F, Derks J, Monje A, Wang H-L. Peri-implantitis. *J Clin Periodontol* 2018;45 Suppl 20:S246–66. <https://doi.org/10.1111/jcpe.12954>.
- [6] Belibasakis GN, Manoil D. Microbial Community-Driven Etiopathogenesis of Peri-Implantitis. *J Dent Res* 2021;100:21–8. <https://doi.org/10.1177/0022034520949851>.
- [7] Kotsakis GA, Olmedo DG. Peri-implantitis is not periodontitis: Scientific discoveries shed light on microbiome-biomaterial interactions that may determine disease phenotype. *Periodontol* 2000 2021. <https://doi.org/10.1111/prd.12372>.
- [8] Lee C-T, Huang Y-W, Zhu L, Weltman R. Prevalences of peri-implantitis and peri-implant mucositis: systematic review and meta-analysis. *J Dent* 2017;62:1–12. <https://doi.org/10.1016/j.jdent.2017.04.011>.
- [9] Chourifa H, Bouloussa H, Migonney V, Falentin-Daudré C. Review of titanium surface modification techniques and coatings for antibacterial applications. *Acta Biomater* 2019;83:37–54. <https://doi.org/10.1016/j.actbio.2018.10.036>.
- [10] Teughels W, Van Assche N, Sliepen I, Quirynen M. Effect of material characteristics and/or surface topography on biofilm development. *Clin Oral Implants Res* 2006;17 Suppl 2:68–81. <https://doi.org/10.1111/j.1600-0501.2006.01353.x>.
- [11] Souza JCM, Sordi MB, Kanazawa M, Ravindran S, Henriques B, Silva FS, et al. Nano-scale modification of titanium implant surfaces to enhance osseointegration. *Acta Biomater* 2019;94:112–31. <https://doi.org/10.1016/j.actbio.2019.05.045>.
- [12] Xue T, Attarilar S, Liu S, Liu J, Song X, Li L, et al. Surface Modification Techniques of Titanium and its Alloys to Functionally Optimize Their Biomedical Properties: Thematic Review. *Front Bioeng Biotechnol* 2020;8:603072. <https://doi.org/10.3389/fbioe.2020.603072>.
- [13] Costa RC, Souza JGS, Cordeiro JM, Bertolini M, de Avila ED, Landers R, et al. Synthesis of bioactive glass-based coating by plasma electrolytic oxidation: Untangling a new deposition pathway toward titanium implant surfaces. *Journal of Colloid and Interface Science* 2020;579:680–98. <https://doi.org/10.1016/j.jcis.2020.06.102>.
- [14] Liu J, Liu J, Attarilar S, Wang C, Tamaddon M, Yang C, et al. Nano-Modified Titanium Implant Materials: A Way Toward Improved Antibacterial Properties. *Front Bioeng Biotechnol* 2020;8:576969. <https://doi.org/10.3389/fbioe.2020.576969>.
- [15] Linklater DP, Baulin VA, Juodkazis S, Crawford RJ, Stoodley P, Ivanova EP. Mechano-bactericidal actions of nanostructured surfaces. *Nat Rev Microbiol* 2021;19:8–22. <https://doi.org/10.1038/s41579-020-0414-z>.
- [16] Souza JGS, Bertolini MM, Costa RC, Nagay BE, Dongari-Bagtzoglou A, Barão VAR. Targeting implant-associated infections: titanium surface loaded with antimicrobial. *IScience* 2021;24:102008. <https://doi.org/10.1016/j.isci.2020.102008>.
- [17] Nadimpalli ML, Chan CW, Doron S. Antibiotic resistance: a call to action to prevent the next epidemic of inequality. *Nat Med* 2021;27:187–8. <https://doi.org/10.1038/s41591-020-01201-9>.
- [18] Derks J, Tomasi C. Peri-implant health and disease. A systematic review of current epidemiology. *J Clin Periodontol* 2015;42 Suppl 16:S158-171. <https://doi.org/10.1111/jcpe.12334>.
- [19] Listl S, Frühauf N, Dannewitz B, Weis C, Tu Y-K, Chang H-J, et al. Cost-effectiveness of non-surgical peri-implantitis treatments. *J Clin Periodontol* 2015;42:470–7. <https://doi.org/10.1111/jcpe.12402>.
- [20] Salvi GE, Cosgarea R, Sculean A. Prevalence and Mechanisms of Peri-implant Diseases. *J Dent Res* 2017;96:31–7. <https://doi.org/10.1177/0022034516667484>.
- [21] Bürgers R, Gerlach T, Hahnel S, Schwarz F, Handel G, Gosau M. In vivo and in vitro biofilm formation on two different titanium implant surfaces. *Clin Oral Implants Res* 2010;21:156–64.

<https://doi.org/10.1111/j.1600-0501.2009.01815.x>.

[22] Bowen WH, Burne RA, Wu H, Koo H. Oral Biofilms: Pathogens, Matrix, and Polymicrobial Interactions in Microenvironments. *Trends in Microbiology* 2018;26:229–42. <https://doi.org/10.1016/j.tim.2017.09.008>.

[23] Costerton JW, Stewart PS, Greenberg EP. Bacterial Biofilms: A Common Cause of Persistent Infections. *Science* 1999;284:1318–22. <https://doi.org/10.1126/science.284.5418.1318>.

[24] Koo H, Falsetta ML, Klein MI. The exopolysaccharide matrix: a virulence determinant of cariogenic biofilm. *J Dent Res* 2013;92:1065–73. <https://doi.org/10.1177/0022034513504218>.

[25] Karygianni L, Ren Z, Koo H, Thurnheer T. Biofilm Matrixome: Extracellular Components in Structured Microbial Communities. *Trends Microbiol* 2020;28:668–81. <https://doi.org/10.1016/j.tim.2020.03.016>.

[26] Flemming H-C, Wingender J, Szewzyk U, Steinberg P, Rice SA, Kjelleberg S. Biofilms: an emergent form of bacterial life. *Nature Reviews Microbiology* 2016;14:563–75. <https://doi.org/10.1038/nrmicro.2016.94>.

[27] Jamal M, Ahmad W, Andleeb S, Jalil F, Imran M, Nawaz MA, et al. Bacterial biofilm and associated infections. *Journal of the Chinese Medical Association* 2018;81:7–11. <https://doi.org/10.1016/j.jcma.2017.07.012>.

[28] Muhammad MH, Idris AL, Fan X, Guo Y, Yu Y, Jin X, et al. Beyond Risk: Bacterial Biofilms and Their Regulating Approaches. *Front Microbiol* 2020;11. <https://doi.org/10.3389/fmicb.2020.00928>.

[29] Mombelli A, Décaillot F. The characteristics of biofilms in peri-implant disease. *J Clin Periodontol* 2011;38 Suppl 11:203–13. <https://doi.org/10.1111/j.1600-051X.2010.01666.x>.

[30] Kolenbrander PE, Palmer RJ, Rickard AH, Jakubovics NS, Chalmers NI, Diaz PI. Bacterial interactions and successions during plaque development. *Periodontol* 2000 2006;42:47–79. <https://doi.org/10.1111/j.1600-0757.2006.00187.x>.

[31] Rosier BT, Marsh PD, Mira A. Resilience of the Oral Microbiota in Health: Mechanisms That Prevent Dysbiosis. *J Dent Res* 2018;97:371–80. <https://doi.org/10.1177/0022034517742139>.

[32] Serino G, Ström C. Peri-implantitis in partially edentulous patients: association with inadequate plaque control. *Clin Oral Implants Res* 2009;20:169–74. <https://doi.org/10.1111/j.1600-0501.2008.01627.x>.

[33] Frisch E, Ziebolz D, Vach K, Ratka-Krüger P. Supportive post-implant therapy: patient compliance rates and impacting factors: 3-year follow-up. *J Clin Periodontol* 2014;41:1007–14. <https://doi.org/10.1111/jcpe.12298>.

[34] Souza JGS, Cury JA, Filho APR, Feres M, Faveri M de, Barão VAR. Effect of sucrose on biofilm formed in situ on titanium material. *Journal of Periodontology* 2019;90:141–8. <https://doi.org/10.1002/JPER.18-0219>.

[35] Souza JGS, Costa Oliveira BE, Bertolini M, Lima CV, Retamal-Valdes B, de Faveri M, et al. Titanium particles and ions favor dysbiosis in oral biofilms. *J Periodont Res* 2020;55:258–66. <https://doi.org/10.1111/jre.12711>.

[36] Costa RC, Souza JGS, Bertolini M, Retamal-Valdes B, Feres M, Barão VAR. Extracellular biofilm matrix leads to microbial dysbiosis and reduces biofilm susceptibility to antimicrobials on titanium biomaterial: An in vitro and in situ study. *Clinical Oral Implants Research* 2020;31:1173–86. <https://doi.org/10.1111/clr.13663>.

[37] Corrêa MG, Pimentel SP, Ribeiro FV, Cirano FR, Casati MZ, Corrêa MG, et al. Host response and peri-implantitis. *Brazilian Oral Research* 2019;33. <https://doi.org/10.1590/1807-3107bor-2019.vol33.0066>.

[38] Berglundh T, Armitage G, Araujo MG, Avila-Ortiz G, Blanco J, Camargo PM, et al. Peri-implant diseases and conditions: Consensus report of workgroup 4 of the 2017 World Workshop on the Classification of Periodontal and Peri-Implant Diseases and Conditions. *Journal of Clinical Periodontology* 2018;45:S286–91. <https://doi.org/10.1111/jcpe.12957>.

[39] Figuero E, Graziani F, Sanz I, Herrera D, Sanz M. Management of peri-implant mucositis and peri-

implantitis. *Periodontol* 2000 2014;66:255–73. <https://doi.org/10.1111/prd.12049>.

[40] Arciola CR, Campoccia D, Montanaro L. Implant infections: adhesion, biofilm formation and immune evasion. *Nature Reviews Microbiology* 2018;16:397–409. <https://doi.org/10.1038/s41579-018-0019-y>.

[41] Heitz-Mayfield LJA, Mombelli A. The therapy of peri-implantitis: a systematic review. *Int J Oral Maxillofac Implants* 2014;29 Suppl:325–45. <https://doi.org/10.11607/jomi.2014suppl.g5.3>.

[42] Campoccia D, Montanaro L, Arciola CR. A review of the biomaterials technologies for infection-resistant surfaces. *Biomaterials* 2013;34:8533–54. <https://doi.org/10.1016/j.biomaterials.2013.07.089>.

[43] Wang F, Shi L, He W-X, Han D, Yan Y, Niu Z-Y, et al. Bioinspired micro/nano fabrication on dental implant–bone interface. *Applied Surface Science* 2013;265:480–8. <https://doi.org/10.1016/j.apsusc.2012.11.032>.

[44] Song F, Koo H, Ren D. Effects of Material Properties on Bacterial Adhesion and Biofilm Formation. *J Dent Res* 2015;94:1027–34. <https://doi.org/10.1177/0022034515587690>.

[45] Koo H, Allan RN, Howlin RP, Stoodley P, Hall-Stoodley L. Targeting microbial biofilms: current and prospective therapeutic strategies. *Nat Rev Microbiol* 2017;15:740–55. <https://doi.org/10.1038/nrmicro.2017.99>.

[46] Liu J, Liu J, Attarilar S, Wang C, Tamaddon M, Yang C, et al. Nano-Modified Titanium Implant Materials: A Way Toward Improved Antibacterial Properties. *Front Bioeng Biotechnol* 2020;8. <https://doi.org/10.3389/fbioe.2020.576969>.

[47] Alipal J, Mohd Pu'ad NAS, Nayan NHM, Sahari N, Abdullah HZ, Idris MI, et al. An updated review on surface functionalisation of titanium and its alloys for implants applications. *Materials Today: Proceedings* 2021. <https://doi.org/10.1016/j.matpr.2021.01.499>.

[48] Nagay BE, Dini C, Cordeiro JM, Ricomini-Filho AP, de Avila ED, Rangel EC, et al. Visible-Light-Induced Photocatalytic and Antibacterial Activity of TiO₂ Codoped with Nitrogen and Bismuth: New Perspectives to Control Implant-Biofilm-Related Diseases. *ACS Appl Mater Interfaces* 2019;11:18186–202. <https://doi.org/10.1021/acsami.9b03311>.

[49] Yuan Z, Tao B, He Y, Mu C, Liu G, Zhang J, et al. Remote eradication of biofilm on titanium implant via near-infrared light triggered photothermal/photodynamic therapy strategy. *Biomaterials* 2019;223:119479. <https://doi.org/10.1016/j.biomaterials.2019.119479>.

[50] Tillmanns HW, Hermann JS, Tiffée JC, Burgess AV, Meffert RM. Evaluation of three different dental implants in ligature-induced peri-implantitis in the beagle dog. Part II. Histology and microbiology. *Int J Oral Maxillofac Implants* 1998;13:59–68.

[51] Rams TE, Roberts TW, Feik D, Molzan AK, Slots J. Clinical and microbiological findings on newly inserted hydroxyapatite-coated and pure titanium human dental implants. *Clin Oral Implants Res* 1991;2:121–7. <https://doi.org/10.1034/j.1600-0501.1991.020304.x>.

[52] He X, Li Y, Guo J, Xu J, Zu H, Huang L, et al. Biomaterials developed for facilitating healing outcome after anterior cruciate ligament reconstruction: Efficacy, surgical protocols, and assessments using preclinical animal models. *Biomaterials* 2021;269:120625. <https://doi.org/10.1016/j.biomaterials.2020.120625>.

[53] Tataru AM, Shah SR, Livingston CE, Mikos AG. Infected animal models for tissue engineering. *Methods* 2015;84:17–24. <https://doi.org/10.1016/j.ymeth.2015.03.025>.

[54] Hashimoto A, Miyamoto H, Kobatake T, Nakashima T, Shobuike T, Ueno M, et al. The combination of silver-containing hydroxyapatite coating and vancomycin has a synergistic antibacterial effect on methicillin-resistant *Staphylococcus aureus* biofilm formation. *Bone Joint Res* 2020;9:211–8. <https://doi.org/10.1302/2046-3758.95.BJR-2019-0326.R1>.

[55] Zhou J, Li B, Zhao L, Zhang L, Han Y. F-Doped Micropore/Nanorod Hierarchically Patterned Coatings for Improving Antibacterial and Osteogenic Activities of Bone Implants in Bacteria-Infected Cases. *ACS Biomater Sci Eng* 2017;3:1437–50. <https://doi.org/10.1021/acsbiomaterials.6b00710>.

[56] Zhou J, Li B, Han Y. F-doped TiO₂ microporous coating on titanium with enhanced antibacterial and

osteogenic activities. *Sci Rep* 2018;8:17858. <https://doi.org/10.1038/s41598-018-35875-6>.

[57] Souza JGS, Tenuta LMA, Del Bel Cury AA, Nóbrega DF, Budin RR, de Queiroz MX, et al. Calcium Prerinse before Fluoride Rinse Reduces Enamel Demineralization: An in situ Caries Study. *Caries Res* 2016;50:372–7. <https://doi.org/10.1159/000446407>.

[58] Al-Ahmad A, Wiedmann-Al-Ahmad M, Fackler A, Follo M, Hellwig E, Bächle M, et al. In vivo study of the initial bacterial adhesion on different implant materials. *Arch Oral Biol* 2013;58:1139–47. <https://doi.org/10.1016/j.archoralbio.2013.04.011>.

[59] de Freitas MM, da Silva CHP, Groisman M, Vidigal GM. Comparative analysis of microorganism species succession on three implant surfaces with different roughness: an in vivo study. *Implant Dent* 2011;20:e14-23. <https://doi.org/10.1097/ID.0b013e31820fb99e>.

[60] Elter C, Heuer W, Demling A, Hannig M, Heidenblut T, Bach F-W, et al. Supra- and subgingival biofilm formation on implant abutments with different surface characteristics. *Int J Oral Maxillofac Implants* 2008;23:327–34.

[61] Vroom MG, Sipos P, de Lange GL, Gründemann LJMM, Timmerman MF, Loos BG, et al. Effect of surface topography of screw-shaped titanium implants in humans on clinical and radiographic parameters: a 12-year prospective study. *Clin Oral Implants Res* 2009;20:1231–9. <https://doi.org/10.1111/j.1600-0501.2009.01768.x>.

[62] Shao J, Kolwijck E, Jansen JA, Yang F, Walboomers XF. Animal models for percutaneous-device-related infections: a review. *Int J Antimicrob Agents* 2017;49:659–67. <https://doi.org/10.1016/j.ijantimicag.2017.01.022>.

[63] Zhang Y, Cheng X, Jansen JA, Yang F, van den Beucken JJJP. Titanium surfaces characteristics modulate macrophage polarization. *Materials Science and Engineering: C* 2019;95:143–51. <https://doi.org/10.1016/j.msec.2018.10.065>.

[64] Elias CN, Oshida Y, Lima JHC, Muller CA. Relationship between surface properties (roughness, wettability and morphology) of titanium and dental implant removal torque. *J Mech Behav Biomed Mater* 2008;1:234–42. <https://doi.org/10.1016/j.jmbbm.2007.12.002>.

[65] Stafford GL. Review found little difference between sandblasted and acid-etched (SLA) dental implants and modified surface (SLActive) implants. *Evidence-Based Dentistry* 2014;15:87–8. <https://doi.org/10.1038/sj.ebd.6401047>.

[66] Hong L, Liu X, Tan L, Cui Z, Yang X, Liang Y, et al. Rapid Biofilm Elimination on Bone Implants Using Near-Infrared-Activated Inorganic Semiconductor Heterostructures. *Adv Healthc Mater* 2019;8:e1900835. <https://doi.org/10.1002/adhm.201900835>.

[67] Hong L, Liu X, Tan L, Cui Z, Yang X, Liang Y, et al. Rapid Biofilm Elimination on Bone Implants Using Near-Infrared-Activated Inorganic Semiconductor Heterostructures. *Advanced Healthcare Materials* 2019;8:1900835. <https://doi.org/10.1002/adhm.201900835>.

[68] Yuan Z, Tao B, He Y, Liu J, Lin C, Shen X, et al. Biocompatible MoS₂/PDA-RGD coating on titanium implant with antibacterial property via intrinsic ROS-independent oxidative stress and NIR irradiation. *Biomaterials* 2019;217:119290. <https://doi.org/10.1016/j.biomaterials.2019.119290>.

[69] Yang Y, Ao H, Wang Y, Lin W, Yang S, Zhang S, et al. Cytocompatibility with osteogenic cells and enhanced in vivo anti-infection potential of quaternized chitosan-loaded titania nanotubes. *Bone Res* 2016;4:1–14. <https://doi.org/10.1038/boneres.2016.27>.

[70] Riool M, Dirks AJ, Jaspers V, de Boer L, Loontjens TJ, van der Loos CM, et al. A chlorhexidine-releasing epoxy-based coating on titanium implants prevents *Staphylococcus aureus* experimental biomaterial-associated infection. *Eur Cell Mater* 2017;33:143–57. <https://doi.org/10.22203/eCM.v033a11>.

[71] Shen J, Gao P, Han S, Kao RYT, Wu S, Liu X, et al. A tailored positively-charged hydrophobic surface reduces the risk of implant associated infections. *Acta Biomaterialia* 2020;114:421–30. <https://doi.org/10.1016/j.actbio.2020.07.040>.

[72] Ye J, Li B, Li M, Zheng Y, Wu S, Han Y. ROS induced bactericidal activity of amorphous Zn-doped

titanium oxide coatings and enhanced osseointegration in bacteria-infected rat tibias. *Acta Biomaterialia* 2020;107:313–24. <https://doi.org/10.1016/j.actbio.2020.02.036>.

[73] Tran PA, O'Brien-Simpson N, Palmer JA, Bock N, Reynolds EC, Webster TJ, et al. Selenium nanoparticles as anti-infective implant coatings for trauma orthopedics against methicillin-resistant *Staphylococcus aureus* and *epidermidis*: in vitro and in vivo assessment. *Int J Nanomedicine* 2019;14:4613–24. <https://doi.org/10.2147/IJN.S197737>.

[74] Song J, Liu H, Lei M, Tan H, Chen Z, Antoshin A, et al. Redox-Channeling Polydopamine-Ferrocene (PDA-Fc) Coating To Confer Context-Dependent and Photothermal Antimicrobial Activities. *ACS Appl Mater Interfaces* 2020;12:8915–28. <https://doi.org/10.1021/acsami.9b22339>.

[75] Yang X, Zhang D, Liu G, Wang J, Luo Z, Peng X, et al. Bioinspired from mussel and salivary acquired pellicle: a universal dual-functional polypeptide coating for implant materials. *Materials Today Chemistry* 2019;14:100205. <https://doi.org/10.1016/j.mtchem.2019.100205>.

[76] Akiyama T, Miyamoto H, Yonekura Y, Tsukamoto M, Ando Y, Noda I, et al. Silver oxide-containing hydroxyapatite coating has in vivo antibacterial activity in the rat tibia. *J Orthop Res* 2013;31:1195–200. <https://doi.org/10.1002/jor.22357>.

[77] Shen X, Zhang Y, Ma P, Sutrisno L, Luo Z, Hu Y, et al. Fabrication of magnesium/zinc-metal organic framework on titanium implants to inhibit bacterial infection and promote bone regeneration. *Biomaterials* 2019;212:1–16. <https://doi.org/10.1016/j.biomaterials.2019.05.008>.

[78] Zeng J, Wang Y, Sun Z, Chang H, Cao M, Zhao J, et al. A novel biocompatible PDA/IR820/DAP coating for antibiotic/photodynamic/photothermal triple therapy to inhibit and eliminate *Staphylococcus aureus* biofilm. *Chemical Engineering Journal* 2020;394:125017. <https://doi.org/10.1016/j.ccej.2020.125017>.

[79] Li M, Li L, Su K, Liu X, Zhang T, Liang Y, et al. Highly Effective and Noninvasive Near-Infrared Eradication of a *Staphylococcus aureus* Biofilm on Implants by a Photoresponsive Coating within 20 Min. *Advanced Science* 2019;6:1900599. <https://doi.org/10.1002/advs.201900599>.

[80] Yang C, Li J, Zhu C, Zhang Q, Yu J, Wang J, et al. Advanced antibacterial activity of biocompatible tantalum nanofilm via enhanced local innate immunity. *Acta Biomater* 2019;89:403–18. <https://doi.org/10.1016/j.actbio.2019.03.027>.

[81] Badar M, Rahim MI, Kieke M, Ebel T, Rohde M, Hauser H, et al. Controlled drug release from antibiotic-loaded layered double hydroxide coatings on porous titanium implants in a mouse model. *J Biomed Mater Res A* 2015;103:2141–9. <https://doi.org/10.1002/jbm.a.35358>.

[82] Su K, Tan L, Liu X, Cui Z, Zheng Y, Li B, et al. Rapid Photo-Sonotherapy for Clinical Treatment of Bacterial Infected Bone Implants by Creating Oxygen Deficiency Using Sulfur Doping. *ACS Nano* 2020;14:2077–89. <https://doi.org/10.1021/acs.nano.9b08686>.

[83] Janson O, Sørensen JH, Strømme M, Engqvist H, Procter P, Welch K. Evaluation of an alkali-treated and hydroxyapatite-coated orthopedic implant loaded with tobramycin. *J Biomater Appl* 2019;34:699–720. <https://doi.org/10.1177/0885328219867968>.

[84] Ao H, Yang S, Nie B, Fan Q, Zhang Q, Zong J, et al. Improved antibacterial properties of collagen I/hyaluronic acid/quaternized chitosan multilayer modified titanium coatings with both contact-killing and release-killing functions. *J Mater Chem B* 2019;7:1951–61. <https://doi.org/10.1039/C8TB02425A>.

[85] Ma M, Liu X, Tan L, Cui Z, Yang X, Liang Y, et al. Enhancing the antibacterial efficacy of low-dose gentamicin with 5 minute assistance of phototherapy at 50 °C. *Biomater Sci* 2019;7:1437–47. <https://doi.org/10.1039/c8bm01539b>.

[86] Zhang E, Zhao X, Hu J, Wang R, Fu S, Qin G. Antibacterial metals and alloys for potential biomedical implants. *Bioactive Materials* 2021;6:2569–612. <https://doi.org/10.1016/j.bioactmat.2021.01.030>.

[87] Alqahtani MS, Kazi M, Alsenaidy MA, Ahmad MZ. Advances in Oral Drug Delivery. *Front Pharmacol* 2021;12:618411. <https://doi.org/10.3389/fphar.2021.618411>.

[88] Jennings JA, Beenken KE, Skinner RA, Meeker DG, Smeltzer MS, Haggard WO, et al. Antibiotic-loaded phosphatidylcholine inhibits staphylococcal bone infection. *World J Orthop* 2016;7:467–74.

<https://doi.org/10.5312/wjo.v7.i8.467>.

[89] Zaugg LK, Astasov-Frauenhoffer M, Braissant O, Hauser-Gerspach I, Waltimo T, Zitzmann NU. Determinants of biofilm formation and cleanliness of titanium surfaces. *Clin Oral Implants Res* 2017;28:469–75. <https://doi.org/10.1111/clr.12821>.

[90] Nicu EA, Van Assche N, Coucke W, Teughels W, Quirynen M. RCT comparing implants with turned and anodically oxidized surfaces: a pilot study, a 3-year follow-up. *J Clin Periodontol* 2012;39:1183–90. <https://doi.org/10.1111/jcpe.12022>.

[91] Morris HF, Ochi S, Spray JR, Olson JW. Periodontal-type measurements associated with hydroxyapatite-coated and non-HA-coated implants: uncovering to 36 months. *Ann Periodontol* 2000;5:56–67. <https://doi.org/10.1902/annals.2000.5.1.56>.

[92] Carinci F, Lauritano D, Bignozzi CA, Pazzi D, Candotto V, Santos de Oliveira P, et al. A New Strategy Against Peri-Implantitis: Antibacterial Internal Coating. *Int J Mol Sci* 2019;20. <https://doi.org/10.3390/ijms20163897>.

[93] Odatsu T, Kuroshima S, Sato M, Takase K, Valanezhad A, Naito M, et al. Antibacterial Properties of Nano-Ag Coating on Healing Abutment: An In Vitro and Clinical Study. *Antibiotics (Basel)* 2020;9. <https://doi.org/10.3390/antibiotics9060347>.

[94] Cucchi A, Molè F, Rinaldi L, Marchetti C, Corinaldesi G. The Efficacy of an Anatase-Coated Collar Surface in Inhibiting the Bacterial Colonization of Oral Implants: A Pilot Prospective Study in Humans. *Int J Oral Maxillofac Implants* 2018;33:395–404. <https://doi.org/10.11607/jomi.5880>.

[95] Shibli JA, Melo L, Ferrari DS, Figueiredo LC, Faveri M, Feres M. Composition of supra- and subgingival biofilm of subjects with healthy and diseased implants. *Clin Oral Implants Res* 2008;19:975–82. <https://doi.org/10.1111/j.1600-0501.2008.01566.x>.

[96] An YH, Friedman RJ. Animal Models of Orthopedic Implant Infection. *Journal of Investigative Surgery* 2009. <https://doi.org/10.3109/08941939809032193>.

[97] Holt J, Hertzberg B, Weinhold P, Storm W, Schoenfisch M, Dahners L. Decreasing bacterial colonization of external fixation pins through nitric oxide release coatings. *J Orthop Trauma* 2011;25:432–7. <https://doi.org/10.1097/BOT.0b013e3181f9ac8a>.

[98] Huang B, Tan L, Liu X, Li J, Wu S. A facile fabrication of novel stuff with antibacterial property and osteogenic promotion utilizing red phosphorus and near-infrared light. *Bioactive Materials* 2019;4:17–21. <https://doi.org/10.1016/j.bioactmat.2018.11.002>.

[99] Ghimire A, Skelly JD, Song J. Micrococcal-Nuclease-Triggered On-Demand Release of Vancomycin from Intramedullary Implant Coating Eradicates *Staphylococcus aureus* Infection in Mouse Femoral Canals. *ACS Cent Sci* 2019;5:1929–36. <https://doi.org/10.1021/acscentsci.9b00870>.

[100] Makvandi P, Josic U, Delfi M, Pinelli F, Jahed V, Kaya E, et al. Drug Delivery (Nano)Platforms for Oral and Dental Applications: Tissue Regeneration, Infection Control, and Cancer Management. *Advanced Science* n.d.;n/a:2004014. <https://doi.org/10.1002/advs.202004014>.

[101] Kantarci A, Hasturk H, Van Dyke TE. Animal models for periodontal regeneration and peri-implant responses. *Periodontol* 2000 2015;68:66–82. <https://doi.org/10.1111/prd.12052>.

[102] Elliott DR, Wilson M, Buckley CMF, Spratt DA. Cultivable oral microbiota of domestic dogs. *J Clin Microbiol* 2005;43:5470–6. <https://doi.org/10.1128/JCM.43.11.5470-5476.2005>.

[103] Bebartha V, Luyten D, Heard K. Emergency medicine animal research: does use of randomization and blinding affect the results? *Acad Emerg Med* 2003;10:684–7. <https://doi.org/10.1111/j.1553-2712.2003.tb00056.x>.

[104] Perel P, Roberts I, Sena E, Wheble P, Briscoe C, Sandercock P, et al. Comparison of treatment effects between animal experiments and clinical trials: systematic review. *BMJ* 2007;334:197. <https://doi.org/10.1136/bmj.39048.407928.BE>.

[105] Gu H, Lee SW, Carnicelli J, Zhang T, Ren D. Magnetically driven active topography for long-term

biofilm control. *Nature Communications* 2020;11:2211. <https://doi.org/10.1038/s41467-020-16055-5>.

[106] Tian J, Feng H, Yan L, Yu M, Ouyang H, Li H, et al. A self-powered sterilization system with both instant and sustainable anti-bacterial ability. *Nano Energy* 2017;36:241–9. <https://doi.org/10.1016/j.nanoen.2017.04.030>.

[107] Wang G, Jin W, Qasim AM, Gao A, Peng X, Li W, et al. Antibacterial effects of titanium embedded with silver nanoparticles based on electron-transfer-induced reactive oxygen species. *Biomaterials* 2017;124:25–34. <https://doi.org/10.1016/j.biomaterials.2017.01.028>.

[108] Souza JGS, Bertolini M, Costa RC, Cordeiro JM, Nagay BE, de Almeida AB, et al. Targeting Pathogenic Biofilms: Newly Developed Superhydrophobic Coating Favors a Host-Compatible Microbial Profile on the Titanium Surface. *ACS Appl Mater Interfaces* 2020;12:10118–29. <https://doi.org/10.1021/acsami.9b22741>.

[109] Skorb EV, Andreeva DV. Surface Nanoarchitecture for Bio-Applications: Self-Regulating Intelligent Interfaces. *Advanced Functional Materials* 2013;23:4483–506. <https://doi.org/10.1002/adfm.201203884>.

[110] Sun T, Qing G. Biomimetic Smart Interface Materials for Biological Applications. *Advanced Materials* 2011;23:H57–77. <https://doi.org/10.1002/adma.201004326>.

[111] de Avila ED, van Oirschot BA, van den Beucken JJJP. Biomaterial-based possibilities for managing peri-implantitis. *J Periodontol Res* 2020;55:165–73. <https://doi.org/10.1111/jre.12707>.

[112] Li X, Wu B, Chen H, Nan K, Jin Y, Sun L, et al. Recent developments in smart antibacterial surfaces to inhibit biofilm formation and bacterial infections. *J Mater Chem B* 2018;6:4274–92. <https://doi.org/10.1039/C8TB01245H>.

[113] Kanamala M, Wilson WR, Yang M, Palmer BD, Wu Z. Mechanisms and biomaterials in pH-responsive tumour targeted drug delivery: A review. *Biomaterials* 2016;85:152–67. <https://doi.org/10.1016/j.biomaterials.2016.01.061>.

[114] Chen J, Shi X, Zhu Y, Chen Y, Gao M, Gao H, et al. On-demand storage and release of antimicrobial peptides using Pandora's box-like nanotubes gated with a bacterial infection-responsive polymer. *Theranostics* 2020;10:109–22. <https://doi.org/10.7150/thno.38388>.

[115] Wei T, Yu Q, Zhan W, Chen H. A Smart Antibacterial Surface for the On-Demand Killing and Releasing of Bacteria. *Advanced Healthcare Materials* 2016;5:449–56. <https://doi.org/10.1002/adhm.201500700>.

[116] Wang B, Xu Q, Ye Z, Liu H, Lin Q, Nan K, et al. Copolymer Brushes with Temperature-Triggered, Reversibly Switchable Bactericidal and Antifouling Properties for Biomaterial Surfaces. *ACS Appl Mater Interfaces* 2016;8:27207–17. <https://doi.org/10.1021/acsami.6b08893>.

[117] Inoue D, Kabata T, Ohtani K, Kajino Y, Shirai T, Tsuchiya H. Inhibition of biofilm formation on iodine-supported titanium implants. *Int Orthop* 2017;41:1093–9. <https://doi.org/10.1007/s00264-017-3477-3>.

[118] Oka Y, Kim W-C, Yoshida T, Hirashima T, Mouri H, Urade H, et al. Efficacy of titanium dioxide photocatalyst for inhibition of bacterial colonization on percutaneous implants. *J Biomed Mater Res B Appl Biomater* 2008;86:530–40. <https://doi.org/10.1002/jbm.b.31053>.

[119] Oosterbos CJM, Vogely HC, Nijhof MW, Fler A, Verbout AJ, Tonino AJ, et al. Osseointegration of hydroxyapatite-coated and noncoated Ti6Al4V implants in the presence of local infection: a comparative histomorphometrical study in rabbits. *J Biomed Mater Res* 2002;60:339–47. <https://doi.org/10.1002/jbm.1288>.

[120] Ravanetti F, Chiesa R, Ossiprandi MC, Gazza F, Farina V, Martini FM, et al. Osteogenic response and osteoprotective effects in vivo of a nanostructured titanium surface with antibacterial properties. *J Mater Sci Mater Med* 2016;27:52. <https://doi.org/10.1007/s10856-015-5661-6>.

[121] Shimazaki T, Miyamoto H, Ando Y, Noda I, Yonekura Y, Kawano S, et al. In vivo antibacterial and silver-releasing properties of novel thermal sprayed silver-containing hydroxyapatite coating. *J Biomed Mater Res B Appl Biomater* 2010;92:386–9. <https://doi.org/10.1002/jbm.b.31526>.

[122] Croes M, Bakhshandeh S, van Hengel I a. J, Lietaert K, van Kessel KPM, Pouran B, et al. Antibacterial

and immunogenic behavior of silver coatings on additively manufactured porous titanium. *Acta Biomater* 2018;81:315–27. <https://doi.org/10.1016/j.actbio.2018.09.051>.

[123] Vogely HC, Oosterbos CJ, Puts EW, Nijhof MW, Nikkels PG, Fleeer A, et al. Effects of hydroxyapatite coating on Ti-6Al-4V implant-site infection in a rabbit tibial model. *J Orthop Res* 2000;18:485–93. <https://doi.org/10.1002/jor.1100180323>.

[124] Moojen DJF, Vogely HC, Fleeer A, Nikkels PGJ, Higham PA, Verbout AJ, et al. Prophylaxis of infection and effects on osseointegration using a tobramycin-periapatite coating on titanium implants--an experimental study in the rabbit. *J Orthop Res* 2009;27:710–6. <https://doi.org/10.1002/jor.20808>.

[125] Williams DL, Epperson RT, Ashton NN, Taylor NB, Kawaguchi B, Olsen RE, et al. In vivo analysis of a first-in-class tri-alkyl norspermidine-biaryl antibiotic in an active release coating to reduce the risk of implant-related infection. *Acta Biomater* 2019;93:36–49. <https://doi.org/10.1016/j.actbio.2019.01.055>.

[126] Xie K, Zhou Z, Guo Y, Wang L, Li G, Zhao S, et al. Long-Term Prevention of Bacterial Infection and Enhanced Osteoinductivity of a Hybrid Coating with Selective Silver Toxicity. *Advanced Healthcare Materials* 2019;8:1801465. <https://doi.org/10.1002/adhm.201801465>.

[127] Xu M, Song Q, Gao L, Liu H, Feng W, Huo J, et al. Single-step fabrication of catechol-ε-poly-L-lysine antimicrobial paint that prevents superbug infection and promotes osteoconductivity of titanium implants. *Chemical Engineering Journal* 2020;396:125240. <https://doi.org/10.1016/j.cej.2020.125240>.

[128] Lovati AB, Bottagisio M, Maraldi S, Violatto MB, Bortolin M, De Vecchi E, et al. Vitamin E Phosphate Coating Stimulates Bone Deposition in Implant-related Infections in a Rat Model. *Clin Orthop Relat Res* 2018;476:1324–38. <https://doi.org/10.1097/01.blo.0000534692.41467.02>.

[129] Gao Q, Feng T, Huang D, Liu P, Lin P, Wu Y, et al. Antibacterial and hydroxyapatite-forming coating for biomedical implants based on polypeptide-functionalized titania nanospikes. *Biomater Sci* 2019;8:278–89. <https://doi.org/10.1039/C9BM01396B>.

[130] Zhou L, Liu Q, Zhou Z, Lu W, Tao J. Efficacy of tobramycin-loaded coating K-wire in an open-fracture rabbit model contaminated by staphylococcus aureus n.d.:13.

[131] Thompson K, Petkov S, Zeiter S, Sprecher CM, Richards RG, Moriarty TF, et al. Intraoperative loading of calcium phosphate-coated implants with gentamicin prevents experimental *Staphylococcus aureus* infection in vivo. *PLoS One* 2019;14:e0210402. <https://doi.org/10.1371/journal.pone.0210402>.

[132] Chen R, Willcox MDP, Ho KKK, Smyth D, Kumar N. Antimicrobial peptide melimine coating for titanium and its in vivo antibacterial activity in rodent subcutaneous infection models. *Biomaterials* 2016;85:142–51. <https://doi.org/10.1016/j.biomaterials.2016.01.063>.

[133] Perni S, Alotaibi HF, Yergeshov AA, Dang T, Abdullin TI, Prokopovich P. Long acting anti-infection constructs on titanium. *Journal of Controlled Release* 2020;326:91–105. <https://doi.org/10.1016/j.jconrel.2020.06.013>.

[134] Liu D, He C, Liu Z, Xu W. Gentamicin coating of nanotubular anodized titanium implant reduces implant-related osteomyelitis and enhances bone biocompatibility in rabbits. *Int J Nanomedicine* 2017;12:5461–71. <https://doi.org/10.2147/IJN.S137137>.

[135] Yuan Z, Huang S, Lan S, Xiong H, Tao B, Ding Y, et al. Surface engineering of titanium implants with enzyme-triggered antibacterial properties and enhanced osseointegration in vivo. *J Mater Chem B* 2018;6:8090–104. <https://doi.org/10.1039/C8TB01918E>.

[136] Secinti KD, Özalp H, Attar A, Sargon MF. Nanoparticle silver ion coatings inhibit biofilm formation on titanium implants. *J Clin Neurosci* 2011;18:391–5. <https://doi.org/10.1016/j.jocn.2010.06.022>.

[137] Yang Y, Ao H, Yang S, Wang Y, Lin W, Yu Z, et al. In vivo evaluation of the anti-infection potential of gentamicin-loaded nanotubes on titania implants. *Int J Nanomedicine* 2016;11:2223–34. <https://doi.org/10.2147/IJN.S102752>.

[138] Ofluoğlu AE, Baris S, Aydin M, Günaldı Ö. The Efficacy of The Titanium Oxide-Coated Screws in The Prevention of Implant-Related Infections; an Experimental Animal Study. *Journal of Neurological Sciences* 2014;31:302–9.

- [139] Zhang H, Wang G, Liu P, Tong D, Ding C, Zhang Z, et al. Vancomycin-loaded titanium coatings with an interconnected micro-patterned structure for prophylaxis of infections: an in vivo study. *RSC Adv* 2018;8:9223–31. <https://doi.org/10.1039/C7RA12347G>.
- [140] Areid N, Söderling E, Tanner J, Kangasniemi I, Närhi TO. Early Biofilm Formation on UV Light Activated Nanoporous TiO₂ Surfaces In Vivo. *International Journal of Biomaterials* 2018;2018:e7275617. <https://doi.org/10.1155/2018/7275617>.
- [141] Cochis A, Azzimonti B, Valle CD, Chiesa R, Arciola CR, Rimondini L. Biofilm formation on titanium implants counteracted by grafting gallium and silver ions. *Journal of Biomedical Materials Research Part A* 2015;103:1176–87. <https://doi.org/10.1002/jbm.a.35270>.
- [142] Conserva E, Generali L, Bandieri A, Cavani F, Borghi F, Consolo U. Plaque accumulation on titanium disks with different surface treatments: an in vivo investigation. *Odontology* 2018;106:145–53. <https://doi.org/10.1007/s10266-017-0317-2>.
- [143] Grössner-Schreiber B, Teichmann J, Hannig M, Dörfer C, Wenderoth DF, Ott SJ. Modified implant surfaces show different biofilm compositions under in vivo conditions. *Clin Oral Implants Res* 2009;20:817–26. <https://doi.org/10.1111/j.1600-0501.2009.01729.x>.
- [144] Ferreira Ribeiro C, Cogo-Müller K, Franco GC, Silva-Concílio LR, Sampaio Campos M, de Mello Rode S, et al. Initial oral biofilm formation on titanium implants with different surface treatments: An in vivo study. *Arch Oral Biol* 2016;69:33–9. <https://doi.org/10.1016/j.archoralbio.2016.05.006>.
- [145] Scarano A, Piattelli M, Vrespa G, Caputi S, Piattelli A. Bacterial adhesion on titanium nitride-coated and uncoated implants: an in vivo human study. *J Oral Implantol* 2003;29:80–5. [https://doi.org/10.1563/1548-1336\(2003\)029<0080:BAOTNA>2.3.CO;2](https://doi.org/10.1563/1548-1336(2003)029<0080:BAOTNA>2.3.CO;2).
- [146] Nicu EA, Van Assche N, Coucke W, Teughels W, Quirynen M. RCT comparing implants with turned and anodically oxidized surfaces: a pilot study, a 3-year follow-up. *J Clin Periodontol* 2012;39:1183–90. <https://doi.org/10.1111/jcpe.12022>.

TABLE 1. Summary of implant surface, animal model, and microbiological data from included experimental studies (study ID, type of method; implant surface: surface treatment, deposition technology and antimicrobial; animal: type and infection model; microbiological assessments: quantitative test, bacterial load, p-value, infection rate, and reference).

Study ID	Type of method	Implant surface			Animal Model		Microbiological assessments					Reference
		Deposition technology	Surface treatment	Antimicrobial (concentration)	Type	Microbial infection	Quantitative test	Bacterial load		p-value	Infection rate	
								Control	Experimental			
1	Physical	Plasma treatment	Machined CaP-coated	Fluoride - F (0.05 to 0.30 M)	Rab	<i>S. aureus</i> (ATCC6538)	CFU/implant	C1= 3.0 (± 0.3) $\times 10^5$ C2= 4.3(± 0.3) $\times 10^5$	F1= 4.6 (± 0.4) $\times 10^5$ F6= 0.7(± 0.5) $\times 10^5$ F9= 0.7 (± 0.2) $\times 10^5$	<.01	NR	[56]
2	Physical	Plasma treatment	PEO coating	Zn (8.79; 16.98; 34.08 wt% - for each group)	R	<i>S. aureus</i> (ATCC 25923)	CFU/cm ²	1.8 $\times 10^8$ (± 1.0)	T1 = 1.4 $\times 10^8$ (± 1.2) T2 = 4.4 $\times 10^7$ (± 0.5) T3 = 0	<.01	NR	[72]
3	Physical	Plasma treatment	Anodic oxide film	Iodine (10–12 $\mu\text{g}/\text{cm}^2$)	R	<i>S. aureus</i> (ATCC 25923)	CFU/implant	<u>24h</u> : Ti = 5.6 (± 2.1) $\times 10^3$ Ti-O = 8.4 (± 2.4) $\times 10^3$ <u>48h</u> : Ti= 6.4 (± 2.1) $\times 10^4$ Ti-O = 7.9 (± 2.3) $\times 10^4$ <u>72h</u> :Ti= 2.0 (± 0.6) $\times 10^5$ Ti-O = 2.9 (± 0.6) $\times 10^5$	<u>24h</u> : Ti-I = 1.2 (± 0.7) $\times 10^3$ <u>48h</u> : Ti-I = 8.6 (± 2.6) $\times 10^3$ <u>72h</u> : Ti-I = 5.0 (± 2.1) $\times 10^4$	<u>24 h</u> : <.05 <u>48h</u> : <.05 <u>72h</u> : <.05	NR	[117]
4	Physical	Plasma treatment	Machined	TiO ₂ (NR)	Rab	MRSA (ATCC 43300)	Log CFU	Ti = 6.1 (± 0.5) Ti-UV = 4.1 (± 1.1)	TiO ₂ = 5.5 (± 0.5) TiO ₂ -UV = 1.8 (± 1.4)	<.05	NR	[118]
5	Physical	Plasma treatment	Grit-blasted surface	HA (NR)	Rab	<i>S. aureus</i> (ATCC 10832)	Rolled out on agar plates test	NR	NR	NR	C: 37,5% (6/16) T: 56,2% (9/16)	[119]

6	Physical	Plasma treatment	Acid-etched surface Anodic coating	Gallium (NR)	Rab	<i>S. aureus</i> (ATCC2592)	CFU/mL	<u>1w:</u> C1 = 7.530 (\pm 788) C2 = 7.485 (\pm 761) <u>2w:</u> C1 = 7.560 (\pm 625) C2 = 7.487 (\pm 788)	<u>1w:</u> 5.999 (\pm 788) <u>2w:</u> 7.469 (\pm 734)	NR	NR	[120]
7	Physical	Plasma and hydrothermal treatment	Machined	Fluoride - F (0.05 to 0.45 M)	Rab	<i>S. aureus</i> (ATCC43300)	CFU/implant	3.0 (\pm 0.2) $\times 10^5$	F0 = 3.9 (\pm 0.3) $\times 10^5$ F1 = 3.7 (\pm 0.3) $\times 10^5$ F2 = 1.9 (\pm 0.2) $\times 10^5$ F5 = 0.2 (\pm 0.1) $\times 10^5$ F7 = 0.1 (\pm 0.2) $\times 10^5$	<.01	NR	[55]
8	Physical	Bi ₂ S ₃ = Hydrothermal method Ag ₃ PO ₄ = Stepwise electrostatic adsorption	Machined + NIR Light	Ag (20 days: 35 μ g/L)	R	<i>S. aureus</i> (ATCC 25923)	Antibacterial efficiency (%)	0	94.3%	<.01	NR	[66]
9	Physical	Hydrothermal method (MoS ₂) + vacuum drying process (gentamicin) + spin-assisted chitosan	Machined + NIR light	NR (only report concentration during process: MoS ₂ = 0.04 g; gentamicin = 1 mg/mL)	R	<i>S. aureus</i> (NR)	Antibacterial ratio (%)	<u>1d:</u> NIR-: 0% (\pm 6.14) NIR+: 0.92% (\pm 7.32) <u>3d:</u> NIR-: 70% (\pm 4.91) NIR+: 82.42% (\pm 2.75) <u>7d:</u> NIR-: 81.05% (\pm 3.68) NIR+: 88.22% (\pm 4.58)	<u>1d:</u> NIR-: 60.75% (\pm 4.91) NIR+: 99.15% (\pm 1.83) <u>3d:</u> NIR-: 88.59% (\pm 2.45) NIR+: 99.67% (\pm 0.91) <u>7d:</u> NIR-: 99.42% (\pm 1.23) NIR+: 99.97% (\pm 0.91)	<u>1d:</u> <.001 <u>3d:</u> <.001 (NIR +) <.05 (NIR -) <u>7d:</u> <.05 (NIR +) <.01 (NIR -)	NR	[85]
10	Physical	Hydrothermal	TiO ₂ nanotubes	MoS ₂ (10 mg)	Rab	<i>S. aureus</i> (ATCC 25923)	Log CFU	1.7 $\times 10^5$ (\pm 27.9)	5.5 $\times 10^3$ (\pm 11)	NR	NR	[68]

11	Physical	Flame Spraying System	HA-coated Ag-HA-coated	Ag ₂ O (0.21 wt% after spraying)	R	MRSA (UOEH6)	CFU/implant	<u>24h</u> : 5.3 (±2.5) x 10 ⁴ <u>48h</u> : 1.2 (±0.5) x 10 ⁵ <u>72h</u> : 4.4 (±3.0) x 10 ⁵	<u>24h</u> : 3.5 (±2.2) x 10 ³ <u>48h</u> : 2.1 (±3.0) x 10 ⁴ <u>72h</u> : 4.0 (±3.5) x 10 ⁴	<u>24h</u> :0.002 <u>48h</u> :0.008 <u>72h</u> :0.041	NR	[76]
12	Physical	Flame Spraying System	Al-sandblasted	Ag ₂ O (3 wt%)	R	MRSA (UOEH6)	CFU/implant	1.5 (± 0.5) x 10 ⁵	1.1 (± 0.4) x 10 ⁴	<.001	NR	[121]
13	Physical	Electrophoretic deposition	Additively manufactured highly porous	Ag (1.69 up to 10.95 at%)	R	<i>S. aureus</i> (ATCC 49230)	CFU/implant	1) AsM = 5x10 ⁶ 2) Ch = 6 x10 ⁶	3) CH1mMAg: 6 x10 ⁶ 4) CH50mMAg: 6 x10 ⁶ 5) CH100mMAg 6 x10 ⁶ 6) CHVan: 5.5 x10 ⁶	>.05	1) 40% (2/5) 2) 100% (8/8) 3) 100% (8/8) 4) 100% (8/8) 5) 100% (8/8) 6) 40% (2/5) p=0.035 (2 vs 6)	[122]
14	Physical	Oxidation process	TiO ₂ nanotubes	Dopamine hydrochloride (2 mg/mL)	R	MRSA (NR)	CFU/implant	1) Ti = 1954 (±221)	2) Ti-Nd = 1727 (±246) 3) Ti-Nd-PDA = 1060 (±67) 4) Ti-Nd-PDA + NIR = 435 (±147) 5) Ti-Nd-PDA-Fc = 484 (±42) 6) Ti-Nd-PDA-Fc + NIR = 79 (±12)	<.05 (6 vs all group)	NR	[74]
15	Physical	Tube furnace	TiO ₂ coating + NIR light + US	Sublimed sulfur (NR)	R	<i>S. aureus</i> (ATCC 29213)	Antibacterial efficiency (%)	0%	99.43%	<.001	NR	[82]
16	Physical	Plasma-sprayed	HA-coated	HA (NR)	D	<i>P. gingivalis</i> ; <i>P. intermedia</i> ; <i>A. actinomycetemcomitans</i> (clinical strain)	DNA counts	<u>Pg</u> : 257.6 (±274.1) x 10 ³ <u>Pi</u> : 21.2 (±21.0) x 10 ³ <u>Aa</u> : 1.0 (±2.4) x 10 ³	<u>Pg</u> : HA = 138.1 (±223.9) x 10 ³	NR	NR	[50]

									TPS = 285.5 (±303.9) x 10 ³ <u>Pi:</u> HA = 12.8 (±10.6) x 10 ³ TPS = 31.5 (±54.1) x 10 ³ <u>Aa:</u> HA = 1.1 (±2.6) x 10 ³ TPS = 1.0 (±2.4) x 10 ³			
17	Physical	Surface-induced nucleation-deposition	Machined	Selenium NP (NR; only report concentration during process = 10 mM)	R	MRSA (ATCC 43300) MRSE (ATCC 35984)	Log CFU	MRSA = 5.9 (±1.2) x 10 ⁶ MRSE = 5.3 (±0.3) x 10 ⁶	MRSA = 2.2 (±0.4) x 10 ⁶ MRSE = 1.0 (±0.5) x 10 ⁶	<.05	NR	[73]
18	Physical	Vacuum plasma-spray	Machined	HA (NR)	Rab	<i>S. aureus</i> (ATCC 10832)	Log CFU	10 ² = 1.3 (±1.3) 10 ³ = 2.1 (±1.2) 10 ⁴ = 3.7 (±1.5) 10 ⁵ = NR	10 ² = 1.6 (±1.6) 10 ³ = 2.0 (±2.0) 10 ⁴ = 5.6 (±1.9) 10 ⁵ = 6.3 (±0.7)	<.05	NR	[123]
19	Physical	Vacuum-drying	Nanotubes - NT	Gentamicin (NR)	R	<i>S. aureus</i> (ATCC 25923)	CFU/implant	Ti = 6.7 × 10 ⁵ (±7.5 × 10 ⁴) Ti-NT = 4.6 x 10 ⁵ (±6.2 × 10 ⁴)	1.5 × 10 ⁴ (±2.0 × 10 ³)	<.01	NR	[69]
20	Physical	Magnetron sputtering	Acid-etched	TaO(at%) Ta-I = 5.52(±0.43) Ta-II = 8.14(±0.04) Ta-III = 6.40(±0.97)	Mic	Luminescent <i>S. aureus</i> (ST1792-Lux) <i>E. coli</i> (ST1)	Log CFU	<i>S. aureus</i> : 5.63 (NR) <i>E. coli</i> : 3.88 (NR)	<u>Ta-I:</u> <i>S. aureus</i> : 4.28 (NR) <i>E. coli</i> : 2.88 (NR) <u>Ta-II:</u> <i>S. aureus</i> : 3.44 (NR) <i>E. coli</i> : 2.23 (NR) <u>Ta-III:</u> <i>S. aureus</i> : 2.82 (NR) <i>E. coli</i> : 1.47 (NR)	<.01	NR	[80]

21	Chemical	Manual application	Machined + Acid etched	Vancomycin (25.0 at%)	Rab	<i>S. aureus</i> (UAMS-1 strain)	CFU/implant	600000 (NR)	20 (\pm 21)	NR	< .001	[88]
22	Chemical	Manual application	Machined or PeriApatite coated	Tobramycin (2.4 mg)	Rab	<i>S. aureus</i> (ATCC 10832)	Log CFU	C1= 3.29 (\pm 0.88) C2= 2.98 (\pm 1.28)	0.05 (\pm 0)	(C1 Vs T) p=.004 (C2 Vs T) p=.045	C1: 67% (12/18) C2: 53% (9/17) T: 6% (1/18)	[124]
23	Chemical	Immersion	Hydroxide coated	(3-aminopropyl) triethoxysilane (NR)	R	<i>S. aureus</i> (ATCC 29213)	CFU/implant	173.9(\pm 33.7)	12.8(\pm 13.2)	<.05	NR	[71]
24	Chemical	Immersion	Si-based coating	CZ-01127 polymer (15.9 \pm 1.5 mg)	S	MRSA (clinical strain)	CFU/g	2.6 x 10 ⁴ (\pm NR)	3.0 x 10 ² (\pm NR)	.035	NR	[125]
25	Chemical	Immersion	Machined	Ag (8.19 wt%)	R	<i>S. aureus</i> (ATCC 25923)	CFU/implant	191.30 (\pm 17.39)	8.69 (\pm 4.35)	<.05	NR	[126]
26	Chemical	Immersion	Machined	ϵ -poly-L-lysine (EPL; 30mM) Catechol (C; 15mM)	R	MRSA (ATCCBAA40)	CFU/implant	5.48 (\pm 0.41)	4.35 (\pm 0.24)	<.01	NR	[127]
27	Chemical	Immersion	Machined + NIR light	NR (only report concentration during process: Red phosphorus = 0.15 g/mL; IR780 = 0.02mg/mL; RGDC peptide = 2 mg/mL)	R	No infection	Rolled out on agar plates test	Not bacterial counted (only photograph)	Not bacterial counted (only photograph)	NR	NR	[98]
28	Chemical	Immersion	Machined	Vitamin E (5 mg/cm ²)	R	<i>S. aureus</i> (UAMS-1Xen40)	Log CFU	3.8 (\pm 0.4)	3.2 (\pm 0.5)	<.001	NR	[128]
29	Chemical	Immobilization	TiO ₂ nanospine coating	Cationic polypeptide (NR)	R	<i>S. aureus</i> (ATCC 6538)	CFU/implant	\sim 3.26 \times 10 ⁸	\sim 28	<.001	NR	[129]
30	Chemical	Immobilization	Machined + NIR light	MPDA (0.09 mg) RGD peptide (5 mg/mL)	R	<i>S. aureus</i> (ATCC 29213)	Antibacterial efficiency (%)	0% (NR)	95.4% (NR)	<.01	NR	[49]

31	Chemical	Immobilization	Machined + NIR light	Daptomycin (634.6 µg)	R	<i>S. aureus</i> (ATCC 25923)	CFU/implant	C - NIR: 192.5 (±12.5) C + NIR: 182.5 (±22.5)	T - NIR: 82.5 (±10.0) T + NIR: 5.00 (±2.5)	< 0.05 (compared to control groups and NIR-)	NR	[78]
32	Chemical	Impregnated on PDLLA coating	PDLLA-coated	Tobramycin (4mg wt%)	Rab	<i>S. aureus</i> (ATCC 25923)	CFU/implant	> 10 ⁴	< 10 ³	NR	C: 100% (6/6) T: 16.7% (1/6) p<.05	[130]
33	Chemical	Dip-coating	Machined Xerogel film	Nitric Oxide - NO (NR)	R	No infection	CFU/implant	<u>Machined:</u> 1.181.000 (±2.717.000) <u>XG:</u> 677.000 (±675.000)	<u>NO:</u> 170.000 (±181,000)	<.05 (NO vs machined and XG)	NR	[97]
34	Chemical	Dip-coating	Machined	CHX (4.9 - 9.5 - 10.0wt%)	Mic	<i>S. aureus</i> (ATCC 49230)	Log CFU	<u>1d:</u> Ti (86) <u>4d:</u> Ti (28)	<u>1d:</u> CHX10% (24) <u>4d:</u> CHX10% (0)	≤.05	<u>1d:</u> Ti: 80% (16/18) CHX10% : (4/17) <u>1d:</u> Ti: (5/18) CHX10% (0/18) (p>0.05 for 1 and 4 days)	[70]
35	Chemical	Dip-coating	CaP-coated	Gentamicin (NR; only report concentration during process = 40 mg/mL)	R	<i>S. aureus</i> (JAR060131)	Log CFU	1.76 (NR) x 10 ⁶	6.43 (NR) x 10 ¹	<.01	C: 100% (9/9) T: 12.5% (1/9)	[131]
36	Chemical	Dip -coating	Machined	2) DDDEEK-G4-(DOPA)4 (5 mg/mL) 3) WRWRWR-G4-(DOPA)4 (5 mg/mL)	R	<i>E. coli</i> (ATCC 8739) <i>S. aureus</i> (ATCC 6538)	CFU/implant	<i>S. aureus</i> : 2.7x10 ⁴ (±1.0) <i>E. coli</i> : 3.2 x 10 ⁴ (±0.5)	<u>2)</u> <i>S. aureus</i> : 0 <i>E. coli</i> : 0 <u>3)</u> <i>S. aureus</i> : 2.8x10 ⁴ (±1.4)	<.05	NR	[75]

				4) DGD+WGD (2.5 mg/mL for each component)					<i>E. coli</i> : 3.2x10 ⁴ (±0.5) 4) <i>S. aureus</i> : 0 <i>E. coli</i> : 0				
37	Chemical	Silanization	Machined	Cys-melimine peptide (3.1 x10 ⁹ mol/cm ²)	Mic R	<i>S. aureus</i> (strain 38)	Log CFU	5 d: (10 ⁷ inoculum) = 4.0x10 ⁶ (10 ⁵ inoculum) = 8.0 x 10 ⁵ 7 d: (10 ⁵ inoculum) = 9.1 x 10 ⁴	5 d: (10 ⁷ inoculum) = 2.1x10 ⁵ (10 ⁵ inoculum) = 4.8x10 ³ 7 d: (10 ⁵ inoculum) = 6.1 x 10 ³	< .05 (Control Vs Tests; 10 ⁵ and 10 ⁷)	NR	[132]	
38	Chemical	Silanization	Polyelectrolyte multi-layers coating	TiO ₂ (1g; wt%) CHX (10 mg/mL)	R	<i>S. aureus</i> (ATCC 29213)	CFU/implant	Median: 5.3(±14.6)x10 ⁵	Median: 3.1(±8.5) x10 ⁵	<.05	NR	[133]	
39	Chemical	Covalently bond	Machined	Vancomycin (90 µg/mm ³)	Mic	<i>S. aureus</i> (Xen29)	Bioluminescence intensity	520 (±40)	0	<.01	NR	[99]	
40	Chemical	Soaking method	Anodized surface	Tobramycin (NR; only report concentration in the stock solution used for loading)	Rab	<i>S. aureus</i> (ATCC 6538)	CFU/implant	10 ⁴ inoculum: 3.4(±2.0) x 10 ⁵ 10 ⁵ inoculum: 2.8(±1.4) x 10 ⁵	10 ⁴ inoculum: 1.35 x 10 ⁵ (only 1 implant) 10 ⁵ inoculum: 0	NR	10 ⁴ CFU: 33.3% (1/3) test; 100.0% control (3/3) 10 ⁵ CFU: 0% test (0/2) 100.0% control (2/2)	[83]	
41	Chemical	Soaking method	Machined + nanotubular anodized surface (NTATi)	Gentamicin - G (10 mg/mL)	Rab	<i>S. aureus</i> (ATCC 25923)	Rolled out on agar plates test	Ti= >1.000 NTATi= >1.000	TiG= 73.75(±10.69) NTATi-G= 40.5(±12.36)	<.05 NTATi-G Vs NTATi and Ti groups.	Ti: 100% (4/4) NTATi: 100% (4/4) Ti-G: 100% (4/4) NTATi-G: 100% (4/4)	[134]	

42	Chemical	Soaking method	Machined or Alkali-heat treatment (AT)	Mg (7.6 ± 0.7 wt%) Zn (1.8 ± 0.1 wt%)	R	<i>S. aureus</i> (ATCC 29213)	% reduction related to machined Ti	AT: 3.16% (± 7.58)	95.99% (± 4.53)	<.01	NR	[77]
43	Chemical	Loading of the drug on nanotubes layer via immersion followed by catechol-functionalized multilayer films (spin coating)	Machined	Vancomycin (200 ug/cm^2) Chitosan-catechol (0.01 g/mL)	R	<i>S. aureus</i> (ATCC 25923)	Log10 CFU	3.4 (± 0.1)	0.9 (± 0.4)	<.01	NR	[135]
44	Chemical	Layered double hydroxides suspension	Porous	Ciprofloxacin ($1.2 \pm 0.2 \text{ mg/cm}^2$)	Mic	<i>P. aeruginosa</i> (PAOI CTX::lux)	Bioluminescence intensity	<u>1w</u> : 100.56 (± 28.4) <u>2w</u> : 99.40 (± 37.64) <u>3w</u> : 289.88 (± 21.30)	<u>1w</u> : 26.47 (± 4.67) <u>2w</u> : 68.45 (± 28.03) <u>3w</u> : 276.19 (± 47.43)	NR	NR	[81]
45	Chemical	Layer-by-layer	TC TC-CH TC-CHH	HACC (Na = 0.14-0.25; Si = 0.44-0.84; Cl = 1.07 at%)	R	MRSA (ATCC 43300)	CFU/implant	$8.65 (\pm 0.66) \times 10^5$	TC-CH: $8.37 (\pm 0.59) \times 10^4$ TC-CHH: $3.6 (\pm 0.95) \times 10^4$	<.05 (Control vs TC-CHH)	NR	[84]
46	Chemical	Sol-gel method	Machined	Ag (NR)	R	<i>S. aureus</i> (NR)	Rolled out on agar plates test (%reduction)	NR	NR	NR	C: 80% (16/20) T: 0% (0/20) p<.001	[136]
47	Physical Chemical	Lyophilization method + vacuum drying	Nanotubes-NT	CS (2 mg)	R	MRSA (ATCC4330)	CFU/implant	Ti = $4.7 \times 10^5 (\pm 8.0 \times 10^4)$ Ti-NT = $2.8 \times 10^5 (\pm 3.0 \times 10^4)$	Ti-NT-C = $1.0 \times 10^4 (\pm 1.6 \times 10^3)$	<.01	NR	[137]
48	Physical Chemical	MoS ₂ = Magnetron sputtering IR780 = dropping	Machined + NIR light	Mo (11.22 at%) S (23.87 at%) I (0.02 at%)	R	<i>S. aureus</i> (ATCC 29213)	Antibacterial ratio (%)	NIR -: 0% (± 4.61) NIR +: 6.15% (± 2.31)	NIR -: 4.62% (± 1.53) NIR +: 98.99% (± 0.42)	<.01 (NIR +)	NIR -: 0% NIR +: ~92.84%	[79]

PDA + RGDC = immersion												
49	Physical Chemical	Thermal spraying (HA and Ag) Immersion (Vancomycin)	HA-coated	Ag (3wt%) Vancomycin - VCM (20µg/ml – topically applied)	R	MRSA (UOEH6)	CFU/implant	HA: 4.2(±3.5) x10 ⁶	HA-VCM: 1.2(±1.3) x10 ⁶ HA-Ag: 1.9 (±2.0) x10 ⁶ HA-Ag- VCM: 1.2(±3.4) x10 ⁵	<.05 (all tested groups vs Control)	NR	[54]
50	NR	NR	Machined	TiO ₂ (NR)	R	<i>S. aureus</i> (ATCC 29213)	Log CFU	2756.25 (±1622.35)	1829.62 (±2939.75)	>.05	NR	[138]
51	Unclear	Unclear	Machined	Vancomycin (NR)	Rab	MRSA (ATCC 43300)	CFU/implant	8.42 (±0.6) x 10 ⁵	4.04 (±0.8) x 10 ⁴	NR	NR	[139]

Notes: Surface treatment (HA – Hydroxyapatite; TC – titanium-coated by plasma vacuum plasma spraying; TC-CH – Collagen I/Hyaluronic acid modified Titanium Coatings; TC-CHH – Collagen I/Hyaluronic acid/Quaternized Chitosan multilayer modified Titanium Coatings; RGDC= Red Phosphorus/IR780/Arginine-Glycine-Aspartic Acid-Cysteine coating; NIR – Near-infrared light; PEG – Polyethylene glycol; CS – Chitosan; PEO – Plasma Electrolytic Oxidation; PDLLA – Poly(D,L-lactide), Deposition technology (NR – Not reported), Antimicrobial (HACC –Hydroxypropyltrimethyl Ammonium Chloride Chitosan; NR– Not reported ; MoS₂– Molybdenum disulfide; CHX – Chlorhexidine; NP – nanoparticles; CS – Chitosan; MPDA – mesoporous polydopamine nanoparticles); Animal type (Rat – Rats; Mic – Mice; Rab – Rabbit; S –Subcutaneous; D – Dog); Infection model (MRSA – methicillin-resistant *Staphylococcus aureus*); Microbial load (C – Control; T – Test; h – Hour; d – Day; w – Week; NR – Not reported).

Table 2. Summary of subjects (study ID, number of male and female, and mean age), intraoral appliance (material and location), sample (shape, location, number/group, and surface treatment), microbiological assessment (quantitative test, microbial species, time points, microbial load, p-value and qualitative tests), and reference from included *in situ* studies.

Study ID	Subjects		Intraoral appliance		Sample			Microbiological assessment					Reference	
	N (M/F)	Mean age (years)	Material (location)	Shape (location, N)	Material	Surface treatment	Quantitative test	Microbial species	Time points	Microbial load		p-value		Qualitative tests
										Control	Experimental			
1	6 (NR)	23 to 54 (range)	Acrylic (upper jaw)	Cylindrical (buccal, 6/group)	cpTi	1) Anodized (TiUnite®) 2) Machined (Ti-m)	DAPI staining (cells/cm²)§	Total oral bacteria	30 min	2) Median: 9.16x10 ⁴ (± 2.75x10 ³)	2) Median: 2.75x10 ⁵ (± 2.33x10 ⁵)	p < .05	FISH and CLSM analysis (Streptococcus spp. represent the largest proportion on all materials)	[58]
									120 min	3) Median: 1.41x10 ⁵ (±1.16x10 ⁵)	2) Median: 2.49x10 ⁵ (± 3.74x10 ⁵)	p < .05		
2	10	39.7	NA - directly attached on the tooth (upper jaw)	Cylindrical (buccal, 10/group)	Ti-6Al-4V	NC: Noncoated UVNC: UV treated NC	Log CFU/mL	<i>S. mutans</i> Non-mutans streptococci Total facultative bacteria	24 h	<u>S.m.:</u> NC = 0.35 (±0.4) <u>N-m:</u> NC = 6.16 (± 0.5) <u>Facult.:</u> NC = 6.26 (±0.5)	<u>S.m.:</u> UVNC = 0.25 (±0.4) HT = 0.07 (±0.2) UVHT = 0.16 (±0.3) <u>N-m:</u> UVNC = 6.06 (±0.6) HT = 6.14 (±0.6) UVHT = 5.97 (±0.5) <u>Facult.:</u>	p > .05		[140]

UVNC =
6.24
(±0.6)
HT = 6.16
(±0.6)
UVHT =
6.09 (±0.4)

Appendix: Supplementary information

1 | Supplementary materials and methods

1.1 | Protocol and registration

This critical evidence-based review was performed following the criteria of the Preferred Reporting Items for Systematic Review and Meta-Analyses (PRISMA) (Moher, Liberati, Tetzlaff & Altman, 2009). The review protocol was registered in the Open Science Framework on February 15, 2021 (osf.io/8m7nz).

1.2 | Focused question

The objective of this review was to address the following clinical question according to the population, intervention, comparison, and outcome (PICO) study design: *“Does titanium surface properties and developed coatings can reduce in vivo bacterial adhesion and microbial accumulation in dental implants?”*. The PICO strategy described below was used:

- (P) – Population: Humans or animals with titanium-based implants installation;
- (I) – Intervention: Titanium surface treatment (chemical/physicochemical topography modifications or antimicrobial deposition) clearly described;
- (C) – Comparison: control (untreated or commercial) implants; and,
- (O) – Outcome: microbial load/implant contamination rate (primary outcome); peri-implant assessment (secondary outcome).

1.3 | Systematic search strategy

An electronic search was performed independently by two examiners (R.C.C. and B.E.N) for identification of studies to be included on four sources: PubMed (MEDLINE), Scopus, The Cochrane Library and EMBASE. The literature search was performed in Aug 2020 using MeSH terms, entry terms and free terms appropriately adapted for syntax rules of each database (Table S1). In addition, search alerts were established to keep the search strategy up to date. A manual screening of the bibliographies of all included studies was performed to complement the electronic search. For the present systematic review, no language and publication time restrictions were applied.

1.4 | Eligibility criteria and study selection

The following inclusion criteria were applied: pre-clinical (animal model and *in situ* model) or clinical studies (N-RCT and RCT) that enrolled animals or adult subjects with titanium-based samples used for microbiological assessments (quantitative data) or peri-implant outcomes (qualitative data). Studies must have used titanium surface with any topography modification and compared the control surface to be included. Studies not meeting the inclusion criteria were excluded. Additionally, the studies designated as literature reviews, case reports, case series, *in vitro*, *in silico*, descriptive and observational were also excluded.

In the first stage, references recorded through all databases were imported to Rayyan QCRI[®] reference manager (Ouzzani, Hammady, Fedorowicz & Elmagarmid, 2016). After duplicates removal, the same two authors (R.C.C. and B.E.N.) independently screened all titles and abstracts on the aforementioned inclusion criteria. Whether data from title and abstracts were insufficient to confirm eligibility, full texts were further evaluated to avoid exclusion of eligible articles. Afterwards, the full text of the selected studies was then obtained and independently assessed by the reviewers. For any disagreements, at any stage, resolution was first resolved through open discussion between the two reviewers. In cases of unsolved disagreements, a third author (J.G.S.S.) was consulted to reach a consensus about eligibility.

1.5 | Data extraction process

Data from the included studies were independently recorded: study features (author(s) and year of publication), study design (preclinical or clinical studies); animal (species, n value, age and infection model), human (patients per group, sex and age), implant information (titanium based-material, surgical site, surface treatment, deposition method), antimicrobial incorporated on surface (type, concentration and *in vitro* drug release) and time of follow-up. Some papers from the same study were associated under a single report (the most recent publication).

The primary outcomes were characterized by mean/median and standard deviation of the microbial load (bacterial counts, area covered by biofilm, bioluminescence intensity, biofilm biovolume or bacterial DNA counts) or implant contamination rate (bacterial presence in the implant surface). For available data only in graphs with no mean/median and standard deviation exact values, data were extracted using the program WebPlotDigitizer[®] which is considered a reliable tool for data extraction (Burda et al.,

2016). Moreover, the secondary outcomes related to peri-implant parameters in animal models (hard and soft tissues) or human studies (plaque index, gingival index, bleeding on probing and bone loss) were qualitatively evaluated. To avoid overlapping, data were collected based on the most recent publication for studies carried out with the same sample population. Due to the different microbiological methods and reported outcomes of the included investigations, only a qualitative descriptive analysis was performed and systematically reviewed using tables. Significant heterogeneity was found preventing a quantitative synthesis of the included studies; therefore, the meta-analysis was precluded.

1.6 | Quality assessment and risk of bias

The methodological quality of each included study was analyzed according to the Systematic Review Centre for Laboratory animal Experimentation (SYRCLE) risk of bias tool for animal studies (Hoojimans et al., 2014) and the Cochrane Collaboration's tool for assessing risk of bias for clinical studies. Currently, no quality assessment method has been developed for analysis of *in situ* studies, thus being the data only descriptively reported. Prior to the bias assessment, some modifications were made to the domains of each methodological instruments to make the tool more suitable for the purpose of this study. Animal studies were evaluated following risk of bias domains by the review authors judgment for sequence generation, baseline characteristics, allocation concealment, blinding, incomplete outcome data, selective outcome reporting, and other sources of bias (apparently free of other sources that could result in high risk; adequate sample size; animal welfare regulation) by SYRCLE guidelines. Bias was assessed as “low risk”, “high risk” or “unclear”.

The Randomized Clinical Trials (RCT) were assessed for randomization process, deviations from intended interventions, missing outcome data, measurement of the outcome, and selection of the reported result based on the revised Cochrane Risk of Bias Tool for RCTs (RoB 2) (Higgins, Savović, Page, Elbers & Sterne 2019). Studies were classified after judgment for each domain as low, some concerns, or high risk-of-bias. Non-Randomized Clinical Trials (N-RCT) were evaluated with the ROBINS-I scoring system, considering bias due to confounding, selection of participants into the study, classification of interventions, deviations from intended interventions, missing data, measurement of the outcomes, and selection of the reported results (Stern et al., 2016). After judgment for each domain, studies were classified as low, moderate, critical, or serious risk-of-bias. Any disagreements between reviewers during the risk-of-bias

evaluation were solved by a third reviewer (J.G.S.S.). Summary assessments of the risk of bias for outcomes (across domains or criteria for the quality assessment used) within and across studies are represented in risk of bias graphics following Cochrane review guidelines.

2 | Supplementary results

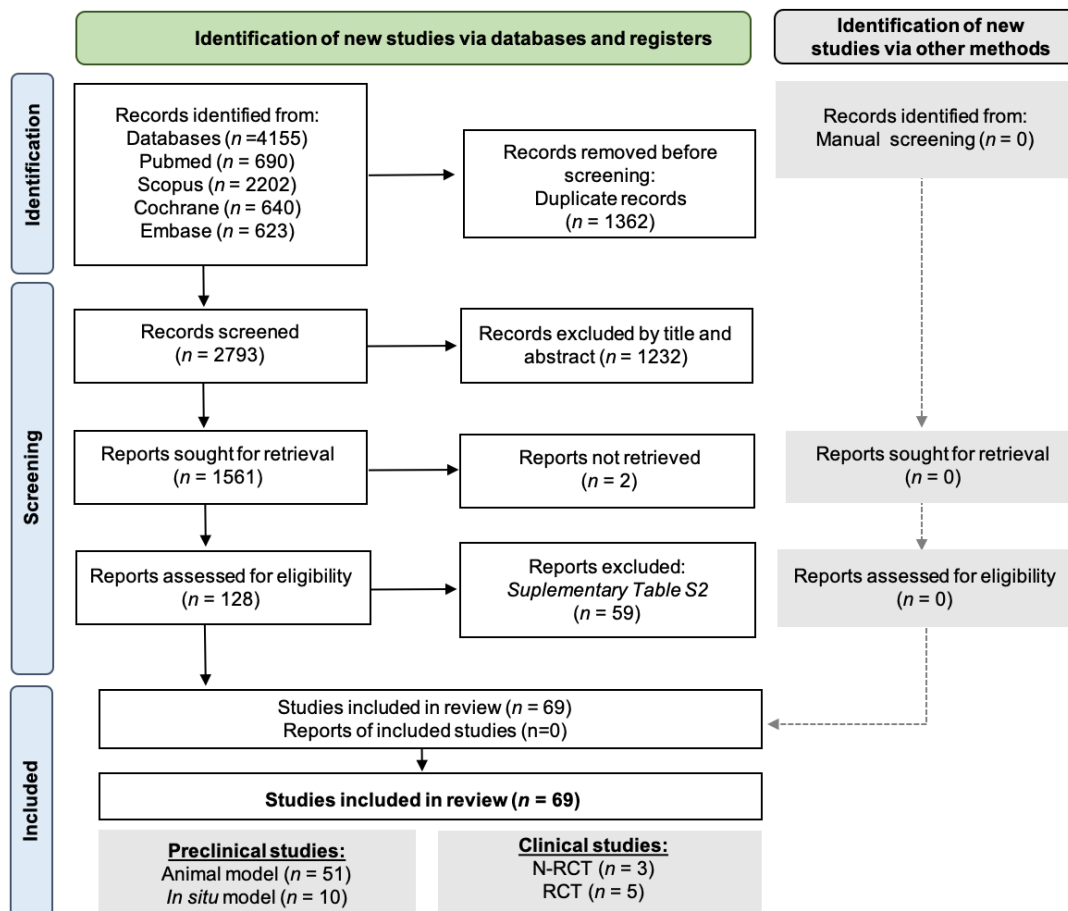


Figure S1. Flow diagram of search results from databases. N-RCT: Non-randomized clinical trial, RCT: Randomized Clinical Trial.

Reason for exclusion	Number	Studies
Does not evaluated microbial colonization quantitatively on implant surface	42	Källicke <i>et al.</i> (2006); Watzak <i>et al.</i> (2006); Visai <i>et al.</i> (2008); Scarano <i>et al.</i> (2010); Shirai <i>et al.</i> (2011); Aykut <i>et al.</i> (2010); Jeyapalina <i>et al.</i> (2012); Schaer <i>et al.</i> (2012); Sinclair <i>et al.</i> (2013); Svensson <i>et al.</i> (2013); Madi <i>et al.</i> (2013); Bitik <i>et al.</i> (2013); Zhang <i>et al.</i> (2014); Li <i>et al.</i> (2014); Wang <i>et al.</i> (2014); Xiao <i>et al.</i> (2015); Harrasser <i>et al.</i> (2016); Diefenbeck <i>et al.</i> (2016); Zhang <i>et al.</i> (2016);

		Nast <i>et al.</i> (2016); Hegazy <i>et al.</i> (2016); Kao <i>et al.</i> (2017); Liao <i>et al.</i> (2017); Li <i>et al.</i> (2017); Maurer <i>et al.</i> (2017); Zhang <i>et al.</i> (2018); Qiu <i>et al.</i> (2019); Shen <i>et al.</i> (2019); Peeters <i>et al.</i> (2019); Gao <i>et al.</i> (2019); Qianli <i>et al.</i> (2019); Jiang <i>et al.</i> (2019); Qiu <i>et al.</i> (2019); Yang <i>et al.</i> (2019); Shevtsov <i>et al.</i> (2019); Li <i>et al.</i> (2019); Mills <i>et al.</i> (2020); Tao <i>et al.</i> (2020); Li <i>et al.</i> (2020); Woelfle <i>et al.</i> (2020); Yavari <i>et al.</i> (2020); Zhang <i>et al.</i> (2020).
Does not used titanium-based implants	7	Lucke <i>et al.</i> (2003); Groessner-Schreiber <i>et al.</i> (2004); López-Píriz <i>et al.</i> (2015); Prinz <i>et al.</i> (2017); Yu <i>et al.</i> (2018); Shiels <i>et al.</i> (2018); Xu <i>et al.</i> (2019).
Does not used healthy rat in the animal model	3	Gerits <i>et al.</i> (2016); Kuchariková <i>et al.</i> (2016); Ma <i>et al.</i> (2017).
Other reasons (Lack of information relevant to review)	7	Tillmanns <i>et al.</i> (1998); Shibli <i>et al.</i> (2008); Kuehl <i>et al.</i> (2016); Liu <i>et al.</i> (2017); Tan <i>et al.</i> (2018); Hong <i>et al.</i> (2019); Masci <i>et al.</i> (2020).

Table S2. Summary of excluded studies

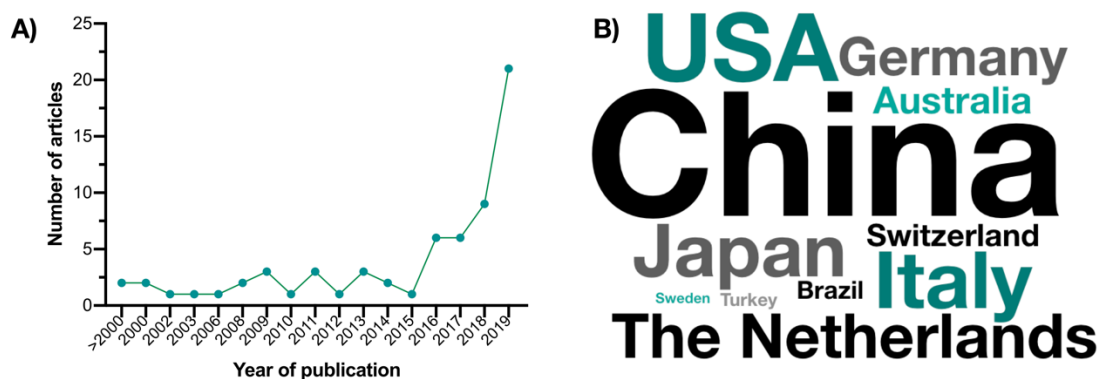


Fig. S2. Bibliometric analysis of included studies. **(A)** Line chart represents the number of published studies included in the systematic review sorted by the year of publishing. **(B)** Word clouds of the country affiliations of all correspondence authors. The font size represents the frequency of countries for each included study in which bigger words mean more frequent country for this purpose, thus predominating research groups from China and the USA.

Table S3. Summary of antimicrobial concentration and release of included studies.

Author (year)	Antimicrobial incorporated		Follow-up
	Concentration	Release	
Akiyama <i>et al.</i> (2013)	Ag not identified in EDX analysis	NR	NR
Ao <i>et al.</i> (2019)	XPS analysis of basic elements composition (HACC – not quantitative described)	1.860 (\pm 120) mg of HACC	18d
Badar <i>et al.</i> (2015)	Ciprofloxacin (1.2 mg/cm ²)	NR	NR
Chen <i>et al.</i> (2016)	NR	3.1 x 10 ⁹ mol/cm ²	NR
Croes <i>et al.</i> (2018)	1) 1.69 Ag (at%) 2) 4.82 Ag (at%) 3) 10.95 Ag (at%) 4) Vancomycin (NR)	NR	NR
Gao <i>et al.</i> (2019)	NR	NR	NR

Ghimire <i>et al.</i> (2019)	90 µg/mm ² hydrogel of vancomycin	~100%	24 h
Hashimoto <i>et al.</i> (2020)	1) HA-VCM (20µg/ml Vancomycin) 2) HA-Ag coating (3wt% Ag)	NR	NR
Holt <i>et al.</i> (2011)	NR	0.28 (± 0.11) mmol/cm ²	4 d
Hong <i>et al.</i> (2019)	NR	34.4 (± 4.4) µg/L	20 d
Huang <i>et al.</i> (2019)	NR	NR	NR
Inoue <i>et al.</i> (2017)	10–12 µg/cm ² of iodine	NR	NR
Janson <i>et al.</i> (2019)	NR	758 µg	15 min
Jennings <i>et al.</i> (2016)	Vancomycin (25.0 at%)	NR	NR
Kao <i>et al.</i> (2017)	NR	NR	NR
Li <i>et al.</i> (2019)	Mo/S (25.0 At%)	NR	NR
Liu <i>et al.</i> (2017)	NR	NR	NR
Lovati <i>et al.</i> (2018)	Vitamin E (5 mg/cm ²)	NR	NR
Ma <i>et al.</i> (2019)	NR	2.8 mg/mL (Without NIR)	25 min
Moojen <i>et al.</i> (2009)	Tobramycin (2.4 mg)	NR	NR
Ofluoglu <i>et al.</i> (2014)	NR	NR	NR
Oosterbos <i>et al.</i> (2002)	NR	NR	NR
Oka <i>et al.</i> (2008)	NR	NR	NR
Perni <i>et al.</i> (2020)	TiO ₂ nanoparticles (1 g; wt%) Chlorhexidine (10 mg/mL)	~ 40 mg/L	60 d
Ravanetti <i>et al.</i> (2016)	NR	NR	NR
Riool <i>et al.</i> (2017)	CHX: 0.369(4.9 wt%), 0.809 (9.5wt%) and 0.858 (10.0wt%)	CHX0 = 0 µg/cm ² CHX5% = 23.0 µg/cm ² CHX10% = 47.1 µg/cm ²	96 h
Sinclair <i>et al.</i> (2013)	5.25 (± 0.50) mg	14.84 (± 1.21) µg/mL	24 h
Shimazaki <i>et al.</i> (2010)	NR	NR	NR
Shen <i>et al.</i> (2019)	Mg: 7.6 ± 0.7; Zn: 1.8 ± 0.1 (EDS analysis, wt%). Total amount after release: Mg (7.4 umol); Zn (0.7 umol)	NR	NR
Shen <i>et al.</i> (2020)	NR	NR	NR
Secinti <i>et al.</i> (2011)	NR	NR	NR
Song <i>et al.</i> (2020)	NR	NR	NR
Su <i>et al.</i> (2020)	NR	NR	NR
Tran <i>et al.</i> (2019)	Sodium selenite (10 mM) L-ascorbic acid (100 mM)	NR	NR
Thompson <i>et al.</i> (2019)	NR	~311.32 µg/ml	15 min
Tillmanns <i>et al.</i> (1998)	NR	NR	NR
Williams <i>et al.</i> (2019)	15.9 (± 1.5 mg) of CZ-01127	NR	NR
Vogely <i>et al.</i> (2000)	NR	NR	NR
Xie <i>et al.</i> (2019)	8.19% of Ag	2.19 (± 0.21) mg/L	30 d
Xu <i>et al.</i> (2020)	ε-poly-L-lysine (EPL; 30 mM) catechol (C; 15mM)	NR	NR
Yang <i>et al.</i> (2016a)	CS (2 mg) HACC (2mg)	1,080 µg of HACC	60h
Yang <i>et al.</i> (2016b)	Gentamicin (100 mg/mL - solution)	91.45 µg	57h
Yang <i>et al.</i> (2019a)	Ta (at %) Ta-I = 17.15 (±0.53) Ta-II = 24.01 (±0.37) Ta-III = 26.66 (±0.12)	No obvious Ta release was observed	14 d
Ye <i>et al.</i> (2020)	1) MZn300V = 10.45 wt%; 2) MZn400V = 17.27 wt%; 3) MZn530V = 34.7 wt %	~14 ppm of Zn for MZn530V group	60 d
Yuan <i>et al.</i> (2018)	Vancomycin (200 µg/cm ²) Chitosan-catechol (0.01 g/mL)	~ 21.2% of VCM	72 h
Yuan <i>et al.</i> (2019a)	10 mg of MoS ₂	NR	NR
Yuan <i>et al.</i> (2019b)	MPDA particle (2 mg/mL) RGD peptide (2 mg/mL) Indocyanine (ICG; 10 µg/mL)	15% of ICG	14d
Zeng <i>et al.</i> (2020)	Daptomycin (634.6 µg - surface) IR-820 (0.02 mg/mL - solution)	408.3 µg of daptomycin	14d
Zhang <i>et al.</i> (2018)	Vancomycin (NR)	NR	NR
Zhou <i>et al.</i> (2017a)	4 mg of tobramycin	26.03 ng/mL (blood)	2 h

(25%; w/w)			
Zhou <i>et al.</i> (2017b)	Fluoride (0.05 to 0.45 M)	> 2 ppm	12 w
Zhou <i>et al.</i> (2018)	Sodium fluoride (0.05 to 0.30 M)	~ 3 ppm	60 d

Notes: EDS – Energy-dispersive X-ray spectroscopy; NR – Not reported; XPS – X-ray photoelectron spectroscopy; HACC –Hydroxypropyltrimethyl Ammonium Chloride Chitosan; VCM – vancomycin; HA – Hydroxyapatite; CHX – Chlorhexidine; CS – Chitosan; Ta – Tantalum; HACC –Hydroxypropyltrimethyl Ammonium Chloride Chitosan; CS – Chitosan; MPDA – mesoporous polydopamine; C – Control; T – Test; h – Hour; d – Day; w – Week; m – Months.

Table S4. Summary of peri-implant outcomes of included studies.

Author (year)	Soft tissue	Hard tissue	Main findings		Follow-up
			Inflammation	Bone loss	
Akiyama <i>et al.</i> (2013)	X-ray and H&E staining	H&E staining	Severe infection and some areas of abscess around the implant was identified in the HA sample but infection in the Ag-HA sample appeared milder.	Bone formation was poor around the HA sample. In the Ag-HA coated implant, bone formation was uniformly good.	10 w
Ao <i>et al.</i> (2019)	X-ray and H&E staining	μCT	Serious infection was observed for TC + MRSA and TC-CH + MRSA, but a controlled infection was noted for the TC-CHH + MRSA group with no evident bone destruction.	TC-CHH presented higher bone volume and mean cortical bone mineral density than the TC-CH group.	6 w
Croes <i>et al.</i> (2018)	H&E staining, Neutrophil viability, phagocytosis assay	μCT Histometry	Antibacterial Ag concentrations were cytotoxic for neutrophils, and that non-toxic Ag concentrations diminished their phagocytic activity.	Ch + Ag implants did not demonstrate antibacterial effects <i>in vivo</i> and even aggravated infection-mediated bone remodeling including increased osteoclast formation and inflammation-induced new bone formation.	4 w
Gao <i>et al.</i> (2019)	H&E staining	NR	The more inflammatory neutrophils were observed in the tissue around the pure Ti implants in comparison with those around the experimental implants	NR	5 d
Ghimire <i>et al.</i> (2019)	H&E, ALP/TRAP and Gram stainings	H&E and μCT	Active bone remodeling was found in the experimental group while control implants showed osteoblastic and osteoclastic activities within the cortical bone.	Normal cortical bone structure and bone marrow morphology in the experimental group while pronounced cortical thickening was found in the control groups.	3 w
Holt <i>et al.</i> (2011)	Surgical site photograph	NR	NO group showed decreases signs of infection score when compared to other groups.	NR	4 w
Hong <i>et al.</i> (2019)	H&E staining	NR	In both groups were exhibited a severe infection induced by biofilm. However, the experimental group showed lower inflammatory cell ratios because the biofilm was eliminated.	NR	3 d
Huang <i>et al.</i> (2019)	H&E staining	μCT	Experimental group implantation has no promoted obvious infection <i>in vivo</i> .	The bone volume around the experimental+Light sample was higher than that around control+light.	2 w
Janson <i>et al.</i> (2019)	Modified Paragon staining	NR	The experimental group showed in general a lower level of tissue lesions related to signs of infection compared to the control group (at both inoculation dose: 10 ⁴ or 10 ⁵ CFU).	NR	9 d
Jennings <i>et al.</i> (2016)	H&E staining	X-ray (only confirmed the implant insertion)	C: characteristics indicative of inflammation such as swelling, redness, increased temperature, inflammatory cell infiltration and pus formation was evident in muscle tissue.	NR	1 w

				T: inflammatory cell presence was minimal and also tissue surrounding the implant had minimal evidence of bacteria.		
Li <i>et al.</i> (2019)	H&E staining	μ CT		For experimental group, a relatively milder inflammatory reaction with fewer inflammatory cells was noted after treatment with 808 nm light irradiation, while acute inflammation was observed for Ti control.	The experimental group exhibited more stimulation for the formation of new bone tissue compared with Ti group.	4 w
Liu <i>et al.</i> (2017)	H&E staining	X-ray score		Signs of infections (development of abscesses, cortical bone destruction, cancellous bone and periosteal new bone formation) were evaluated in NTATi and Ti groups, while NTATi-G and Ti-G groups showed no signs of apparent bone infection.	The bone volume in NTATi-G group was greater than Ti-G group, and little bone formation was seen in NTATi and Ti groups.	6 w
Lovati <i>et al.</i> (2018)	H&E staining	μ CT		The experimental group did not show any presence of abscesses.	The higher bone mineral density at the knee and femoral metaphysis was in the vitamin E-treated group compared with uncoated implants.	42 d
Ma <i>et al.</i> (2019)	H&E staining	NR		The experimental group + NIR light exhibits a milder inflammatory response with fewer inflammatory cells infiltrating into the tissues.	NR	7 d
Moojen <i>et al.</i> (2009)	Fuch sine and methylene blue staining	Histomorphometry		The average histopathology scores of the rabbits in the test group were lower; however, this was only significant compared to the rabbits in the uncoated titanium group.	Analysis showed that there was a large difference in osseointegration between rabbits that did or did not develop an infection; especially the PA and PA-tobra rabbits showed a large reduction	4 w
Ofluoglu <i>et al.</i> (2014)	H&E staining	NR		Inflammatory signs were milder in the animals implanted with TiO ₂ -coated screws.	NR	3 w
Oosterbos <i>et al.</i> (2002)	H&E staining	Histomorphometry		Only compared between infection and not infection implants, not evaluated the different Ti surfaces.	In terms of bone contact was demonstrated higher bacterial concentration in experimental group	4 w
Perni <i>et al.</i> (2020)	H&E staining	NR		The histological analysis suggests that the healing time of infected wounds reduced to about half by using the chlorhexidine releasing formulation (Experimental group).	NR	2 w
Ravanetti <i>et al.</i> (2016)	H&E staining	X-ray (only confirmed the implant insertion)		C: Peri-implant tissue was extensively degenerated with osteolysis and foci of osteomyelitis. T: Peri-implant tissue was more safeguarded, however; large bacterial colonies were observed in all groups, even in gallium-doped titanium.	NR	2 w
Riool <i>et al.</i> (2017)	H&E staining	NR		The CHX10-coated implants were well-tolerated by the animals, with no signs of toxicity observed by histological analysis.	NR	4 d
Shen <i>et al.</i> (2019)	H&E and CD68 stainings	μ CT		More monocytes gathered around Ti and AT implants in both osteoepiphysis and medullary cavity than that of AT-Mg/Zn3 group.	The higher bone volume in osteoepiphysis or medullary cavity were detected around AT-Mg/Zn3 implants than those of other groups in both normal and bacterial models.	4 w
Shen <i>et al.</i> (2020)	H&E staining	NR		There was little to no inflammation or infection found in experimental implant-tissue interface with few inflammatory cells.	NR	7 d
Song <i>et al.</i> (2020)	H&E staining	NR		For Ti-Nd-PDAFc + NIR group, a significant decrease of inflammatory cells could also be observed.	NR	3 d

Su <i>et al.</i> (2020)	H&E staining	μ CT	There were fewer inflammatory cells in the Ti-S-TiO ₂ -x + Light + US group, and the amount of <i>S. aureus</i> also clearly declined, indicating that the inflammation reaction can be significantly reduced under photothermal and sonodynamic treatments.	The new bone mass in the Ti-S-TiO ₂ -x + Light + US group was much greater than that of the control.	2 w (soft tissue) 4 w (hard tissue)
Thompson <i>et al.</i> (2019)	NR	Giemsa-Eosin staining	NR	No significant difference was observed between the control and treated groups regarding bone-to-implant contact and bone density.	1 w
Tillmanns <i>et al.</i> (1998)	NR	Toluidine blue, basic fuchsin, and alizarin red stainings Histomorphometry	NR	Vertical bone loss (mm ²) 3 months - Ti-A: 1.1/ HA: 3.19/ TPS: 0.45	3 m 6 m
Williams <i>et al.</i> (2019)	Sanderson's Rapid Bone Stain	X-ray	Si-based implants showed high amounts of osteoclast activity and significant inflammatory response. Histological data from experimental group demonstrated a mixture of osteoclast and osteoblast activity in the coated region.	The radiographs showed radiolucent areas around the Si and CZ-coated regions in all 3 groups. Similarly, bone ingrowth could not be determined from radiography.	24 w
Xie <i>et al.</i> (2019)	H&E and Giemsa stainings	μ CT	In the Ti group, bone tissue destruction accompanied by inflammatory cell infiltration and fibrosis was observed, while in the experimental group a slight inflammatory reaction was visualized.	The quantitative analysis of bone volume showed a significant bone mineral density decrease in the Ti group; however, no sign of implant-related infection was observed in the Ti/HA/Ag/CS group after 4-week implantation.	4 w
Xu <i>et al.</i> (2020)	H&E staining	NR	The tissue slices revealed that more inflammatory cells (black arrow) appeared in the control group compared with that in experimental group.	NR	5 d
Yang <i>et al.</i> (2016a)	H&E staining	X-ray μ CT	C: destruction of cortical bone T: no signs of cortical bone destruction	C: signs of massive destruction of cortical bone, accompanied by intracortical abscesses and inflammatory cell infiltration, medullary sequestrum formation and fibrosis T: no evident abscess formation and significantly lightened bone destruction	42 d
Yang <i>et al.</i> (2016b)	H&E staining	X-ray μ CT	C: destruction of cortical bone, intracortical abscesses and inflammatory cell infiltration, medullary sequestrum formation and fibrosis, and many bacteria observed in the intramedullary cavity T: relatively slight inflammatory cell infiltration, no evident bone destruction, and reduced bacterial numbers.	C: Radiographic signs of obvious osteolysis and slight periosteal reactions around the distal femur. MicroCT analysis showed obvious implant loosening and porous changes in the femoral cortical bones. T: exhibited obvious signs of bone infection, including osteolysis and periosteal reactions. MicroCT analysis showed good implant osseointegration and cortical integrity.	6 w (soft tissue) 1 d, 3 w, 6 w (hard tissue)
Yang <i>et al.</i> (2019a)	H&E and Giemsa stainings	X-ray μ CT	Morphological changes indicative of severe infection were observed in the Ti group, including massive inflammatory exudates, tissue damage and numerous neutrophils revealed by H&E staining, and a large number of bacteria revealed by Giemsa staining. In contrast, milder inflammatory reactions and smaller bacterial loads were present in the Ta groups and decreased in a film-thickness dependent manner.	X-ray test revealed that the degrees of bone destruction, osteolysis and the periosteal reaction were significantly alleviated in the Ta groups in a film thickness-dependent manner. Compared with the X-ray findings, the micro-CT results revealed a similar trend.	2 w

Yang <i>et al.</i> (2019b)	H&E staining	μCT	The infection signs, including bone destruction and osteolysis, were obviously more severe in the Ti group.	NR	24 h
Ye <i>et al.</i> (2020)	H&E staining	μCT	M Zn- 400 V coated pillar induced more amount of newly formed bone than M Zn- 300 V coated pillar, which exhibited the comparable osteogenesis to M Zn-free coated pillar; however, M Zn- 530 V coated pillar induced the smallest amount of new bone due to its cytotoxicity.	M Zn- 400 V coated pillar showed the highest bone-implant contact ratio.	4 w
Yuan <i>et al.</i> (2018)	H&E and Giemsa stainings	H&E staining	The number of neutrophils on the TNT@Van-LBLc implant was remarkably lower than on the native Ti sample, indicating a relatively minor inflammatory reaction and impactful antibacterial ability.	The newly formed bone around the TNT@Van-LBLc implant obviously increased in comparison with the native Ti sample.	4 w
Yuan <i>et al.</i> (2019a)	H&E staining	μCT	In experimental group (MoS ₂ /PDA-RGD + NIR) there was few neutrophils, eosinophils and bacteria, and a large amount of cells were normal, revealing insignificant inflammatory reaction.	Quantitative analysis of new bone volume (BV) and percentage of bone volume to tissue volume (BV/TV), the MoS ₂ /PDA-RGD group displayed significant higher level than control group.	4 w
Yuan <i>et al.</i> (2019b)	H&E and Gram staining	NR	Experimental samples + NIR treatment revealing minor inflammatory reaction and effective antibacterial performance.	NR	4 w
Zeng <i>et al.</i> (2020)	H&E staining	μCT	The inflammation reaction was quite mild and the bone tissue maintained its integrity in the Ti-PDA-IR820-DAP group.	The newly formed bone on the surface of Ti-PDAIR820-DAP groups were much thicker compared with that in the Ti group.	2 w (soft tissue) 8 w (hardtissue)
Zhang <i>et al.</i> (2018)	H&E staining	μCT	The bone destruction was not observed clearly in the TV group, and the medullary cavity exhibited infiltration of a small number of inflammatory cells. NT did not exhibit a distinct infiltration of inflammatory cells.	The bone tissue of the TV group remained intact, and the bone volume was 16.6 - 2.63%, which showed no significant difference as compared to the NT group.	6 w
Zhou <i>et al.</i> (2017a)	H&E staining	X-ray score	T: Reactive trabecular bone hyperplasia without signs of bone infection is evident.	5/6 = showed healed fractures and did not present any of radiographic appearance of infection on X-rays. 1/6 = appeared to be less severe radiographic signs of infection with healed fractures	8 w
Zhou <i>et al.</i> (2017b)	NR	Van Gieson's picrofuchsin staining	NR	Ti and the coated implants induced new bone formation on their surfaces but of different amounts, following the trend of MNR-F5 > MNR-F7 > MNR-F2 > MNR-F1 ≈ MNR-F0 > Ti.	8 w
Zhou <i>et al.</i> (2018)	NR	Van Gieson's staining	NR	All Ti coatings induced new bone formation on their surfaces but with different amount, presenting the rank of TiCP-F6>TiCP-F9>TiCP-F1≈TiCP>Ti.	8 w

Notes: NR – Not reported; C – Control; T – Test; h – Hour; d – Day; w – Week; m – Months.

Animal studies

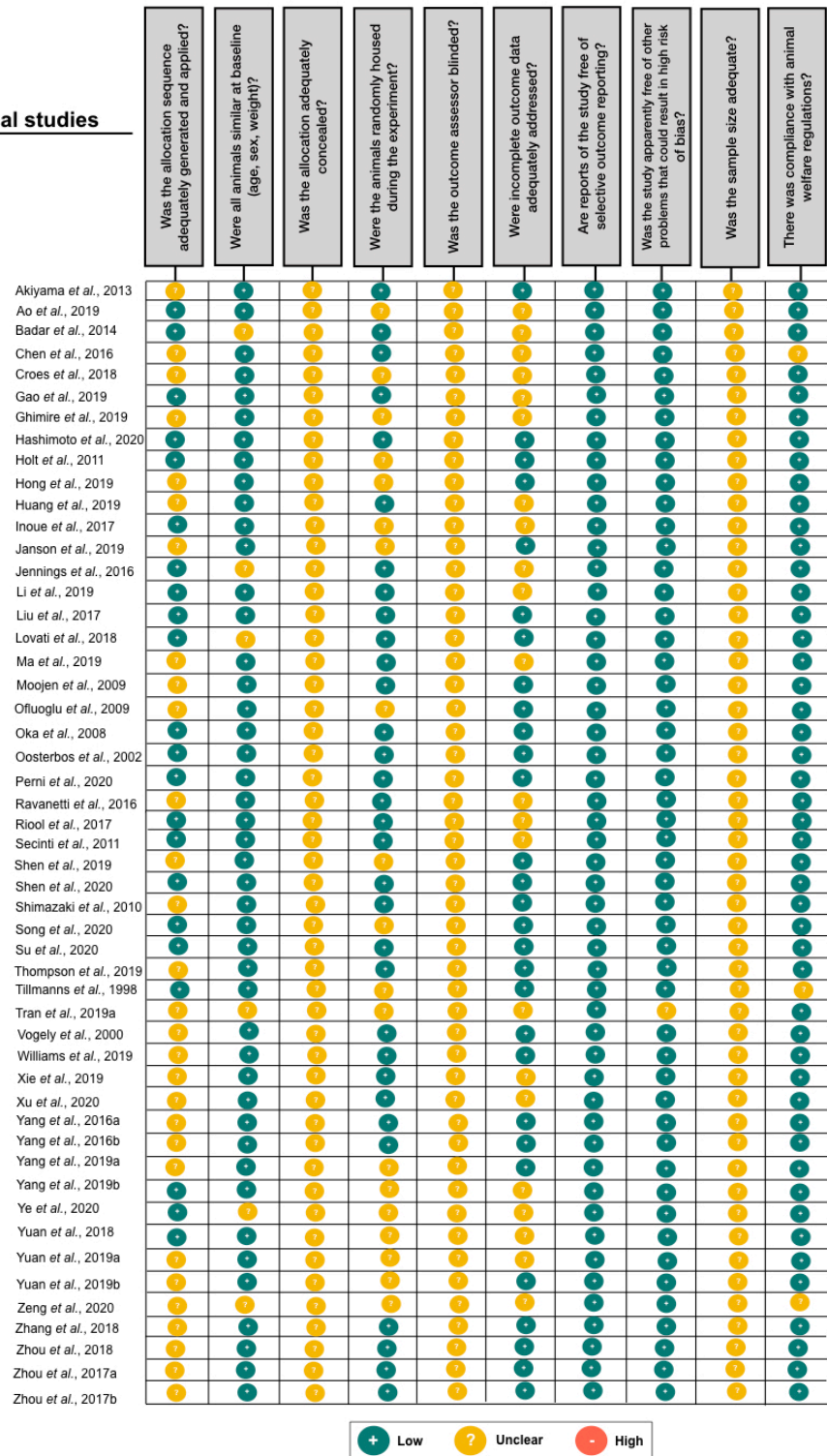


Figure S3. Risk of bias of the individual animal studies included. The items were scored as low risk (green / +), high risk (red / -), or nuclear (yellow / ?).

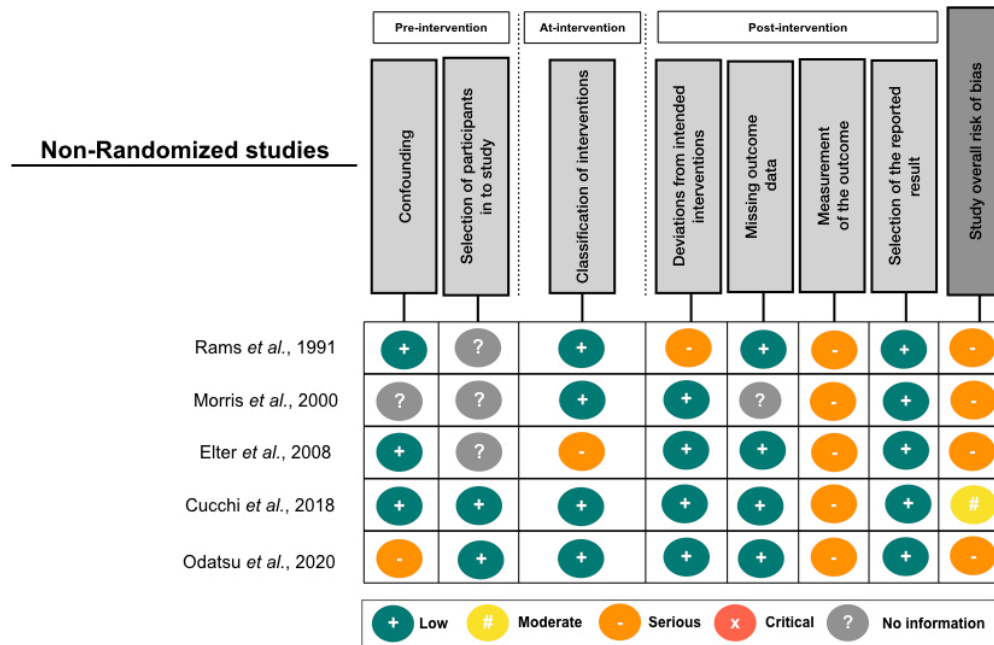


Figure S4. Quality assessment for risk of bias in non-randomized studies included. The items were scored as low risk (green / +), moderate risk (yellow / #), serious risk (orange / -), critical risk (red / x) or no information (gray / ?).

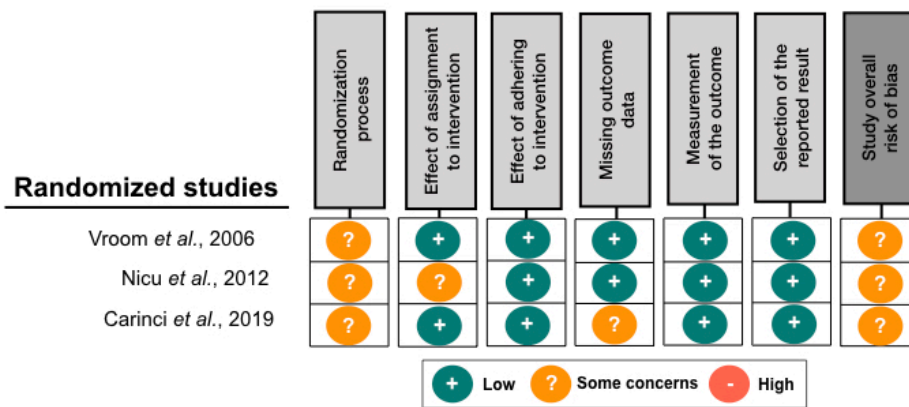


Figure S5. Quality assessment for risk of bias in randomized studies included. The items were scored as low risk (green / +), some concerns (orange / ?), or high risk (red / -).

Supplementary References

- Burda BU, O'Connor EA, Webber EM, Redmond N, Perdue LA. Estimating data from figures with a Web-based program: Considerations for a systematic review. *Res Synth Methods*, 8 (2017) 258-262.
- Higgins JPT, Altman DG, Gøtzsche PC, Jüni P, Moher D, Oxman AD, Sterne JAC. The Cochrane Collaboration's tool for assessing risk of bias in randomised trials. *BMJ* 343 (2011) d5928.
- Hooijmans CR, Rovers MM, de Vries RB, Leenaars M, Ritskes-Hoitinga M, Langendam MW. SYRCLE's risk of bias tool for animal studies. *BMC Med Res Methodol* 26 (2014) 43.
- Moher D, Liberati A, Tetzlaff J, Altman DG; PRISMA Group. Preferred reporting items for systematic reviews and meta-analyses: the PRISMA statement. *PLoS Med* 21 (2009) e1000097.
- Mourad O, Hossam H, Zbys F, Ahmed E. Rayyan — a web and mobile app for systematic reviews. *Systematic Reviews*. 5 (2016) 210.
- Sterne JAC, Hernán MA, Reeves BC, Savović J, Berkman ND, Viswanathan M, Henry D, Altman DG, Ansari MT, Boutron I, Carpenter JR, Chan AW, Churchill R, Deeks JJ, Hróbjartsson A, Kirkham J, Jüni P, Loke YK, Pigott TD, Ramsay CR, Regidor D, Rothstein HR, Sandhu L, Santaguida PL, Schünemann HJ, Shea B, Shrier I, Tugwell P, Turner L, Valentine JC, Waddington H, Waters E, Wells GA, Whiting PF, Higgins JP. ROBINS-I: a tool for assessing risk of bias in non-randomised studies of interventions. *BMJ* 355 (2016) i4919.
- Zaugg LK, Astasov-Frauenhoffer M, Braissant O, Hauser-Gerspach I, Waltimo T, Zitzmann NU. Determinants of biofilm formation and cleanability of titanium surfaces. *Clin Oral Implants Res* 28 (2017) 469-475.
- Al-Ahmad A, Wiedmann-Al-Ahmad M, Fackler A, Follo M, Hellwig E, Bächle M, Hannig C, Han JS, Wolkewitz M, Kohal R. In vivo study of the initial bacterial adhesion on different implant materials. *Arch Oral Biol*. 58 (2013) 1139-1147.
- Svensson S, Suska F, Emanuelsson L, Palmquist A, Norlindh B, Trobos M, Bäckros H, Persson L, Rydja G, Ohrlander M, Lyvén B, Lausmaa J, Thomsen P. Osseointegration of titanium with an antimicrobial nanostructured noble metal coating. *Nanomed* 9 (2013) 1048-56.
- Akiyama T, Miyamoto H, Yonekura Y, Tsukamoto M, Ando Y, Noda I, Sonohata M, Mawatari M. Silver oxide-containing hydroxyapatite coating has in vivo antibacterial activity in the rat tibia. *J Orthop Res* 31 (2013) 1195-200.
- Sinclair KD, Pham TX, Williams DL, Farnsworth RW, Loc-Carrillo CM, Bloebaum RD. Model development for determining the efficacy of a combination coating for the prevention of perioperative device related infections: a pilot study. *J Biomed Mater Res B* 101 (2013) 1143-1153.
- Masci G, Cazzato G, Milano G, et al. The stiff elbow: Current concepts. *Orthop Rev (Pavia)*. 12 (2020) 8661.
- Holt J, Hertzberg B, Weinhold P, Storm W, Schoenfish M, Dahners L. Decreasing bacterial colonization of external fixation pins through nitric oxide release coatings. *J Orthop Trauma* 25 (2011) 432-437.
- Scarano A, Piattelli A, Polimeni A, Di Iorio D, Carinci F. Bacterial adhesion on commercially pure titanium and anatase-coated titanium healing screws: an in vivo human study. *J Periodontol* (2010) Oct;81(10):1466-71. doi: 10.1902/jop.2010.100061. PMID: 20528698.
- Aykut S, Oztürk A, Ozkan Y, Yanik K, Ilman AA, Ozdemir RM. Evaluation and comparison of the antimicrobial efficacy of teicoplanin- and clindamycin-coated titanium implants: an experimental study. *J Bone Joint Surg Br* 92 (2010):159-163.
- Shimazaki T, Miyamoto H, Ando Y, Noda I, Yonekura Y, Kawano S, Miyazaki M, Mawatari M, Hotokebuchi T. In vivo antibacterial and silver-releasing properties of novel thermal sprayed silver-containing hydroxyapatite coating. *J Biomed Mater Res B* 92 (2010) 386-389.
- Grössner-Schreiber B, Teichmann J, Hannig M, Dörfer C, Wenderoth DF, Ott SJ. Modified implant surfaces show different biofilm compositions under in vivo conditions. *Clin Oral Implants Res* 20 (2009) 817-826.
- Moojen DJ, Vogely HC, Fleer A, Nikkels PG, Higham PA, Verbout AJ, Castelein RM, Dhert WJ. Prophylaxis of infection and effects on osseointegration using a tobramycin-periapatite coating on titanium implants--an experimental study in the rabbit. *J Orthop Res* 27 (2009) 710-716.
- Visai L, Rimondini L, Giordano C, Del Curto B, Sbarra MS, Franchini R, Della Valle C, Chiesa R. Electrochemical surface modification of titanium for implant abutments can affect oral bacteria contamination. *J Appl Biomater Biomech* 6 (2008) 170-177.
- Groessner-Schreiber B, Hannig M, Dück A, Griepentrog M, Wenderoth DF. Do different implant surfaces exposed in the oral cavity of humans show different biofilm compositions and activities? *Eur J Oral Sci* 112 (2004) 516-522.
- Scarano A, Piattelli M, Vrespa G, Caputi S, Piattelli A. Bacterial adhesion on titanium nitride-coated and uncoated implants: an in vivo human study. *J Oral Implantol* 29 (2003) 80-85.

- Lucke M, Schmidmaier G, Sadoni S, Wildemann B, Schiller R, Haas NP, Raschke M. Gentamicin coating of metallic implants reduces implant-related osteomyelitis in rats. *Bone* 32 (2003) 521-531.
- Morris HF, Ochi S, Spray JR, Olson JW. Periodontal-type measurements associated with hydroxyapatite-coated and non-HA-coated implants: uncovering to 36 months. *Ann Periodontol* 5 (2000) 56-67.
- Tillmanns HW, Hermann JS, Tiffée JC, Burgess AV, Meffert RM. Evaluation of three different dental implants in ligature-induced peri-implantitis in the beagle dog. Part II. Histology and microbiology. *Int J Oral Maxillofac Implants* 13 (1998) 59-68.
- Vogely HC, Oosterbos CJM, Puts EWA, Nijhof MW, Nikkels PGJ, Fleer A, Tonino AJ, Dhert WJA, Verbout AJ. Effects of Hydroxyapatite Coating on Ti-6Al-4V Implant-Site Infection in a Rabbit Tibial Model. *J Orth* 18 (2000) 3.
- Tillmanns HW, Hermann JS, Tiffée JC, Burgess AV, Meffert RM. Evaluation of three different dental implants in ligature-induced peri-implantitis in the beagle dog. Part II. Histology and microbiology. *Int J Oral Maxillofac Implants* 13 (1998) 59-68.
- Thompson K, Petkov S, Zeiter S, Sprecher CM, Richards RG, Moriarty TF, Eijer H. Intraoperative loading of calcium phosphate-coated implants with gentamicin prevents experimental *Staphylococcus aureus* infection in vivo. *PLoS One* 14 (2019) e0210402.
- Qiu, J.; Qian, W.; Zhang, J.; Chen, D.; Yeung, K.W.; Liu, X. Minocycline hydrochloride loaded graphene oxide enables enhanced osteogenic activity in the presence of Gram-positive bacteria, *Staphylococcus aureus*. *J. Mater. Chem. B* 7 (2019) 3590.
- Hong L, Liu X, Tan L, Cui Z, Yang X, Liang Y, Li Z, Zhu S, Zheng Y, Yeung KWK, Jing D, Zheng D, Wang X, Wu S. Rapid Biofilm Elimination on Bone Implants Using Near-Infrared-Activated Inorganic Semiconductor Heterostructures. *Adv Healthc Mater* 8 (2019) e1900835.
- Tran PA, O'Brien-Simpson N, Palmer JA, Bock N, Reynolds EC, Webster TJ, Deva A, Morrison WA, O'Connor AJ. Selenium nanoparticles as anti-infective implant coatings for trauma orthopedics against methicillin-resistant *Staphylococcus aureus* and *epidermidis*: in vitro and in vivo assessment. *Int J Nanomed* 14 (2019) 4613-4624.
- Zhou J, Li B, Han Y. F-doped TiO₂ microporous coating on titanium with enhanced antibacterial and osteogenic activities. *Sci Rep.* 14 (2018) 17858.
- Yu, X.; Wang, S.; Zhang, X.; Qi, A.; Qiao, X.; Liu, Z.; Wu, M.; Li, L.; Wang, Z.L. Heterostructured nanorod array with piezophototronic and plasmonic effect for photodynamic bacteria killing and wound healing. *Nano Energy* 46 (2018) 29-38.
- Zhang Y, Liu X, Li Z, Zhu S, Yuan X, Cui Z, Yang X, Chu PK, Wu S. Nano Ag/ZnO-Incorporated Hydroxyapatite Composite Coatings: Highly Effective Infection Prevention and Excellent Osteointegration. *ACS Appl Mater Interfaces* 10 (2018) 1266-1277.
- Cucchi A, Molè F, Rinaldi L, Marchetti C, Corinaldesi G. The Efficacy of an Anatase-Coated Collar Surface in Inhibiting the Bacterial Colonization of Oral Implants: A Pilot Prospective Study in Humans. *Int J Oral Maxillofac Implants* 33 (2018) 395-404.
- Zhang, H.; Wang, G.; Liu, P.; Tong, D.; Ding, C.; Zhang, Z.; Xie, Y.; Tang, H.; Ji, F. Vancomycin-loaded titanium coatings with an interconnected micro-patterned structure for prophylaxis of infections: an in vivo study *RSC Adv* 8 (2018) 9223-9231.
- Zhang Y., Suzhou H., Shaoxiong L., Haizhou X., Bailong T., Yao D., Yisi L., Peng L., Kaiyong C. Surface engineering of titanium implants with enzyme-triggered antibacterial properties and enhanced osseointegration in vivo. *J. Mater. Chem. B* 6 (2018) 8090.
- Nagat A., Eva S., Johanna T., Ilkka K., Timo O.N. Early Biofilm Formation on UV Light Activated Nanoporous TiO₂ Surfaces *In Vivo*. *Int J Biomat* (2018) ID 7275617.
- Shiels SM, Bouchard M, Wang H, Wenke JC. Chlorhexidine-releasing implant coating on intramedullary nail reduces infection in a rat model. *Eur Cell Mater* 22 (2018) 178-194.
- Prinz C, Elhensheri M, Rychly J, Neumann HG. Antimicrobial and bone-forming activity of a copper coated implant in a rabbit model. *J Biomater Appl.* 32 (2017) 139-149.
- Zhou J, Li B, Zhao L, Zhang L, Han Y. F-Doped Micropore/Nanorod Hierarchically Patterned Coatings for Improving Antibacterial and Osteogenic Activities of Bone Implants in Bacteria-Infected Cases. *ACS Biomater Sci Eng* 3 (2017) 1437-1450.
- Kao WK, Gagnon PM, Vogel JP, Chole RA. Surface charge modification decreases *Pseudomonas aeruginosa* adherence in vitro and bacterial persistence in an in vivo implant model. *Laryngoscope* 127 (2017) 1655-1661.
- Inoue D, Kabata T, Ohtani K, et al. Inhibition of biofilm formation on iodine-supported titanium implants. *International Orthopaedics* 41(2017) 1093-1099.

- Zhou L, Liu Q, Zhou Z, Lu W, Tao J. Efficacy of tobramycin-loaded coating K-wire in an open-fracture rabbit model contaminated by staphylococcus aureus. *Int J Clin Exp Med* 10 (2017) 6004-6016.
- Liao H, Miao X, Ye J, Wu T, Deng Z, Li C, Jia J, Cheng X, Wang X. Falling Leaves Inspired ZnO Nanorods-Nanoslices Hierarchical Structure for Implant Surface Modification with Two Stage Releasing Features. *ACS Appl Mater Interfaces* 9 (2017) 13009-13015.
- Ma K, Cai X, Zhou Y, Wang Y, Jiang T. In Vitro and In Vivo Evaluation of Tetracycline Loaded Chitosan-Gelatin Nanosphere Coatings for Titanium Surface Functionalization. *Macromol Biosci* 17 (2017) s/n.
- Gerits E, Kucharíková S, Van Dijck P, Erdtmann M, Krona A, Lövenklev M, Fröhlich M, Dovgan B, Impellizzeri F, Braem A, Vleugels J, Robijns SC, Steenackers HP, Vanderleyden J, De Brucker K, Thevissen K, Cammue BP, Fauvart M, Verstraeten N, Michiels J. Antibacterial activity of a new broad-spectrum antibiotic covalently bound to titanium surfaces. *J Orthop Res* 12 (2016) 2191-2198.
- Harrasser N, de Wild M, Gorkotte J, Obermeier A, Feihl S, Straub M, von Eisenhart-Rothe R, Gollwitzer H, Rüegg J, Moser W, Gruner P, Burgkart R. Evaluation of calcium dihydroxide- and silver-coated implants in the rat tibia. *J Appl Biomater Funct Mater*. 14 (2016) e441-e448.
- Yang, Y., Ao, H., Wang, Y. *et al.* Cytocompatibility with osteogenic cells and enhanced *in vivo* anti-infection potential of quaternized chitosan-loaded titania nanotubes. *Bone Res* 4 (2016) 16027.
- Ferreira Ribeiro C, Cogo-Müller K, Franco GC, et al. Initial oral biofilm formation on titanium implants with different surface treatments: An in vivo study. *Arch Oral Biol* 69 (2016) 33-39.
- Jennings JA, Beenken KE, Skinner RA, Meeker DG, Smeltzer MS, Haggard WO, Troxel KS. Antibiotic-loaded phosphatidylcholine inhibits staphylococcal bone infection. *World J Orthop* 18 (2016) 467-474.
- Yang Y, Ao HY, Yang SB, et al. In vivo evaluation of the anti-infection potential of gentamicin-loaded nanotubes on titania implants. *Int J Nanomed* 11 (2016) 2223-2234.
- Kucharíková S, Gerits E, De Brucker K, Braem A, Ceh K, Majdič G, Španič T, Pogorevc E, Verstraeten N, Tournu H, Delattin N, Impellizzeri F, Erdtmann M, Krona A, Lövenklev M, Knezevic M, Fröhlich M, Vleugels J, Fauvart M, de Silva WJ, Vandamme K, Garcia-Forgas J, Cammue BP, Michiels J, Van Dijck P, Thevissen K. Covalent immobilization of antimicrobial agents on titanium prevents Staphylococcus aureus and Candida albicans colonization and biofilm formation. *J Antimicrob Chemother* 71 (2016) 936-945.
- Kuehl R, Brunetto PS, Woischnig AK, Varisco M, Rajacic Z, Vosbeck J, Terracciano L, Fromm KM, Khanna N. Preventing Implant-Associated Infections by Silver Coating. *Antimicrob Agents Chemother* 60 (2016) 2467-75.
- Ravanetti F, Chiesa R, Ossiprandi MC, et al. Osteogenic response and osteoprotective effects in vivo of a nanostructured titanium surface with antibacterial properties. *J Mater Sci Mater Med*. 27 (2016) 52.
- López-Píriz R, Solá-Linares E, Rodriguez-Portugal M, Malpica B, Díaz-Güemes I, Enciso S, Esteban-Tejeda L, Cabal B, Granizo JJ, Moya JS, Torrecillas R. Evaluation in a Dog Model of Three Antimicrobial Glassy Coatings: Prevention of Bone Loss around Implants and Microbial Assessments. *PLoS One* 10 (2015) e0140374.
- Badar M, Rahim MI, Kieke M, et al. Controlled drug release from antibiotic-loaded layered double hydroxide coatings on porous titanium implants in a mouse model. *J Biomed Mater Res A* 103 (2015) 2141-2149.
- Li Y, Xiong W, Zhang C, Gao B, Guan H, Cheng H, Fu J, Li F. Enhanced osseointegration and antibacterial action of zinc-loaded titania-nanotube-coated titanium substrates: in vitro and in vivo studies. *J Biomed Mater Res A* 102 (2014) 3939-3950.
- Wang Z, Wang G, Shan SQ, Hui G, Guo T, Liu G, Zhao Y. In vitro and in vivo study of a sodium chloride impregnated microarc oxidation-treated titanium implant surface. *J. Mater. Chem. B* 2 (2014) 3549.
- Madi M, Zakaria O, Noritake K, Fuji M, Kasugai S. Peri-implantitis progression around thin sputtered hydroxyapatite-coated implants: clinical and radiographic evaluation in dogs. *Int J Oral Maxillofac Implants* 28 (2013) 701-709.
- Bitik, O.; Uzun, H.; Kecik, A. In-Vivo Analysis of Antibacterial Silver Coated Titanium Implants in a Contaminated Rabbit Knee Model. *Turkiye Klinikleri J Med Sci* 33 (2013) 1462-1472.
- Xiao, W., Luo, S., Wei, X., Zhang, C., Huang, W., Chen, J., Rahaman, M. Evaluation of Ti implants coated with Ag-containing borate bioactive glass for simultaneous eradication of infection and fracture fixation in a rabbit tibial model – ERRATUM. *J Mat Res*, 30(2015), 3151-3151.
- Jeyapalina S, Beck JP, Bachus KN, Williams DL, Bloebaum RD. Efficacy of a porous-structured titanium subdermal barrier for preventing infection in percutaneous osseointegrated prostheses. *J Orthop Res* 30 (2012):1304-1311.
- Schaer TP, Stewart S, Hsu BB, Klibanov AM. Hydrophobic polycationic coatings that inhibit biofilms and support bone healing during infection. *Biomaterials* 33 (2012) 1245-1254.
- Secinti KD, Özalp H, Attar A, Sargon MF. Nanoparticle silver ion coatings inhibit biofilm formation on titanium implants. *J Clin Neurosci*. 18 (2011) 391-395.

- Shirai T, Shimizu T, Ohtani K, Zen Y, Takaya M, Tsuchiya H. Antibacterial iodine-supported titanium implants. *Acta Biomater* 7 (2011) 1928-1933.
- Bürgers R, Gerlach T, Hahnel S, Schwarz F, Handel G, Gosau M. In vivo and in vitro biofilm formation on two different titanium implant surfaces. *Clin Oral Implants Res* 21 (2010) 156-164.
- Oka, Y.; Kim, W.-C.; Yoshida, T.; Hirashima, T.; Mouri, H.; Urade, H.; Itoh, Y.; Kubo, T. Efficacy of Titanium Dioxide Photocatalyst for Inhibition of Bacterial Colonization on Percutaneous Implants. *J. Biomed. Mater. Res.* 86 (2008) 530–540.
- Källicke T, Schierholz J, Schlegel U, Frangen TM, Köller M, Printzen G, Seybold D, Klöckner S, Muhr G, Arens S. Effect on infection resistance of a local antiseptic and antibiotic coating on osteosynthesis implants: an in vitro and in vivo study. *J Orthop Res* 24(2006) 1622-1640.
- Watzak G, Zechner W, Tangl S, Vasak C, Donath K, Watzek G. Soft tissue around three different implant types after 1.5 years of functional loading without oral hygiene: a preliminary study in baboons. *Clin Oral Implants Res.* 17 (2006) 229-236.
- Oosterbos CJ, Vogely HCh, Nijhof MW, et al. Osseointegration of hydroxyapatite-coated and noncoated Ti6Al4V implants in the presence of local infection: a comparative histomorphometrical study in rabbits. *J Biomed Mater Res.* 60 (2002) 339-347.
- Carinci F, Lauritano D, Bignozzi CA, et al. A New Strategy Against Peri-Implantitis: Antibacterial Internal Coating. *Int J Mol Sci* 20 (2019) 3897.
- Zhang L, Zhang L, Yang Y, Zhang W, Lv H, Yang F, Lin C, Tang P. Inhibitory effect of super-hydrophobicity on silver release and antibacterial properties of super-hydrophobic Ag/TiO₂ nanotubes. *J Biomed Mater Res B* 104 (2016) 1004-1012.
- Nast S, Fassbender M, Bormann N, Beck S, Montali A, Lucke M, Schmidmaier G, Wildemann B. In vivo quantification of gentamicin released from an implant coating. *J Biomater Appl.* 31 (2016) 45-54.
- Shibli JA, Melo L, Ferrari DS, Figueiredo LC, Faveri M, Feres M. Composition of supra- and subgingival biofilm of subjects with healthy and diseased implants. *Clin Oral Implants Res* 19 (2008) 975-982.
- Vroom MG, Sipos P, de Lange GL, et al. Effect of surface topography of screw-shaped titanium implants in humans on clinical and radiographic parameters: a 12-year prospective study. *Clin Oral Implants Res.* 20 (2009) 1231-1239.
- Rams TE, Roberts TW, Feik D, Molzan AK, Slots J. Clinical and microbiological findings on newly inserted hydroxyapatite-coated and pure titanium human dental implants. *Clin Oral Implants Res* 2 (1991) 121-127.
- de Freitas MM, da Silva CH, Groisman M, Vidigal GM Jr. Comparative analysis of microorganism species succession on three implant surfaces with different roughness: an in vivo study. *Implant Dent* 20 (2011) e14-e23.
- Nicu EA, Van Assche N, Coucke W, Teughels W, Quirynen M. RCT comparing implants with turned and anodically oxidized surfaces: a pilot study, a 3-year follow-up. *J Clin Periodontol.* 39 (2012) 1183-1190.
- Cochis A, Azzimonti B, Della Valle C, Chiesa R, Arciola CR, Rimondini L. Biofilm formation on titanium implants counteracted by grafting gallium and silver ions. *J Biomed Mater Res A.* 103 (2015) 1176-1187.
- Hegazy S, Elmekawy N, Emera RM. Peri-implant Outcomes with Laser vs Nanosurface Treatment of Early Loaded Implant-Retaining Mandibular Overdentures. *Int J Oral Maxillofac Implants* 31 (2016) 424-30.
- Croes M, Bakhshandeh S, van Hengel IAJ, et al. Antibacterial and immunogenic behavior of silver coatings on additively manufactured porous titanium. *Acta Biomater* 81 (2018) 315-327.
- Lovati AB, Bottagisio M, Maraldi S, Violatto MB, Bortolin M, De Vecchi E, Bigini P, Drago L, Romanò CL. Vitamin E Phosphate Coating Stimulates Bone Deposition in Implant-related Infections in a Rat Model. *Clin Orthop Relat Res* 476 (2018) 1324-1338.
- Conserva E, Generali L, Bandieri A, Cavani F, Borghi F, Consolo U. Plaque accumulation on titanium disks with different surface treatments: an in vivo investigation. *Odontology* 106 (2018) 145-153.
- Li D, Lv P, Fan L, Huang Y, Yang F, Mei X, Wu D. The immobilization of antibiotic-loaded polymeric coatings on osteoarticular Ti implants for the prevention of bone infections. *Biomater Sci* 5 (2017) 2337.
- Liu D, He C, Liu Z, Xu W. Gentamicin coating of nanotubular anodized titanium implant reduces implant-related osteomyelitis and enhances bone biocompatibility in rabbits. *Int J Nanomed* 12 (2017) 5461-5471.
- Liu D, He C, Liu Z, Xu W. Gentamicin coating of nanotubular anodized titanium implant reduces implant-related osteomyelitis and enhances bone biocompatibility in rabbits. *Int J Nanomed* 12 (2017) 5461-5471.
- Mauerer A, Stenglein S, Schulz-Drost S, et al. Antibacterial Effect of a 4x Cu-TiO₂ Coating Simulating Acute Periprosthetic Infection-An Animal Model. *Molecules.* 22 (2017) 1042.

- Riool M, Dirks AJ, Jaspers V, de Boer L, Loontjens TJ, van der Loos CM, Florquin S, Apachitei I, Rijk LN, Keul HA, Zaat SA. A chlorhexidine-releasing epoxy-based coating on titanium implants prevents *Staphylococcus aureus* experimental biomaterial-associated infection. *Eur Cell Mater* 14 (2017) 143-157.
- Diefenbeck M, Schrader C, Gras F, Mückley T, Schmidt J, Zankovych S, Bossert J, Jandt KD, Völpel A, Sigusch BW, Schubert H, Bischoff S, Pfister W, Edel B, Faucon M, Finger U. Gentamicin coating of plasma chemical oxidized titanium alloy prevents implant-related osteomyelitis in rats. *Biomaterials* 101 (2016) 156-164.
- Chen R, Willcox MD, Ho KK, Smyth D, Kumar N. Antimicrobial peptide melimine coating for titanium and its in vivo antibacterial activity in rodent subcutaneous infection models. *Biomaterials* 85 (2016) 142-151.
- Zhang L, Yan J, Yin Z, et al. Electrospun vancomycin-loaded coating on titanium implants for the prevention of implant-associated infections. *Int J Nanomed* 9 (2014) 3027-3036.
- Yang C, Li J, Zhu C, Zhang Q, Yu J, Wang J, Wang Q, Tang J, Zhou H, Shen H. Advanced antibacterial activity of biocompatible tantalum nanofilm via enhanced local innate immunity. *Acta Biomater* 89 (2019) 403-418.
- Tan L, Li J, Liu X, Cui Z, Yang X, Zhu S, Li Z, Yuan X, Zheng Y, Yeung KWK, Pan H, Wang X, Wu S. Rapid Biofilm Eradication on Bone Implants Using Red Phosphorus and Near-Infrared Light. *Adv Mater* 30 (2018) e1801808.
- Ofluoglu AE, Baris YS, Aydin MD, Gunaldi M. The Efficacy of The Titanium Oxide-Coated Screws in The Prevention of Implant-Related Infections; an Experimental Animal Study. *J Neurol Science* 31 (2013) 302-309.
- Janson O, Sörensen JH, Strømme M, Engqvist H, Procter P, Welch K. Evaluation of an alkali-treated and hydroxyapatite-coated orthopedic implant loaded with tobramycin. *J Biomater Appl* 34 (2019) 699-720.
- Shen X, Zhang Y, Ma P, Sutrisno L, Luo Z, Hu Y, Yu Y, Tao B, Li C, Cai K. Fabrication of magnesium/zinc-metal organic framework on titanium implants to inhibit bacterial infection and promote bone regeneration. *Biomaterials* 212 (2019) 1-16.
- Shen X, Al-Baadani MA, He H, et al. Antibacterial and osteogenesis performances of LL37-loaded titania nanopores in vitro and in vivo. *Int J Nanomed* 14 (2019) 3043-3054.
- Shen X, Al-Baadani MA, He H, Cai L, Wu Z, Yao L, Wu X, Wu S, Chen M, Zhang H, Liu J. Antibacterial and osteogenesis performances of LL37-loaded titania nanopores in vitro and in vivo. *Int J Nanomed* 14 (2019) 3043-3054.
- Xu X, Li Y, Wang L, Li Y, Pan J, Fu X, Luo Z, Sui Y, Zhang S, Wang L, Ni Y, Zhang L, Wei S. Triple-functional polyetheretherketone surface with enhanced bacteriostasis and anti-inflammatory and osseointegrative properties for implant application. *Biomaterials* 212 (2019) 98-114.
- Peeters E, Hooyberghs G, Robijns S, De Weerd A, Kuchariková S, Tournu H, Braem A, Čeh K, Majdič G, Španič T, Pogorevc E, Claes B, Dovgan B, Girandon L, Impellizzeri F, Erdtmann M, Krona A, Vleugels J, Fröhlich M, Garcia-Forgas J, De Brucker K, Cammue BPA, Thevissen K, Van Dijk P, Vanderleyden J, Van der Eycken E, Steenackers HP. An antibiofilm coating of 5-aryl-2-aminoimidazole covalently attached to a titanium surface. *J Biomed Mater Res B* 107 (2019) 1908-1919.
- Huanga, B.; Tana, L.; Xiangmei, L.; Lib, J.; Wua, S.A facile fabrication of novel stuffwith antibacterial property and osteogenicpromotion utilizing red phosphorus and near-infrared light. *Bioactive Mat* 4 (2019) 2118.
- Yuan Z, Tao B, He Y, Mu C, Liu G, Zhang J, Liao Q, Liu P, Cai K. Remote eradication of biofilm on titanium implant via near-infrared light triggered photothermal/photodynamic therapy strategy. *Biomaterials* 223 (2019) 119479.
- Ao, H.; Yang, S.; Nie, B.; Fan, Q.; Zhang, Q.; Zong, J.; Guo, S.; Zheng, X.; Tang, T. Improved antibacterial properties of collagen I/hyaluronic acid/quaternized chitosan multilayer modified titanium coatings with both contact-killing and release-killing functions. *J. Mater. Chem. B* 7 (2019) 1951.
- Gao C, Cheng H, Xu N, Li Y, Chen Y, Wei Y, Gao B, Fu J, Huo K, Xiong W. Poly(dopamine) and Ag nanoparticle-loaded TiO₂ nanotubes with optimized antibacterial and ROS-scavenging bioactivities. *Nanomed* 14 (2019) 803-818.
- Ma M, Liu X, Tan L, Cui Z, Yang X, Ling Y, Li Z, Zheng Y, Yeung Z. Enhancing the antibacterial efficacy of low-dose gentamicin with 5 minute assistance of phototherapy at 50 °C. *Biomater Sci* 7 (2019) 1437.
- Ghimire A, Skelly JD, Song J. Micrococcal-Nuclease-Triggered On-Demand Release of Vancomycin from Intramedullary Implant Coating Eradicates *Staphylococcus aureus* Infection in Mouse Femoral Canals. *ACS Cent Sci* 5 (2019) 1929-1936.
- Hong L, Liu X, Tan L, Cui Z, Yang X, Liang Y, Li Z, Zhu S, Zheng Y, Yeung KWK, Jing D, Zheng D, Wang X, Wu S. Rapid Biofilm Elimination on Bone Implants Using Near-Infrared-Activated Inorganic Semiconductor Heterostructures. *Adv Healthc Mater* 8 (2019) e1900835.
- Li M, Li L, Su K, et al. Highly Effective and Noninvasive Near-Infrared Eradication of a *Staphylococcus aureus* Biofilm on Implants by a Photoresponsive Coating within 20 Min. *Adv Sci* 6 (2019) 1900599.
- Qianli H, Zhengxiao O, Yanni T, Hong W, Yong L. Activating macrophages for enhanced osteogenic and bactericidal performance by Cu ion release from micro/nano-topographical coating on a titanium substrate. *Acta Biomaterialia* 100 (2019) 415-426.

- Jiang J, Han G, Zheng X, Chen G, Zhu P. Characterization and biocompatibility study of hydroxyapatite coating on the surface of titanium alloy. *Surface & Coatings Technology* 375 (2019) 645–651.
- Qiu J, Qian W, Zhang J, Chen D, Yeung KWK, Liu X. Minocycline hydrochloride loaded graphene oxide enables enhanced osteogenic activity in the presence of Gram-positive bacteria, *Staphylococcus aureus*. *J. Mater. Chem. B* 7 (2019) 3590.
- Thompson K, Petkov S, Zeiter S, Sprecher CM, Richards RG, Moriarty TF, Eijer H. Intraoperative loading of calcium phosphate-coated implants with gentamicin prevents experimental *Staphylococcus aureus* infection in vivo. *PLoS One* 14 (2019) e0210402.
- Williams DL, Epperson RT, Ashton NN, Taylor NB, Kawaguchi B, Olsen RE, Haussener TJ, Sebahar PR, Allyn G, Looper RE. In vivo analysis of a first-in-class tri-alkyl norspermidine-biaryl antibiotic in an active release coating to reduce the risk of implant-related infection. *Acta Biomater* 93 (2019) 36–49.
- Xie K, Zhou Z, Guo Y, Wang L, Li G, Zhao S, Liu X, Li J, Jiang W, Wu S, Hao Y. Long-Term Prevention of Bacterial Infection and Enhanced Osteoinductivity of a Hybrid Coating with Selective Silver Toxicity. *Adv Healthc Mater* 8 (2019) e1801465.
- Yang Y, Liu L, Luo H, Zhang D, Lei S, Zhou K. Dual-Purpose Magnesium-Incorporated Titanium Nanotubes for Combating Bacterial Infection and Ameliorating Osteolysis to Realize Better Osseointegration. *ACS Biomater Sci Eng* 5 (2019) 5368–5383.
- Yang X, Zhang D, Liu G, Wang J, Luo Z, Peng X, Zeng Z, Wang H, Tan JL. Bioinspired from mussel and salivary acquired pellicle: a universal dual-functional polypeptide coating for implant materials. *Materials Chemistry Today* 14 (2019) 100205.
- Yuan Z, Tao B, He Y, Liu J, Lin C, Shen X, Ding Y, Yu Y, Mu C, Liu P, Cai K. Biocompatible MoS₂/PDA-RGD coating on titanium implant with antibacterial property via intrinsic ROS-independent oxidative stress and NIR irradiation. *Biomaterials* 217 (2019) 119290.
- Tran PA, O'Brien-Simpson N, Palmer JA, Bock N, Reynolds EC, Webster TJ, Deva A, Morrison WA, O'Connor AJ. Selenium nanoparticles as anti-infective implant coatings for trauma orthopedics against methicillin-resistant *Staphylococcus aureus* and *epidermidis*: in vitro and in vivo assessment. *Int J Nanomed* 14 (2019) 4613–4624.
- Shevtsov MA, Yuditceva NM, Blinova MI, Voronkina IV, Suslov DN, Galibin OV, Gavrilov DV, Akkaoui M, Raykhtsaum G, Albul AV, Pitkin E, Pitkin M. Evaluation of the temporary effect of physical vapor deposition silver coating on resistance to infection in transdermal skin and bone integrated pylon with deep porosity. *J Biomed Mater Res B* 107 (2019) 169–177.
- Li D, Li Y, Shrestha A, Wang S, Wu Q, Li L, Guan C, Wang C, Fu T, Liu W, Huang Y, Ji P, Chen T. Effects of Programmed Local Delivery from a Micro/Nano-Hierarchical Surface on Titanium Implant on Infection Clearance and Osteogenic Induction in an Infected Bone Defect. *Adv Healthc Mater* 8 (2019) e1900002.
- Gao Q, Feng T, Huang D, Liu P, Lin P, Wu Y, Ye Z, Ji J, Li P, Huang W. Antibacterial and hydroxyapatite-forming coating for biomedical implants based on polypeptidefunctionalized titania nanospikes. *Biomater Sci* 8 (2020) 278–289.
- Odatsu T, Kuroshima S, Sato M, et al. Antibacterial Properties of Nano-Ag Coating on Healing Abutment: An In Vitro and Clinical Study. *Antibiotics (Basel)* 9 (2020) 347.
- Song J, Liu H, Lei M, Tan H, Chen Z, Antoshin A, Payne GF, Qu X, Liu C. Redox-Channelling Polydopamine-Ferrocene (PDA-Fc) Coating to Confer Context-Dependent and Photothermal Antimicrobial Activities. *ACS Appl Mater Interfaces* 12 (2020) 8915–8928.
- Mills, R.J.; Boyling, A.; Cheng, T.L.; Peacock, L.; Savage, P.B.; Tägil, M.; Little, D.G.; Schindeler, A. CSA-90 reduces periprosthetic joint infection in a novel rat model challenged with local and systemic *Staphylococcus aureus*. *J Orthop Res* 38 (2020) 2065–2073.
- Hashimoto A, Miyamoto H, Kobatake T, Nakashima T, Shobuike T, Ueno M, Murakami T, Noda I, Sonohata M, Mawatari M. The combination of silver-containing hydroxyapatite coating and vancomycin has a synergistic antibacterial effect on methicillin-resistant *Staphylococcus aureus* biofilm formation. *Bone Joint Res* 9 (2020) 211–218.
- Tao B, Zhao W, Lin C, Yuan Z, He Y, Lu L, Chen M, Ding Y, Yang Y, Xia Z, Cai K. Surface modification of titanium implants by ZIF-8@Levo/LBL coating for inhibition of bacterial-associated infection and enhancement of in vivo osseointegration. *Chem Eng J* 390 (2020) 124621.
- Li Y, Li L, Ma Y, Zhang K, Li G, Lu B, Lu C, Chen C, Wang L, Wang H, Cui X. 3D-Printed Titanium Cage with PVA-Vancomycin Coating Prevents Surgical Site Infections (SSIs). *Macromol Biosci* 20 (2020) e1900394.
- Zeng J, Wang Y, Sun Z, Chang H, Cao M, Lin K, Xie Y. A novel biocompatible PDA/IR820/DAP coating for antibiotic/photodynamic/photothermal triple therapy to inhibit and eliminate *Staphylococcus aureus* biofilm. *Chem Eng* 394 (2020) 1250172.
- Perni S, Alotaibi HF, Yergeshov AA, Dang T, Abdullin TI, Prokopovich P. Long acting anti-infection constructs on titanium. *J Control Rel* 326 (2020) 91.

- Xu M, Song Q, Gao L, Liu H, Feng W, Huo J, Jin H, Huang L, Chai J, Pei Y, Qu X, Li P, Huang W. Single-step fabrication of catechol- ϵ -poly-L-lysine antimicrobial paint that prevents superbug infection and promotes osteoconductivity of titanium implants. *Chem Eng* 396 (2020) 125240.
- Woelfle UC, Briggs T, Bhattacharyya S, Qu H, Sheth N, Knabe C, Ducheyne P. Dual local drug delivery of vancomycin and farnesol for mitigation of MRSA infection in vivo - a pilot study. *Eur Cell Mater* 40 (2020) 38-57.
- Ye J, Li B, Li M, Zheng Y, Wu S, Han Y. ROS induced bactericidal activity of amorphous Zn-doped titanium oxide coatings and enhanced osseointegration in bacteria-infected rat tibias. *Acta biomaterialia* 107 (2020) 313-324.
- Shen J, Gao P, Han S, Kao RYT, Wu S, Liu XY, Paul SQ, Chu K, Cheung KMC, Yeung KWK. A tailored positively-charged hydrophobic surface reduces the risk of implant associated infections. *Acta biomaterialia* 114 (2020) 421-430.
- Yavari, S.A.; Croes, M.; Akhavan, B; Jahanmards, F.; Eigenhuis, C.C.; Dadbakhsh, S.; Vogely, H.C.; Bilek, M.M.; Fluit, C.C.; Boel, C.H.E. Van der Wal, B.C.H.; Vermonden, T.; Weinans, H.; Zadpoor, A.A. Layer by layer coating for bio-functionalization of additively manufactured meta-biomaterials. *Additive Manufacturing* 32 (2020) 100991.
- K. Su, L. Tan, X. Liu, Z. Cui, Y. Zheng, B. Li, Y. Han, Z. Li, S. Zhu, Y. Liang, X. Feng, X. Wang, S. Wu. Rapid phototherapy for clinical treatment of bacterial infected bone implants by creating oxygen deficiency using sulfur doping. *ACS Nano* (2020) 2077-2089.
- Zhang G, Zhang X, Yang Y, Chi R, Shi J, Hang R, Huang X, Yao X, Chu PC, Zhang X. Dual light-induced in situ antibacterial activities of biocompatible TiO₂/MoS₂/PDA/RGD nanorod arrays on titanium. *Biomater Sci* 8 (2020) 391.

2.2 Polymicrobial biofilms related to dental implant diseases: unraveling the critical role of extracellular biofilm matrix #

Raphael C. Costa¹, Martinna Bertolini², Barbara E. Costa Oliveira³, Bruna E. Nagay¹, Caroline Dini¹, Bruna Benso⁴, Marlise I. Klein⁵, Valentim A. R. Barão^{1,*}, João Gabriel S. Souza^{1,6,7,*}

1 Department of Prosthodontics and Periodontology, Piracicaba Dental School, University of Campinas (UNICAMP), Piracicaba, Brazil.

2 Department of Oral Health and Diagnostic Sciences, University of Connecticut Health Center, Farmington, USA.

3 Graduate Program in Dentistry, University Ceuma (UNICEUMA), São Luís, Brazil.

4 School of Dentistry, Faculty of Medicine, Pontificia Universidad Católica de Chile, Santiago, Chile

5 Department of Dental Materials and Prosthodontics, São Paulo State University, São Paulo, Brazil

6 Dental Science School (Faculdade de Ciências Odontológicas - FCO), Montes Claros, Minas 10 Gerais, 39401-303, Brazil.

7 Dental Research Division, Guarulhos University, Guarulhos, São Paulo, 07023-070, Brazil.

*** Corresponding Authors:**

Valentim A. R. Barão (vbarao@unicamp.br)

João Gabriel S. Souza (jgabriel.ssouza@yahoo.com.br)

Costa RC, Bertolini M, Costa Oliveira BE, Nagay BE, Dini C, Benso B, Klein MI, Barão VAR, Souza JGS. Polymicrobial biofilms related to dental implant diseases: unravelling the critical role of extracellular biofilm matrix. Crit Rev Microbiol. 2023 May;49(3):370-390. doi: 10.1080/1040841X.2022.2062219.

Abstract

Biofilms are complex tri-dimensional structures encase microbial cells in an extracellular matrix comprising self-produced polymeric substances. This matrix rich in extracellular polymeric substance (EPS) contributes to the unique features of biofilm lifestyle and structure, enhancing microbial accretion, biofilm virulence, and antimicrobial resistance. The role of the EPS matrix of biofilms growing on biotic surfaces, especially dental surfaces, is largely unraveled. To date, there is a lack of a broad overview of existing literature concerning the relationship between the EPS matrix and the dental implant environment and its role in implant-related infections. Here, we discuss recent advances in the critical role of the EPS matrix on biofilm growth and virulence on the implant surface and its effect on the etiopathogenesis and progression of implant-related infections. Similar to other biofilms associated with human diseases/conditions, EPS-enriched biofilms on implant surfaces promote microbial accumulation, microbiological shift, cross-kingdom interaction, antimicrobial resistance, biofilm virulence, and, consequently, peri-implant tissue damage. But intriguingly, the protagonism of EPS role on implant-related infections and the development of matrix-target therapeutic strategies has been neglected. Finally, we highlight the need for more in-depth analyses of polymicrobial interactions within EPS matrix and EPS-targeting technologies' rationale for disrupting the complex biofilm microenvironment with more outstanding translation to implant applications in the near future.

Keywords: extracellular matrix; extracellular polymeric substances (EPS); microenvironments; polymicrobial biofilm; spatial organization; virulence.

1. Introduction

Polymicrobial biofilms are complex structures that comprise microbial cells in highly organized communities encased in an extracellular matrix containing self-produced extracellular polymeric substances (EPS), the scaffold for biofilms' three-dimensional architecture (Costerton et al., 1995; Flemming; Wingender, 2010a; Guggenheim, 1970). In the oral cavity, the microbiota is organized in biofilms on teeth and mucosa surfaces (and on restorative and implant materials); although some microorganisms can be free-floating in saliva (or gingival crevicular fluid), representing the microbial cells dispersed or dislodged from distinct surfaces (Baker et al., 2017; Dewhirst et al., 2010). Microorganisms growing as biofilms have several advantages when compared to planktonic cells, and this is primarily due to the presence of an extracellular matrix that favors their aggregation, maturation, nutrient availability, and antimicrobial protection, factors that enhance these microorganisms virulence (Bowen et al., 2018). Although the biofilm matrix comprises a complex array of components, this unique environment has been attributed to the EPS matrix, which favors cell-cell communication and cross-kingdom interactions (Flemming; Wingender, 2010a; Koo et al., 2017). In a range of oral biofilms, only ~ 5-35% of the total volume represents microbial cells, while the remaining content comprises their respective EPS matrix (Dragoš; Kovács, 2017; Guzmán-Soto et al., 2021).

Although the role of EPS matrix on biofilms growing on native human surfaces, especially oral tissues, has been widely discussed (Flemming; Wingender, 2010b; Karygianni et al., 2020; Koo; Falsetta; Klein, 2013; Serrage et al., 2021), further information is still missing for biofilms growing on dental implanted devices, where biofilms may also synthesize high amounts of EPS and could directly affect its potential to trigger infectious diseases. In this perspective, the EPS matrix of implant-related biofilms has been considered a relevant factor to promote the microbial shift from health-associated condition to a dysbiotic and more pathogenic biofilm (Arciola; Campoccia; Montanaro, 2018; Costerton; Montanaro; Arciola, 2005; Daubert; Weinstein, 2019; Mombelli; Décaillot, 2011). Furthermore, since the microbial composition of biofilms reflects the environmental conditions (Mombelli; Décaillot, 2011), the EPS matrix can create a suitable microenvironment responsible for disrupting the commensal state leading to microbiological shift due to the overgrowth of putative and pathogenic anaerobic microbial species (Costa et al., 2020; Souza et al., 2019). These pathogenic biofilms formed on implant surfaces have been associated with increased mucosal

damage (Costa et al., 2020) and the development of peri-implant diseases (Berglundh et al., 2018a). Moreover, previous evidence from our group has shown that titanium (Ti) implant surfaces can modulate the expression of bacterial exoenzymes responsible for synthesizing EPS, thus enhancing microbial accumulation (Souza et al., 2020c).

For dental implant-related infections, this microbiological shift often leads to the development of inflammatory disease processes known as peri-implant mucositis and peri-implantitis around infected implant devices (Berglundh et al., 2018a), which has been considered the main reason for late dental implant treatment failures (Salvi; Cosgarea; Sculean, 2017). Nowadays, although systemic antimicrobial therapies are considered the gold standard as adjuncts to mechanical debridement for infections around natural teeth (Teughels et al., 2020), they are often inefficient against implant-related biofilms (Shibli et al., 2019). This trait has been attributed to the EPS presence and its ability to form a protective barrier for microbial communities and difficulties associated with removing biofilm from the complex implant surface (Costa et al., 2020). In this regard, EPS targeting therapies have been proposed as potential strategies for digesting biofilms' protective matrix barrier, facilitating antimicrobial access and diffusion into the EPS structure, and killing the exposed microbial cells in dental (Kim et al., 2018a) and implant (Costa et al., 2020) surfaces.

Several outstanding reviews have discussed the role of biofilm matrix or bacteria-matrix interactions in dental biofilms (Bowen et al., 2018; Branda et al., 2005; Flemming; Wingender, 2010a; Karygianni et al., 2020), but its effect on the pathogenesis of implant-related infections has been neglected. Here, we primarily focused on recent scientific evidence towards the critical role of the EPS matrix in the growth and virulence of the polymicrobial biofilms related to Ti-based dental implants. Furthermore, we summarized relevant concepts concerning biofilm matrix biology to generate novel questions and hypotheses for innovative research advances in the field of implant dentistry.

2. Dental implant-related biofilms: matrix-encased polymicrobial communities

The oral cavity supports the second largest and diverse microbiome in the human body (Baker et al., 2017; Dewhirst et al., 2010), and, therefore, it is a suitable environment for microbial adhesion and accumulation. Upon implant placement, the surface is immediately coated by a protein layer adsorbed from biological fluids, such as saliva or blood plasma, named pellicle (Arciola; Campoccia; Montanaro, 2018). Since proteins'

adsorption on implants is the first critical step for microbial colonization and host cell adhesion (Rabe; Verdes; Seeger, 2011; Souza et al., 2020b), we can expect some differences between dental implants and oral surfaces for biofilm growth. The substrate (*i.e.*, the surface on which biofilm develops) physicochemical properties, such as surface topography, electrochemical charges, wettability, chemical composition, and roughness, may dictate the proteomic profile of each substrate (Dodo et al., 2013; Fürst et al., 2007). Particularly, Ti material has shown specificity to protein layers adsorbed from saliva and blood plasma, which in turn will select the adhesion of certain early colonizers (Souza et al., 2020b). In addition, the recognition of some protein pellicle receptors by early colonizing bacteria allows the selection of key species to adhere and accumulate on exposed biomedical surfaces (Kolenbrander et al., 2006). Thus, the complex dynamics of biofilm-assembly comprises several events co-occurring across space and time, on a surface, whereby microenvironments factors, host interactions, and unique properties can influence this entire process (Branda et al., 2005; Xiao et al., 2012). We have previously shown an adaptation of the ecological plaque hypothesis for implant-related biofilm describing a microbiological transition from a healthy oral community to a disease-associated community on biomaterials, as well as factors leading to microbiological shift or controlling biofilm growth and disease progression (Costa et al., 2021b; Souza et al., 2021).

Dental implant-related biofilms are dynamic and well-structured, including many more components than just viable microbial cells (Daubert; Weinstein, 2019). During biofilm assembly, a complex three-dimensional matrix structure composed of extracellular polymers, proteins, eDNA, and others contributes to biofilms' matrix scaffold and architecture (Branda et al., 2005). Among the biofilm matrix components, extracellular polysaccharides synthesized by bacterial enzymes modulate biofilm architecture, drastically promoting microbial accumulation (Karygianni et al., 2020). Clustering and microcolony assembly depend on the EPS matrix (Flemming; Wingender, 2010a). Oppositely, in the absence of the extracellular polysaccharides, the bacterial cells cannot aggregate and expand three-dimensionally (Xiao et al., 2012). A recent study developed by Paula and coworkers (2020) using a 3D-morphometric analysis has shown that the dynamics of microbial population growth in biofilms resemble spatial and structural aspects of urbanization (Figure 1). This urbanization analogy is related to the fact that bacterial can colonize the surfaces ("terrains"), and a subset of the bacterial species can continue to grow/co-aggregate when structuring molecules are produced

("buildings"). The EPS matrix-encased polymicrobial communities drive the development of larger structures with distinct community organization and structural patterns ("cities"), which in turn merge, resulting in a larger biofilm superstructure ("megacity") (Paula; Hwang; Koo, 2020). We emphasize that this conceptual framework may lead to alternative ways of studying the biofilm-assembly mechanisms and developing therapeutic strategies to prevent or reduce EPS matrix synthesis on dental as well as implant surfaces.

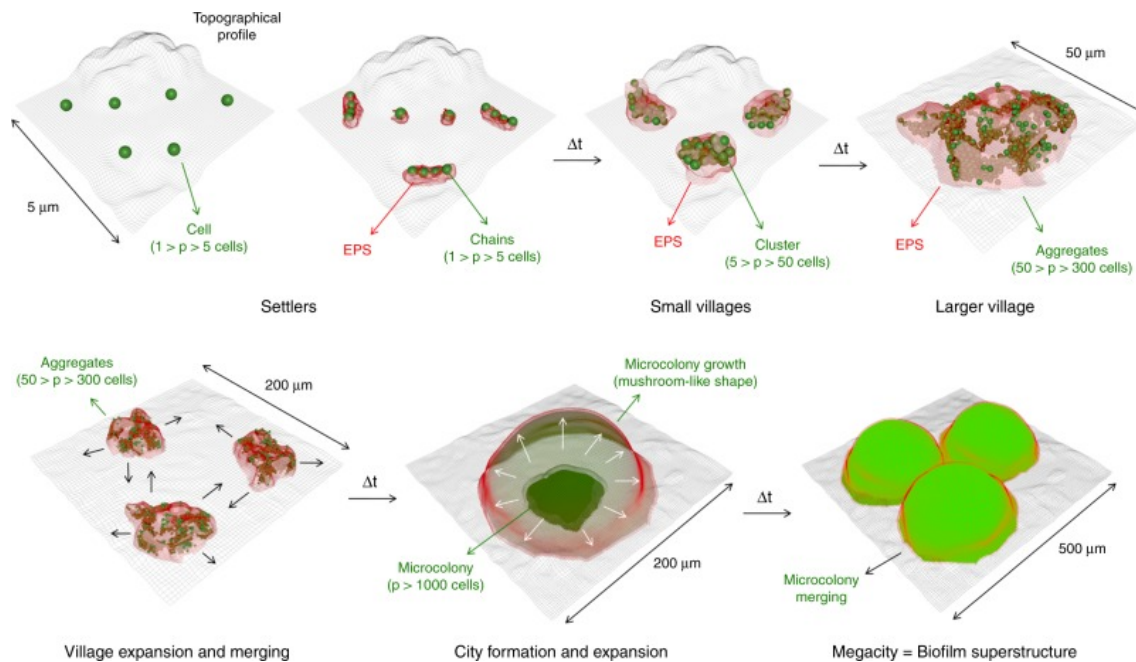


Figure 1. Schematic depiction for the spatiotemporal microbial population growth during biofilm development on the dental surface (from submicron to submillimeter-scale). The biofilm assembly can be modulated by the type of settlers, neighboring cells, and further community merging and scaffolding are occurring at various scales. It was reprinted (adapted) from Paula, Hwang, and Koo (2020); Copyright (2020), with permission from Springer Nature in terms of Creative Commons CC BY license. Of note, Δt = difference between two-time scales; p = population of bacterial cells.

3. EPS matrix: Assembling a complex microenvironment around the dental implant

Oral biofilm studies have increased the knowledge on composition and functions of the EPS matrix, which is associated with the properties of these biofilms (Bowen et al., 2018; Flemming; Wingender, 2010a). However, it is noteworthy that biofilm formation on Ti implant surfaces has unique features related to material composition, surface properties, microenvironment conditions, and host-material interactions (Al-Ahmad et al., 2010). Consequently, the knowledge on biofilm formation on oral surfaces cannot be transferred to implant surfaces (Souza et al., 2021); this is a developing research field with few studies investigating EPS matrix related to polymicrobial communities on dental implant surfaces. Thus, this section summarizes what is currently known and refines

critical concepts and mechanisms in EPS matrix attributes with possible translatability for dental implant applications.

3.1 EPS matrix composition

Biofilm matrix is an essential feature of polymicrobial communities, mainly attributed to EPS content (Figure 2) (Flemming; Wingender, 2010a). Interestingly, the term "matrixome" was recently coined to describe the vast array of biomolecules on EPS matrix content and their molecular, structural, and functional diversity, creating a unique lifestyle for biofilm assembly and growth (Karygianni et al., 2020). However, EPS content is directly affected by microbial species in the biofilm, the surface where the biofilm is growing, and, mainly, the type and availability of nutrients (Flemming; Wingender, 2010a). Since carbohydrates from the human diet have been considered the primary substrate for exopolysaccharides synthesis, the role of carbohydrates has been extensively investigated in the literature (Costa-Oliveira; Cury; Ricomini-Filho, 2017a; Koo; Falsetta; Klein, 2013; Paes Leme et al., 2008; Souza et al., 2019), the reason why it will be firstly approached in this subtopic.

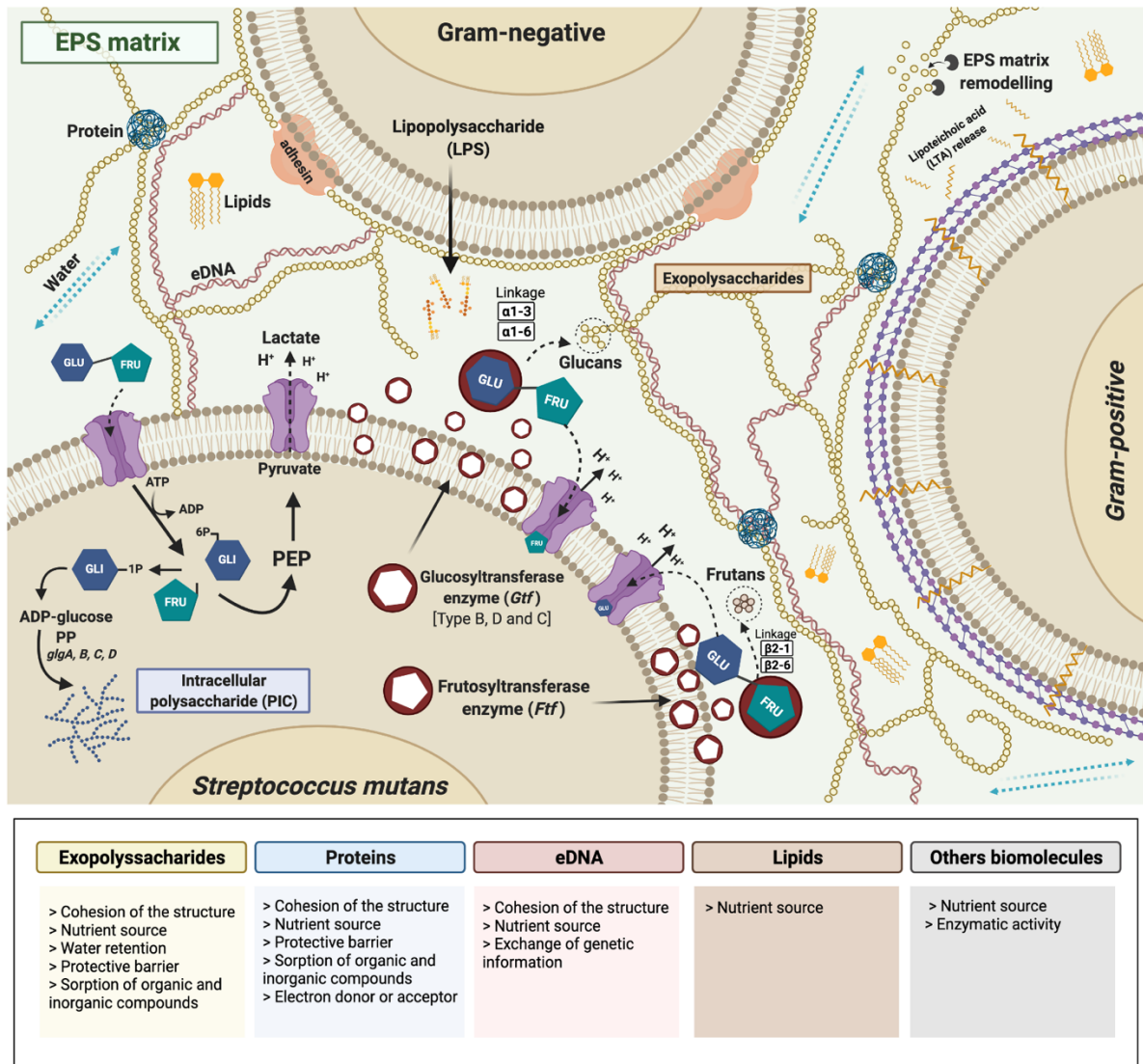


Figure 2. The schematic representation of the EPS biofilm matrix (top panel) and their main components and functions (bottom panel). The biofilm matrix (in green) consists of a wide array of functional biomolecules such as exopolysaccharides, proteins, eDNA, lipids, and others organized into a confined space with unique attributes that provide a functional versatility for biofilm lifestyle. The drawing was created with BioRender.com (License number: VH22WQBLSE).

Among dietary sugars, sucrose is the central molecule that can negatively affect the biofilm symbiosis in distinct polymicrobial diseases (Costa-Oliveira; Cury; Ricomini-Filho, 2017b; Lula et al., 2014; Souza et al., 2019). Furthermore, sucrose is the only substrate for insoluble polysaccharides formation, the main component of EPS biofilm matrix, due to its molecular structure (Russell et al., 1988). This process occurs because of the atypical glycosidic linkage presented in this disaccharide (composed of glucose and fructose molecules) that, upon breaking, releases enough energy for starting a

polysaccharide chain synthesis (Bowen; Koo, 2011; Colby; Russell, 1997). Distinct enzymes can promote the rupture of that linkage, but, apart from invertases that only release the free monosaccharides, the transferases start the transfer of glucose or fructose units for developing glucans and fructans polymers (Bowen; Koo, 2011; Colby; Russell, 1997; Takahashi, 2015), through glucosyltransferase (Gtf) and fructosyltransferase (Ftf) action, respectively. Therefore, extracellular Gtfs hydrolyze sucrose from the host diet to synthesize glucans, formed in various proportions of α -1,6 and α -1,3-linkages (Vacca-Smith et al., 1996). These polymers are pivotal components of the EPS matrix and present distinguished functions as described afterward (please, see Matrix function subtopic).

Despite the purely chemical approach, it is essential to understand how the differences among polysaccharides linkages are decisive when evaluating biofilm resistance or virulence to conventional antimicrobials and disinfectants. In other words, glucans (glucose-based polysaccharides) derived from sucrose metabolism by Gtf bacterial exoenzymes can be water-soluble or water-insoluble molecules (Bowen; Koo, 2011). The differences in solubility are due to the linkages between glucose units, thereby being soluble when predominately presenting α 1,6(Glc \rightarrow Glc) bonds, insoluble when showing α 1-3(Glc \rightarrow Glc) bonds, or mixed when comprising α 1-3 and α 1-6(Glc \rightarrow Glc) bonds (Bowen; Koo, 2011; Hayacibara et al., 2004; Russell et al., 1988). A range of microorganisms can produce and secrete Gtf enzymes, but we bring readers' attention firstly to *Streptococcus mutans* and other *Streptococcus* species.

S. mutans in a polymicrobial biofilm associated with sucrose can significantly alter the entire biofilm composition by different mechanisms (Souza et al., 2019; Xiao et al., 2012). In this context, GtfB from *S. mutans* is important not only due to the synthesis of a particular insoluble polymer but also because this enzyme can attach to other microorganisms non-producers of exopolysaccharides and help on co-aggregation of bacteria and fungi, such as the fungal *Candida albicans* (Gregoire et al., 2011; Souza et al., 2020c), an opportunistic pathogen of interest. Furthermore, since the sticky and well-structured EPS matrix can be produced by other microorganisms not abundant in the community, focusing on the interkingdom interaction could bring us significant findings for understanding biofilm virulence traits (Lamont; Koo; Hajishengallis, 2018). Interkingdom interactions may generate modified patterns of exopolymeric matrix scaffold, since microorganisms produce polymers holding specific features. As previously reported, we can consider there is a matrixome in oral biofilms that ensemble diverse biomolecules holding distinct structures and functions (Karygianni et al., 2020). In this

way, the association between *S. mutans* and its α 1-3 glucan rich matrix and the β -glucans and mannans produced by *C. albicans* (Hwang et al., 2017), can result in a more structured scaffold that might shelter diverse microorganisms, enhancing antifungal resistance (Kim et al., 2018a), impairing the inner pH buffering by saliva (Sampaio et al., 2019), being a source for different biomolecules (Flemming; Wingender, 2010a), or even inducing the complete quorum-sensing system in the bacteria (Sztajer et al., 2014), events that assure biofilm development and allow the biofilm virulence.

C. albicans is a dysmorphic microorganism, and its ability to switch between yeast and hyphal forms is crucial to its ability to form biofilms and invade the host tissues (Bertolini et al., 2021). In addition, the different polysaccharides produced by this fungus are also pivotal for biofilm formation and architecture, being the chemical differences a crucial factor for this purpose. *C. albicans* can synthesize β -1,3-glucan, β -1,6-glucan, and mannans, which together form a mannan–glucan complex that composes the biofilm matrix (Khoury et al., 2020; Mitchell et al., 2015). In the past, it was questioned whether the polymers found in the *C. albicans* biofilm matrix originated from shed cell components. However, it is currently known that there are differences between fungal cell-wall components and the produced matrix, including the number of monomers in the mannan matrix and the branching characteristics of the β -glucans, for example, hence supporting the ability of fungal species to produce EPS-rich matrix as well (Lopez-Ribot, 2014; Pierce et al., 2017).

Combining these fungal polymers and streptococcal exopolysaccharides can generate a more virulent biofilm, favoring the overgrowth of both species (Khoury et al., 2020; Martorano-Fernandes et al., 2020). Furthermore, early colonizers, such as those Streptococci from the mitis group, also synthesize carbohydrate polymers that are of great importance for biofilm establishment, development, and virulence traits (Souza et al., 2020d). For example, *S. oralis* secretes the extracellular enzyme GtfR (Fujiwara et al., 2000), responsible for producing an α -glucan (mostly α -1,6 linked glucose) that is part of the biofilm matrix. When interacting with *C. albicans*, hypervirulent biofilms are originated due to the cross-kingdom interaction favored by the polymers synthesized by GtfR (Souza et al., 2020c). According to Souza *et al.* (2020c), on Ti surface compared to a plastic surface, *C. albicans* co-inoculation with *S. oralis* augmented the amount of α -glucan matrix by increasing bacterial cell numbers or *gtfR* gene expression, suggesting an essential role of implant material properties to enhance EPS matrix assembly (Souza et al., 2020c). Moreover, GtfG from *S. gordonii* also play a role in promoting bacterial

binding to *C. albicans* which leads to increased accretion of streptococcal cells in dual-species model and enhanced biofilm growth (Ricker; Vickerman; Dongari-Bagtzoglou, 2014)

Another relevant point is that EPS synthesis enhances microbial attachment and increases biofilm thickness and volume, which may determine biofilm viscoelasticity (Karygianni et al., 2020). This modification can also change the oxygen availability and hence biofilm composition in terms of the microbial population, depending on the evaluated niche, whether in more profound or more superficial layers, considering that a gradient emerges in the biofilm as it develops, modifying its balance (Marsh; Bradshaw, 1997). As an example, it was recently suggested that cariogenic, periodontal, and peri-implant biofilms might share a common risk factor that is the exposure to carbohydrates on dental (Lula et al., 2014; Nyvad; Takahashi, 2020) and implant (Souza et al., 2019) surfaces.

Thus, if sucrose negatively modulates biofilm virulence, its role was questioned in a periodonto-pathogenic biofilm, for example. However, recently Costa and coworkers (2020) pointed out that the presence of an EPS-enrich matrix can shift the microbial composition of supragingival biofilms by favoring anaerobic species overgrowth, including microorganisms often associated with implant-related infections (Costa et al., 2020). In a nutshell, exopolysaccharides synthesized under sucrose exposure changed biofilm structure and biovolume so that more virulent microorganisms, commonly found in periodontal pockets, could grow and persist in a seemingly adverse condition (Costa et al., 2020). It is essential to highlight that the EPS matrix is still synthesized in the absence of sucrose (Russell et al., 1988). However, the matrix constituents acquire another composition and structural profile that is still not well understood.

Carbohydrates have also been suggested as the main component of the periodontal biofilm matrix, as shown in *Porphyromonas gingivalis* and *Fusobacterium nucleatum* dual-species biofilms, which can produce excellent protein content (Ali Mohammed et al., 2013). However, protein content is dynamic and seems to be modified by the carbohydrate exposure and by the presence of sucrose-induced extracellular polysaccharides (Moi et al., 2012; Paes Leme et al., 2008). The types of exopolysaccharides produced by some bacteria species associated with periodontal disease development and detected in dental implant biofilms were characterized using *in vitro* single-species biofilms in the absence of sucrose. These included PGA, a β -1,6-linked N-acetyl-D-glucosamine (GlcNAc) polymer, by *Aggregatibacter*

actinomycetemcomitans (Izano et al., 2008; Kaplan et al., 2004), mannose by *Prevotella intermedia* and *Prevotella nigrescens* (Yamanaka et al., 2009; Yamane et al., 2005), a mix of mostly mannose with low levels of rhamnose, glucose, galactose, and 2-acetamido-2-deoxy-D-glucose by *Porphyromonas gingivalis* (Comstock; Kasper, 2006; Farquharson; Germaine; Gray, 2000), and glycoproteins by *Tannerella forsythia* (Honma et al., 2007). Despite of implant-related diseases are polymicrobial infections, there are still many unanswered questions regarding the role of the EPS biofilm matrix in the complex interplay between bacteria and host, which is only possible when evaluated simplified models of oral biofilms in mechanistic studies.

3.2 Metabolic changes in biofilm composition and EPS

Within the context of polymicrobial bacterial communities *Streptococci* and *Actinomyces* species are the major initial colonizers, helping to further mediate the biofilm community as the maturation process occur, this process has been shown in enamel (Kolenbrander, 2000) and titanium dental implants (Bermejo et al., 2019). At early stages fructans and soluble glucans present in the biofilm are metabolized by the early colonizers to produce exo- and/or endo-hydrolytic enzymes (Koo; Falsetta; Klein, 2013). It is apparent that glucan synthesized by *Streptococci* Gtf in salivary pellicle provides increased binding for not only other *Streptococci*, but also for *Actinomyces* species (Banas; Vickerman, 2003). In titanium, *Streptococcus* colonization increases over time, with a positive correlation with *A. naeslundii* loads, while *Fusobacterium nucleatum* increases in a later time (Bermejo et al., 2019). Importantly, *Fusobacterium* plays a central role as it mediates coaggregation and allows late colonizers anaerobes to become part of the biofilm, and it has been shown to promote *P. gingivalis* and *A. actinomycetemcomitans* co-aggregation in mature biofilms (Bermejo et al., 2019). At this stage, a very complex nutritional bacterial relationships will take place in polymicrobial biofilms communities because metabolic communication will start to develop with the main source of nutrients for some bacteria being the products of metabolism of other bacteria (Hojo et al., 2009), as a results specific metabolic pathways can be associated with the different biofilm layers, depending on the gradient of metabolic requirements across the biofilm (Mazumdar; Amar; Segrè, 2013). Hence, this matrix composition (enriched of protein and acid nucleic) in the presence of these key later colonizers can optimize its metabolism and adapts/survives within the mixed-species community in response to a dynamically changing environment. Consequently, this condition reflects

the intricate physiological processes linked to the expression of virulence by periodontopathogens within complex biofilms, favoring the overgrowth of late microbial species and leading to more aggressive and pathogenic biofilm (Jakubovics et al., 2021). An *in vitro* study by Ali Mohammed *et al.* (2013) suggests that *F. nucleatum* has helped the growth of *P. gingivalis* in co-culture of the two species, with proteins and carbohydrates being the major components of the biofilm matrix. Importantly treatment with proteinase K was shown to be insufficient to disperse this carbohydrate-rich matrix and, therefore, would not be an effective treatment to allow increased diffusion of antimicrobial drugs within the biofilm complex (Ali Mohammed et al., 2013). Thus, the better understanding of EPS on these polymicrobial biofilms should lead to more efficient control strategies on wheatear the EPS is highly composed by carbohydrates or proteins.

Other bacteria cells interactions can also be mediated by EPS content. For instance, studies on *S. mutans* mixed with *A. naeslundii* and *Streptococcus oralis* demonstrated critical differences in the exopolysaccharide matrix assembly (Klein et al., 2012). Notably, the virulence genes expression related to glucan synthesis and remodeling (e.g.; *gtfBC*, *dexA*, *gbpB*) are generally augmented in an acidic environment in three-species biofilms compared with monospecies biofilms (Klein et al., 2012). Overall, biofilms composed with *Aggregatibacter actinomycetemcomitans* form microcolonies with the tight formation with fibrils of fimbriae observed, which help on cell-to-surface and cell-to-cell interactions (Inoue et al., 2017). Furthermore, lipoteichoic acids from *S. gordonii* and *Lactobacillus plantarum* are present outside the cell and associated with glucosyltransferases, particularly over the later stages during maturation of the matrix (Pierre et al., 2012). Regarding eDNA content, few periodontal pathogen biofilms have been thoroughly examined for their reliance on extracellular DNA. However, recent reviews (Jakubovics et al., 2021; Serrage et al., 2021) have summarized that biofilm matrix stability depends on eDNA in living biofilms, thus being a relevant factor considered in the design of EPS strategy approaches (Peterson et al., 2013). Additionally, fungi-bacterial interactions can also be modulated by the EPS matrix, which is composed mainly of α -mannan, β -1,6 glucan, and β -1,3 glucan, essential components for cross-kingdom microbial interactions and diseases progression (Bertolini et al., 2021).

3.3 EPS matrix functions

Due to the presence of long carbohydrate polymeric chains, the main functions of the EPS matrix include structuration, protection, nutrition, and survival (Costa-Oliveira et al., 2021; Costa-Oliveira; Cury; Ricomini-Filho, 2017a; Klein et al., 2015). Moreover, the presence of EPS allows assembling a three-dimensional organization that characterizes a biofilm (Costa et al., 2020; Koo; Falsetta; Klein, 2013; Xiao et al., 2012). In this regard, the formation of organized niches (or structures), named microcolonies, is responsible for heterocompartments creation that can generate distinct microenvironments inside the same community, including areas with very reduced oxygen availability (Koo et al., 2010; Paula; Hwang; Koo, 2020). Consequently, one single biofilm harbors species and pH variation in different areas due to the specific environmental changes, allowing adaptation and biodiversity (Bowen et al., 2018).

The well-structured matrix has a significant effect when evaluating the impact of antimicrobials on oral biofilms (Jakubovics et al., 2021; Ren et al., 2019). An EPS-enriched biofilm shows a reduced antimicrobial susceptibility on dental (Xiao et al., 2012) and implant (Costa et al., 2020) surfaces. Recently, our group demonstrated that exopolysaccharides reduce the biofilm susceptibility to chlorhexidine treatments on Ti material (Figure 3) (Costa et al., 2020). These findings have been explained by the higher biofilm volume, which impairs the diffusion of antimicrobials in all the biofilm layers due to the protection that polymeric substances could exert on the microbial cell by sheltering it (Koo et al., 2017). Additionally, it is hypothesized that carbohydrate-based polysaccharides are negatively charged due to the presence of lipoteichoic acid and eDNA, thereby binding to the chlorhexidine (a cationic molecule - positively charged) and inactivating it (Hope; Wilson, 2004). Another trait in biofilms that accounts for increased tolerance to antimicrobials of inhabiting microbial cells is that these cells can be at distinct growth phases, influenced by the different gradients that the matrix provides (Marsh; Bradshaw, 1997). Also, the enrichment of EPS in the matrix affects the diversity of the members in the microbial community (Costa et al., 2020); thereby, an antimicrobial molecule that may target preferable Gram-negative bacteria might not affect Gram-positive bacteria or fungi. In fungal biofilms, the drug resistance properties were found to occur also due to the presence of β -glucans and mannans, especially when organized as mannan–glucan complexes (Mitchell et al., 2015). Moreover, Gtf enzymes bound to *Candida* can also produce glucan polymers and promote antifungal resistance (Kim et al., 2018a). In summary, the exopolysaccharides can protect microorganisms from external factors, which also occurs in dual-species biofilms containing *C. albicans* and hence

mannans synthesis (Montelongo-Jauregui et al., 2018). This protection trait can arise upon antibiotics exposure and against host immune responses (also exerted by the eDNA), bringing advantages to this well-organized community (Flemming; Wingender, 2010a; Jakubovics et al., 2021).

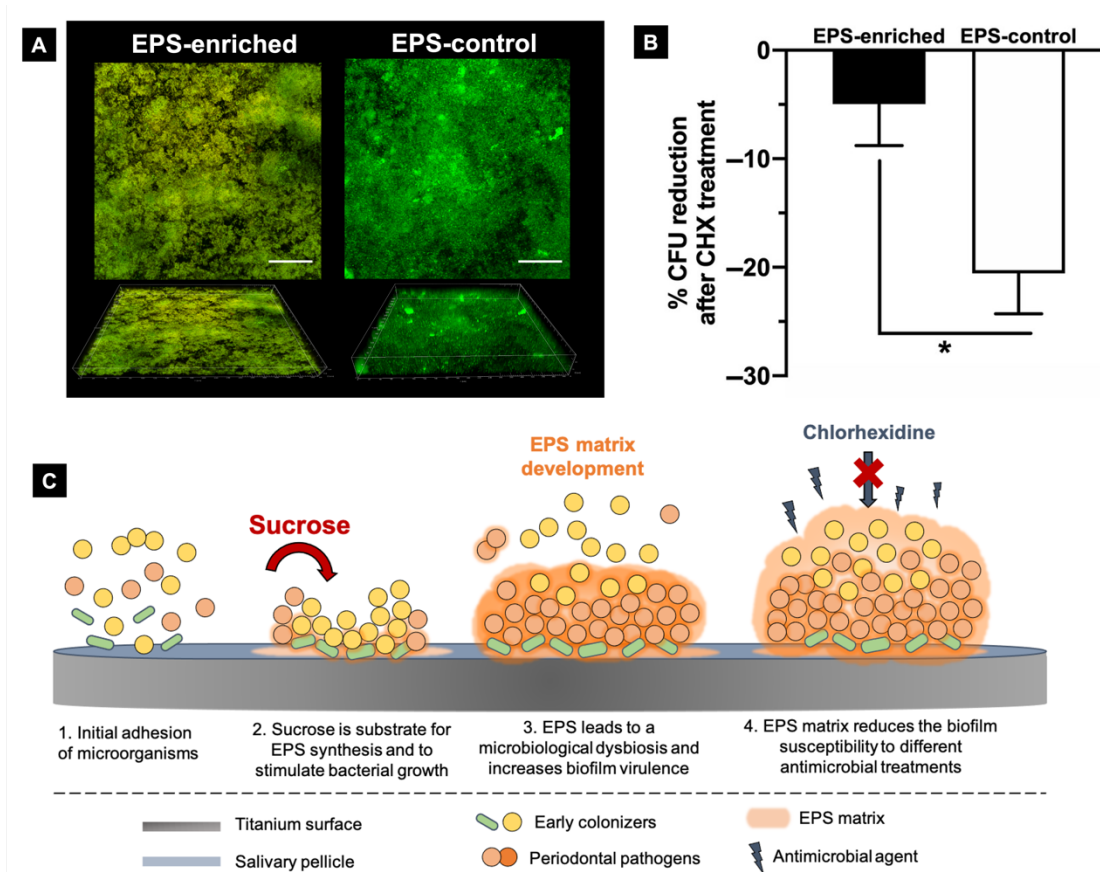


Figure 3. *In vitro* *S. mutans* 48-hr biofilms were grown on Ti surface to test the effect of EPS matrix on antimicrobial susceptibility. **(A)** Representative confocal laser scanning microscopy images (scale bars 50 μm) showing the live bacterial cells (green; stained with Syto-9) and biofilm matrix (red; stained with Alexa Fluor 647-labeled dextran conjugate probe) in biofilms treated to sucrose (EPS-enriched) or glucose (EPS-control). **(B)** Biofilms were exposed to 0.2% chlorhexidine (CHX) and the results revealed the protective effect of EPS matrix on bacterial survival in EPS-enriched biofilms (* $p < .05$). **(C)** Schematic representation of the possible impact of EPS matrix in the microbiological shift of biofilms growing on Ti surface; and their mechanism in reducing antimicrobials diffusion and reducing bacterial killing. Reprinted (adapted) from ref (Costa et al., 2020a); Copyright (2020), with permission from John Wiley and Sons (License number: 5140250601407).

Another component that has been shown involved in the structural properties of the biofilm matrix is eDNA (Schlafer et al., 2017). Studies have suggested that eDNA is more than vestiges of dead cells, but it is a necessary component for biofilm assembling

instead (Jakubovics et al., 2021). This statement is confirmed by studies that uncovered that the eDNA protects biofilms against mechanical stress (Peterson et al., 2013), and the digestion of eDNA in biofilm matrix with DNases reduced biofilm accumulation of *P. gingivalis* and *F. nucleatum* (Ali Mohammed et al., 2013), as well as *P. aeruginosa* (Whitchurch et al., 2002). In other words, enzymatic degradation of exopolymeric matrix components can disorganize the biofilm structure (Baelo et al., 2015; Koo et al., 2017), releasing free cells from the biofilm matrix, evidencing the structural importance of the eDNA and also revealing a novel therapeutic option for oral biofilm management (Serrage et al., 2021). Another feature of eDNA presence in the oral biofilm is the horizontal transfer of antibiotic resistance genes due to the genomic incorporation of sequences by competent microorganisms (*i.e.*, those that can uptake DNA from the milieu), an issue of great importance in dentistry and medicine (Flemming; Wingender, 2010a).

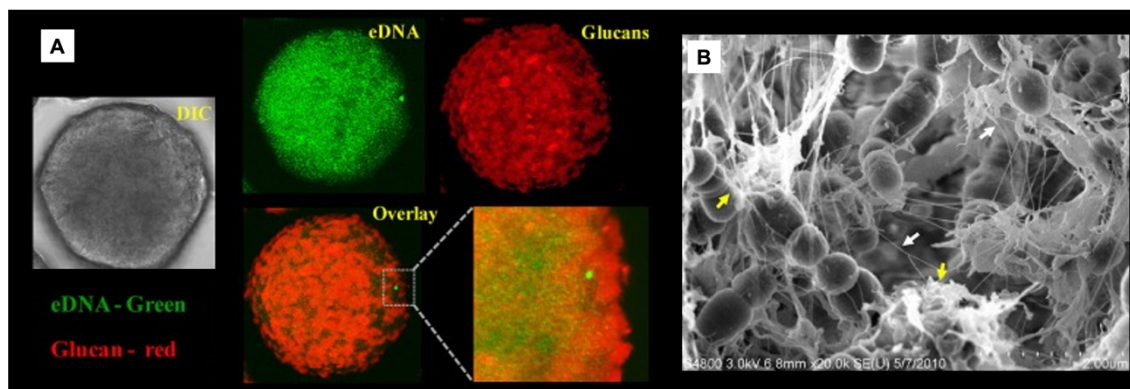


Figure 4. The role of eDNA on glucans synthesis and microbial adhesion on dental surfaces. (A) Representative confocal laser scanning microscopy images of saliva-coated hydroxyapatite samples (DIC; in gray), eDNA associated to the surface (in green), and glucans formed (in red), showing the eDNA interspersed with glucans. (B) Scanning electronic microscopy analysis highlights the interaction of nanofibrous eDNA (white arrows) and wool-like glucans (yellow arrows). Reprinted (adapted) from ref (KLEIN et al., 2015); Copyright (2015), with permission from Frontiers in terms of Creative Commons CC BY license.

EPS matrix is also responsible for enhancing bacterial adhesion since the EPS favors bacterial attachment to surfaces, cellular co-aggregation, and biofilm assembling (Klein et al., 2015; Peterson et al., 2013). The α 1-3 glucans have been considered as a "biological glue", binding the cells through cell-surface proteins that work as glucan-receptors (Matsumoto-Nakano, 2018; Takahashi, 2015). Glucans synthesized *in situ* by Gtf in salivary pellicle adsorbed on dental surface promote the initial adherence of *S.*

mutans (Schilling; Bowen, 1992). Similar findings were described for *C. albicans* adhesion on a dental surface mimetic (Gregoire et al., 2011). GtfB can effectively adhere to the *C. albicans* yeast cell surface, and the presence of glucans on the yeast promotes the co-aggregation with *S. mutans* (via its glucan-binding proteins in the cell wall). Therefore, EPS content is essential for fostering microbial adhesion and co-aggregation.

It is noteworthy that the biofilm matrix is also a nutrient source that provides energy for biofilm communities (Karygianni et al., 2020). This property is closely related to how exopolymers can be degraded by extracellular hydrolases enzymes present in the matrix, releasing carbohydrates for metabolization (Bowen et al., 2018). In the presence of sucrose, those synthesized glucans and fructans are sources of glucose and fructose that are released by dextranase and fructanase action (Paes-Leme et al., 2008). Specifically, dextranases break $\alpha 1,6(\text{Glc} \rightarrow \text{Glc})$ bonds and fructanases break $\beta 2,1$ and $\beta 2,6(\text{Fru} \rightarrow \text{Fru})$ bonds, allowing continuous carbohydrate release (Costa-Oliveira; Cury; Ricomini-Filho, 2017b; Walker; Hare; Morrey-Jones, 1983). This carbohydrate releasing is paramount for microbial survival during periods of nutrient absence in oral biofilms, which generally occurs between the meals and during the night (Bowden; Hamilton, 1998; Costa-Oliveira; Cury; Ricomini-Filho, 2017b). Furthermore, the biofilm matrix formed under sucrose exposure can favor glycogen accumulation and delay its degradation, which could increase biofilm virulence under carbohydrate depletion moments (Costa-Oliveira et al., 2021). Hence, the biofilm matrix of oral biofilms might be able to increase bacterial persistence. Therefore, bringing new insights and revealing another feature of EPS-rich matrix formed under sucrose exposure. However, besides carbohydrate polymers, proteins, glycoproteins, and amino acids in the biofilm matrix can similarly act as a nutrient source. Unlike carbohydrate metabolism that allows mainly acid generation in the biofilm, protein and amino acids metabolism provide alkali production, which is responsible for increasing the pH of the biofilm and contributing to periodontopathogenic microorganism selection (Souza et al., 2019; Takahashi, 2015).

4. The EPS matrix as a microbial virulence factor in the development of peri-implant diseases

The etiopathogenesis of peri-implant diseases involves the biofilm accumulation and host immune response and are classified as peri-implant mucositis or peri-implantitis (Schwarz et al., 2018). Peri-implant mucositis is an inflammatory reaction of the soft tissue around dental implants, whereas peri-implantitis involves the inflammation of the

peri-implant soft tissue and the progressive bone loss around dental implants (Berglundh et al., 2018b; Heitz-Mayfield; Salvi, 2018). According to the current evidence, highlighting the last consensus report (2017) of peri-implant diseases (Berglundh et al., 2018b), polymicrobial biofilms induce these clinical conditions. As biofilms are matrix-encased polymicrobial communities (Karygianni et al., 2020), it is conceived that EPS matrix exerts a fundamental role in the biofilm pathogenicity and can be considered as a microbial virulence factor for peri-implant diseases.

The development of peri-implant diseases and ecological transitions from implant-host homeostasis to disease-associated microbiome is not adequately understood (Lafaurie et al., 2017). However, the EPS matrix and the complex interaction with the environment seem to play a critical role in the pathogenesis of the peri-implant disease. Classic animal studies have described the cause-effect relationship between increased biofilm accumulation and worse peri-implant clinical measures (Elliott et al., 2005; Lang et al., 1993). Disease progression was also linked to the microbiological shift in the implant-related biofilms to a more pathogenic composition (Padial-Molina et al., 2016; Shibli et al., 2008). Microbiological shifts on implant surfaces are closely related to sucrose exposure (Souza et al., 2019), a substrate for exopolysaccharides synthesis, and an EPS matrix-enriched environment (Costa et al., 2020). Our group has shown that *in situ* biofilms grown on Ti and under increasing sucrose exposure led to a significant microbiological shift, increasing putative anaerobe pathogens, such as *P. gingivalis*, *Tannerella forsythia*, and *Treponema denticola* (Souza et al., 2019); these bacteria species are strongly related with the etiology of peri-implant infections (Pérez-Chaparro et al., 2016) and oral tissues damage around the implant (Belibasakis; Manoil, 2021). This effect has been attributed to the higher biofilm biomass under sucrose exposure since the carbohydrate is a substrate for bacterial metabolism and with the areas of reduced oxygen availability, which may have been the driving force towards the increased loads of anaerobic peri-implant pathogens, as above mentioned. Moreover, higher sucrose exposure led to increased EPS content, which may change biofilm architecture, creating a suitable environment for bacterial growth and co-aggregation (Souza et al., 2019). These findings suggest that sucrose can trigger this ecologic transition even without the host inflammatory process, possibly acting as a stress factor leading to a microbiological shift.

Thereafter, we evaluated whether EPS-enriched matrix was responsible for modulating microbiological shifts in sucrose exposed biofilms. EPS-enriched

environment favored a transition condition from a commensal to a pathogenic community on Ti material by creating a suitable environment for anaerobic pathogens, compared to EPS-control (without sucrose exposed). EPS content promoted the growth of *Streptococcus*, *Campylobacter* and *Fusobacterium* species and even strict anaerobic species (Costa et al., 2020). Putative and peri-implant pathogens were ~3-fold higher in EPS-enriched biofilms developed on the Ti surfaces (Costa et al., 2020). Therefore, EPS content is a crucial factor for creating a favorable ecological environment that allows facultative and anaerobic pathogens growth that has been found in implant-related infections. Since there is a clinical transition from mucositis to peri-implantitis, and it reflects the microbiological shift in peri-implant sites (Belibasakis; Manoil, 2021), higher EPS matrix content may be a virulence factor to be considered in the pathogenesis of implant-related infection. EPS-enriched biofilms led to higher host cell death, showing the effect of tissue damage (Costa et al., 2020). Hence, the selection of microbial species triggered by sucrose and the production of exopolysaccharides could influence the host's response towards inflammation.

As mentioned above, *gtfR* from *S. oralis* was overexpressed in mixed-biofilms with *C. albicans* on Ti surface (Souza et al., 2020c), compared to other abiotic surfaces. Wild-type *S. oralis* strain encoded *gtfR* gene promoted mixed-biofilm growth, compared to mutant strain with *gtfR* gene deletion. Moreover, in mixed biofilms, GtfR promotes fungal accretion on Ti surfaces. Therefore, EPS content promotes cross-kingdom interaction on the Ti surface, increasing biofilm biomass and fungal growth (Souza et al., 2020c). *C. albicans* is the most frequent oral fungal opportunistic pathogen that forms biofilms on implanted materials and can cause disseminated infection (Bertolini et al., 2021; Ghannoum et al., 2010). Moreover, *Candida* has been found on peri-implant disease sites (Alrabiah et al., 2019) and previous evidence showed that the cross-kingdom interaction with streptococci from mitis group on Ti material led to increased mucosal damage (Souza et al., 2020d)

As biofilm becomes established, the EPS matrix difficult bacterial eradication from the macro-and microgeometry of the implant surface (Al-Ahmad et al., 2010). For implant decontamination, mechanical instruments and chemical agents have been widely used in clinical settings over the years (Renvert; Roos-Jansåker; Claffey, 2008). However, a systematic review (Heitz-Mayfield; Mombelli, 2014) has not identified a completely effective therapy, which probably may be due to difficulties associated with EPS-enriched biofilms removal. Additionally, EPS acts as a protective barrier due to its

negative charge hampering the diffusion of antimicrobial agents with positive charges and binding ability, neutralizing antimicrobial agents that enter its complex structure before attacking bacterial cells (Falsetta et al., 2014; Xiao et al., 2012). Notably, our group and others have shown that EPS content reduces antimicrobial susceptibility of oral biofilms, even for antifungal and antibiotics agents (Costa et al., 2020; Klein et al., 2015; Ren et al., 2019). Previous evidence (Gil et al., 2014) also showed that exoproteomes of exopolysaccharide-based and protein-based biofilm matrices produced by *Staphylococcus aureus* and injected in mice induced an immune response against bacterial strains and promoted cytokine production. These findings show the role of EPS content to promote antimicrobial resistance and interact directly with host response in implant surfaces.

Considering that exopolysaccharides, proteins, and acid nucleic (eDNA and eRNA) are extracellularly released to ensure matrix scaffolding, the presence of different bacterial species may produce other components; thereby it is not expected a unique behavior for peri-implant biofilms (Bowen et al., 2018; Flemming et al., 2016). Gram-negative bacteria present in the peri-implant biofilm can produce beta-lactamases. In addition, peri-implant communities also include Gram-positive bacteria resistant to beta-lactam antibiotics (Branda et al., 2005). Specific Gram-positive bacteria identified in peri-implantitis are also known to provide low-affinity penicillin-binding proteins shareable to other bacteria through gene transfer and confer high resistance to beta-lactam antibiotics (Drawz; Bonomo, 2010). This broad and complex microbiological composition of polymicrobial biofilms associated with the tridimensional structure and several advantages provided by the EPS matrix make the implant-related infections a challenge to be controlled and treated using traditional antibiotics therapies (Arciola; Campoccia; Montanaro, 2018).

Another relevant point is that metal particles and ions from Ti dental implant have been identified within the EPS matrix of *in vivo* peri-implant biofilms (Safioti et al., 2017). Those particles that originated from the bio-tribocorrosion process occurring on implant surfaces are known to produce inflammatory reactions as a response to the foreign material and have been suggested to be involved in microbial shift and clinical development of peri-implantitis (Costa et al., 2021a; Dini et al., 2020). Furthermore, our group has shown that Ti particles drive microbial community shift increases the population of *Streptococcus anginosus*, *Capnocytophaga sputigena*, *Prevotella nigrescens*, and *Actinomyces israeli* (Souza et al., 2020a). Similarly, Ti ions showed

higher levels of some putative pathogens growing in *in situ* model (Souza et al., 2020a). Therefore, the microbiome composition of biofilm-related to dental implants is strongly influenced by Ti dissolution products, which may shift the peri-implant microbiome within the EPS matrix. Overall, the EPS matrix remains an unexploited resource thus far in the implantology field, which can potentially be the driving force to shift the paradigm about peri-implant diseases etiopathogenesis in the near future.

Therefore, the biological plausibility of EPS matrix role on implant-related infections is based on the following hypothesis and findings: (1) EPS matrix promotes microbial adhesion, biofilm growth, and biomass accretion and, consequently, exacerbates the role of biofilm to induce peri-implant disease; (2) higher biomass and structural and functional changes due to EPS-enriched environment lead to a microbiological shift in implant-related biofilms promoting anaerobic microbial growth; (3) EPS matrix favor cross-kingdom interaction with *C. albicans* which promote bacterial enzymes expression, exopolysaccharides synthesis and fungal growth in implant-related biofilms; (4) EPS matrix reduce antimicrobial susceptibility of biofilms creating a protective layer and hampering antimicrobial diffusion; (5) the microbiological shift found on EPS-enriched biofilms on implant surfaces increase host cells damage. Thus, the EPS matrix plays a crucial role in the pathogenesis of dental implant-related infections, but biomaterials science and the implantology fields have neglected it.

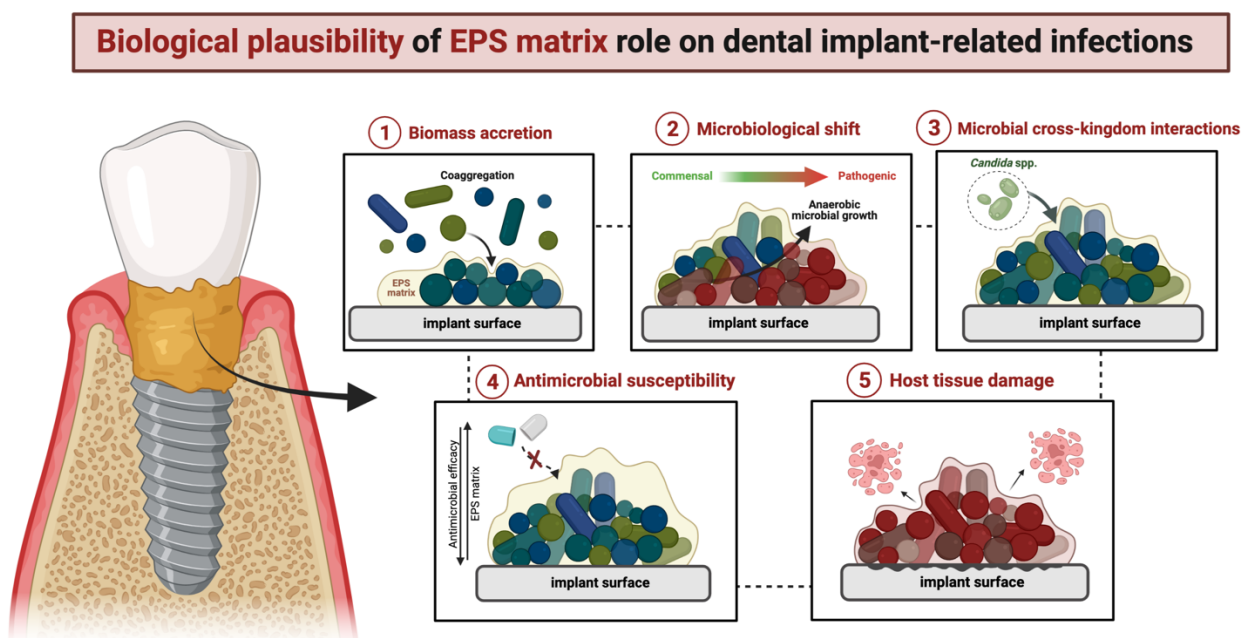


Figure 5. Schematic representation of the role of EPS matrix to promote biofilm accumulation and virulence with expected higher host tissue damage on dental implant-related infections. Biological plausibility hypothesis of EPS matrix role on peri-implantitis was considered based on current evidence and Bradford Hill criteria. The drawing was created with BioRender.com (License number: VH22WQBLSE).

5. EPS targeting therapies for biofilm disruption: a potential alternative to dental implant-related infections

The unique properties of the EPS matrix represent fundamental challenges for the consolidation of effective and rational antibiofilm therapeutics to control implant-related infections (Arciola; Campoccia; Montanaro, 2018). As mentioned before, the EPS matrix can limit the diffusion of antimicrobials and is challenging to remove biofilms from implant surfaces (Costerton; MONTANARO; Arciola, 2005; Karygianni et al., 2020). Conventional monotherapies focusing solely on microbial killing may not achieve relevant clinical efficacy within the complex microenvironment surrounding the dental implant (Shibli et al., 2019). Furthermore, antibiotic therapy may change resident microbiota and promote drug resistance over time, providing an ever-prevalent issue (Smith, 2005). To address these hurdles, several non-antimicrobial methods to manipulate polymicrobial biofilm communities have emerged, including EPS targeting therapies (Koo; Falsetta; Klein, 2013; Xiao et al., 2012). These therapies can be applied entirely alone to prevent the assembly of EPS matrix or in combination with antimicrobials to potentially disrupt this protective matrix and optimize bacterial killing efficacy (Fulaz et al., 2019). Targeting the EPS matrix is a promising strategy, but it is still underexploited in the context of peri-implant biofilm control. The current knowledge is derived mainly from oral biofilm research using dental surfaces and cariogenic microorganisms (Kim et al., 2018a; Ren et al., 2019). Consequently, some concepts need to be adapted for suitable transfer to implant applications in the future. This section aims to provide an overview of the rationale technologies currently developed that appears to be also promising to enhance current therapeutic modalities' efficacy for dental implants (Table 1).

Table 1. Overview of current and potential therapeutic strategies targeting the EPS matrix component of biofilms.

Type	Strategy	Proposed mechanism	Targeted biofilm component	Biofilm phase	Related disease	State of development	Advantages	Disadvantages
Biochemical agents	EPS-degrading enzymes	Disassembly of biofilm matrix and dispersion	Exopolysaccharides	Early/Mature biofilm	Dental caries, chronic infections of the wounds, biomedical implant-related diseases	<i>In vitro/in vivo</i>	1. Biofilm disruption independent on killing cells; 2. Effective against established biofilms; 3. Weaken biofilm's physical structure, facilitating mechanical removal; 4. Disrupt pathogenic microenvironment; 5. Readily combined with antimicrobials irrigants.	1. Limited efficacy when used alone due to no/limited antimicrobial activity; 2. Possible pathogen recolonization; 3. Poor enzymatic activity and high cost of the enzymes; 4. Cytotoxicity (high dose needed).
	EPS synthesis inhibitors	Direct inhibition of glucosyltransferases that catalyze glucan formation	Exopolysaccharides	Early biofilm	Dental caries, biomedical implant-related diseases	<i>In vitro/in vivo</i>	1. Biofilm prevention independent on killing cells; 2. Prevention of early biofilm formation; 3. Less microecological consequences; 4. Readily combined with antimicrobials.	1. Poor retention in biofilm; 2. Polysaccharides chemistry and synthesis highly complex; 3. Limited effect on formed biofilms.
	Inhibitors of c-di-GMP signaling	Modulation of c-di-GMP to inhibit polysaccharides synthesis and promote biofilm disassembly	Exopolysaccharides	Early/Mature biofilm	Chronic infections, biomedical implant-related diseases	<i>In vitro</i>	1. Potential strategy to target polymicrobial infection; 2. Multi-mode of action; 3. Indirect modulation of polysaccharide production.	1. Complexity of c-di-GMP signaling network; 2. Poor retention in biofilm.
	Inhibitors of adhesin production	Inhibition of cell-surface-associated adhesin to disrupt cell binding to host surfaces	Exopolysaccharides	Early biofilm	Catheter-associated infection, urinary tract infection	<i>In vivo</i>	1. Selective depletion of the pathogen at the early stage of biofilm formation	1. Poor retention in biofilm 2. Complex structure and immunity of the adhesin 3. Limited effect on formed biofilms
	Antibody against DNA-binding proteins	Targeting DNABII family of DNA-binding proteins that protect the	Microbial cells, Nucleic acids	Mature biofilm	Periodontal disease, urinary tract infections, lung infections	<i>In vitro/in vivo</i>	1. Effective against biofilms formed by numerous types of bacteria	1. Limited efficacy when used alone 2. High cost of the antibodies

		structural integrity of eDNA					
	DNases	Disruption of early biofilm development by degrading scaffolding eDNA	Nucleic acids	Early biofilms	Wide range of chronic infections	<i>In vitro/in vivo</i>	1. Biofilm disruption independent on killing cells; 2. Weakens biofilm' physical structure; 3. Readily combined with antimicrobials. 1. Limited efficacy when used alone.
	Proteases	Degradation of the protein components in the matrix or the protein adhesins on the cell surface	Proteins	Mature biofilms	Wide range of chronic infections	<i>In vitro/in vivo</i>	1. Biofilm disruption independent on killing cells; 2. Effective against established biofilms; 3. Weakens biofilm' physical structure; 4. Readily combined with antimicrobials. 1. Limited efficacy when used alone; 2. Complexity of protein components in the matrix; 3. Poor enzymatic stability; 4. Cytotoxicity.
Chemical agents	Detergent/Surfactant irrigants	Topical drug-delivery capacity to bacterial killing	Microbial cell/ Exopolysaccharides	All stages	Dental caries, biomedical implant-related diseases	Clinical	1. Active on dormant cells; 2. Readily combine for multi-targeting therapeutics. 1. Not all biofilm removed; 2. Release of pathogens may result in recolonization; 3. Bacterial resistance.
	Natural products	Topical drug-delivery capacity to bacterial killing	Microbial cell/ Exopolysaccharides	All stages	Wide range of chronic infections	<i>In vivo, clinical</i>	1. Selected for broad-range of bioactivity; 2. Chemical diversity with drug-like properties; 3. Multi-mode of action. 1. Bacterial resistance; 2. Complex chemistry and isolation procedures; 3. Chemical composition variability; 4. Cytotoxicity.
	Rinsing fluid/Irrigators	Topical drug-delivery capacity to bacterial killing	Microbial cell/ Exopolysaccharides	All stages	Dental caries, biomedical implant-related diseases	Clinical	1. Can be readily combined with antimicrobial agents. 1. Accessibility; 2. Biofilm viscoelasticity can resist removal.
Physical/Electric methods	High-velocity spray/jet irrigators	Mechanical disruption of biofilm scaffold	Microbial cell/ Exopolysaccharides	All stages	Surgical-site infections, biomedical implant decontamination	<i>In vitro/in vivo/Clinical</i>	1. Physical mechanism reduces the probability of antimicrobial resistance; 2. Readily combined with antimicrobials. 1. Limited efficacy when used alone; 2. Biofilm viscoelasticity can resist removal; 3. Recolonization.
	Electric currents/fields	Physical disruption of biofilm scaffold	Microbial cell/ Exopolysaccharides	All stages	Surgical-site infections, biomedical implant decontamination	<i>In vitro/in vivo/Clinical</i>	1. Projected through induction or connected wires; 2. Physical mechanism reduces the probability of antimicrobial resistance; 1. Accessibility. 2. Recolonization; 3. Delivery of fields and currents to deep tissue; 3. Cytotoxicity.

Smart Delivery Systems	Nanocarriers (polymeric nanoparticles/liposomes)	On-demand drug release triggered by biological stimulus (pH, O ₂ , temperature)	Microbial cell/ Exopolysaccharides	Early/Mature biofilm	Wide range of infections	<i>In vivo</i> / Pre-clinical	3. Readily combined with antimicrobials. 1. Small size allows transport into the EPS; 2. Carry/release different drug combinations; 3. Suitable delivery during infection.	1. Charge may limit penetration into the biofilm EPS; 2. Prolonged retention needed for optimal drug activity; 3. Cytotoxicity.
-------------------------------	---	--	---------------------------------------	----------------------	--------------------------	----------------------------------	---	---

Source: Table modified from Karygianni *et al.* 2020.

EPS matrix compounds, mainly exopolysaccharides, can serve as anti-biofilm targets to prevent early microbial accumulation (Koo et al., 2017). Because of the wide range of biomolecules that forms the biofilm matrix, matrix degradation likely requires a combination of various small molecules with different specificities (Fulaz et al., 2019). Of particular interest, EPS-degrading enzymes have been widely investigated for caries management decades ago (Guggenheim, 1970; Hamada et al., 1975; Koo; Falsetta; Klein, 2013). Mechanistically, the inhibition of streptococcal glucosyltransferases (Gtf) can hamper EPS synthesis and disrupt its assembly, leading to biofilm disruption, independent of killing bacterial cells (Guggenheim, 1970; Hamada et al., 1975; Koo; Falsetta; Klein, 2013). Thus, despite the lack of intrinsic antimicrobial effect, EPS-degrading enzymes may be adjuvants to overcome EPS matrix-induced antimicrobial recalcitrance (Karygianni et al., 2020). *Studies in vitro* (Ren et al., 2016) and *in vivo* (Kim et al., 2018a) have proven this intriguing mechanism in oral biofilms. Instead of focusing efforts on degrading exopolysaccharides, other alternative strategies drive on destabilizing the interactions between eDNA and other biomolecules in the biofilm matrix (Okshevsky; Regina; Meyer, 2015). Such approaches include inhibitors of c-di-GMP signaling (Christensen et al., 2013), inhibitors of adhesin production (Cozens; Read, 2012), antibodies against DNA-binding proteins (Novotny et al., 2016), DNases (Baelo et al., 2015; Panariello et al., 2019), and proteases (Conlon et al., 2013), all of which have also been gaining attention in dental medicine. However, for almost all the EPS targeting methods applied alone, the most significant limitations are uncontrolled agent release, poor bioavailability, lower pharmacokinetics; hence, limited treatment effectiveness.

The optimal approach for dental implant application would be to prevent the matrix from forming to arrest the transition to a pathogenic biofilm state (Jakubovics et al., 2021). Similar to dental surfaces (Kim et al., 2018a), our group recently showed that povidone-iodine [(C₆H₉NO)_nI] is a matrix-targeting disruption strategy to disassemble the EPS matrix and increase the antibiotic effect in *in vitro* and *in situ* biofilms formed on Ti surfaces (Costa et al., 2020). The povidone-iodine is a potent EPS-degrading agent due to inhibition of GtfB (Kim et al., 2018a), promoting disruption of biofilm scaffold in early and mature biofilms. Moreover, this agent also displays moderate antibacterial activity against multiple oral

bacteria and may act concurrently with amoxicillin and metronidazole to improve the current peri-implant biofilm treatment (Shibli et al., 2019). Beyond the advantages mentioned, povidone-iodine is a low-cost agent compared to other synthetic EPS-degrading enzymes (Sahrman et al., 2010). Together, our findings demonstrated that using a dual-targeting approach by combining matrix biofilm disruption (first step) may potentially improve antibiotic therapy (second step), representing a feasible treatment for implant-related infections. To the best of our knowledge, our study (Costa et al., 2020) was the first to provide experimental evidence on the EPS-targeting therapy towards dental implant biofilms.

Once a polymicrobial biofilm is established, more aggressive methods are needed to eradicate microbial cells and EPS matrix from the implant surface (Barootchi et al., 2020). These methods include synergistic combinations of antimicrobial action (antibiotics, natural products, or rinsing fluid) with mechanical debridement (Renvert; Roos-Jansåker; Claffey, 2008). However, relevant concerns related to bacterial resistance, microbial recolonization, and cytotoxicity had discouraged chemical approaches, mainly when used alone (Arciola; Campoccia; Montanaro, 2018). More recently, the physical/electric disruption techniques such as high-velocity spray/jet irrigators (Peterson et al., 2015) or electromagnetic methods (Faveri et al., 2020) have been proposed to disrupt the EPS matrix at difficult-to-reach and retentive regions of implant-abutment connections. However, it is essential to highlight that the mechanical resistance of biofilms is another fundamental mechanism that leads to microbial cells persistently attaching to implant surfaces, making physical removal challenging (Peterson et al., 2015). To date, there is no common consensus about which mechanical and chemical therapy is more effective for implant-related diseases (Berglundh et al., 2018a; Heitz-Mayfield; Mombelli, 2014).

The advancement of nanotechnology has opened up the possibility of on-demand EPS targeting systems (Fulaz et al., 2019). Notably, these smart delivery systems are a new weapon in antimicrobial warfare (Makvandi et al., 2021). Lipid- and polymer-based nanoparticles are of major interest in the biomedical field due to their adequate biocompatibility, higher versatility to incorporate drugs, and potential as platforms for targeted/triggered release (Alqahtani et al., 2021). Hence, the potential exists to use nanocarriers to penetrate the biofilm matrix. For instance, nanocarriers should be designed to protect the antimicrobial from enzymatic inactivation provided by bacterial or host

immune defense and, therefore, actively bind to the biofilm matrix or other components surrounding the biofilm infection site (Fulaz et al., 2019). The use of nanocarriers provides an alternative path to overcome the limitations of classic drug delivery systems, such as burst drug release and microbial resistance development (Alqahtani et al., 2021; Fulaz et al., 2019). Nevertheless, for most of the approaches described herein, many questions still need to be answered before these agents can be suitably produced on a large scale and for clinical application. The technologies for matrix disassembly, disruptive agents, and promising nanocarriers for implant devices are outlined (Figure 6).

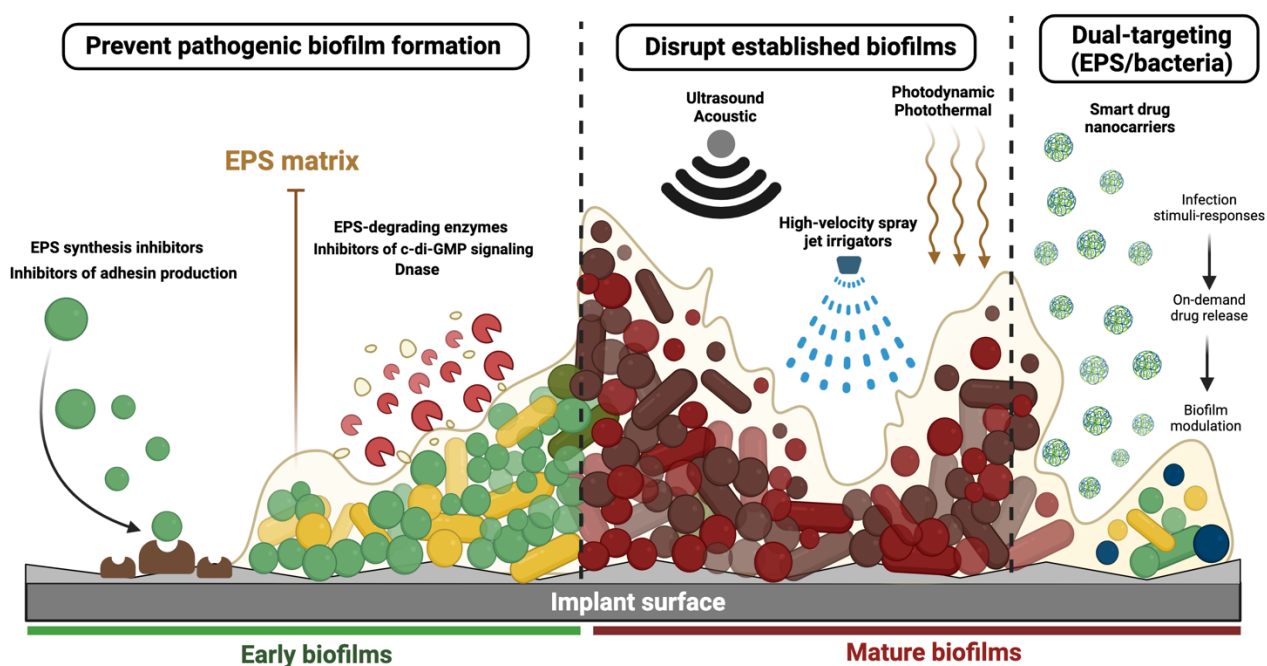


Figure 6. Therapeutic strategies for targeting the biofilm matrix. The drawing was created with BioRender.com (License number: RH22WRCM9V).

6. Future outlook

As discussed already, it is clear that the EPS matrix can be considered an attractive target for anti-biofilm therapies in implant dentistry (Costa et al., 2020a). Although this treat-to-target approach focusing on EPS is effective, the greatest challenge of this elegant treatment is the *in vivo* long-term effects (Baelo et al., 2015; Karygianni et al., 2020; Koo et al., 2017). Since biofilm formation is a chronic and continuous process, the matrix-degrading or biofilm-dispersing strategies have been questionable for "real-world" applications.

Traditionally, matrix-degrading or biofilm-dispersing strategy can be used alone or associated with antimicrobials; however, the long-term effects have been questionable. To rationally design of EPS-targeting strategy is essential to deeply recognize EPS composition from different microorganisms to understand the precise mechanism of etiopathogenesis and the risk factors of the peri-implant disease.

To overcome these limitations, smart delivery systems with 'on-demand' stimulus responsive mechanisms for drug release have been indicated as the most relevant strategies in the implantology field that could be utilized moving forward (Sun; Qing, 2011). So far, there are various cutting-edging emerging technologies using smart biomaterial development (Costa et al., 2021b). The so-called molecularly imprinted polymers (MIP) are an efficient, versatile, and simple way to form self-regulated EPS-targeting strategies is the so-called molecularly imprinted polymers (MIP) (Zhang, 2020). These MIP-based materials have become one of the most remarkable innovations in the biomedical field due to the possibility of being used as a powerful drug delivery system (Gagliardi; Bertero; Bifone, 2017; Zhang, 2020). Compared to classic drug delivery systems, MIPs have superior chemical stability to degradation, promoting a more controlled drug release *in vivo* (He et al., 2020). Their brilliant therapeutic features generally depend upon the different biological stimuli (e.g., enzymatic activity, O₂ level, temperature, and pH) designed to start the drug release in the infection locally (Belbruno, 2019). Hence, MIP functionalized with a drug to disrupt EPS seems to be a promising adjunctive approach for biofilm control that could potentially enhance the killing efficacy of antimicrobial agents and promote biofilm removal when co-administered in implant surroundings. Additionally, host modulation therapies to benefit encouraged the microbiological shift drives symbiotic status of biofilm from implants have been investigated using bioactive implant surfaces (COSTA et al., 2020b) and probiotics (BELIBASAKIS; MANOIL, 2021). These valuable strategies should also be tested in association with EPS-targeting approaches.

7. Conclusion

There is emergent evidence suggesting that EPS matrix could be a critical virulence factor in oral biofilm-related to dental implants. In this way, the EPS matrix seems to be a potential target for developing biofilm control strategies and promoting peri-implant health

status. However, further studies are needed to fully elucidate the *in vivo* mechanisms that modulate the synthesis of polysaccharides considering peri-implant conditions. Effective targeting of EPS on implant surfaces will also require improved insight into the molecular basis of polysaccharides, EPS matrix architecture, and bacterial interactions within the EPS matrix for such strategies to become a clinical reality and be translated into commercial products.

Research involving human participants and or animals

This review article does not contain any data from unpublished studies associated with human participants or animals performed by any authors.

Disclosure statement

The authors declare that they have no conflict of interest.

Funding

This study was supported by the IADR Regional Development Program, Cordenção de Aperfeiçoamento de Pessoal de Nível Superior – Brasil (CAPES) – Finance code 001, and São Paulo Research Foundation (FAPESP) (grant numbers: 2020/05231-4 and 2020/10436-4).

Author contribution

RCC and JGSS conceived the idea. The literature was searched, and the manuscript was written by RCC, MB, BECO, BEN, CD, and BB. Correction, editing, and supervision by VARB, MFK, and JGSS.

References

- AL-AHMAD, A. et al. Biofilm formation and composition on different implant materials *in vivo*. **Journal of Biomedical Materials Research. Part B, Applied Biomaterials**, v. 95, n. 1, p. 101–109, out. 2010.
- ALI MOHAMMED, M. M. et al. Characterization of extracellular polymeric matrix, and treatment of *Fusobacterium nucleatum* and *Porphyromonas gingivalis* biofilms with DNase I and proteinase K. **Journal of Oral Microbiology**, v. 5, 2013.

- ALQAHTANI, M. S. et al. Advances in Oral Drug Delivery. **Frontiers in Pharmacology**, v. 12, p. 618411, 2021.
- ALRABIAH, M. et al. Presence of Candida species in the subgingival oral biofilm of patients with peri-implantitis. **Clinical Implant Dentistry and Related Research**, v. 21, n. 4, p. 781–785, ago. 2019.
- ARCIOLA, C. R.; CAMPOCCIA, D.; MONTANARO, L. Implant infections: adhesion, biofilm formation and immune evasion. **Nature Reviews Microbiology**, v. 16, n. 7, p. 397–409, jul. 2018.
- BAELO, A. et al. Disassembling bacterial extracellular matrix with DNase-coated nanoparticles to enhance antibiotic delivery in biofilm infections. **Journal of Controlled Release: Official Journal of the Controlled Release Society**, v. 209, p. 150–158, 10 jul. 2015.
- BAKER, J. L. et al. Ecology of the oral microbiome: beyond bacteria. **Trends in microbiology**, v. 25, n. 5, p. 362–374, maio 2017.
- BANAS, J. A.; VICKERMAN, M. M. Glucan-binding proteins of the oral streptococci. **Critical Reviews in Oral Biology and Medicine: An Official Publication of the American Association of Oral Biologists**, v. 14, n. 2, p. 89–99, 2003.
- BAROOTCHI, S. et al. Nonsurgical treatment for peri-implant mucositis: A systematic review and meta-analysis. **International journal of oral implantology (New Malden, London, England)**, v. 13, n. 2, p. 123–139, 2020.
- BELBRUNO, J. J. Molecularly Imprinted Polymers. **Chemical Reviews**, v. 119, n. 1, p. 94–119, 9 jan. 2019.
- BELIBASAKIS, G. N.; MANOIL, D. Microbial Community-Driven Etiopathogenesis of Peri-Implantitis. **Journal of Dental Research**, v. 100, n. 1, p. 21–28, 1 jan. 2021.
- BERGLUNDH, T. et al. Peri-implant diseases and conditions: Consensus report of workgroup 4 of the 2017 World Workshop on the Classification of Periodontal and Peri-Implant Diseases and Conditions. **Journal of Clinical Periodontology**, v. 45 Suppl 20, p. S286–S291, 2018a.
- BERGLUNDH, T. et al. Peri-implant diseases and conditions: Consensus report of workgroup 4 of the 2017 World Workshop on the Classification of Periodontal and Peri-Implant Diseases and Conditions. **Journal of Clinical Periodontology**, v. 45, n. S20, p. S286–S291, 2018b.
- BERMEJO, P. et al. Topographic characterization of multispecies biofilms growing on dental implant surfaces: An in vitro model. **Clinical Oral Implants Research**, v. 30, n. 3, p. 229–241, mar. 2019.
- BERTOLINI, M. et al. Mucosal Bacteria Modulate Candida albicans Virulence in Oropharyngeal Candidiasis. **mBio**, p. e0193721, 17 ago. 2021.
- BERTOLINI, M. et al. Mucosal Bacteria Modulate Candida albicans Virulence in Oropharyngeal Candidiasis. **mBio**, v. 0, n. 0, p. e01937-21, [s.d.].
- BOWDEN, G. H.; HAMILTON, I. R. Survival of oral bacteria. **Critical Reviews in Oral Biology and Medicine: An Official Publication of the American Association of Oral Biologists**, v. 9, n. 1, p. 54–85, 1998.
- BOWEN, W. H. et al. Oral Biofilms: Pathogens, Matrix, and Polymicrobial Interactions in Microenvironments. **Trends in Microbiology**, v. 26, n. 3, p. 229–242, 1 mar. 2018.
- BOWEN, W. H.; KOO, H. Biology of Streptococcus mutans-derived glucosyltransferases: role in extracellular matrix formation of cariogenic biofilms. **Caries Research**, v. 45, n. 1, p. 69–86, 2011.
- BRANDA, S. S. et al. Biofilms: the matrix revisited. **Trends in Microbiology**, v. 13, n. 1, p. 20–26, jan. 2005.

- CHRISTENSEN, L. D. et al. Clearance of *Pseudomonas aeruginosa* foreign-body biofilm infections through reduction of the cyclic Di-GMP level in the bacteria. **Infection and Immunity**, v. 81, n. 8, p. 2705–2713, ago. 2013.
- COLBY, S. M.; RUSSELL, R. R. Sugar metabolism by mutans streptococci. **Society for Applied Bacteriology Symposium Series**, v. 26, p. 80S-88S, 1997.
- COMSTOCK, L. E.; KASPER, D. L. Bacterial glycans: key mediators of diverse host immune responses. **Cell**, v. 126, n. 5, p. 847–850, 8 set. 2006.
- CONLON, B. P. et al. Activated ClpP kills persisters and eradicates a chronic biofilm infection. **Nature**, v. 503, n. 7476, p. 365–370, nov. 2013.
- COSTA OLIVEIRA, B. E. et al. The Route of Sucrose Utilization by *Streptococcus mutans* Affects Intracellular Polysaccharide Metabolism. **Frontiers in Microbiology**, v. 12, p. 636684, 2 fev. 2021.
- COSTA OLIVEIRA, B. E.; CURY, J. A.; RICOMINI FILHO, A. P. Biofilm extracellular polysaccharides degradation during starvation and enamel demineralization. **PLoS One**, v. 12, n. 7, p. e0181168, 2017a.
- COSTA OLIVEIRA, B. E.; CURY, J. A.; RICOMINI FILHO, A. P. Biofilm extracellular polysaccharides degradation during starvation and enamel demineralization. **PLoS ONE**, v. 12, n. 7, 17 jul. 2017b.
- COSTA, R. C. et al. Extracellular biofilm matrix leads to microbial dysbiosis and reduces biofilm susceptibility to antimicrobials on titanium biomaterial: An in vitro and in situ study. **Clinical Oral Implants Research**, v. 31, n. 12, p. 1173–1186, 2020a.
- COSTA, R. C. et al. Synthesis of bioactive glass-based coating by plasma electrolytic oxidation: Untangling a new deposition pathway toward titanium implant surfaces. **Journal of Colloid and Interface Science**, v. 579, p. 680–698, 1 nov. 2020b.
- COSTA, R. C. et al. Microbial Corrosion in Titanium-Based Dental Implants: How Tiny Bacteria Can Create a Big Problem? **Journal of Bio- and Tribo-Corrosion**, v. 7, n. 4, p. 136, 23 ago. 2021a.
- COSTA, R. C. et al. Fitting pieces into the puzzle: The impact of titanium-based dental implant surface modifications on bacterial accumulation and polymicrobial infections. **Advances in Colloid and Interface Science**, v. 298, p. 102551, 1 dez. 2021b.
- COSTERTON, J. W. et al. Microbial biofilms. **Annual Review of Microbiology**, v. 49, p. 711–745, 1995.
- COSTERTON, J. W.; MONTANARO, L.; ARCIOLA, C. R. Biofilm in implant infections: its production and regulation. **The International Journal of Artificial Organs**, v. 28, n. 11, p. 1062–1068, nov. 2005.
- COZENS, D.; READ, R. C. Anti-adhesion methods as novel therapeutics for bacterial infections. **Expert Review of Anti-infective Therapy**, v. 10, n. 12, p. 1457–1468, 1 dez. 2012.
- DAUBERT, D. M.; WEINSTEIN, B. F. Biofilm as a risk factor in implant treatment. **Periodontology** **2000**, v. 81, n. 1, p. 29–40, 2019.
- DEWHIRST, F. E. et al. The human oral microbiome. **Journal of Bacteriology**, v. 192, n. 19, p. 5002–5017, out. 2010.
- DINI, C. et al. Progression of Bio-Tribocorrosion in Implant Dentistry. **Frontiers in Mechanical Engineering**, v. 6, 2020.
- DODO, C. G. et al. Proteome analysis of the plasma protein layer adsorbed to a rough titanium surface. **Biofouling**, v. 29, n. 5, p. 549–557, 2013.

- DRAGOŠ, A.; KOVÁCS, Á. T. The Peculiar Functions of the Bacterial Extracellular Matrix. **Trends in Microbiology**, v. 25, n. 4, p. 257–266, abr. 2017.
- DRAWZ, S. M.; BONOMO, R. A. Three decades of beta-lactamase inhibitors. **Clinical Microbiology Reviews**, v. 23, n. 1, p. 160–201, jan. 2010.
- ELLIOTT, D. R. et al. Cultivable oral microbiota of domestic dogs. **Journal of Clinical Microbiology**, v. 43, n. 11, p. 5470–5476, nov. 2005.
- FALSETTA, M. L. et al. Symbiotic relationship between *Streptococcus mutans* and *Candida albicans* synergizes virulence of plaque biofilms in vivo. **Infection and Immunity**, v. 82, n. 5, p. 1968–1981, maio 2014.
- FARHA, M. A.; BROWN, E. D. Strategies for target identification of antimicrobial natural products. **Natural Product Reports**, v. 33, n. 5, p. 668–680, 4 maio 2016.
- FARQUHARSON, S. I.; GERMAINE, G. R.; GRAY, G. R. Isolation and characterization of the cell-surface polysaccharides of *Porphyromonas gingivalis* ATCC 53978. **Oral Microbiology and Immunology**, v. 15, n. 3, p. 151–157, jun. 2000.
- FAVERI, M. et al. Antimicrobial effects of a pulsed electromagnetic field: an in vitro polymicrobial periodontal subgingival biofilm model. **Biofouling**, v. 36, n. 7, p. 862–869, 8 ago. 2020.
- FLEMMING, H.-C. et al. Biofilms: an emergent form of bacterial life. **Nature Reviews Microbiology**, v. 14, n. 9, p. 563–575, set. 2016.
- FLEMMING, H.-C.; WINGENDER, J. The biofilm matrix. **Nature Reviews Microbiology**, v. 8, n. 9, p. 623–633, set. 2010a.
- FLEMMING, H.-C.; WINGENDER, J. The biofilm matrix. **Nature Reviews Microbiology**, v. 8, n. 9, p. 623–633, set. 2010b.
- FUJIWARA, T. et al. Purification, characterization, and molecular analysis of the gene encoding glucosyltransferase from *Streptococcus oralis*. **Infection and Immunity**, v. 68, n. 5, p. 2475–2483, maio 2000.
- FULAZ, S. et al. Nanoparticle–Biofilm Interactions: The Role of the EPS Matrix. **Trends in Microbiology**, v. 27, n. 11, p. 915–926, 1 nov. 2019.
- FÜRST, M. M. et al. Bacterial colonization immediately after installation on oral titanium implants. **Clinical Oral Implants Research**, v. 18, n. 4, p. 501–508, ago. 2007.
- GAGLIARDI, M.; BERTERO, A.; BIFONE, A. Molecularly Imprinted Biodegradable Nanoparticles. **Scientific Reports**, v. 7, n. 1, p. 40046, 10 jan. 2017.
- GHANNOUM, M. A. et al. Characterization of the oral fungal microbiome (mycobiome) in healthy individuals. **PLoS pathogens**, v. 6, n. 1, p. e1000713, 8 jan. 2010.
- GIL, C. et al. Biofilm matrix exoproteins induce a protective immune response against *Staphylococcus aureus* biofilm infection. **Infection and Immunity**, v. 82, n. 3, p. 1017–1029, mar. 2014.
- GREGOIRE, S. et al. Role of glucosyltransferase B in interactions of *Candida albicans* with *Streptococcus mutans* and with an experimental pellicle on hydroxyapatite surfaces. **Applied and Environmental Microbiology**, v. 77, n. 18, p. 6357–6367, set. 2011.
- GUGGENHEIM, B. Extracellular polysaccharides and microbial plaque. **International Dental Journal**, v. 20, n. 4, p. 657–678, dez. 1970.
- GUZMÁN-SOTO, I. et al. Mimicking biofilm formation and development: Recent progress in In

Vitro and In Vivo biofilm models. **iScience**, p. 102443, 17 abr. 2021.

HAMADA, S. et al. Effect of dextranase on the extracellular polysaccharide synthesis of *Streptococcus mutans*; chemical and scanning electron microscopy studies. **Infection and Immunity**, v. 12, n. 6, p. 1415–1425, dez. 1975.

HAYACIBARA, M. F. et al. The influence of mutanase and dextranase on the production and structure of glucans synthesized by streptococcal glucosyltransferases. **Carbohydrate Research**, v. 339, n. 12, p. 2127–2137, 23 ago. 2004.

HE, Y. et al. Targeted MIP-3 β plasmid nanoparticles induce dendritic cell maturation and inhibit M2 macrophage polarisation to suppress cancer growth. **Biomaterials**, v. 249, p. 120046, ago. 2020.

HEITZ-MAYFIELD, L. J. A.; MOMBELLI, A. The therapy of peri-implantitis: a systematic review. **The International Journal of Oral & Maxillofacial Implants**, v. 29 Suppl, p. 325–345, 2014.

HEITZ-MAYFIELD, L. J. A.; SALVI, G. E. Peri-implant mucositis. **Journal of Clinical Periodontology**, v. 45, n. S20, p. S237–S245, 2018.

HOJO, K. et al. Bacterial interactions in dental biofilm development. **Journal of Dental Research**, v. 88, n. 11, p. 982–990, nov. 2009.

HONMA, K. et al. Role of a *Tannerella forsythia* exopolysaccharide synthesis operon in biofilm development. **Microbial Pathogenesis**, v. 42, n. 4, p. 156–166, abr. 2007.

HOPE, C. K.; WILSON, M. Analysis of the effects of chlorhexidine on oral biofilm vitality and structure based on viability profiling and an indicator of membrane integrity. **Antimicrobial Agents and Chemotherapy**, v. 48, n. 5, p. 1461–1468, maio 2004.

HWANG, G. et al. *Candida albicans* mannans mediate *Streptococcus mutans* exoenzyme GtfB binding to modulate cross-kingdom biofilm development in vivo. **PLoS pathogens**, v. 13, n. 6, p. e1006407, jun. 2017.

INOUE, D. et al. Inhibition of biofilm formation on iodine-supported titanium implants. **International Orthopaedics**, v. 41, n. 6, p. 1093–1099, jun. 2017.

IZANO, E. A. et al. Poly-N-acetylglucosamine mediates biofilm formation and detergent resistance in *Aggregatibacter actinomycetemcomitans*. **Microbial Pathogenesis**, v. 44, n. 1, p. 52–60, jan. 2008.

JAKUBOVICS, N. S. et al. The dental plaque biofilm matrix. **Periodontology 2000**, v. 86, n. 1, p. 32–56, 2021a.

JAKUBOVICS, N. S. et al. The dental plaque biofilm matrix. **Periodontology 2000**, v. 86, n. 1, p. 32–56, jun. 2021b.

KAPLAN, J. B. et al. Genes involved in the synthesis and degradation of matrix polysaccharide in *Actinobacillus actinomycetemcomitans* and *Actinobacillus pleuropneumoniae* biofilms. **Journal of Bacteriology**, v. 186, n. 24, p. 8213–8220, dez. 2004.

KAPLAN, J. B. Biofilm matrix-degrading enzymes. **Methods in Molecular Biology (Clifton, N.J.)**, v. 1147, p. 203–213, 2014.

KARYGIANNI, L. et al. Biofilm Matrixome: Extracellular Components in Structured Microbial Communities. **Trends in Microbiology**, v. 28, n. 8, p. 668–681, ago. 2020.

KHOURY, Z. H. et al. The Role of *Candida albicans* Secreted Polysaccharides in Augmenting *Streptococcus mutans* Adherence and Mixed Biofilm Formation: In vitro and in vivo Studies. **Frontiers in Microbiology**, v. 11, p. 307, 28 fev. 2020.

KIM, D. et al. Bacterial-derived exopolysaccharides enhance antifungal drug tolerance in a cross-

- kingdom oral biofilm. **The ISME journal**, v. 12, n. 6, p. 1427–1442, 2018a.
- KIM, H. E. et al. Intervening in Symbiotic Cross-Kingdom Biofilm Interactions: a Binding Mechanism-Based Nonmicrobicidal Approach. **mBio**, v. 12, n. 3, p. e00651-21, [s.d.].
- KLEIN, M. I. et al. Streptococcus mutans protein synthesis during mixed-species biofilm development by high-throughput quantitative proteomics. **PloS One**, v. 7, n. 9, p. e45795, 2012.
- KLEIN, M. I. et al. Streptococcus mutans-derived extracellular matrix in cariogenic oral biofilms. **Frontiers in Cellular and Infection Microbiology**, v. 5, 13 fev. 2015.
- KOLENBRANDER, P. E. Oral microbial communities: biofilms, interactions, and genetic systems. **Annual Review of Microbiology**, v. 54, p. 413–437, 2000.
- KOLENBRANDER, P. E. et al. Bacterial interactions and successions during plaque development. **Periodontology 2000**, v. 42, p. 47–79, 2006.
- KOO, H. et al. Exopolysaccharides Produced by Streptococcus mutans Glucosyltransferases Modulate the Establishment of Microcolonies within Multispecies Biofilms. **Journal of Bacteriology**, v. 192, n. 12, p. 3024–3032, 15 jun. 2010.
- KOO, H. et al. Targeting microbial biofilms: current and prospective therapeutic strategies. **Nature Reviews. Microbiology**, v. 15, n. 12, p. 740–755, dez. 2017.
- KOO, H.; FALSETTA, M. L.; KLEIN, M. I. The exopolysaccharide matrix: a virulence determinant of cariogenic biofilm. **Journal of Dental Research**, v. 92, n. 12, p. 1065–1073, dez. 2013.
- LAFRAURIE, G. I. et al. Microbiome and Microbial Biofilm Profiles of Peri-Implantitis: A Systematic Review. **Journal of Periodontology**, v. 88, n. 10, p. 1066–1089, 2017.
- LAMONT, R. J.; KOO, H.; HAJISHENGALLIS, G. The oral microbiota: dynamic communities and host interactions. **Nature Reviews Microbiology**, v. 16, n. 12, p. 745–759, dez. 2018.
- LANG, N. P. et al. Ligature-induced peri-implant infection in cynomolgus monkeys. I. Clinical and radiographic findings. **Clinical Oral Implants Research**, v. 4, n. 1, p. 2–11, mar. 1993.
- LOPEZ-RIBOT, J. L. Large-Scale Biochemical Profiling of the Candida albicans Biofilm Matrix: New Compositional, Structural, and Functional Insights. **mBio**, v. 5, n. 5, p. e01781-14, [s.d.].
- LULA, E. C. O. et al. Added sugars and periodontal disease in young adults: an analysis of NHANES III data. **The American Journal of Clinical Nutrition**, v. 100, n. 4, p. 1182–1187, out. 2014.
- MAKVANDI, P. et al. Drug Delivery (Nano)Platforms for Oral and Dental Applications: Tissue Regeneration, Infection Control, and Cancer Management. **Advanced Science**, v. n/a, n. n/a, p. 2004014, [s.d.].
- MARSH, P. D.; BRADSHAW, D. J. Physiological approaches to the control of oral biofilms. **Advances in Dental Research**, v. 11, n. 1, p. 176–185, abr. 1997.
- MARTORANO-FERNANDES, L. et al. Interkingdom interaction between C. albicans and S. salivarius on titanium surfaces. **BMC oral health**, v. 20, n. 1, p. 349, 1 dez. 2020.
- MATSUMOTO-NAKANO, M. Role of Streptococcus mutans surface proteins for biofilm formation. **The Japanese Dental Science Review**, v. 54, n. 1, p. 22–29, fev. 2018.
- MAZUMDAR, V.; AMAR, S.; SEGRÉ, D. Metabolic Proximity in the Order of Colonization of a Microbial Community. **PLOS ONE**, v. 8, n. 10, p. e77617, 30 out. 2013.
- MITCHELL, K. F. et al. Community participation in biofilm matrix assembly and function. **Proceedings of the National Academy of Sciences of the United States of America**, v. 112, n. 13, p. 4092–4097, 31 mar. 2015.

- MOI, G. P. et al. Proteomic Analysis of Matrix of Dental Biofilm Formed under Dietary Carbohydrate Exposure. **Caries Research**, v. 46, n. 4, p. 339–345, 2012.
- MOMBELLI, A.; DÉCAILLET, F. The characteristics of biofilms in peri-implant disease. **Journal of Clinical Periodontology**, v. 38 Suppl 11, p. 203–213, mar. 2011.
- MONTELONGO-JAUREGUI, D. et al. An In Vitro Model for *Candida albicans*-*Streptococcus gordonii* Biofilms on Titanium Surfaces. **Journal of Fungi (Basel, Switzerland)**, v. 4, n. 2, p. E66, 4 jun. 2018.
- NODZO, S. R. et al. Cathodic Voltage-controlled Electrical Stimulation Plus Prolonged Vancomycin Reduce Bacterial Burden of a Titanium Implant-associated Infection in a Rodent Model. **Clinical Orthopaedics and Related Research**, v. 474, n. 7, p. 1668–1675, jul. 2016.
- NOVOTNY, L. A. et al. Monoclonal antibodies against DNA-binding tips of DNABII proteins disrupt biofilms in vitro and induce bacterial clearance in vivo. **EBioMedicine**, v. 10, p. 33–44, ago. 2016.
- NYVAD, B.; TAKAHASHI, N. Integrated hypothesis of dental caries and periodontal diseases. **Journal of Oral Microbiology**, v. 12, n. 1, p. 1710953, [s.d.].
- OKSHEVSKY, M.; REGINA, V. R.; MEYER, R. L. Extracellular DNA as a target for biofilm control. **Current Opinion in Biotechnology**, Environmental biotechnology • Energy biotechnology. v. 33, p. 73–80, 1 jun. 2015.
- OTZEN, D. E. Biosurfactants and surfactants interacting with membranes and proteins: Same but different? **Biochimica et Biophysica Acta (BBA) - Biomembranes**, Lipid order/lipid defects and lipid-control of protein activity. v. 1859, n. 4, p. 639–649, 1 abr. 2017.
- PADIAL-MOLINA, M. et al. Microbial Profiles and Detection Techniques in Peri-Implant Diseases: a Systematic Review. **Journal of Oral & Maxillofacial Research**, v. 7, n. 3, p. e10, 9 set. 2016.
- PAES LEME, A. F. et al. Effects of sucrose on the extracellular matrix of plaque-like biofilm formed in vivo, studied by proteomic analysis. **Caries Research**, v. 42, n. 6, p. 435–443, 2008.
- PANARIELLO, B. H. D. et al. DNase increases the efficacy of antimicrobial photodynamic therapy on *Candida albicans* biofilms. **Photodiagnosis and Photodynamic Therapy**, v. 27, p. 124–131, set. 2019.
- PAULA, A. J.; HWANG, G.; KOO, H. Dynamics of bacterial population growth in biofilms resemble spatial and structural aspects of urbanization. **Nature Communications**, v. 11, p. 1354, 13 mar. 2020.
- PÉREZ-CHAPARRO, P. J. et al. The Current Weight of Evidence of the Microbiologic Profile Associated With Peri-Implantitis: A Systematic Review. **Journal of Periodontology**, v. 87, n. 11, p. 1295–1304, nov. 2016.
- PETERSON, B. W. et al. A distinguishable role of eDNA in the viscoelastic relaxation of biofilms. **mBio**, v. 4, n. 5, p. e00497-00413, 15 out. 2013.
- PETERSON, B. W. et al. Viscoelasticity of biofilms and their recalcitrance to mechanical and chemical challenges. **FEMS microbiology reviews**, v. 39, n. 2, p. 234–245, mar. 2015.
- PIERCE, C. G. et al. The *Candida albicans* Biofilm Matrix: Composition, Structure and Function. **Journal of Fungi (Basel, Switzerland)**, v. 3, n. 1, p. 14, mar. 2017.
- PIERRE, G. et al. Biochemical composition and changes of extracellular polysaccharides (ECPS) produced during microphytobenthic biofilm development (Marennes-Oléron, France). **Microbial Ecology**, v. 63, n. 1, p. 157–169, jan. 2012.
- PLESZCZYŃSKA, M. et al. (1→3)- α -D-Glucan hydrolases in dental biofilm prevention and control:

- A review. **International Journal of Biological Macromolecules**, v. 79, p. 761–778, ago. 2015.
- RABE, M.; VERDES, D.; SEEGER, S. Understanding protein adsorption phenomena at solid surfaces. **Advances in Colloid and Interface Science**, v. 162, n. 1, p. 87–106, 17 fev. 2011.
- REN, Z. et al. Molecule Targeting Glucosyltransferase Inhibits Streptococcus mutans Biofilm Formation and Virulence. **Antimicrobial Agents and Chemotherapy**, v. 60, n. 1, p. 126–135, jan. 2016.
- REN, Z. et al. Dual-Targeting Approach Degrades Biofilm Matrix and Enhances Bacterial Killing. **Journal of Dental Research**, v. 98, n. 3, p. 322–330, 2019.
- RENVERT, S.; ROOS-JANSÅKER, A.-M.; CLAFFEY, N. Non-surgical treatment of peri-implant mucositis and peri-implantitis: a literature review. **Journal of Clinical Periodontology**, v. 35, n. 8 Suppl, p. 305–315, set. 2008.
- RICKER, A.; VICKERMAN, M.; DONGARI-BAGTZOGLOU, A. Streptococcus gordonii glucosyltransferase promotes biofilm interactions with Candida albicans. **Journal of Oral Microbiology**, v. 6, 2014.
- RUSSELL, R. R. et al. Streptococcus mutans gtfA gene specifies sucrose phosphorylase. **Infection and Immunity**, v. 56, n. 10, p. 2763–2765, out. 1988.
- SAFIOTI, L. M. et al. Increased Levels of Dissolved Titanium Are Associated With Peri-Implantitis - A Cross-Sectional Study. **Journal of Periodontology**, v. 88, n. 5, p. 436–442, maio 2017.
- SAHRMANN, P. et al. Systematic review on the effect of rinsing with povidone-iodine during nonsurgical periodontal therapy. **Journal of Periodontal Research**, v. 45, n. 2, p. 153–164, abr. 2010.
- SALVI, G. E.; COSGAREA, R.; SCULEAN, A. Prevalence and Mechanisms of Peri-implant Diseases. **Journal of Dental Research**, v. 96, n. 1, p. 31–37, 1 jan. 2017.
- SAMPAIO, A. A. et al. Candida albicans Increases Dentine Demineralization Provoked by Streptococcus mutans Biofilm. **Caries Research**, v. 53, n. 3, p. 322–331, 2019.
- SCHILLING, K. M.; BOWEN, W. H. Glucans synthesized in situ in experimental salivary pellicle function as specific binding sites for Streptococcus mutans. **Infection and Immunity**, v. 60, n. 1, p. 284–295, jan. 1992.
- SCHLAFER, S. et al. Extracellular DNA Contributes to Dental Biofilm Stability. **Caries Research**, v. 51, n. 4, p. 436–442, 2017.
- SCHWARZ, F. et al. Peri-implantitis. **Journal of Clinical Periodontology**, v. 45 Suppl 20, p. S246–S266, jun. 2018.
- SERRAGE, H. J. et al. Understanding the Matrix: The Role of Extracellular DNA in Oral Biofilms. **Frontiers in Oral Health**, v. 2, p. 7, 2021.
- SHIBLI, J. A. et al. Composition of supra- and subgingival biofilm of subjects with healthy and diseased implants. **Clinical Oral Implants Research**, v. 19, n. 10, p. 975–982, out. 2008.
- SHIBLI, J. A. et al. Microbiological and clinical effects of adjunctive systemic metronidazole and amoxicillin in the non-surgical treatment of peri-implantitis: 1 year follow-up. **Brazilian Oral Research**, v. 33, 2019.
- SMITH, A. W. Biofilms and antibiotic therapy: Is there a role for combating bacterial resistance by the use of novel drug delivery systems? **Advanced Drug Delivery Reviews**, v. 57, n. 10, p. 1539–1550, 2005.

- SOUZA, J. G. S. et al. Effect of sucrose on biofilm formed in situ on titanium material. **Journal of Periodontology**, v. 90, n. 2, p. 141–148, fev. 2019.
- SOUZA, J. G. S. et al. Titanium particles and ions favor dysbiosis in oral biofilms. **Journal of Periodontal Research**, v. 55, n. 2, p. 258–266, abr. 2020a.
- SOUZA, J. G. S. et al. Proteomic profile of the saliva and plasma protein layer adsorbed on Ti–Zr alloy: the effect of sandblasted and acid-etched surface treatment. **Biofouling**, v. 36, n. 4, p. 428–441, 20 abr. 2020b.
- SOUZA, J. G. S. et al. Role of glucosyltransferase R in biofilm interactions between *Streptococcus oralis* and *Candida albicans*. **The ISME journal**, v. 14, n. 5, p. 1207–1222, maio 2020c.
- SOUZA, J. G. S. et al. Targeting implant-associated infections: titanium surface loaded with antimicrobial. **iScience**, v. 24, n. 1, p. 102008, 22 jan. 2021.
- SOUZA, J. G. S. et al. Biofilm Interactions of *Candida albicans* and Mitis Group *Streptococci* in a Titanium-Mucosal Interface Model. **Applied and Environmental Microbiology**, v. 86, n. 9, p. e02950-19, [s.d.].
- SUN, T.; QING, G. Biomimetic Smart Interface Materials for Biological Applications. **Advanced Materials**, v. 23, n. 12, p. H57–H77, 2011.
- SZTAJER, H. et al. Cross-feeding and interkingdom communication in dual-species biofilms of *Streptococcus mutans* and *Candida albicans*. **The ISME journal**, v. 8, n. 11, p. 2256–2271, nov. 2014.
- TAKAHASHI, N. Oral Microbiome Metabolism: From “Who Are They?” to “What Are They Doing?” **Journal of Dental Research**, v. 94, n. 12, p. 1628–1637, dez. 2015.
- TEUGHEL, W. et al. Adjunctive effect of systemic antimicrobials in periodontitis therapy: A systematic review and meta-analysis. **Journal of Clinical Periodontology**, v. 47 Suppl 22, p. 257–281, jul. 2020.
- URISH, K. L. et al. Pulse lavage is inadequate at removal of biofilm from the surface of total knee arthroplasty materials. **The Journal of Arthroplasty**, v. 29, n. 6, p. 1128–1132, jun. 2014.
- VACCA-SMITH, A. M. et al. Interactions of streptococcal glucosyltransferases with alpha-amylase and starch on the surface of saliva-coated hydroxyapatite. **Archives of Oral Biology**, v. 41, n. 3, p. 291–298, mar. 1996.
- WALKER, G. J.; HARE, M. D.; MORREY-JONES, J. G. Activity of fructanase in batch cultures of oral streptococci. **Carbohydrate Research**, v. 113, n. 1, p. 101–112, 16 fev. 1983.
- WHITCHURCH, C. B. et al. Extracellular DNA required for bacterial biofilm formation. **Science (New York, N.Y.)**, v. 295, n. 5559, p. 1487, 22 fev. 2002.
- XIAO, J. et al. The exopolysaccharide matrix modulates the interaction between 3D architecture and virulence of a mixed-species oral biofilm. **PLoS pathogens**, v. 8, n. 4, p. e1002623, 2012.
- YAMANAKA, T. et al. Gene expression profile and pathogenicity of biofilm-forming *Prevotella intermedia* strain 17. **BMC Microbiology**, v. 9, n. 1, p. 11, 16 jan. 2009.
- YAMANE, K. et al. A novel exopolysaccharide from a clinical isolate of *Prevotella nigrescens*: purification, chemical characterization and possible role in modifying human leukocyte phagocytosis. **Oral Microbiology and Immunology**, v. 20, n. 1, p. 1–9, fev. 2005.
- ZHANG, H. Molecularly Imprinted Nanoparticles for Biomedical Applications. **Advanced Materials**, v. 32, n. 3, p. 1806328, 2020.

2.3 Novel 3-step nonsurgical decontamination protocol for titanium-based dental implants: An *in vitro* and *in situ* study

Short running title: Decontamination protocol for titanium-based dental implants

Raphael Cavalcante Costa¹ | Thais Terumi Sadamitsu Takeda¹ | Caroline Dini¹ | Martinna Bertolini² | Raquel Carla Ferreira³ | Gabriele Pereira³ | Catharina Marques Sacramento¹ | Karina Gonzales S. Ruiz¹ | Magda Feres^{3,4} | Jamil A. Shibli³ | Valentim A. R. Barão^{1*} | João Gabriel S. Souza^{3,5*}

¹Department of Prosthodontics and Periodontology, Piracicaba Dental School, University of Campinas (UNICAMP), Av. Limeira, 901, Piracicaba, São Paulo 13414-903, Brazil

²Department of Periodontics and Preventive Dentistry, School of Dental Medicine, University of Pittsburgh, Pittsburgh, PA 15106, USA

³Dental Research Division, Guarulhos University, Guarulhos, SP, 07023-070, Brazil.

⁴Department of Oral Medicine, Infection and Immunity, Harvard School of Dental Medicine, Boston, MA 02115, USA.

⁵Dentistry Science School (Faculdade de Ciências Odontológicas - FCO), Montes Claros, Minas Gerais 39401-303, Brazil.

***Corresponding authors:**

1. Valentim A. R. Barão, University of Campinas (UNICAMP), Piracicaba Dental School, Department of Prosthodontics and Periodontology, Av. Limeira, 901, Piracicaba, São Paulo, 13414-903, Brazil. Email: vbarao@unicamp.br

2. João Gabriel S. Souza, Dental Research Division, Guarulhos University, Guarulhos, SP, 07023-070, Brazil. Email: jgabriel.ssouza@yahoo.com.br

Note: VARB and JGSS share the position of senior authors.

ACKNOWLEDGMENTS

This study was funded by The São Paulo Research Foundation (FAPESP), Grant/Award numbers: 2020/10436-4 to R.C.C, and 2020/05231-4 to V.A.R.B.; Conselho Nacional de Desenvolvimento Científico e Tecnológico (CNPq), Grant/Award number: #307471/2021-7 to V.A.R.B; and Coordenação de Aperfeiçoamento de Pessoal de Nível Superior (CAPES), Finance code 001. The authors are indebted to Plenum[®] Company for supplying the samples used in this study. The authors also thank the Brazilian Nanotechnology National Laboratory (LNNano) at the Brazilian Center of Research in Energy and Materials (CNPEM) for the CLSM analysis facility and the Richard Landers for the XPS analysis facility. Finally, the authors express their gratitude to the volunteers for their valuable participation.

DISCLAIMERS

Jamil A. Shibli is currently the chief science officer at the M3 Health Ind. Com. de Prod. Med. Odont. e Correlatos S.A. (Plenum[®] Company; Jundiaí, São Paulo, Brasil) and declares conflicts of interest. The other authors certify that they have no commercial or associative interest that represents a conflict of interest in the manuscript.

AUTHOR CONTRIBUTIONS

RCC, JGSJ, and VARB contributed to conception and design, data acquisition, analysis, and interpretation, drafted and critically revised the manuscript; RCF, GP, CMS, KGSR, MF, JAS, contributed to design, data acquisition, drafted and critically revised the manuscript. All authors gave final approval and agreed to be accountable for all aspects of the work ensuring integrity and accuracy.

DATA AVAILABILITY STATEMENT

The data that support the findings of this study are available from the corresponding author upon reasonable request.

ABSTRACT

There is no agreement on the most efficient nonsurgical decontamination protocol for peri-implantitis treatment, especially when rough titanium (Ti) surfaces are exposed. Therefore, we aimed to evaluate several mechanical and chemical decontamination methods and the possible harmful effects of implant surfaces to propose a new protocol for exposed surfaces. Ti discs were obtained by additive manufacturing. Polymicrobial biofilm-covered Ti disc surfaces were decontaminated with mechanical [Ti curette, Teflon curette, Ti brush, water-air jet device, and Er:YAG laser] or chemical [iodopovidone (PVPI) 0.2% to disrupt the extracellular matrix, along with amoxicillin; minocycline; tetracycline; H₂O₂ 3%; chlorhexidine 0.2%; NaOCl 0.95%; or hydrocarbon-oxo-borate-based antiseptic] protocols. The optimal *in vitro* mechanical/chemical protocol was then tested in combination using an *in situ* oral biofilm model. Er:YAG laser treatment displayed optimum surface cleaning by biofilm removal with minimal deleterious damage to the surface, smaller Ti release, good corrosion stability, and improved fibroblast readhesion. NaOCl 0.95% was the most promising agent to reduce *in vitro* and *in situ* biofilms and was even more effective when associated with PVPI 0.2% as a pretreatment to disrupt the biofilm matrix. The combination of Er:YAG laser followed by PVPI 0.2% plus NaOCl 0.95% promoted efficient decontamination of rough Ti surfaces by disrupting the biofilm matrix and killing remnants of *in situ* biofilms (the only protocol to lead to ~99% biofilm eradication). We conclude that Er:YAG laser + PVPI 0.2% + NaOCl 0.95% can be an reliable decontamination protocol for Ti surfaces, eliminating microbial biofilms without damaging the implant surface.

Keywords:

Decontamination

Dental implant

Biofilm

Peri-implantitis

Word count: 6263

1 | Introduction

Dental implants are a reliable and predictable treatment option for supporting dental prostheses with high clinical longevity and survival rates (Howe et al. 2019). However, immune-mediated biological complications attributed to polymicrobial biofilms formed around the implant often lead to peri-implant diseases, such as peri-implant mucositis and peri-implantitis (Berglundh et al. 2018). Once the biofilm accumulates on the implant surface, treatment involving effective microbial removal becomes very challenging for clinicians due to the complex biofilm architecture, which is highly specialized to favor coaggregation and cell protection through the extracellular biofilm matrix (Costa et al. 2020; Yang et al. 2023). Meta-analyses have shown that peri-implantitis can affect 12%–24% of patients 5–10 years after implant placement (Derks & Tomasi 2015; Lee et al. 2017). Furthermore, peri-implant diseases continue to rise worldwide due to the popularity of dental implants and population aging and are considered an emergent global public health problem (Costa et al. 2021). Therefore, since pathogenic biofilm accumulation on implant material is a major cause of peri-implant diseases, surface decontamination is a prerequisite to successful therapy for implant-related diseases (Cosgarea et al. 2022).

Implant decontamination can be performed with nonsurgical and surgical interventions using a plethora of physical and chemical protocols (Ntrouka et al. 2011; Louropoulou et al. 2014). Regarding nonsurgical therapies, conventional mechanical debridement with various types of scalers, ultrasonic tips, brushes, or alternative approaches such as oral irrigators, air-abrasive devices, and laser therapies are commonly used to clean contaminated implants (Figuera et al. 2014; Cosgarea et al. 2022). Nevertheless, these mechanical therapies have shortcomings due to their limited accessibility for cleaning the complex rough titanium (Ti) implant surface, hindering effective biofilm removal (Costa et al. 2020). If the remaining biofilm structure is not removed, it may promote microbial recolonization and persistent infection (Bowen et al. 2018). For this reason, chemotherapeutic agents have also been applied as an adjunct to subgingival instrumentation (Balderrama et al. 2020). However, the effectiveness of disinfection protocols remains unpredictable, and reported beneficial clinical outcomes might be restricted to a short-term period, especially if implant surfaces are left exposed in the oral cavity (Renvert et al. 2008; Shibli et al. 2019). Currently, no particular treatment is considered the gold standard for disrupting the biofilm matrix and efficiently reducing the bacterial load below the threshold level for predictable nonsurgical treatment outcomes, raising the need for biofilm-focused treatment modalities (Figuera et al. 2014; Heitz-Mayfield and Mombelli 2014; Cosgarea et al. 2022). In this context, strategies for disrupting bacterial clustering and the exopolysaccharide matrix to enhance biofilm removal have been suggested to overcome the

therapeutic limitation of peri-implantitis treatment, but this novel strategy is still being underutilized (Costa et al. 2022; Souza et al. 2022; Yang et al. 2023).

The 2017 World Workshop on the Classification of Periodontal and Peri-Implant Diseases and Conditions consensus report recognized that an optimal decontamination protocol should ensure both cleaning potential by biofilm removal and maintenance of implant surface features to possibly achieve the biological seal of the implant-soft tissue interface and reosseointegration afterward (Berglundh et al. 2018). However, this protocol has not yet been established. This goal becomes a particular challenge with the rough Ti surfaces currently used in dental implants compared to the classic turned implants initially used by Branemark (Howe et al. 2019). Here, we conducted *in vitro* and *in situ* studies aiming to examine not only Ti surface decontamination efficacy but also their possible deleterious effects on a 3D printed rough surface, including Ti release, corrosion behavior, and posterior fibroblast cytocompatibility. Collectively, we unveil a promising combined mechanical/chemical protocol based on the initial biofilm matrix disruption strategy associated with bacterial killing and removal to effectively decontaminate complex rough dental implant surfaces.

2 | Material and methods

2.1 Experimental design and ethical aspects

This study was designed with emerging mechanical and chemical protocols for dental implant decontamination currently used in the clinic setting. Importantly, a matrix-degrading agent was used prior to chemical therapy to further enhance bacterial killing on the implant surface. In brief, *in vitro* tests were conducted to evaluate the best treatment for promoting minimum surface damage without altering the posterior fibroblasts adhesion, morphology, and spreading. Additionally, polymicrobial biofilm-covered surfaces were also tested to confirm efficient biofilm removal and bacteria viability using mechanical and chemical protocols. Next, chemotherapeutics agents were tested in combination with a pre-treatment with PVPI 0.2% to determine the best *in vitro* surface disinfection. Last, the best mechanical/chemical protocol, optimized by PVPI 0.2% application, was evaluated against biofilms formed in the oral environment using our validated *in situ* model for implant surfaces with healthy volunteers (Souza et al. 2019b) to determine the efficiency of the established 3-step decontamination protocol. This study was approved by the Local Research and Ethics Committee (protocol 53844321.2.0000.5418) and was conducted in according to Brazilian ethical regulations (National Health Council, resolution 466/12) and the Declaration of Helsinki.

2.2 | Rough Ti implant surfaces

Rough Ti surface discs ($N = 80$; $\emptyset 12$ mm x 2 mm) were made of Ti-6Al-4 V powders with a particle size of 25–45 μm by additive manufacturing technology (Pinguero et al. 2019). The titanium discs presented a hierarchical surface referent to the commercial Plenum[®] implant surface (Jundiaí, São Paulo, Brazil). The selection of this implant surface was based on the difficulty to remove bacteria from the highly rougher surfaces (Ra value: 7.70 μm), thus being a relevant condition to determine the best effect of decontamination protocols.

2.3 | Mechanical instrumentation protocols

A calibration process was performed prior to the commencement of the study to ensure the reproducibility of the decontamination methods. Two examiners (R.C.C. and T.T.S.T.) were calibrated by calculating the intraclass correlation coefficient (ICC = 0.834; $p < 0.0001$; two-way random-effects model) based on the load applied (N) in hand instruments during the decontamination of implant surfaces on two separate occasions, 1 week apart. After a pilot study, each sample was instrumented for 60 s utilizing a sterile technique. The discs were randomly and equally allocated to the following decontamination protocols:

[1] **As-received:** control group without instrumentation.

[2] **Titanium curette** (M. Polachini, São Paulo, SP, Brazil): manually treated with a working force of ~ 0.25 N and an angle of 70–80°, moving in an imbricate style with 20 strokes, and immersed in deionized water.

[3] **Teflon curette** (M. Polachini, São Paulo, SP, Brazil): manually treated with a working force of ~ 0.25 N and an angle of 70–80°, moving in an imbricate style with 20 strokes, and immersed in deionized water.

[4] **Titanium brush** (Salvin Dental, Charlotte, NC, USA): rotatory brushes were coupled in the oscillating dental handpiece at 600 rpm, with irrigation of deionized water, light pressure, and at an angle of approximately 45–60° as recommended in the instructions for use by the manufacturer for nonflap cases.

[5] **Water–air jet** (Oraljet, Campinas, SP, Brazil): A standard handpiece was mounted with a holder to maintain the nozzle at a static position, perpendicular to the disc, to treat each sample at a distance of 10 mm with a static pressure of 7 bar (101.5 psi) and 60 mL of deionized water/min.

[6] **Erbium-doped yttrium aluminum garnet (Er:YAG) laser** (Life touch[®], Light Instruments, São Paulo, SP, Brazil): laser irradiation with the tip 1.3×17 mm, perpendicular to the disc, at a distance of 10 mm with laser beam parameters using the manufacturers' recommended setting for implant recovery (40 mJ, 0.80 W, 20 Hz, in continuous mode).

To simulate clinical practice, the force exerted in hand instruments (protocols 2 and 3) is consistent with those that would be used to remove adherent calculus deposits from implant surfaces (Lang et al. 2016). For the automatic tools (protocols 4, 5, and 6), each disc received treatment by being consistently rotated opposing the nozzle from the center to the periphery in ten circular motions. After instrumentation, all the discs were cleaned with deionized water. These mechanical instrumentations were performed in the presence and absence of oral biofilms.

2.4 | Chemical decontamination protocols

Biofilm-covered implant surfaces were treated by immersion in a 24-well plate with 1 mL (v/v) of seven different chemotherapeutic agents and incubated under static conditions (± 37 °C; 10% CO₂) for 10 min, as follows:

- [1] **Sterile saline [NaCl; 0.9% - v/v]**: control group without disinfection treatment.
- [2] **Amoxicillin [AMX; 4.14 µg/mL]** (Sigma–Aldrich, St. Louis, MO, USA) to simulate the concentrations detected in the pocket environment following systemic administration (Tenenbaum et al. 1997).
- [3] **Minocycline [MIN; 1.49 µg/mL]** (Sigma–Aldrich, St. Louis, MO, USA) to simulate the concentrations detected in the pocket environment following systemic administration (Sakellari et al. 2000).
- [4] **Tetracycline [TEC; 0.61 µg/mL]** (Sigma–Aldrich, St. Louis, MO, USA) to simulate the concentrations detected in the pocket environment following systemic administration (Sakellari et al. 2000).
- [5] **Hydrogen peroxide [H₂O₂; 3% - v/v]** (Sigma–Aldrich, St. Louis, MO, USA) to mimic the local irrigation performed by professionals during clinical practice (Jervøe-Storm et al. 2021).
- [6] **Chlorhexidine [CHX; 0.2% - v/v]** (Sigma–Aldrich, St. Louis, MO, USA) to mimic the local irrigation performed by professionals during clinical practice (Souza et al. 2018).
- [7] **Hydrocarbon-oxo-borate-based formula antiseptic [HCOBc; 1 mL - v/v]** (BlueM®, Curitiba, PR, Brazil): to mimic the mouthwashes performed by patients in the oral care routine (Shibli et al. 2021).
- [8] **Sodium hypochlorite [NaOCl; 0.95% - v/v]** (Sigma–Aldrich, St. Louis, MO, USA) to mimic local administration by professionals during clinical practice (Radulescu et al. 2022).

After each treatment, samples were washed in 0.9% NaCl solution, and biofilm analysis was immediately conducted.

2.5 | Implant surface degradation

Rough Ti surfaces were analyzed after each mechanical instrumentation protocol. Three-dimensional images and roughness line profiles ($n = 3$) were acquired by laser scanning confocal microscopy (LSCM, VK-X200 series; Keyence, Osaka, Japan)(Souza et al. 2020a). Image processing was performed by software (VK Analyzer, Keyence v3.3.0.0; Osaka, Japan). Average surface roughness (Ra) ($n = 6$) was assessed by profilometry (Dektak D150; Veeco, Plainview, NY, USA) and acquired with a cutoff of 0.25 mm at 0.05 mm/s for 12 s (Borges et al. 2022). The water contact angle with mechanically treated samples was analyzed using a goniometer (Ramé-Hart 100–00; Ramé-Hart Instrument Co., Succasunna, NJ, USA) by the sessile drop (2 μ L) method ($n = 5$) (Borges et al. 2022). Ti ion release from the substrate ($n = 5$) was measured by an inductively coupled plasma optical emission spectrometer (ICP–OES, iCAP model, 7000 series; Thermo Scientific, MA, USA) (Costa et al. 2020).

2.6 | Corrosion performance

The electrochemical tests (OCP = open circuit potential, EIS = electrochemical impedance spectroscopy, and potentiodynamic polarization) were conducted following our previous protocol (Costa et al. 2020; Souza et al. 2020; Borges et al. 2022). To simulate the oral conditions, artificial saliva at 37 ± 1 °C (pH 6.5) was adopted as the electrolytic solution (10 mL). Prior to the tests, a cathodic potential (-0.9 V vs. SCE) was applied for 600 s to reduce the naturally formed TiO₂ oxide layer on the Ti surfaces. Subsequently, the OCP was scanned for 3600 s, followed by EIS measurements made at frequencies of 100 kHz to 5 mHz, with an AC curve in the range of ± 10 mV applied to the electrode. Such data were used to estimate the real (Z_{real}) and imaginary (Z_{imag}) components of the impedance, which were presented as a Nyquist plot, impedance ($|Z|$), and phase angle. The EIS data were modeled by means of a simple equivalent circuit that features a single dense oxide layer, in which R_{sol} represents the resistance of the electrolyte, R_p is the polarization resistance, and Q is the constant phase element (CPE). The polarization of the samples was conducted from -0.8 V to 1.8 V (2 mV/s scan rate). A Tafel extrapolation method was used to determine the polarization curves, which provided electrochemical variables such as corrosion potential (E_{corr}), corrosion current density (i_{corr}), and corrosion rate. For data analyses ($n = 5$), an exposed area of 1 cm² was considered.

In addition to electrochemical tests, X-ray photoelectron spectroscopy (XPS) analysis was used to determine the chemical composition of the outermost oxide layer ($n = 1$) of rough Ti surfaces. A spectrometer (K-Alpha X-ray XPS; Thermo Scientific, Finland) with a hemispheric analyzer was operated with an energy step at 0.100 eV and spot size at 400 μ m as previously described (Costa et al. 2020).

2.7 | Cell behavior

Primary human gingival fibroblasts (HGFs) collected from a single periodontal health patient were cultivated (passage 4) on mechanically treated surfaces ($n = 5$) to check the cytocompatibility (Souza et al. 2020a; Borges et al. 2022). Cells were seeded at a density of 1×10^4 cells/well in 48-well plates in Dulbecco's modified Eagle medium (Gibco, Life Technologies) supplemented with 2% fetal bovine serum, penicillin (100 U/mL), and streptomycin (100 mg/mL: Gibco, Life Technologies) in a humidified incubator at 37 °C in a 5% CO₂ atmosphere. The cell metabolism was evaluated after 24h by MTT 3-(4,5-dimethylthiazol-2-yl)-2,5-diphenyltetrazolium bromide method according to the manufacturer's instructions. Briefly, células lavadas com PBS, MTT concentracao (0,5 mg/ml) em meio de cultura. Incubadora 4 h, soltar cristais com etanol 100%. Leitura no espectofotometro a 570. Moreover, HGFs were fixed with Karnovsky's solution overnight at 4 °C and dehydrated through a grade ethanol series (35, 50, 70, 90, and 100%) at room temperature. The samples were critical-point-dried and gold-sputtered to analyze cell adhesion, morphology, and spreading by scanning electron microscopy (SEM; JEOL JSM-5600LV, Peabody, MA, USA) at 500× magnification. Additionally, the cell adhered area (in μm^2) on the surfaces was calculated on SEM micrographs using ImageJ software (National Institutes of Health, Bethesda, Maryland, USA) (Pantaroto et al. 2021). Experiments were independently performed at least twice with similar results.

2.8 | *In vitro* biofilm cleaning potential

Polymicrobial biofilms were formed using our saliva-coated Ti disc model, as previously detailed (Costa et al. 2020). In brief, a pool of fresh stimulated human saliva was collected from 4 healthy volunteers and used as microbial inoculum to mimic the oral microbiome composition ($\sim 10^8$ bacterial cells/mL) (Souza et al. 2018). Ti discs were incubated with BHI medium (Becton-Dickinson, Sparks, MD, USA) supplemented with 1% sucrose and saliva (1:10 v/v) for 48 h to promote biofilm accumulation at 37 °C with 10% CO₂. Media were changed every 24 h. Afterward, biofilms were treated as mentioned above under two protocols, mechanical and chemical isolation. Then, samples (2 experiments, $n = 3$ /experiment) were washed, vortexed, sonicated, serially diluted, and plated on BHI blood agar for colony-forming unit (CFU) counting of residual biofilm remnants. The recolonization potential of mechanically treated surfaces was also tested (2 experiments, $n = 3$ /experiment) (Souza et al. 2019). For this, discs used in the prior experiment were cleaned by UV light (4 W, $\lambda = 280$ nm, 20 min) to promote new microbial adhesion using fresh human saliva (same volunteers) for 1 h, following the conditions mentioned above. Bacterial recolonization was determined by CFU counts. Additionally, biofilm-covered discs after mechanical treatment were dehydrated in a series of ethanol washes, dried, mounted on stubs, sputter-coated with gold, and examined using SEM at 15 kV to visualize the structure of remnant biofilm (Bertolini et al. 2021).

Checkerboard DNA–DNA hybridization was used to identify periodontal pathogens in the residual biofilm remnants on the surface after mechanical instrumentation (2 experiments, $n = 6$ /experiment) (Costa et al. 2020; Souza et al. 2020). One hundred microliters of bacterial suspension from disrupted biofilms used for CFU analysis was collected. The samples were inserted into a tube containing 150 μL of TE solution (Tris HCl 10 mM + ethylenediaminetetraacetic acid 1 mM, pH 7.6) and a 100 μL quantity of 0.5 M NaOH was added to each tube. The samples were dispersed in a vortex mixer and then boiled for 10 min, and the final solution was neutralized with 0.8 mL of 5 M ammonium. The released DNA was then placed into the extended slots of a Minislot 30 apparatus (Immuntics, Cambridge, MA, USA), concentrated on a 15/15 cm positively charged nylon membrane (Boehringer Mannheim, Indianapolis, IN, USA), and fixed to the membrane by being baked at 121 °C for 20 min. The membrane was then placed in a Miniblotter 45 (Immuntics) with the lanes of DNA at 90° to the lanes of the device. Digoxigenin-labeled whole genomic DNA probes for 40 bacterial species were hybridized in individual lanes of the Miniblotter. After hybridization, the membranes were washed at high stringency, and the DNA probes were detected with the antibody to digoxigenin conjugated with alkaline phosphate and chemiluminescence detection. Signals were detected with the AttoPhos substrate (Amersham Life Sciences, Arlington Heights, IL, USA), and results were obtained with Typhoon Trio Plus (Molecular Dynamics, Sunnyvale, CA, USA). Data are expressed as the levels and proportions of 40 periodontal pathogens.

2.9 | *In vitro* disinfection therapies

After establishing the mechanical method that promoted enhanced biofilm cleaning potential, chemotherapeutic agents were tested to improve bacterial killing. Polymicrobial biofilm-covered discs (2 independent experiments, $n = 3$ /experiment) were then used to apply chemical protocols, as mentioned above. The antimicrobial effect was measured by CFU counts. An XTT reduction assay was also performed to determine the impact of each chemotherapeutic on bacterial metabolism (Silva et al. 2008). For this, XTT (Sigma–Aldrich, St. Louis, MO, USA) was dissolved in sterilized purified water at a final concentration of 0.5 mg/mL and mixed with 0.32 mg/mL phenazine methosulfate (PMS; Sigma–Aldrich, St. Louis, MO, USA) solution at a volume ratio of 9:1 (v/v). One hundred microliters of biofilm-containing solution was transferred to 96-well plates with 100 μL of XTT/PMS solution. Subsequently, the plates were kept in the dark (wrapped in foil) and incubated at 37 °C for 30 min. The colorimetric changes were measured at 492 nm using a spectrophotometer (DU 800 UV–visible Spectrophotometer, Beckman Coulter, Inc., Brea, CA).

CLSM (Confocal Laser Scanning Microscopy; CARLS ZEISS LSM 800 Airyscan with GaAsp detector, Germany) was used for live/dead cell and 3D-structure analyses of 48-hour

polymicrobial biofilms after chemotherapeutic exposure (Costa et al. 2020). Viable cells were stained using SYTO-9 green-fluorescent nucleic acid (480–500 nm; Thermo Fischer Scientific Inc.), and the nonviable cells were stained with propidium iodide solution (490–635 nm; Sigma–Aldrich). At least 3 random regions were selected to acquire stacks of the z-plane. The images were analyzed using ZEN Blue software (version 2.3) for reconstruction. Fluorescence intensity by area ($400 \mu\text{m}^2$) for each fluorescence emission corresponding to each fluorophore was also estimated (Souza et al. 2022). Region of interest (R.O.I.) was the same area for all images to allow comparisons. A.U. (arbitrary unit) was used to estimate fluorescence intensity. The fluorescence intensity was estimated by ZEN Blue software (version 2.3).

2.10 | Biofilm matrix-degrading therapy

Biofilm matrix-targeting therapy using PVPI 2% (v/v) to disrupt extracellular matrix compounds was previously tested on smooth Ti surfaces by our group (Costa et al. 2020). We are now in a position to deepen and improve the method to completely clean contaminated implant surfaces, including highly rough Ti implant surfaces. First, a dose–response assay was conducted to determine the minimum therapeutic concentration of PVPI. An *S. mutans* biofilm model was used due to its ability to produce extracellular polymers (EPS; exopolysaccharides) by glucosyltransferase exoenzymes (Costa et al. 2022). *S. mutans* UA159 strain overnight cultures cultivated in ultrafiltered tryptone-yeast extract broth (UTYEB) were adjusted to obtain 10^7 cells/mL (OD 1.0 at 600 nm) (Souza et al. 2022). The bacterial inoculum was incubated in UTYEB + 1% sucrose on discs for 24 h at 37 °C with 10% CO₂. PVPI (Sigma–Aldrich, St. Louis, MO, USA) at concentrations ranging from 0.01 to 3% (v/v) or NaCl 0.9% control were topically applied on biofilm-covered discs for 10 min to disrupt the extracellular biofilm matrix and then washed to remove excess. Afterward, samples were plated on BHI agar (Becton-Dickinson, Sparks, MD, USA), and CFU counts were quantified. For the EPS analyses, a 400- μL aliquot of the sonicated biofilm suspension was used for the extraction of soluble (S-EPS) and insoluble (I-EPS) extracellular polysaccharides, as described in detail previously (Souza et al. 2019). The total amount of carbohydrates in each sample was quantified by the phenol sulfuric method, with glucose as the standard. The total number of viable *S. mutans* after PVPI treatment was determined by CFU counts.

2.11 | *In situ* antimicrobial efficacy

The optimal mechanical/chemical protocol was tested in combination with PVPI treatment using an *in situ* model. The protocol includes 3 steps as follows: *i*) mechanical debridement; *ii*) biofilm matrix-degradating therapy with PVPI (10 min); and *iii*) adjuvant chemical administration (10 min). For this, four healthy volunteers wore a palatal appliance containing Ti discs for three days,

as described elsewhere (Costa et al. 2020). Samples ($n = 6$ per group) were exposed extraorally, 4 times/per day, to 20% (v/v) sucrose solution to allow the increase of peri-implant associated pathogens with bacterial loads similar to that found on periimplantitis (Souza et al. 2019). On the morning of the fourth day, discs were removed, randomized, and treated by the established mechanical/chemical protocol. Untreated biofilms were used as controls. The antimicrobial efficacy was determined by CFU counts and reported as % of bacterial count reduction after treatment vs. control. After decontamination, the biofilm remnants were fully collected and inserted into a tube (weight verified previously), and then the tube containing the sample was weighed to estimate the biofilm wet weight (in mg) as an indicator of residual biomass (Souza et al. 2019).

2.12 | Statistical analysis

GraphPad Prism software (GraphPad, La Jolla, CA, USA) was used for statistical analyses and to prepare the final graphs. The normality of errors and homoscedasticity of data were checked for each response variable, considering each sample as a statistical unit. The quantitative data were subjected to analysis of variance (ANOVA) in Tukey's HSD test for multiple comparisons. A significance level of 5% was considered to be statistically significant. The statistical power was calculated using the software G*Power version 3.1.9.2 (Program written, conceptualized, and designed by Franz, Universitat Kiel, Germany). Freely available Windows application software) ($\beta > 0.8$, $\alpha = 0.05$) considering the main variables of the study (CFU counts of *in vitro* and *in situ* biofilms). The entire dataset is available in a spreadsheet format and registered in a web-based institutional repository from the University of Campinas (UNICAMP).

3 | Results

3.1 | Mechanical instrumentation changes the implant surface topography

Two- and three-dimensional confocal images showed distinct effects on both the macro- and microstructure of the implant surface, leading to different roughness profiles for each treatment (Figure 1A). Mechanical instrumentation using a titanium brush, titanium curette, and Teflon curette generated significant surface damage and flattening peaks, leading to greater vertical discrepancies. The Er:YAG laser group showed an overall polished appearance with reduced sharpness of the peaks, while the valley area appeared unaffected. Finally, the water-air jet group showed no evident surface alterations. The two-dimensional average surface roughness values (Ra) of the as-received surface ($7.70 \pm 1.18 \mu\text{m}$) remained unchanged even after each method of instrumentation ($p > 0.05$; Figure 1B). The wettability property for all surfaces remained stable when compared to the as-received group ($p > 0.05$; Figure 1C), with similar average contact angles and a tendency for hydrophobicity (From

as-received: $111.24^\circ \pm 9.9$ up to Er:YAG: $90.31^\circ \pm 7.5$). Regarding surface degradation, titanium brush instrumentation induced the greatest Ti ion release (~ 4 -fold increases compared to as-received), and this concentration was statistically significant in all groups ($p < 0.05$; Figure 1D). The other groups showed no statistical difference among them, except with the as-received control group ($p < 0.05$).

Mechanical protocols

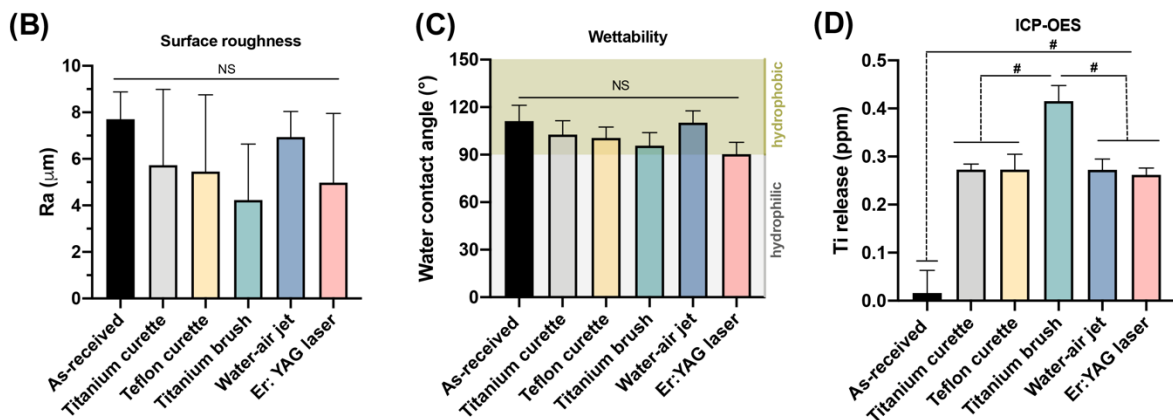
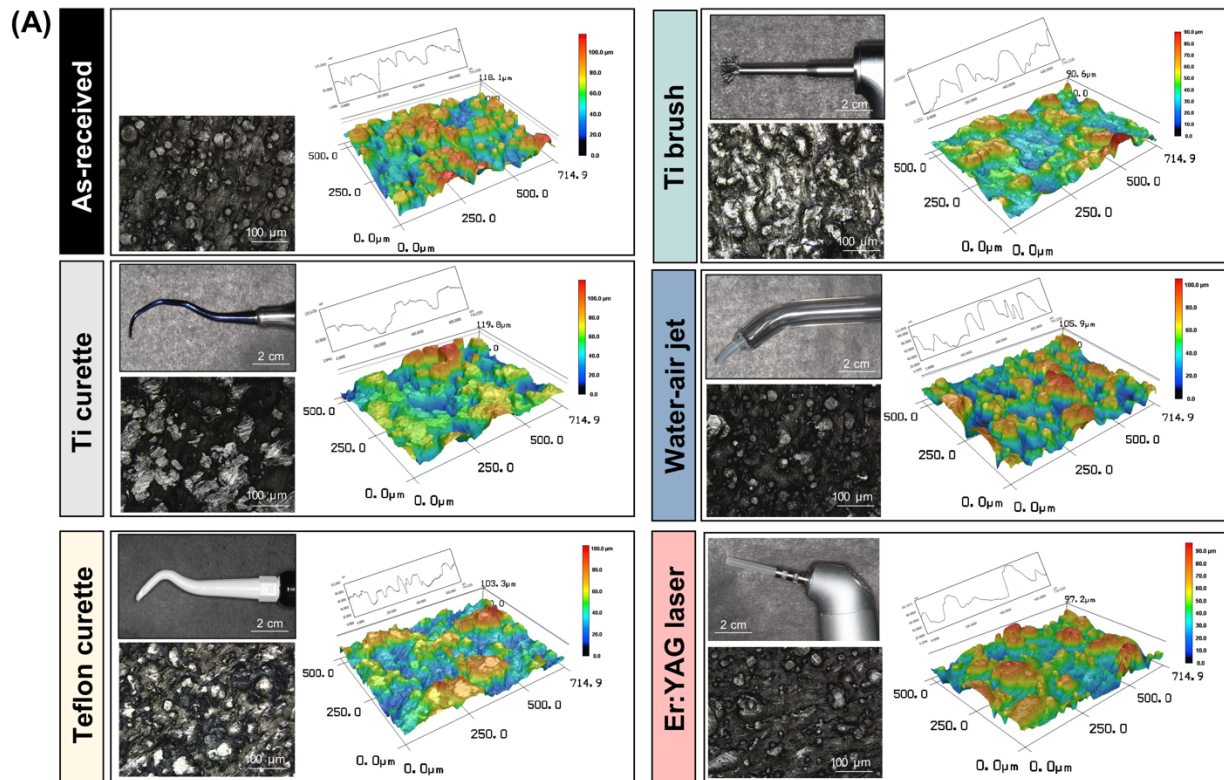


Figure 1. Mechanical instrumentation protocols on 3D-printed implant surfaces. **(A)** Photographic images of each mechanical instrument (top panel, on the left); representative two- (bottom panel, on the left) and three- (bottom panel, on the right) dimensional images, and roughness profile (top panel, right) from each group ($n = 2$) obtained by confocal laser scanning microscopy (CLSM; 150 \times magnification). **(B)** Roughness average (Ra) obtained by profilometry after mechanical instrumentation ($n = 6$). **(C)** Water contact angle after mechanical instrumentation ($n = 5$). Different background colors for the graph indicate the hydrophilicity scale. **(D)** Ti ion release was measured by inductively coupled plasma–optical emission spectrometry (ICP–OES) after mechanical instrumentation ($n = 3$). Data are expressed as the mean \pm standard deviation. Statistically significant differences between groups are indicated by symbols: # $p < 0.05$, Tukey’s HSD test. *NS* = no statistically significant differences.

3.2 | Er:YAG-treated surfaces demonstrate appropriate electrochemical stability

The open circuit potential (OCP) curves of the Er:YAG laser stabilized in nobler potentials with the most positive values (Figure 2A). The electrochemical impedance spectroscopy (EIS) data were modeled using a simple equivalent electrical circuit (Figure 2B). For the Er:YAG laser group, the semicircular diameter of the Nyquist arch was the widest, while in the Bode plot (Figure 2D) and phase angle (Figure 2E), the data remained rather stable throughout all groups at low frequencies. Polarization resistance (R_p ; Figure 2F), and capacitance (Q ; Figure 2G) showed excellent agreement between the experimental and simulated EIS data ($\chi^2 \leq 10^{-3}$; Supplementary Table 1). Notably, higher values of R_p ($2.99 \pm 1.3 \Omega \text{cm}^2$) and smaller values of Q ($2.09 \pm 1.3 \Omega^{-1} \text{s}^n \text{cm}^{-2}$) of the Ti oxide film can be seen for the Er:YAG group ($p < 0.05$). For the potentiodynamic polarization (Figure 2H), the Er:YAG curves are shifted to more electropositive potentials and slightly lower current densities than the as-received group. Regarding electrochemical parameters (Supplementary Table 2), the Er:YAG laser exhibited significantly lower i_{corr} (Figure 2I; $2.54 \pm 4.1 \mu\text{A}\cdot\text{cm}^{-2}$) and corrosion rate (Figure 2J; $1.16 \pm 1.9 \text{ mpy}$) than those of the as-received group. Altogether, the Er:YAG laser group exhibited slight improvement in some electrical and electrochemical parameters compared to the other groups. In addition to corrosion assessments, XPS analysis (Supplementary Figure 1) revealed a minimal impact of mechanical instrumentation on the chemical composition in the outermost oxide layer formed on the Ti substrates.

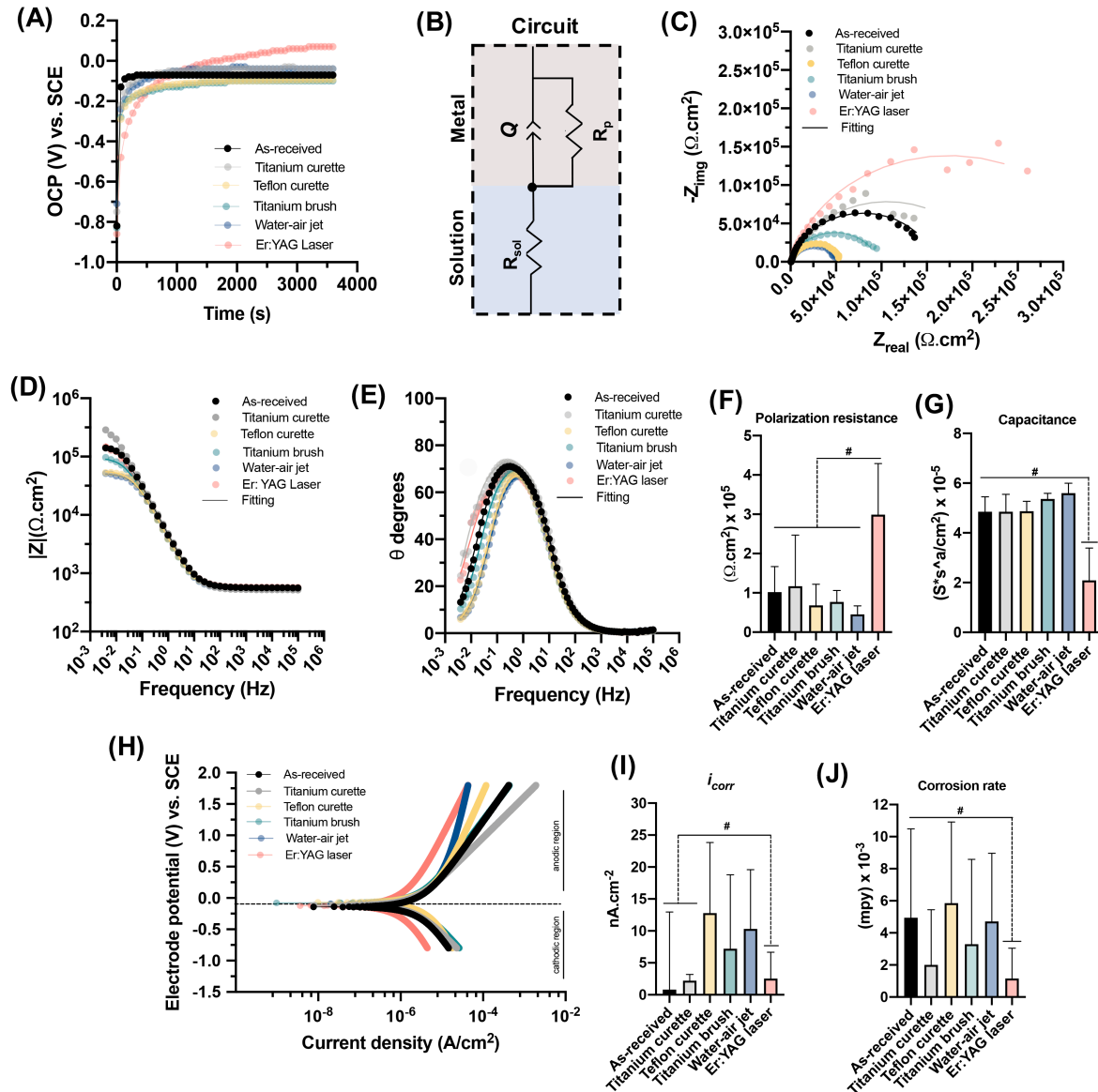


Figure 2. Corrosion performance of titanium implant surface in artificial saliva as a function of different mechanical instrumentation ($n = 5$). **(A)** Representative curve of open circuit potential (OCP) evolution (in V vs. SCE - saturated calomel electrode) for 3600 s. **(B)** The equivalent electric circuit used for electrochemical impedance spectroscopy (EIS) data, in which R_{sol} represents the resistance of the electrolyte, R_p is the polarization resistance, and Q is the constant phase element. Representative **(C)** Nyquist diagrams, **(D)** impedance modulus, and **(E)** phase angles of EIS. Electrical parameter values such as **(F)** polarization resistance and **(G)** capacitance are obtained from EIS (goodness of fit on the order of 10^{-3}). **(H)** Potentiodynamic polarization curves (in V vs. SCE). **(I)** Corrosion current density (i_{corr}) and **(J)** corrosion rate values. Data are expressed as the mean \pm standard deviation. Statistically significant differences between groups are indicated by symbols: # $p < 0.05$, Tukey's HSD test.

3.3 | Er:YAG laser treatment allows fibroblast readhesion and effectively removes polymicrobial biofilms by reducing putative pathogens

An adequate cell-surface interaction was observed after all mechanical instrumentation modalities (Figures 3A and 3A'), evidencing greater fibroblasts metabolism in the titanium brush and Er:YAG laser groups (~20% increase vs. as-received group; $p < 0.05$). However, no significant difference was found in the cell-adhered area ($p > 0.05$; Figure 3B), which was around 10-20 μm^2 of cell coverage. SEM micrographs showed that fibroblasts were able to attach and spread on the treated surfaces with a preferred orientation in the valley area (Figure 3C). Regarding microbiological findings, none of the protocols promoted total polymicrobial biofilm eradication from rough Ti implant surfaces (Figure 3D). However, the water-air jet and Er:YAG laser successfully removed the majority of the bacteria (~ 4-log reduction, compared to the as-received group), resulting in a small load of residual biofilm remnants ($p < 0.05$). The Er:YAG laser was the only mechanical protocol to slightly reduce bacterial recolonization after instrumentation ($p < 0.05$; Figure 3E). The 40 bacterial species assessed were detected in all treatment groups (Figure 3F). Some periodontal pathogens such as *Treponema denticola*, *Porphyromonas gingivalis*, *Campylobacter showae*, *Prevotella intermedia*, *Campylobacter gracilis*, *Prevotella nigrescens*, *Parvimonas micra*, *Campylobacter rectus*, and *Eubacterium nodatum*, were reduced on the laser-treated surface (~1 log of DNA count reduction vs. as-received group; $p < 0.05$), promoting the reduction of red and orange complexes load (Figure 3G). Therefore, Er:YAG laser led to biofilm removal and less virulent remnant biofilm. SEM micrographs (Figure 3H) indicated the presence of microbial clusters hiding in the pits and valleys from the implant surface. The titanium brush, water-air jet, and Er:YAG laser reached and dislodged the bacteria in these valley areas.

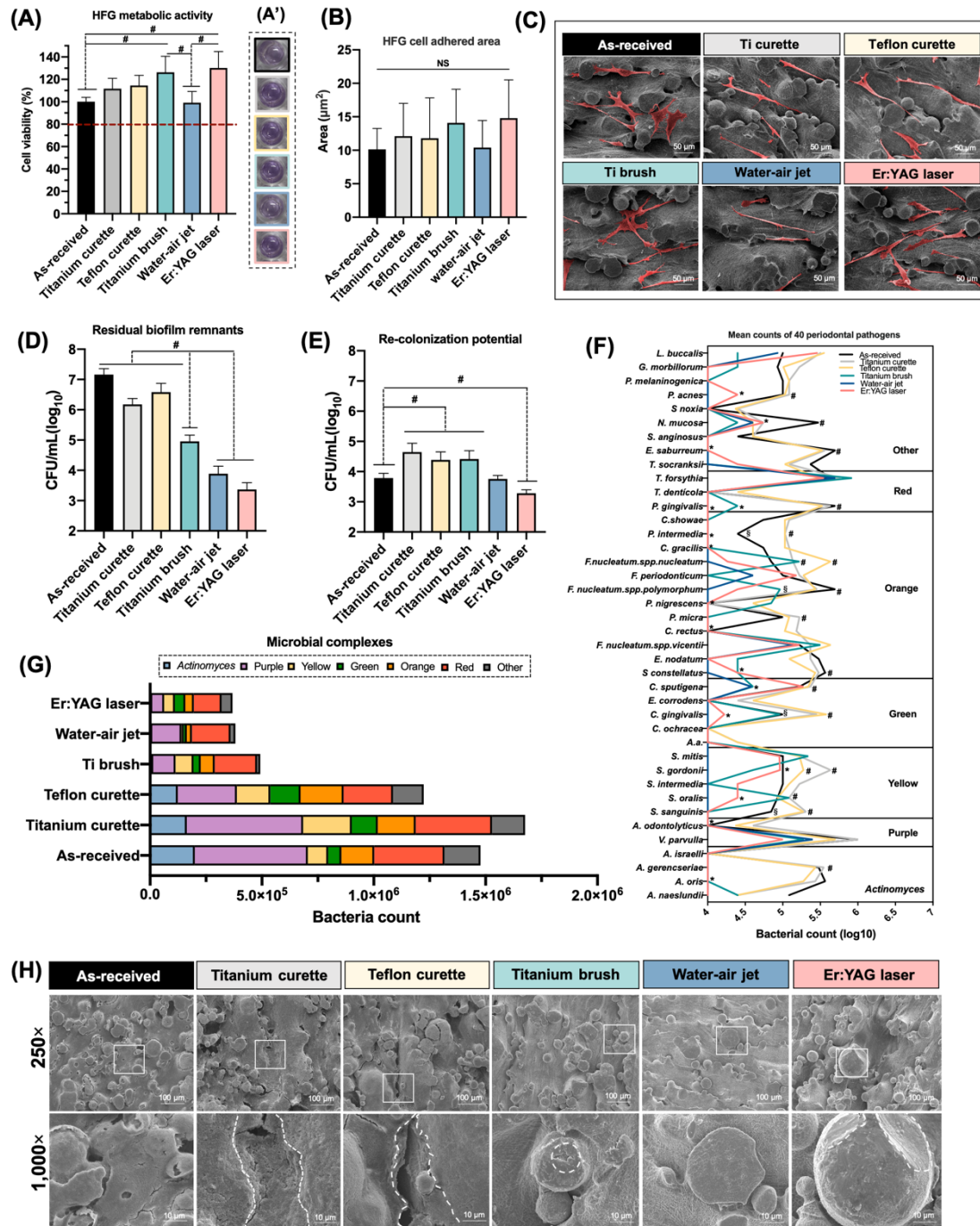


Figure 3. *In vitro* cellular and microbiological results after mechanical instrumentation. (A) Human gingival fibroblast (HGF) metabolic activity (%) was evaluated by MTT assay after culturing in the mechanically treated surfaces from 1 day ($n = 6$) with (A') its photography of colorimetric changes in each group. (B) The HGF cell adhered area (μm^2) for each group was obtained from SEM micrographs (250 \times magnification) and calculated using ImageJ software. HGF were colored in red using Adobe Photoshop CC 2018. (C) Representative SEM micrographs of HGF cell morphology and adhesion-treated surfaces after 1 day of cell culture (250 \times magnification) using 15 kV. (D) Residual polymicrobial biofilm remnants formed *in vitro* (48 h) after

mechanical decontamination reported as log-transformed viable colony-forming units (Log₁₀ CFU/mL) ($n = 6$). **(E)** The recolonization potential of treated surfaces after 1 h of bacterial adhesion reported as log-transformed viable colony-forming units (Log₁₀ CFU/mL) ($n = 6$). **(F)** Profile of mean levels of 40 bacterial species in biofilm samples (48 h) after mechanical instrumentation by checkerboard DNA–DNA hybridization ($n = 6$). Levels of individual species were computed in each sample and then averaged for each group. **(G)** Proportions of periodontal complexes using the mean of total levels of the species evaluated ($n = 6$). **(H)** SEM ($n = 2$) micrographs (magnification = 250× and 1000×) after mechanical instrumentation in polymicrobial biofilm (48 h) formed *in vitro*. The white lines represent the biofilm-removed areas and surface damage. Sterilized saline (0.9%) rinse was used as a control. Data are expressed as the mean ± standard deviation. Statistically significant differences between groups are indicated by symbols: # $p < 0.05$, Tukey's HSD test. For checkerboard DNA–DNA hybridization analysis (F), different symbols indicate statistically significant differences between groups ($p < 0.05$, Tukey's HSD test). NS = no statistically significant differences.

3.4 | PVPI 0.2% disrupts extracellular biofilm matrix and improves NaOCl 0.95% antimicrobial activity on polymicrobial biofilms

Compared with saline rinsing (control), all chemical protocols significantly reduced the microbial viability, although with significant differences among the treatment regimens (Figure 4A). The best antimicrobial protocol was found for NaOCl 0.95%, followed by HCOBc, with an almost 6-fold and 5-fold decrease in bacterial viability compared to the control, respectively. The metabolic activity of biofilms exposed to NaOCl 0.95% and HCOBc also displayed the greatest reduction compared to the control ($p < 0.05$; Figure 4B). These data were validated by fluorescence images (Figure 4C), in which polymicrobial biofilms were more susceptible to NaOCl 0.95% and HCOBc application with a higher proportion of dead cells (in red) among all groups. In fact, the total fluorescence intensity of dead bacterial cells was more pronounced in NaOCl 0.95% (Figure 4D). For matrix-targeted therapy (Figure 4E and Supplementary Figure 2), 0.2% PVPI was the most effective for both soluble and insoluble exopolysaccharide matrix degradation ($p < 0.05$). Therefore, PVPI 0.2% treatment before NaOCl and HCOBc antimicrobials was the standard protocol to demonstrate the proof-of-concept for this approach (Figure 4F). Although PVPI 0.2% is devoid of strong antimicrobial ability alone, when used as a pretreatment, it significantly enhanced the antimicrobial activity of NaOCl 0.95% (~ 4.5-log more effective killing vs. antimicrobial alone; $p < 0.05$). When comparing NaOCl and HCOBc, in the dual therapy, the PVPI + NaOCl combination was more effective than PVPI + HCOBc ($p < 0.05$; Figure 4F).

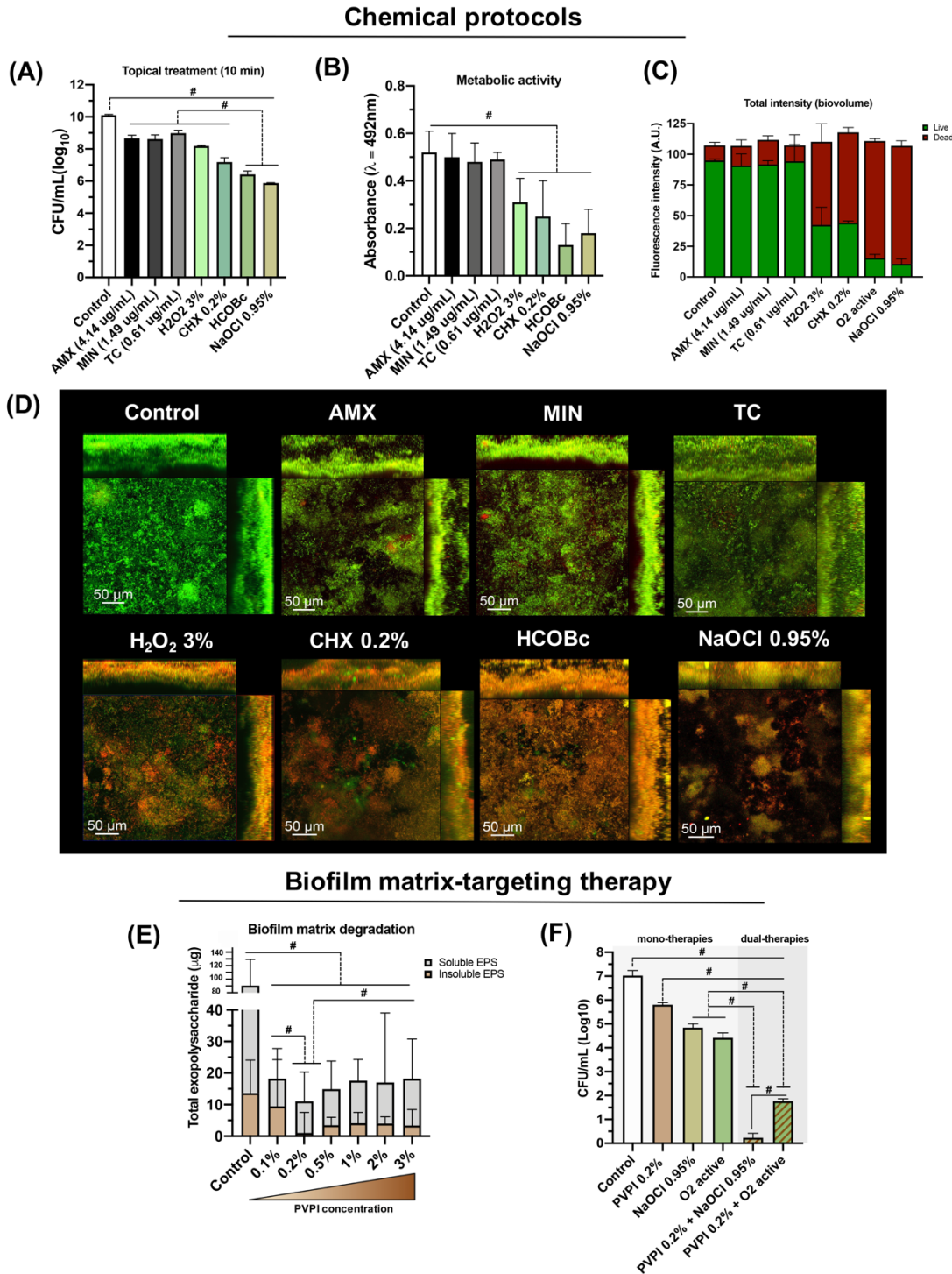


Figure 4. Adjuvant chemical protocols and biofilm matrix-degrading therapy on 3D-printed implant surfaces. **(A)** Log-transformed viable colony-forming units (Log₁₀ CFU/mL) and **(B)** bacterial metabolic activity evaluated by XTT assay after topical chemical protocol applications (10 min) on 48-hour biofilm formed *in vitro* ($n = 5$). **(C)** Average total fluorescence intensity (by area - 400 μm^2) of live and dead cells in A.U. (arbitrary units) from fluorescence images ($n = 2$). **(D)** Bacterial cell viability ($n = 3$) after chemical treatments via

live/dead analysis (green for live cells, red for dead cells). **(E)** Dose–response assay quantified by the phenol sulfuric method to determine the amounts of soluble extracellular polysaccharides and insoluble extracellular polysaccharides ($n = 6$). Data are expressed in μg polysaccharides. **(F)** Log-transformed viable colony-forming units (Log_{10} CFU/mL) after topical mono- and dual-therapy applications (10 min of each) on 48-hour biofilm formed *in vitro* ($n = 5$). Different graph background colors show the type of therapy regarding the number of treatment immersions. Sterilized saline (0.9%) rinse was used as a control. Data are expressed as the mean \pm standard deviation. Statistically significant differences between groups are indicated by symbols: # $p < 0.05$, Tukey's HSD test. Abbreviations: AMX = amoxicillin; MIN = minocycline; TEC = tetracycline; H_2O_2 = hydrogen peroxide; CHX = chlorhexidine; HCOBc = hydrocarbon-oxo-borate; NaOCl = sodium hypochlorite.

3.5 | 3-step decontamination protocol with Er:YAG laser + PVPI 0.2% + NaCl 0.95% guarantees an effective cleaning potential for *in situ* biofilms

The combination of mechanical/chemical protocol was validated using a *in situ* model (Figure 5A), showing higher bacterial cell death (Figure 5B) than each therapy alone ($\sim 99\%$ bacterial reduction; $p < 0.05$). The Er:YAG laser application (alone or in combination with antimicrobial) demonstrated greater cleaning potential with less adhered biofilm biomass on the surfaces ($p < 0.05$; Figure 5C).

Mechanical/chemical protocol

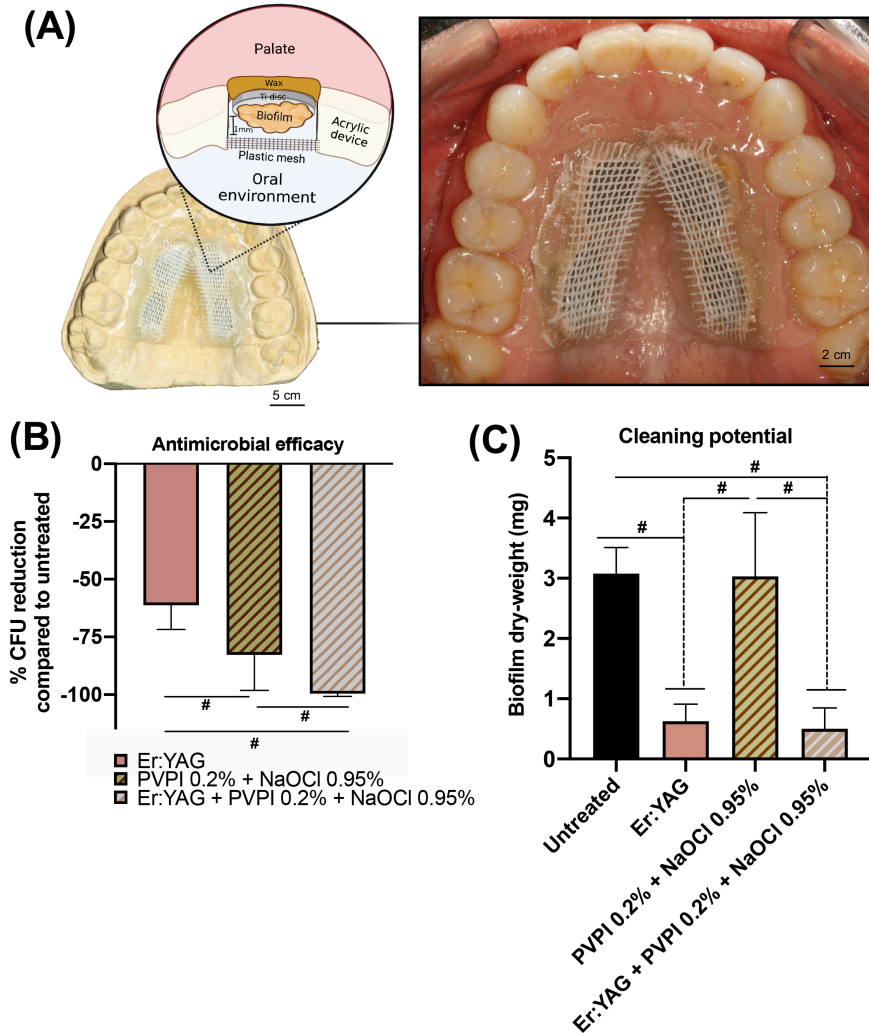


Figure 5. *In situ* antimicrobial effect of mechanical/chemical decontamination protocols. **(A)** Representative scheme of the *in situ* model used to form biofilms in the oral cavity. Figure created by Biorender (license number: YT24Y6OGOR). **(B)** % reduction of log-transformed viable colony-forming units (Log₁₀ CFU/mL) to check *in situ* antimicrobial efficacy and **(C)** biofilm-dry weight after mechanical/chemical (Er:YAG laser + PVPI 0.2% + NaOCl 0.95%) protocol ($n = 6$). Data are expressed as the mean \pm standard deviation. Statistically significant differences between groups are indicated by symbols: # $p < 0.05$, Tukey's HSD test.

4 | Discussion

This study was the pioneer to establish a 3-step nonsurgical decontamination protocol for implant surfaces based on biofilm matrix disruption to enhance bacterial removal by antimicrobial and mechanical debridement and to evaluate possible surface damage. The biggest strength of this

study was that we established a protocol for a 3D-printed Ti surface with a high surface roughness, which is the proof-of-concept for our biofilm matrix-degrading therapy. For the first time, we showed that the Er:YAG laser application led to minor morphological changes on Ti, with higher corrosion performance, effectively removing the biofilms and reducing recolonization, and favoring readhesion of gingival fibroblasts. After testing most of the commercially available chemical protocols currently used in the clinic, we also showed that the NaOCl 0.95% agent was able to drastically reduce the viability and metabolism of polymicrobial biofilms. Finally, we indicated a novel additional step to disrupt bacterial clustering and the exopolysaccharide matrix, creating a protocol that guarantees a surface almost free of live bacterial cells. Based on our findings, we defined a 3-step protocol to remove biofilms from rough titanium implant surfaces as follows: Er:YAG laser [Step 1: to mechanically remove biofilms and possible calculus deposits] + PVPI 0.2% [Step 2: to disrupt biofilm matrix of any microbial clustering left behind on valleys of rough implant surfaces] + NaOCl 0.95% [Step 3: to eradicate remaining live bacteria] (Figure 6).

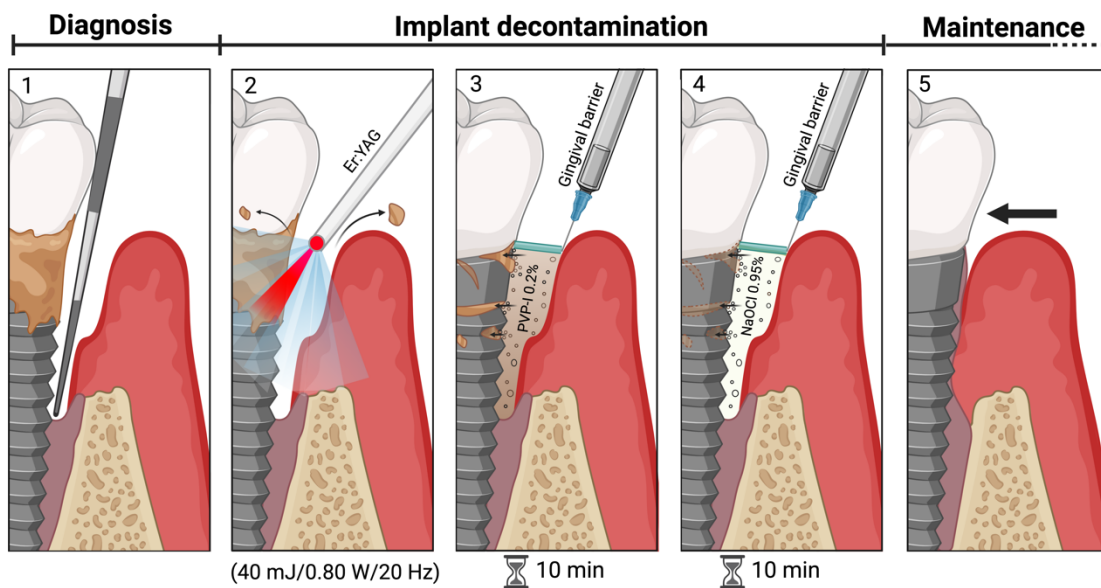


Figure 6. Proposed 3-step decontamination protocol.

The rough titanium surfaces used in our study are fabricated through a novel 3D-printing technology. They have a unique and complex micro- and macrotopography and geometry (Pinguero et al. 2019; Lee et al. 2021), resulting in an ideal substrate to test effective decontamination protocols. Within our investigation, except for the water–air jet group, all other mechanical protocols tested altered the original surface patterns, although they were unable to significantly change the surface roughness and wettability. Regarding the Ti surface degradation, the rotating titanium brush promoted higher Ti particles, which can be explained by the simultaneous surface degradation and brush

deterioration. Although the cause-effect relationship between Ti dissolution and peri-implant diseases is still not completely comprehended, Ti subproducts have been associated with an increased inflammatory response (Eger et al. 2018) and to stimulate putative pathogens grown on the Ti surface (Souza et al. 2020b). Importantly, the cumulative Ti subproducts released from the implant surface and brush (~ 0.4 ppm concentration) need further investigation to verify whether they could harm the peri-implant tissues and lead to further progression of peri-implantitis.

In addition to surface deterioration, mechanical instrumentation may remove the oxide film that is naturally formed on Ti-based implants, leading to oxidation and active attack on the material surface (Costa, et al. 2021). Er:YAG laser-treated surfaces displayed similar or slightly improved electric and electrochemical parameters compared to the as-received control. As we know, the characteristics of the TiO₂ film to be formed after laser irradiation are strongly dependent on the working parameters applied. Herein, the Er:YAG laser protocol with 40 mJ, 0.80 W, and 20 Hz follows the manufacturer's recommendation for implant cleaning. We believe that the Er:YAG laser significantly reduces surface heterogeneities (smoothing), which are responsible for delaying the achievement of the equilibrium condition and behaving as a nonideal capacitor (Costa et al. 2020). At the same time, the TiO₂ layer is probably thickened after laser irradiation. The residual energy from laser-assisted therapy can induce the formation of a duplex structure of the TiO₂ film with an inner compact high corrosion-resistant layer and an outer porous layer (AlMoharib et al. 2021). These modifications in the classic pattern of rough Ti surfaces likely induce a high homogeneity and compactness of the protective TiO₂ film, which can be associated with the best values in the electrical and electrochemical parameters found for this group. Thus, Er:YAG laser application seems to be a nondamaging decontamination method that improves the Ti oxide layer protective behavior without jeopardizing the Ti chemical composition. Regarding the cell readhesion onto treated surfaces after mechanical instrumentations, all groups resulted in low cytotoxicity and high metabolic activity of fibroblasts after 24 h of culture. This finding can be associated with the direct preservation of the valleys region microstructure (Balderrama et al. 2020), which are the preferred cell adhesion sites on the surfaces, avoiding the peaks. This first phase determines the further behavior of the cells in contact with the implant surface (*i.e.*, cell proliferation and differentiation), which could facilitate successful re-osseointegration (Cao et al. 2018; Stein et al.).

Mechanical debridement with hand curettes has been fronted as a preferred alternative in clinical practice (Figuro et al. 2014). Our findings do not fully support this recommendation, which indicates that titanium and Teflon curettes were ineffective in significantly reducing bacterial loads. A handful of studies (John et al. 2014; Park et al. 2015; Sanz-Martín et al. 2021; Luengo et al. 2022) have already demonstrated that the cleaning potential of rotatory titanium brushes outperformed hand

curettes for several implant surfaces. Despite this superior cleaning performance, the irreversible surface damage and Ti release shown in this study make this a less attractive therapy. The present study shows that the water–air jet and Er:YAG laser groups successfully lowered microbial counts on implant surfaces without leading to surface deterioration. Notably, the water–air jet is ablative only and has no antimicrobial action, which, when used alone, leads to suboptimal clinical outcomes for sandblasted and etched implants (Al-Hashedi et al. 2017). In this study, Er:YAG laser-assisted therapy was advocated as a bactericidal strategy that causes bacterial vaporization and no implant surface damage, and was the only treatment that promoted less bacterial recolonization and microbial profile modulation. The Er:YAG mechanism of action is related to the energy that ruptures the cell membranes of bacteria when absorbed into intracellular water (AlMoharib et al. 2021), even at low energy densities (40 mJ), as tested here.

Concerning the efficacy of the chemical agents, oxygenating products such as NaOCl 0.95% agent and HCOBc-based antiseptic were more effective for rough Ti surface disinfection than conventional antibiotics and chlorhexidine. NaOCl as a subgingival rinse for periodontitis has been proposed since the early 2000s for home care performed by patients as an effective, safe, and affordable periodontal antimicrobial therapy (Slots 2002, 2012; Jorgensen et al. 2005). Since its mechanism of action is rather nonselective (oxidative burst), bacterial resistance toward NaOCl seems less likely than toward chemical agents, including antibiotics and chlorhexidine-based products. A recent clinical trial (Radulescu et al. 2022) demonstrated that a single topical application of NaOCl 0.95% in a gel form (Periosolv®) promotes a beneficial effect on clinical outcomes during supportive periodontal therapy. Multi-omics analysis of periodontal pocket microbial communities pre- and post-treatment with 0.25% sodium hypochlorite showed at baseline periodontal pathogens, such as *Porphyromonas*, *Treponema*, *Desulfovibrio*, and *Mycoplasma*, and after 2 weeks dramatic shifts in the most abundant taxa were observed, with only the genus *Desulfovibrio* remaining among the 20 most abundant taxa (Califf et al. 2017). Moreover, our study used PVPI 0.2% as a biofilm matrix-degrading therapy, which showed a synergistic antimicrobial effect with HCOBc and NaOCl, demonstrating that it as an emerging strategy with a high safety profile. Thus, an important finding in this study was that pretreatment with PVPI made the greatest difference in the antimicrobial efficacy of NaOCl, which was shown to be even better than HCOBc-based antiseptic. These data suggest a possible synergistic effect when PVPI was used in combination with NaOCl, but the specific chemical reaction and mechanism of action for this synergism remain to be further explored.

To mimic the clinical conditions of biofilm formation over rough Ti surfaces, we employed an *in situ* model (Souza et al. 2019b) to develop oral biofilms inside subjects' mouths and validate the proposed mechanical/chemical protocol. With this model, we ascertained that Er:YAG laser +

PVPI 0.2% + NaOCl 0.95% guarantees an effective action elimination of ~99% of oral biofilm formed over a rough Ti surface. Although the combination of PVPI + NaOCl was successful and could be continued by the patient as a home care measure on exposed rough implant surfaces, it is essential to remember that the Er:YAG laser as the first step is an important step for in-office decontamination because it helps to physically remove calculus deposits and biofilm.

Although we believe we developed a promising 3-step biofilm removal technique for rough Ti surface decontamination without causing damage to the surface and altered cellular regrowth, we acknowledge some limitations in the present study. The presence of submucosal hard deposits (i.e., calculus) could not be simulated with the present design, which is a more challenging situation and another reason we suggested Er. YAG as the first step of the proposed decontamination protocol. Moreover, we consider that this optimized mechanical/chemical decontamination protocol needs to be further explored by clinical studies. Nevertheless, the combination of Er:YAG laser + PVPI 0.2% + NaOCl 0.95% can be considered a reliable decontamination protocol for rough implant surfaces, providing enough biological plausibility and theoretical evidence for successful clinical translation and open new perspectives to improve nonsurgical implant-related infection therapies.

REFERENCES

- Al-Hashedi, A.A., Laurenti, M., Benhamou, V. & Tamimi, F. (2017) Decontamination of titanium implants using physical methods. *Clinical Oral Implants Research* 28: 1013–1021.
- AlMoharib, H.S., Steffensen, B., Zoukhri, D., Finkelman, M. & Gyurko, R. (2021) Efficacy of an Er:YAG laser in the decontamination of dental implant surfaces: An in vitro study. *Journal of Periodontology* 92: 1613–1621.
- Balderrama, Í. de F., Cardoso, M.V., Stuani, V.T., Oliveira, R.C., Matos, A.A., Gregghi, S.L.A. & Sant'Ana, A.C.P. (2020) Residual decontamination chemical agents negatively affect adhesion and proliferation of osteoblast-like cells on implant surface. *International Journal of Implant Dentistry* 6: 84.
- Berglundh, T., Armitage, G., Araujo, M.G., Avila-Ortiz, G., Blanco, J., Camargo, P.M., Chen, S., Cochran, D., Derks, J., Figuero, E., Hämmerle, C.H.F., Heitz-Mayfield, L.J.A., Huynh-Ba, G., Iacono, V., Koo, K.-T., Lambert, F., McCauley, L., Quirynen, M., Renvert, S., Salvi, G.E., Schwarz, F., Tarnow, D., Tomasi, C., Wang, H.-L. & Zitzmann, N. (2018) Peri-implant diseases and conditions: Consensus report of workgroup 4 of the 2017 World Workshop on the Classification of Periodontal and Peri-Implant Diseases and Conditions. *Journal of Clinical Periodontology* 45: S286–S291.
- Bertolini, M., Vazquez Munoz, R., Archambault, L., Shah, S., Souza, J.G.S., Costa, R.C., Thompson, A., Zhou, Y., Sobue, T. & Dongari-Bagtzoglou, A. Mucosal Bacteria Modulate Candida albicans Virulence in Oropharyngeal Candidiasis. *mBio* 0: e01937-21.
- Borges, M.H.R., Nagay, B.E., Costa, R.C., Sacramento, C.M., Ruiz, K.G., Landers, R., van den Beucken, J.J.J.P., Fortulan, C.A., Rangel, E.C., da Cruz, N.C. & Barão, V.A.R. (2022) A tattoo-inspired electrosynthesized polypyrrole film: crossing the line toward a highly adherent

- film for biomedical implant applications. *Materials Today Chemistry* 26: 101095.
- Bowen, W.H., Burne, R.A., Wu, H. & Koo, H. (2018) Oral Biofilms: Pathogens, Matrix, and Polymicrobial Interactions in Microenvironments. *Trends in Microbiology* 26: 229–242.
- Califf, K.J., Schwarzberg-Lipson, K., Garg, N., Gibbons, S.M., Caporaso, J.G., Slots, J., Cohen, C., Dorrestein, P.C. & Kelley, S.T. (2017) Multi-omics Analysis of Periodontal Pocket Microbial Communities Pre- and Posttreatment. *mSystems* 2: e00016-17.
- Cao, J., Wang, T., Pu, Y., Tang, Z. & Meng, H. (2018) Influence on proliferation and adhesion of human gingival fibroblasts from different titanium surface decontamination treatments: An in vitro study. *Archives of Oral Biology* 87: 204–210.
- Cosgarea, R., Rocuzzo, A., Jepsen, K., Sculean, A., Jepsen, S. & Salvi, G.E. (2022) Efficacy of mechanical/physical approaches for implant surface decontamination in nonsurgical submarginal instrumentation of peri-implantitis. A systematic review. *Journal of Clinical Periodontology*.
- Costa, R.C., Abdo, V.L., Mendes, P.H.C., Mota-Veloso, I., Bertolini, M., Mathew, M.T., Barão, V.A.R. & Souza, J.G.S. (2021a) Microbial Corrosion in Titanium-Based Dental Implants: How Tiny Bacteria Can Create a Big Problem? *Journal of Bio- and Tribo-Corrosion* 7: 136.
- Costa, R.C., Bertolini, M., Costa Oliveira, B.E., Nagay, B.E., Dini, C., Benso, B., Klein, M.I., Barão, V.A.R. & Souza, J.G.S. (2022) Polymicrobial biofilms related to dental implant diseases: unravelling the critical role of extracellular biofilm matrix. *Critical Reviews in Microbiology* 0: 1–21.
- Costa, R.C., Nagay, B.E., Bertolini, M., Costa-Oliveira, B.E., Sampaio, A.A., Retamal-Valdes, B., Shibli, J.A., Feres, M., Barão, V.A.R. & Souza, J.G.S. (2021b) Fitting pieces into the puzzle: The impact of titanium-based dental implant surface modifications on bacterial accumulation and polymicrobial infections. *Advances in Colloid and Interface Science* 298: 102551.
- Costa, R.C., Souza, J.G.S., Bertolini, M., Retamal-Valdes, B., Feres, M. & Barão, V.A.R. (2020a) Extracellular biofilm matrix leads to microbial dysbiosis and reduces biofilm susceptibility to antimicrobials on titanium biomaterial: An in vitro and in situ study. *Clinical Oral Implants Research* 31: 1173–1186.
- Costa, R.C., Souza, J.G.S., Cordeiro, J.M., Bertolini, M., de Avila, E.D., Landers, R., Rangel, E.C., Fortulan, C.A., Retamal-Valdes, B., da Cruz, N.C., Feres, M. & Barão, V.A.R. (2020b) Synthesis of bioactive glass-based coating by plasma electrolytic oxidation: Untangling a new deposition pathway toward titanium implant surfaces. *Journal of Colloid and Interface Science* 579: 680–698.
- Derks, J. & Tomasi, C. (2015) Peri-implant health and disease. A systematic review of current epidemiology. *Journal of Clinical Periodontology* 42 Suppl 16: S158-171.
- Eger, M., Hiram-Bab, S., Liron, T., Sterer, N., Carmi, Y., Kohavi, D. & Gabet, Y. (2018) Mechanism and Prevention of Titanium Particle-Induced Inflammation and Osteolysis. *Frontiers in Immunology* 9: 2963.
- Figuro, E., Graziani, F., Sanz, I., Herrera, D. & Sanz, M. (2014) Management of peri-implant mucositis and peri-implantitis. *Periodontology 2000* 66: 255–273.
- Heitz-Mayfield, L.J.A. & Mombelli, A. (2014) The therapy of peri-implantitis: a systematic review. *The International Journal of Oral & Maxillofacial Implants* 29 Suppl: 325–345.
- Howe, M.-S., Keys, W. & Richards, D. (2019) Long-term (10-year) dental implant survival: A systematic review and sensitivity meta-analysis. *Journal of Dentistry* 84: 9–21.

- Jervøe-Storm, P.-M., Hablützel, A.S., Bartels, P., Kraus, D., Jepsen, S. & Enkling, N. (2021) Comparison of irrigation protocols for the internal decontamination of dental implants-results of in vitro and in vivo studies. *Clinical Oral Implants Research* 32: 1168–1175.
- John, G., Becker, J. & Schwarz, F. (2014) Rotating titanium brush for plaque removal from rough titanium surfaces – an in vitro study. *Clinical Oral Implants Research* 25: 838–842.
- Jorgensen, M.G., Aalam, A. & Slots, J. (2005) Periodontal antimicrobials--finding the right solutions. *International Dental Journal* 55: 3–12.
- Lang, M.S., Cerutis, D.R., Miyamoto, T. & Nunn, M.E. (2016) Cell Attachment Following Instrumentation with Titanium and Plastic Instruments, Diode Laser, and Titanium Brush on Titanium, Titanium-Zirconium, and Zirconia Surfaces. *The International Journal of Oral & Maxillofacial Implants* 31: 799–806.
- Lee, C.-T., Huang, Y.-W., Zhu, L. & Weltman, R. (2017) Prevalences of peri-implantitis and peri-implant mucositis: systematic review and meta-analysis. *Journal of Dentistry* 62: 1–12.
- Lee, J., Lee, J.-B., Yun, J., Rhyu, I.-C., Lee, Y.-M., Lee, S.-M., Lee, M.-K., Kim, B., Kim, P. & Koo, K.-T. (2021) The impact of surface treatment in 3-dimensional printed implants for early osseointegration: a comparison study of three different surfaces. *Scientific Reports* 11: 10453.
- Louropoulou, A., Slot, D.E. & Van der Weijden, F. (2014) The effects of mechanical instruments on contaminated titanium dental implant surfaces: a systematic review. *Clinical Oral Implants Research* 25: 1149–1160.
- Luengo, F., Sanz-Esporrín, J., Noguerol, F., Sanz-Martín, I., Sanz-Sánchez, I. & Sanz, M. (2022) In vitro effect of different implant decontamination methods in three intraosseous defect configurations. *Clinical Oral Implants Research* 33: 1087–1097.
- Ntrouka, V.I., Slot, D.E., Louropoulou, A. & Van der Weijden, F. (2011) The effect of chemotherapeutic agents on contaminated titanium surfaces: a systematic review. *Clinical Oral Implants Research* 22: 681–690.
- Pantaroto, H.N., de Almeida, A.B., Gomes, O.P., Matos, A.O., Landers, R., Casarin, R.C.V., da Silva, J.H.D., Nociti, F.H. & Barão, V.A.R. (2021) Outlining cell interaction and inflammatory cytokines on UV-photofunctionalized mixed-phase TiO₂ thin film. *Materials Science and Engineering: C* 118: 111438.
- Park, J.-B., Jeon, Y. & Ko, Y. (2015) Effects of titanium brush on machined and sand-blasted/acid-etched titanium disc using confocal microscopy and contact profilometry. *Clinical Oral Implants Research* 26: 130–136.
- Pingueiro, J., Piattelli, A., Paiva, J., Figueiredo, L.C. de, Feres, M., Shibli, J. & Bueno-Silva, B. (2019) Additive manufacturing of titanium alloy could modify the pathogenic microbial profile: an in vitro study. *Brazilian Oral Research* 33: e065.
- Radulescu, V., Boariu, M.I., Rusu, D., Roman, A., Surlin, P., Voicu, A., Didilescu, A.C., Jentsch, H., Siciliano, V.I., Ramaglia, L., Vela, O., Kardaras, G., Sculean, A. & Stratul, S.-I. (2022) Clinical and microbiological effects of a single application of sodium hypochlorite gel during subgingival re-instrumentation: a triple-blind randomized placebo-controlled clinical trial. *Clinical Oral Investigations* 26: 6639–6652.
- Renvert, S., Roos-Jansåker, A.-M. & Claffey, N. (2008) Non-surgical treatment of peri-implant mucositis and peri-implantitis: a literature review. *Journal of Clinical Periodontology* 35: 305–315.
- Sakellari, D., Goodson, J.M., Kolokotronis, A. & Konstantinidis, A. (2000) Concentration of 3

tetracyclines in plasma, gingival crevice fluid and saliva. *Journal of Clinical Periodontology* 27: 53–60.

- Sanz-Martín, I., Paeng, K., Park, H., Cha, J.-K., Jung, U.-W. & Sanz, M. (2021) Significance of implant design on the efficacy of different peri-implantitis decontamination protocols. *Clinical Oral Investigations* 25: 3589–3597.
- Shibli, J.A., Ferrari, D.S., Siroma, R.S., Figueiredo, L.C. de, Faveri, M. de, Feres, M., Shibli, J.A., Ferrari, D.S., Siroma, R.S., Figueiredo, L.C. de, Faveri, M. de & Feres, M. (2019) Microbiological and clinical effects of adjunctive systemic metronidazole and amoxicillin in the non-surgical treatment of peri-implantitis: 1 year follow-up. *Brazilian Oral Research* 33.
- Shibli, J.A., Rocha, T.F., Coelho, F., de Oliveira Capote, T.S., Saska, S., Melo, M.A., Pinguero, J.M.S., de Faveri, M. & Bueno-Silva, B. (2021) Metabolic activity of hydro-carbon-oxo-borate on a multispecies subgingival periodontal biofilm: a short communication. *Clinical Oral Investigations* 25: 5945–5953.
- Silva, W.J. da, Seneviratne, J., Parahitiyawa, N., Rosa, E.A.R., Samaranayake, L.P. & Cury, A.A.D.B. (2008) Improvement of XTT assay performance for studies involving *Candida albicans* biofilms. *Brazilian Dental Journal* 19: 364–369.
- Slots, J. (2012) Low-cost periodontal therapy. *Periodontology 2000* 60: 110–137.
- Slots, J. (2002) Selection of antimicrobial agents in periodontal therapy. *Journal of Periodontal Research* 37: 389–398.
- Souza, J.G.S., Bertolini, M., Costa, R.C., Cordeiro, J.M., Nagay, B.E., de Almeida, A.B., Retamal-Valdes, B., Nociti, F.H., Feres, M., Rangel, E.C. & Barão, V.A.R. (2020a) Targeting Pathogenic Biofilms: Newly Developed Superhydrophobic Coating Favors a Host-Compatible Microbial Profile on the Titanium Surface. *ACS Applied Materials & Interfaces* 12: 10118–10129.
- Souza, J.G.S., Cordeiro, J.M., Lima, C.V. & Barão, V.A.R. (2019a) Citric acid reduces oral biofilm and influences the electrochemical behavior of titanium: An in situ and in vitro study. *Journal of Periodontology* 90: 149–158.
- Souza, J.G.S., Costa Oliveira, B.E., Bertolini, M., Lima, C.V., Retamal-Valdes, B., de Faveri, M., Feres, M. & Barão, V.A.R. (2020b) Titanium particles and ions favor dysbiosis in oral biofilms. *Journal of Periodontal Research* 55: 258–266.
- Souza, J.G.S., Costa Oliveira, B.E., Costa, R.C., Bechara, K., Cardoso-Filho, O., Benso, B., Shibli, J.A., Bertolini, M. & Barão, V.A.R. (2022) Bacterial-derived extracellular polysaccharides reduce antimicrobial susceptibility on biotic and abiotic surfaces. *Archives of Oral Biology* 142: 105521.
- Souza, J.G.S., Cury, J.A., Ricomini Filho, A.P., Feres, M., Faveri, M. de & Barão, V.A.R. (2019b) Effect of sucrose on biofilm formed in situ on titanium material. *Journal of Periodontology* 90: 141–148.
- Souza, J.G.S., Lima, C.V., Costa Oliveira, B.E., Ricomini-Filho, A.P., Faveri, M., Sukotjo, C., Feres, M., Del Bel Cury, A.A. & Barão, V.A.R. (2018) Dose-response effect of chlorhexidine on a multispecies oral biofilm formed on pure titanium and on a titanium-zirconium alloy. *Biofouling* 34: 1175–1184.
- Stein, J.M., Conrads, G., Abdelbary, M.M.H., Yekta-Michael, S.S., Buttler, P., Glock, J., Sadvandi, G., Kaufmann, R. & Apel, C. Antimicrobial efficiency and cytocompatibility of different decontamination methods on titanium and zirconium surfaces. *Clinical Oral Implants Research* n/a:

- Tenenbaum, H., Jehl, F., Gallion, C. & Dahan, M. (1997) Amoxicillin and clavulanic acid concentrations in gingival crevicular fluid. *Journal of Clinical Periodontology* 24: 804–807.
- Yang, T., Xie, L., Hu, X., He, K., Zhu, Z., Fan, L. & Tian, W. (2023) Residual extracellular polymeric substances (EPS) detected by fluorescence microscopy on dental implants after different decontamination. *Materials Chemistry and Physics* 296: 127242.

2.4 Pathogenesis-guided engineering: pH-responsive imprinted polymer co-delivering folate for inflammation-resolving as immunotherapy in implant infections

Raphael C. Costa¹ | Bruna E. Nagay¹ | Javier E. L. Villa^{2,3} | Maria D. P. T. Sotomayor³ | Bruna Benso⁴ | Sebastian Aguayo⁴ | Martinna Bertolini⁵ | Catarina M. Sacramento¹ | Karina G. S. Ruiz¹ | Fernanda P. Spada⁶ | Erica Dorigatti de Avila⁷ | Leonardo P. Faverani⁸ | Luciano T. A. Cintra⁹ | João Gabriel S. Souza^{10,*} | Valentim A. R. Barão^{1,*}

¹ Department of Prosthodontics and Periodontology, Piracicaba Dental School, University of Campinas (UNICAMP), Piracicaba, São Paulo, 13414-903, Brazil.

² Institute of Chemistry, University of Campinas (UNICAMP), Campinas, São Paulo, 13081-970, Brazil.

³ Institute of Chemistry, State University of São Paulo (UNESP), Araraquara, São Paulo, 14801-970, Brazil.

⁴ School of Dentistry, Faculty of Medicine, Pontificia Universidad Católica de Chile, Santiago, 8330024, Chile.

⁵ Department of Periodontics and Preventive Dentistry, School of Dental Medicine, University of Pittsburgh, Pittsburgh, PA 15106, USA.

⁶ Department of Agri-food industry, Food and Nutrition, “Luiz de Queiroz” College of Agriculture, University of São Paulo, Piracicaba, São Paulo, 13418-900, Brazil.

⁷ Department of Dental Materials and Prosthodontics, School of Dentistry, São Paulo State University (UNESP), Araçatuba, São Paulo, 16015-050, Brazil.

⁸ Department of Diagnosis and Surgery, School of Dentistry, São Paulo State University (UNESP), Araçatuba, São Paulo, 16015-050, Brazil.

⁹ Department of Preventive and Restorative Dentistry, School of Dentistry, São Paulo State University (UNESP), Araçatuba, São Paulo, 16015-050, Brazil.

¹⁰ Dental Research Division, Guarulhos University, Guarulhos, SP, 07023-070, Brazil.

*Corresponding authors:

1. Valentim A. R. Barão, University of Campinas (UNICAMP), Piracicaba Dental School, Department of Prosthodontics and Periodontology, Av. Limeira, 901, Piracicaba, São Paulo, 13414-903, Brazil. Email: ybarao@unicamp.br

2. João Gabriel S. Souza, Dental Research Division, Guarulhos University, Guarulhos, SP, 07023-070, Brazil. Email: jgabriel.ssouza@yahoo.com.br

Note: VARB and JGSS share the position of senior authors.

Abstract

Host-modulation therapies have been recognized as an important therapeutic approach that can dictate the fate of chronic diseases, including dental implant-related infections. Folate (FT) is a suitable targeting ligand for folate receptor (FOLR) overexpressed on inflamed cells. Thus, FT-based polymers can be employed as FOLRS-targeted immunotherapy to positively modulate the inflammatory process. We herein present a novel biodegradable imprinted polymer with a folate delivery mechanism driven by pH changes [PCL-MIP@FT]. Molecularly imprinted technology synthesized the newly developed polymer successfully in a facile manner. The pH mechanism was validated *in vitro*, demonstrating that an acidic environment accelerates and increases the FT release (~100 µg/mL). As a proof-of-concept, inflammation was induced in human gingival fibroblasts (HGF) by *Porphyromonas gingivalis* protein extract (1 µg/mL) for 3h. For the first time, we discovered that folate receptors (FOLR-1 and FOLR-3) are also overexpressed on activated HGFs, representing a favorable target in the peri-implant site. Moreover, FT-induced alterations on biofilm nanomechanics can be used to enhance mechanical decontamination from implant surfaces. *In vivo* systemic toxicity of PCL-MIP@FT eluate was determined using *Galleria mellonella* larvae model, demonstrating to be a safe biomaterial. The PCL-MIP@FT, when locally administered to subcutaneous tissue in rats, promotes an alleviating inflammatory reaction and can be able to stimulate the repair. The current findings that demonstrate reliable anti-inflammatory actions of PCL-MIP@FT *in vitro* and *in vivo* support their use as a novel drug-free therapeutic platform for the treatment of dental implant infections.

Keywords: biomaterial, folate, inflammation, implant infection.

1. Introduction

Dental implant-related infections are chronic inflammatory diseases associated with a pathogenic microbial community that progressively affects the integrity of the supporting tissues (1,2). Peri-implant tissue destruction results from the breakdown of homeostasis between the resident commensal microbiota and host, which drives the disease pathology (3). The non-resolving inflammation offers a nourishing environment for the disease-associated microbial communities that develop immune subversion strategies to counteract the host immune response, creating a dysbiotic state with increased bacterial load (3–5). In individuals susceptible to peri-implant diseases, the host response is ineffective, dysregulated, and destructive (6). Current clinical therapies aim to remove the disease-causing biofilm by mechanical debridement occasionally with adjunctive antimicrobial approaches (7). However, is not always effective, particularly to reverse biofilm dysbiosis and to control inflammation (8). Therefore, there is an unmet need for effective host-modulation therapies as an adjunct to the standard treatment.

Folic acid, a synthetic form of folate (FT), is an ancient agent in periodontal treatment due to its modulating role in disease progression (9,10). The FT (e.i.; B9 vitamin) is a pivotal micronutrient obtained from the diet involved in DNA synthesis and repair, and consequently, is essential for normal cell metabolism especially in infancy and pregnancy (11,12). In the oral environment, insufficient dietary FT intake (> 3 ng/mL per day) is manifested as epithelial aberrations in the maturation and keratinization process and may predispose to infection, ulceration, and poor wound healing (13). Considering that the tissue uptake and storage of FT is a key event of the folate metabolic pathway (14), topical FT supplementation is quite promising due to prolonged contact with the target, decreasing the overuse and toxicity. Despite the use of FT as immunotherapy being promised, it remains underexplored in the implantology field.

FT has also been revealed as an optimal targeting ligand for the selective delivery of therapeutic agents to sites of chronic inflammation (12). Mechanistically, FT can be internalized by a folate receptor (FOLR) that is overexpressed on the surfaces of some inflamed and malignant mammalian cells, whereas FOLR expression in normal cell tissues is relatively lower (15). There are four isoforms of the FOLR identified in humans (isoforms 1,2,3 and 4), which can be used as targets for diagnostics and therapy in different diseases

(16). FT and its conjugates bind to FOLRs with high affinity ($K_d \sim 10^{-9}$ M) and enter FOLR-expressing cells by receptor-mediated endocytosis (15,16). As a result, FT-triggered anti-inflammatory functions might be through the multiple signaling pathways that have been generally recognized to get involved in many other anti-inflammatory actions (17). Nowadays, it is known that FR expression is not limited to malignant cells and activated macrophages. A prior study showed a high level of serum FOLRs in gingival crevicular fluid with different periodontal status(18). This opens up a broader array of possibilities to use FT also as a targeting ligand in peri-implant tissue to modulate the inflammation surrounding the implant.

In order to promote the active delivery of FT, a plethora of bio-carriers can be used (19). However, chemical stability is the main factor to be considered in the design of systems for the oral cavity (20). In this line, molecularly imprinted polymers (MIPs) are cross-linked polymers that exhibit specific binding sites for the template molecule(19,21). Briefly, a template molecule is introduced in a mixture of monomers and cross-linker dissolved in a solvent resulting in a three-dimensional polymer matrix(22). Due to their high selectivity and stability, MIPs have been used for numerous biomedical applications and have a rapid growth in the last few decades (21–23). Recently, biodegradable MIPs have been proposed as a fascinating drug-delivery system(24). Concerning the polymer approved by Food and Drug Administration (FDA), polycaprolactone (PCL) is one of the well-known synthetic polymers, hydrophobic, blend compatible, thermoplastic, semicrystalline, and nonimmunogenic (25). Thus, it seems to be promising to design a PCL-based polymer via molecularly imprinted technology as a folate-delivery system. Herein, we propose a pathogenesis-guided strategy to engineer functionally integrating folate co-delivery therapy for promoting inflammation-resolving in peri-implant tissue.

2. Materials & Methods

2.1 *In silico* theoretical calculations

Computational simulations based on the ab initio density functional theory (DFT) method were first conducted using ORCA software (26) to obtain adequate complexation stoichiometry. B3LYP was used as the hybrid functional (27), and SVP was used as the basis set for H, C, N, and O were used for such calculations (28). The calculations were performed

under the condition of explicit solvent (chloroform). All the structures were built using AVOGADRO® software (29). The figures of merit were obtained by Visual Molecular Dynamics (VMD) software (30). The formalism used in the calculation of atomic charges was obtained from the self-consistent field, and with the population analysis of the molecular orbital, using this type of analysis, it was possible to extract the Mulliken charges (21). No symmetry constraints were imposed during the geometry optimization processes. The interaction energies (ΔE) for the complexation process were calculated (Eq. 1), as follows:

$$\Delta E = (E_{\text{folate}} + E_{\text{monomer}}) - E_{\text{complex}} \quad (1)$$

2.2 Synthesis of poly(ϵ -caprolactone) as a biodegradable cross-linker

The poly(ϵ -caprolactone; PCL) was synthesized following the previous protocol (25). In brief, 4.0 g [2 mmol] of PCL diol (molecular weight 2,000; Sigma Aldrich) was dissolved in 40 mL of benzene (Exodo). Afterward, 0.63 mL [4.5 mmol] of triethylamine (Sigma Aldrich) and 0.37 mL [4.5 mmol] of acryloyl chloride (Sigma Aldrich) were added for end-chain functionalization. The reaction mixture was stirred for 3 h at 80°C. After the reaction, it was filtered to remove triethylamine hydrochloride. PCL triol was obtained by pouring the filtrate in 400 mL of hexane (Neon). The solid precipitate was dried under a vacuum for 24 h in a dissector. Finally, the PCL was grounded manually with a mortar and pestle and sieved.

2.3 Polymerization of biodegradable PCL-based imprinted polymer (MIP)

PCL-MIP@FT was synthesized by photopolymerization as described elsewhere with slight modifications (25). Firstly, FT solution (0.8 mg/100 chloroform; Sigma Aldrich) was mixed with 0.1 mL of acrylic acid under stirring (400 rpm) at room temperature. After 5 min incubation, 0.6 g of crosslinking agent (PCL triol) and 0.05 mL of the initiator solution [0.1 g of dimethoxy-2-phenylacetophenone (Sigma Aldrich) dissolved in 1 mL of 1-vinylpyrrolidinone (Sigma Aldrich)] were added to the reaction mixture. The system was sealed, put in water bath at 5 °C, and the photopolymerization was conducted using a 125 W high-pressure mercury lamp (spectrum at 280, 370, 405, 430, 550, and 580 nm)(22) for 20 minutes to ensure thorough gelation. The final product was thoroughly flushed with water, freeze-dried for 24 h, and kept at 4 °C until further use.

2.3 Physicochemical characterizations

The tri-dimensional structure of the freeze-dried polymers was visualized using confocal laser scanning microscopy (CLSM; VK- X200 series, Keyence, Japan)(31). Moreover, polymers were dropped on a double-stick carbon tape and gold-sputtered to visualize their morphology by scanning electron microscopy (SEM; JEOL JSM-6010LA, Peabody, MA, USA)(21). The average size in the dry state was determined by measuring the diameter of 100 polymers in SEM images from five random regions and then analyzed by ImageJ (National Institutes of Health, Bethesda, MD, USA) (32). The chemical bond structure was examined by attenuated total reflectance–Fourier transform infrared spectroscopy (FTIR; Vertex 70 FTIR spectrometer, Bruker, USA) in the spectral range of 400–4000 cm^{-1} at room temperature(25).

2.4 Folate release kinetics and PCL Biodegradation

UV–vis spectrophotometry (Lambda 750, PerkinElmer Inc., Shelton, CT) at 290 nm was used to measure the amount of unbound FT in the washed supernatants. The incorporation efficiency (IE) and incorporation coefficient (IC) of FT for PCL-MIPs ($n = 3$) were calculated, as follows:

$$\text{IE}(\%) = \frac{(\text{feed FT content} - \text{free FT content})}{\text{feed FT content}} \times 100\% \quad (2)$$

$$\text{IC}(\%) = \frac{(\text{feed FT content} - \text{free FT content})}{(\text{feed FT content} + \text{polymer content} - \text{free FT content})} \times 100\% \quad (3)$$

Regarding the drug release ($n = 5$), 10 mg of freshly prepared PCL-NIP and PCL-MIP@FT were individually added in an eppendorf with 1 mL of phosphate-buffered saline (PBS; Gibco™, Life Technologies) at pH 4.5, 7.4, 9.0 to study the effect of pH of the release media on drug release kinetics. The samples were maintained hermetically closed in an incubator at 37 °C. After scheduled time points (1, 3, 7, 10, 14, 21, and 28 days), the supernatant was collected and filtrated (0.22 μm membrane filter) to determine FT concentrations ($\mu\text{g/mL}$) and replaced with fresh PBS solution. The cumulative FT release percentage was calculated relative to the total amount of FT added to each sample.

To study the biodegradation of the PCL, samples ($n = 3$) were placed in 10 ml PBS and incubated at 37 °C for 1, 7, 14, and 28 days. After each time point, samples were removed

from the PBS and freeze-dried overnight. The remaining material of the samples was calculated as below:

$$\% \text{ Remaining material} = 100 - \frac{(m_i - m_f)}{m_i} \times 100\% \quad (4)$$

, where m_n = final mass of the sample and m_i = initial mass of the sample.

2.5. In vitro microbiological tests

2.5.1 MIC and MBC determination for FT

To examine the possible antibacterial effect of the FT, the Minimum Inhibitory Concentration (MIC) and Minimum Bacterial Concentration (MBC) were determined by the broth microdilution method based on the Clinical and Laboratory Standards Institute guidelines [M07-A9]. Briefly, *Staphylococcus aureus* (ATCC 25,923) was initially grown aerobically on Mueller Hinton (MH) agar under aerobic conditions for 2 days at 37 °C. Five bacterial colonies were transferred to MH broth medium and incubated overnight. Afterward, 500 µL from this culture was transferred to a new tube with 9.5 mL of fresh MH broth medium and kept for 4 h (37°C; aerobic condition). *S. aureus* bacteria were adjusted to OD_{600nm} = 0.597 (1×10^7 colony forming units-CFU/mL) and inoculated into 96-well microliter plates to a final bacterial density of 10^5 CFU/mL containing two-fold serial dilution of each drug in broth culture medium. The samples were incubated at 37 °C under aerobic conditions, and the absorbance at OD_{600nm} was read after 24 h. The concentrations of FT were plated and the number of viable bacteria determined the minimal bactericidal concentration (MBC).

2.5.2. Nanoscale bacterial characterization and biofilm nanomechanics after FT exposed

In order to verify the possible effect of FT on the mechanical properties of biofilm, nanomechanics tests using atomic force microscopy (AFM) was performed (33,34). For all AFM-based experiments, an *S. aureus* biofilm model was developed as mentioned above. In brief, glass slices (12-mm; Electron Microscopy Sciences, US) were coated with 50 µL of a 0.1 M solution of poly-L-lysine (PLL, Sigma) for 5 minutes, washed 3x with PBS, and dried at room temperature. Subsequently, a 100µL of bacterial inoculum (10^5 CFU/mL of *S. aureus*) and 900µL of BHI broth were used to form biofilms for 24h under static conditions

(37°C; 10%CO₂). Pre-formed *S. aureus* biofilms (24h) were treated with PCL-NIP and PCL-MIP@FT eluates [10mg/mL for 3 days of release in BHI medium before microbiological tests; ~100µg/mL of FT] and incubated overnight. Lastly, Biofilm-coated slices were washed 3x with PBS, dried under a gentle stream of N₂, and carried out on the AFM immediately after sample preparation. For all AFM imaging ($n = 3$), an Asylum MFP 3D-SA AFM(Asylum Research, US) was utilized in intermittent contact mode (AC mode) with TAP300GD-G cantilevers(BudgetSensors, Bulgaria), obtaining height, amplitude, and phase channel images of substrates in air. For nanomechanical analysis, individually calibrated MNSL-10 cantilevers (0.1N/m, Bruker, US) were employed to obtain force-distance curves on the surface of selected EVs in buffer, with a soft loading force of 0.5nN and a 2µm/s rate.

2.6. *In vitro* inflammatory response

2.6.1. *Isolation of human gingival fibroblasts (HGF)*

Three populations (NLA, RG, TB) of primary human gingival fibroblast cells (HGF) were obtained from patients with periodontal health and characterized in a previous study(35). This study was approved by the Research Ethics Committee (CEP/FOP-UNICAMP, CAAE number: 53844321.2.0000.5418). All patients provided written informed consent for participation in the study.

2.6.2. *HGF cell morphology and viability*

To confirm the impact of the FT treatment on cell behavior, HGF cell morphology and viability were examined by confocal microscopy analyses. For this, HGF were cultured in high-glucose Dulbecco's modified Eagle's medium (Sigma Chemical Co., St. Louis, MO, USA), supplemented with 10% fetal bovine serum (Gibco, Grand Island, NY, USA) and 1% penicillin/streptomycin (Sigma-Aldrich, St. Louis, MO, USA), in a humidified atmosphere containing 5% CO₂ at 37 °C. Cells were plated in 96-well plates (2 × 10⁵ cells/well) in standard medium. After 24 hours, the medium was changed to DMEM supplemented with 2% FBS and 1% penicillin/streptomycin containing 0 to 10 mg/mL FT concentration. The plates were then incubated at 37 °C under 5% CO₂ conditions for 24 h to form a monolayer cell culture. HGF cells at the same sampling concentration were inoculated directly on a 24-

well polystyrene plate to serve as a positive control, and cells treated with Triton X-100 (Sigma-Aldrich, St Louis, MO, USA) represented the death control (negative control).

The experiment was carried out 1 day post-seeding. Then, 2 µg/mL Hoescht 33342 (Thermo Fisher Scientific, Waltham, MA, USA) and 20 µg/mL propidium iodide (PI) solution were added into each well to stain live and dead cells, respectively, and cells were incubated for 20 min at 37 °C. Stained cells were then washed with PBS buffer, and cell viability was then examined by confocal laser scanning microscopy (Zeiss LSM 800, Jena, Germany). The blue fluorescence of Hoescht and the red color of PI were examined at 405 nm (405–450 nm) and 488 nm (575–630 nm), respectively, to reveal the distribution of live/dead cells. Images were acquired through 10 and 20× dry (Plan NeoFluar NA 0.3 air) objective lenses and analyzed with Zen Blue 2.3 software (Carl Zeiss). The experiment was performed in duplicate to ensure the reliability of the experiment.

2.6.3. HGF cell metabolism

In order to check the effect of FT in the metabolism of HGF cells, a 3-(4,5-dimethylthiazol-2-yl)-2,5-diphenyl tetrazolium bromide (MTT) assay was also conducted(36). As mentioned above mentioned, HGFs were plated in 96-well plates (0.5×10^4 cells/well) in a standard medium. After 24 hours, the medium was changed to DMEM supplemented with 2% FBS and 1% penicillin/streptomycin containing 0 to 1 mg/mL FT concentration, and HGF cells were cultured for 3 days. At days 1 and 3, MTT reagent was added to each well and incubated for 4 hours at 37°C in a humidified 5% CO₂ incubator. At the end of the incubation period, the medium was removed, and the converted dye was solubilized with 100% ethanol. The absorbance of converted dye was measured at a wavelength of 570 nm with background subtraction at 630 to 690 nm.

2.6.4. *Porphyromonas gingivalis* protein extract (PgPE) preparation

To induce cell inflammation, the *Porphyromonas gingivalis* total protein extract was used as described previously(35,37). *P. gingivalis* (ATCC 53987) was grown anaerobically on blood agar plates, supplemented with hemin and vitamin K1, at 37°C under anaerobic conditions (80% N₂, 10% CO₂, 10% H₂) for 5 days. Isolated colonies were resuspended in cold NaCl 0.9% solution, transferred to microcentrifuge tubes, centrifuged ($\sim 13,000 \times g$ for

4 minutes at 2°C), and stored at -80°C. Total protein was extracted by adding 700 µL ultrapure water and ~0.16 g zirconia beads (0.1-mm diameter) to bacterial solutions. Bacteria were mechanically disrupted with 3 cycles of 1 minute at maximum power and 1 minute on ice. Samples were centrifuged twice (13,000 × g for 8 minutes at 4°C). Protein integrity was evaluated by sodium dodecyl sulfate-polyacrylamide gel electrophoresis and the total protein concentration was determined by the Bradford method. Single-use aliquots were stored at -80°C. At the time of each experiment, a fresh solution of PgPE was prepared by diluting the frozen stock solution in a cell culture medium.

2.6.4. Time course and dose-response evaluation

Considering the lack of information about the FOLRs expression in HGF cells, time course and dose-response experiments were firstly performed. In this step, we propose to assess whether evaluate which concentration of PgPE and which period of exposure promote maximum FOLR1, FOLR2, and FOLR3 expression by the HGFs. After analyzing the PgPE concentrations that did not compromise cell viability in a maximum period of 3 days by MTT assays, the FOLRs expression was evaluated for two different extract concentrations: a lower of 1 µg/ml and a higher of 10 µg/ml (data not shown).

HGFs from a single population (NLA) were seeded in 6-well cell culture plates at a concentration of 15×10^4 cells per well and grown in a standard culture medium for 24 h in a 37°C, 5% CO₂, and 98% humidity incubator. After this period, the medium was replaced with medium containing PgPE at the predetermined concentrations. The cells were maintained in these culture conditions for 1.5, 3, 6, 12, and 24 h. Negative controls were represented by unstimulated cells for all experiments (data not shown).

2.6.5 FOLRs expression by RT-PCR

At the end of each period, the total RNA of the cells was collected using a specific reagent, extracted according to its manufacturer's protocol, and treated with deoxyribonuclease (DNase; DNA-free™, Ambion Inc.)(35,38). The RNA concentration and quality were measured using a spectrophotometer (Nanodrop 2000, ThermoFisher Scientific), and a 10 µl aliquot of the sample was used for the synthesis of complementary single-stranded DNA (cDNA; Roche Diagnostic Co.) in a final volume of 20 µl. Quantitative

polymerase chain reaction (qPCR) was performed using the cDNA in a concentration of 25 ng/ml and the kit LightCycler 480 SYBR Green I Master (Roche Diagnostic Co.). The primers for 18S, ACBT, GAPDH, FOLR1, FOLR2, and FOLR3 (Table 1) were designed using Primer3web version 4.1.0 and sequences confirmed by UCSC PCR *in silico*(38). Each experiment was performed in triplicate, using the water as a negative control. The relative gene expression level was determined using the cycle threshold (Ct) method. GAPDH and ACBT were used as the reference genes ("housekeeping") for the normalization of values. δ Ct formula was used to calculate the expression of the target gene.

Table 1. Primer sequences used for RT-qPCR.

Gene	Primer (5' - 3' sequence)	Annealing temperature	Product Size
18S	F: CGGACAGGATTGACAGATTGATAGC R: TGCCAGAGTCTCGTTTCGTTATCG	61°C	530 bp
ACTB	F: CCAACCGCGAGAAGATGA R: CCAGAGGCGTACAGGGATAG	61°C	538 bp
GAPDH	F: ACATCATCCCTGCCTCTAC R: CCACCTTCTTGATGTCATCATATTTG	51°C	171 pb
FOLR-1	F: CGGGCACCATGAAGGAAA R: GGCCAGACCAAAGATAGAGTT	55°C	184 pb
FOLR-2	F: CCAACCGCGAGAAGATGA R: CCAAGCAAGGTCTTCCAAAG	60°C	223 pb
FOLR-3	F: CTTCCACCCCTCTTTCTTCC R: GTCTCCCGGAAACACTTGAA	58°C	221 pb

ACTB: β -actin; GAPDH: Glyceraldehyde 3-Phosphate Dehydrogenase; 18S: 18S ribosomal RNA.

2.7. *In vivo* systemic toxicity

The systemic acute toxicity of PCL-MIP@FT was determined on the *Galleria mellonella* larvae model(39,40). *G. mellonella* larvae (200 to 300 mg) with no signs of melanization were randomly selected for each group ($n = 15$). Prior to the experiment, PCL-MIP@FT and PCL-NIP samples (10 mg) were immersed in the PBS solution (1 mL) as previously described for drug release and solutions were collected on days 0, 7, and 21. PBS was administered to a negative control group ($n = 15$). A 10 μ L aliquot of PCL-MIP@FT eluate or PCL-NIP eluate was injected into the hemocoel of each larva via the last left proleg using a 1 mL syringe. The prick area was decontaminated with 70% ethanol before the administration of each eluate. The larvae were incubated at 30° C (Bio-Oxygen Demand incubator, SP labor, Sao Paulo, Brazil), and their survival was monitored at selected intervals

for up to 72 h. Larvae with no movements upon touch were counted as dead. The experiment was repeated two times.

2.8. *In vivo* biocompatibility and inflammatory profile

2.8.1. *Animals*

Wistar rats (*Rattus norvegicus albinus*; $N = 6$), six weeks old, weighing between 250 and 300 g, were purchased after approval by the Institutional Ethics Committee on Animal Research (CEUA/FOA-UNESP, Protocol Number 433-2023). All animals were housed in a vivarium under humidity (40–60%) and temperature (22 ± 2 °C) control in 12 h light–dark cycle, with access to food and water *ad libitum*. The general health of the animals was monitored throughout the experimental period. This study was carried out in strict accordance with the guidelines for the care and use of animals by ARRIVE guidelines (41).

2.8.2. *Subcutaneous implantation of the polymers*

Polyethylene tubes (Abbot Labs of Brazil; $N=15$) with 1.0-mm internal diameter, 1.6-mm external diameter, and 10.0-mm length (ISO 10993-6, 2007) sterilized in ethylene oxide were used in a subcutaneous model(42). They were filled with 10 mg of PCL-NIP or PCL-MIP@FT and empty tubes were used as a control. In brief, the rats were anesthetized by intramuscular administration of ketamine, 87 mg/kg (Francotar; Virbac do Brasil Ind. E Com. Ltda) and xylazine, 13 mg/kg (Rompum; Bayer SA). Then, their dorsal were shaved, and cleaned with topic polyvinylpyrrolidone Iodine (PVPI; 2%), and a 2.0-cm incision was made in a head-to-tail orientation with a #15 Bard-Parker blade (BD, Franklin Lakes, NJ). The skin was reflected to create two pockets on the right side and two pockets on the left side of the incision. Four tubes were randomly implanted into the pockets of each animal, and the skin was sutured.

After the experimental procedures, the animals received intraperitoneally 150 mg/kg of Dipyrone (Sanofi Medley Indústria Farmacêutica Ltda) for pain relief. Animals were euthanized at 3 days postoperatively with an overdose of sodium thiopental anesthetic (240 mg/kg – Thiopentax, Cristalia Produtos Quimicos Farmaceuticos Ltda.). Subsequently, the tubes and the surrounding tissues were removed and fixed in 10% formalin solution at a pH of 7.0. The fixed specimens were processed and embedded in paraffin and serially

sectioned into 5- μ m slices for staining with hematoxylin-eosin for histological analysis. Three slides with three sections each were obtained for each sample and the best section was used in the analysis.

2.8.3. Histological analysis

Histological analysis was performed by a single calibrated operator (R.C.C.) under light microscopy (400 \times , DM 4000 B; Leica). To evaluate inflammatory cells the ImageJ software (National Institutes of Health, Bethesda, MD, USA) was used. For the image quantifying, an objective of \times 100 magnification was used, and a grid with 130 points was applied to allow the count of cells.

2.9. Statistical analysis

The results were expressed as mean \pm standard deviation (SD). The data were checked for normality and homogeneity of variance. The differences between groups were analyzed using one-way or two-way analysis of variance (ANOVA), followed by Tukey's or Bonferroni's post-hoc tests. Survival curves of treated and untreated larvae were compared using the Log-rank (Mantel-Cox) test. The results were considered significant at $p < 0.05$.

3. Results and discussion

The molecularly imprinted technique is a straightforward and effective strategy for developing a drug-delivery system of folate in biological tissues. Herein, biodegradable PCL-based polymers were fabricated and functionalized with folate in a facile manner to achieve suitable release by pH for active participation in inflammatory events involved in implant infections. For the first time, we demonstrated that FOLR receptors are overexpressed in gingival fibroblasts during inflammation, thus being crucial targets for host-modulating therapies. In general, PCL-MIP@FT has optimal anti-inflammatory actions *in vitro* and *in vivo* supporting their use as a novel drug-free therapeutic platform for the treatment of chronic inflammatory disorders.

3.1. Molecularly imprinted technology successfully produces biodegradable polymers as a promising folate-delivery system

The MIP technique used in this study has been progressively applied in the biomedical field (43,44) due to its favorable chemical stability in harsh environments, including the oral cavity. In the first step, we rationally designed a biodegradable MIP utilizing computational simulations to reduce the time and resources usually required. For this, density functional theory (DFT) was applied to understand the interaction between folate and the functional monomers. The functional monomers chosen were acrylamide, acrylic acid, styrene, and 2-vinylpyridine because are most widely used in the synthesis of biodegradable and biocompatibility imprinted polymers for healthcare materials(27,28). The formulation of the complexes was conducted manually as reported elsewhere(21,23). Despite some favorable molecular interactions (Supplementary Figure 1), the most promising interaction for drug release is the folate-acrylic acid complex (Fig. 1A). Since the solvent and functional monomer play a key role in producing high-affinity MIPs with controlled binding strength(22), their binding energies were calculated (Fig. 1B). Traditionally, the more negative this binding energy is, the more favorable the complex formation. On the other hand, drug delivery systems need to have a weakened intermolecular interaction for efficient oral drug delivery(20). Thus, based on our calculations, the folate-acrylic acid complex in chloroform solvent was selected for this purpose.

Based on the theoretical predictions, PCL-based non-imprinted polymer (PCL-NIP; control) and imprinted polymer with folate (PCL-MIP@FT) were successfully produced. The final formulation of PCL-MIP@FT is composited as follows: folate (analyte), acrylic acid (functional monomer), PCL-triol (structural monomer), and chloroform (solvent). Regarding the polymer characterizations, the presence of folate changed the PCL polymer color from off-white to shades of yellow (Fig. 1D). CLSM (Fig. E) and SEM (Fig. F) images show micro-particles with a high degree of agglomeration due to the polymer self-assembly by the photopolymerization method (25). The comparison of FTIR spectra of PCL-NIP and PCL-MIP@FT, with and without folate (Fig. 1G), demonstrated the similarity of chemical bonds. In particular, the characteristic signals of the hydroxyl and amine groups of PCL, detected between 3630 cm^{-1} and 1072 cm^{-1} (O-H and C-H stretching, broad signal) appear in both spectra. For PCL-MIP@FT there is the peak at 2250 cm^{-1} is ascribed to the carboxylic group due to folate functionalities (C = O stretching, broad signal) that is not observed in PCL-NIP. Our results revealed that even with folate incorporated the PCL has the same functional

group. The polymer size was considered acceptable in the range of 1–5 μm with homogeneous distribution (Fig. F).

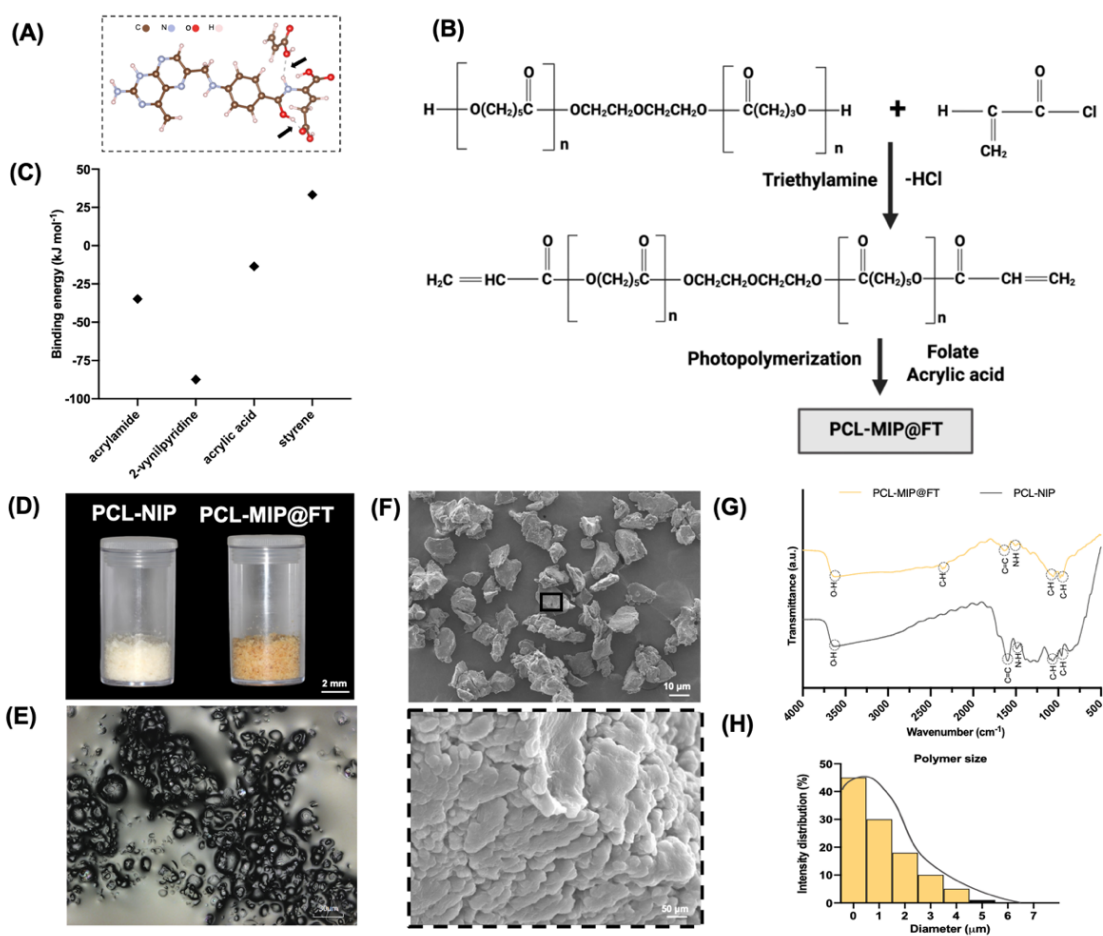


Figure 1. Theoretical prediction and synthesis characterizations. (A) The best interaction for drug release is the folate-acrylic acid complex (on top). The hydrogen bonds were drawn in dotted lines and highlighted by black arrows. (B) Theoretically calculated energies (kJ mol⁻¹) for complexes of folate and distinct functional monomers in chloroform (solvent). (C) Overall reaction scheme for the synthesis of polymerizable on PCL and the crosslinked MIP network. (D) Photograph of polymers. (E) Representative three-dimensional images obtained by confocal laser scanning microscopy (CLSM; 50× of magnification). (F) Scanning electron microscopy (WD = 12 mm, 3 kV). (G) FTIR spectra with the assignment of the main bands for PCL-NIP and PCL-MIP@FT. (H) Polymer size distribution (μm).

3.2. Acidic environment accelerates and increases the release of folate by polymer biodegradability

PCL has exceptional potential to be blended with other polymers for achieving specific mechanical and degradation properties(45). In fact, controllable factors such as polymer composition and molecular weight as well as other factors like temperature and pH strongly influence the degradation rate, reflected by a decreasing molecular weight of the polymer (19). Herein, we validated the mechanism of folate release from the polymer by pH changes (Figure 2A). As expected, PCL-MIP@FT has higher stability under physiologic (pH = 7.4) and alkaline conditions (pH = 9.0) (Figure 2B). At acidic conditions, folate was released from the polymer much faster and almost completely within 10 days, a convenient perspective to clinical situations where the inflammatory disease is already has been established. This phenomenon may be a consequence of secondary interactions (hydrogen bonds) and intermolecular associations order upon changes in the local pH, which affect drug release(11,46). Thus, we assume that the folate release mechanism is related to PCL chain mobility after ionization by pH and its hydrolytic susceptibility. The successful folate incorporation in PCL-MIP was confirmed by IE and IC values achieving at least 97 % and 26%, respectively (Figure 2C). Overall, ~ 180 ug of folate was released in total from PCL-MIP@FT in the acid condition, while only ~ 135 ug and ~ 58 ug of folate incorporated into the polymers were released from neutral and alkaline conditions, respectively (Figure 2D). Moreover, a more substantial polymer degradation (~35% at day 28) was found in the acidic environments (Figure 2E), and this supports our assumption that the overall increase in folate release at pH = 4.5 was triggered by PCL deterioration. Concerning the temperature mechanism, both the PCL-NIP and PCL-MIP@FT exhibited almost similar thermal behavior with stability up to high temperatures (Figure 2F). These TGA results confirmed that PCL-MIP@FT is not dependent on temperature for drug delivery.

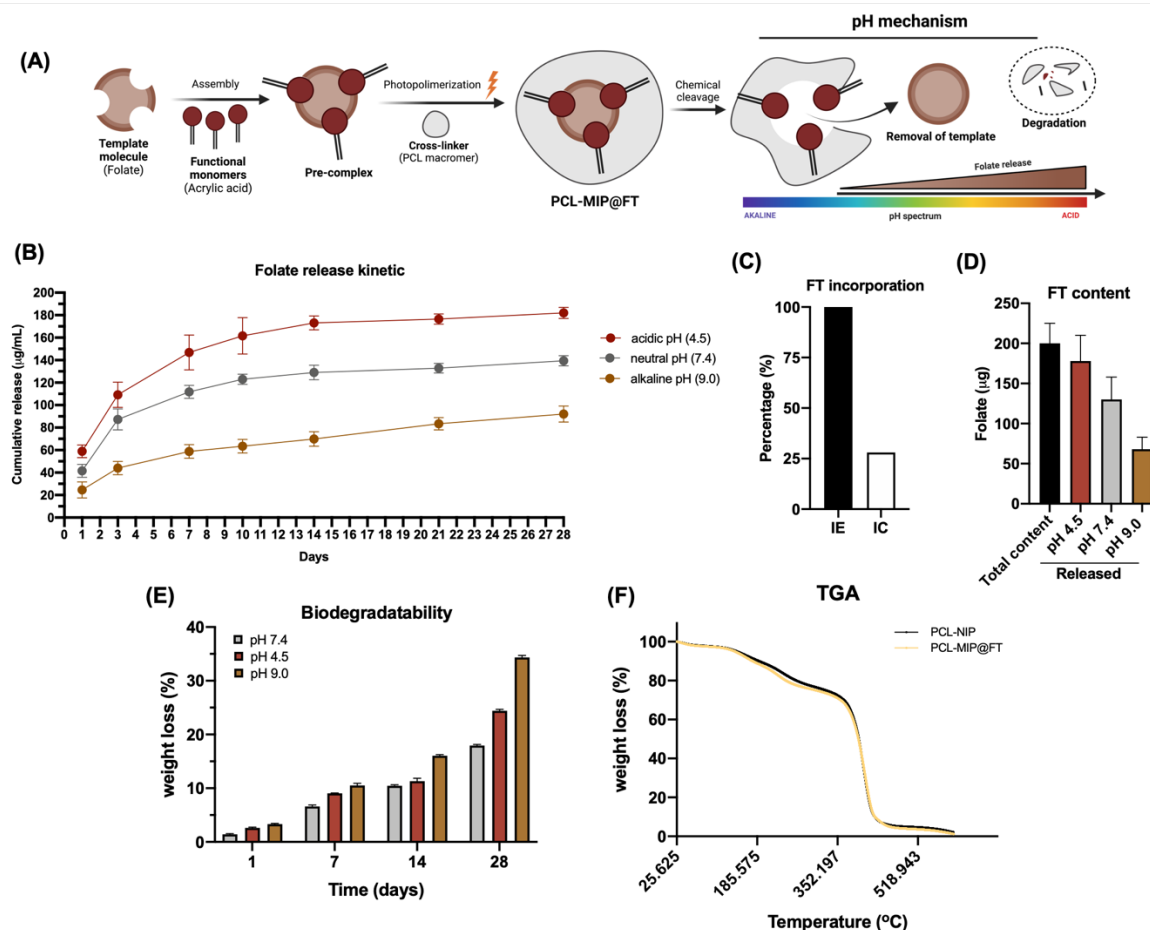


Figure 2. Proof-of-concept of pH mechanism to trigger folate release and PCL degradation. (A) Schematic representation of polymer synthesis and degradation from pH changes. **(B)** Cumulative folate release profile [$n = 5$; 2 independent experiments] in neutral [7.4], acidic [4.5], and alkaline [9.0] conditions. **(C)** Percentage levels of incorporation efficiency [IE] and incorporation coefficient [IC] of folate in the polymer. **(D)** Relation between folate total content in polymer and folate release after 28 days. **(E)** Biodegradation profile in each pH condition ($n = 3$; 2 independent experiments). **(F)** TGA thermograms of PCL-NIP and PCL-MIP@FT.

3.3. FT-induces alterations on *S. aureus* biofilm nanomechanics

Motivated by the contradictory results about the possible antimicrobial effect of FT, a CIM/CBM assay was performed. Notably, FT did not have any antibacterial effect as demonstrated in the CIM assay (Figure 3A). A substantial *S. aureus* growth was observed in all concentration tested (Figure 3B). Regarding AFM imaging (Figure 3C), control biofilms showed a very defined morphology and marked division features, such as septa. On the other

hand, biofilms treated with PCL-MIP@FT eluate displayed an altered and irregular morphology, where cells appear enlarged, with less pronounced division septa and the presence of wrinkling and other features consistent with cell damage and surface disorganization. This finding can be partially attributed to folate-bacteria interaction, which leads to the membrane disruption effect, as observed with AFM in a previous study(34). Moreover, polymer-treated biofilms were found to have a significant increase in Young's modulus compared to the control (Figure 3D and 3E), supporting the hypothesis that PCL-MIP@FT significantly alters wall morphology and properties in *S. aureus*. Further research is necessary to fully elucidate the particular effect of FT on the elastic properties of other Gram-positive and Gram-negative bacteria.

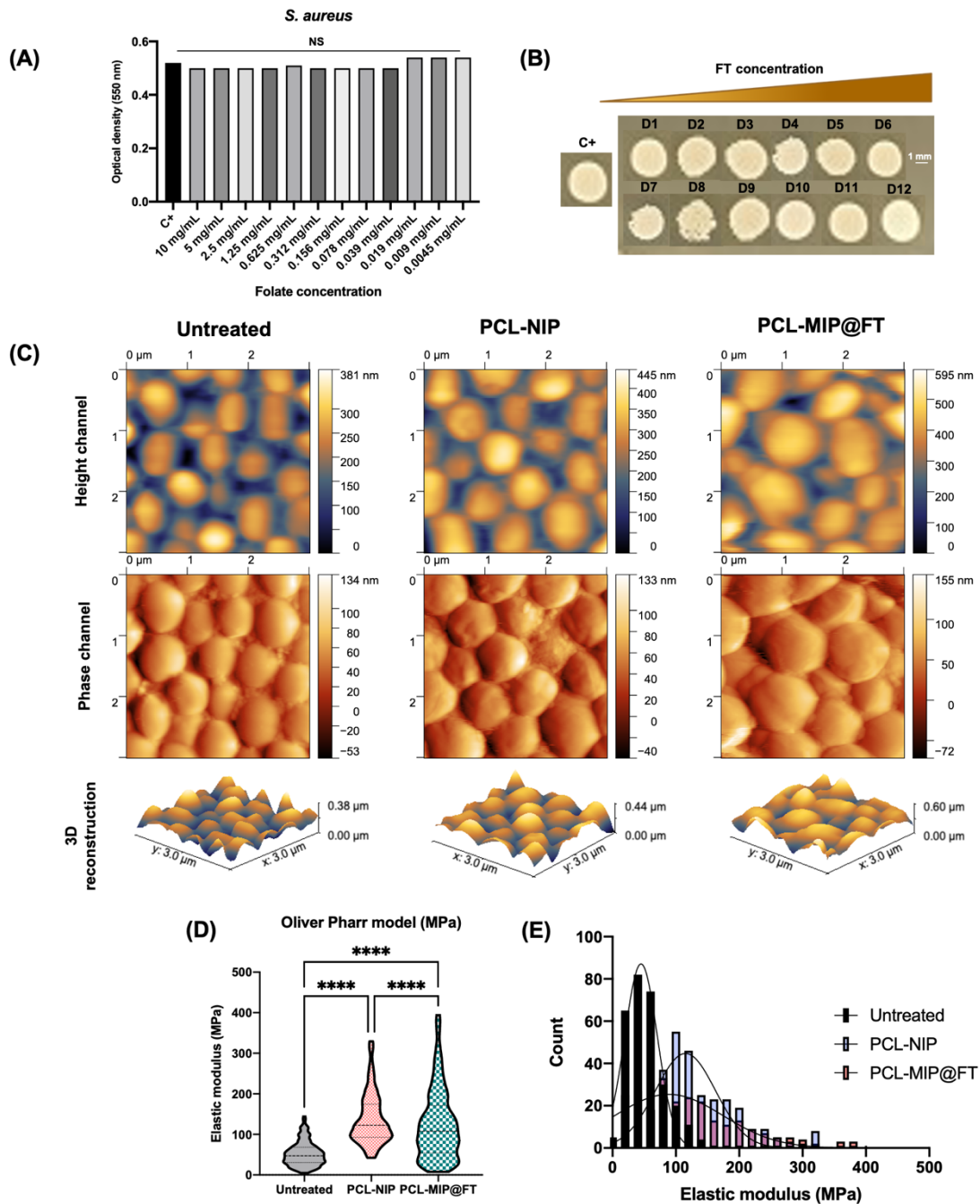


Figure 3. Effect of FT in *S. aureus* viability and biofilm nanomechanics. **(A)** Minimum inhibition concentration assay for folate. **(B)** Photography of bacteria colonies from 10 mg [D1] up to 0.0045 mg [D2]. **(C)** AFM-based nano-characterization of *S. aureus* after polymer exposure. **(D)** Oliver Pharr model and **(E)** the histogram of elastic modulus (in MPa).

Statistically significant differences between groups are indicated by symbols: **** $p < 0.001$; NS= No statistical difference.

3.4. Overexpressed of FOLR-1 e FOLR-3 in HGFs by *PgPE*-induced inflammation regulates the folate-target immunotherapy

Based on the knowledge acquired thus far, we also evaluated the specific effect of folate on HGF cells as *in vitro* validation of its mechanisms. FT concentration up to 1 mg/mL did not affect cell viability compared to the control (Figure 4A). As expected, FT 0.1 and 0.5 $\mu\text{g/mL}$ stimulate the growth of HGF cells. Moreover, higher metabolic activity ($> 100\%$) was found for FT 0.1 mg/mL at 1 and 3 days (Figure 4B). These findings corroborated with a previous study that demonstrated similar cytocompatibility and stimulatory effects under keratinocytes using 100 $\mu\text{g/day}$ of FT released from scaffolds(17), confirming the safety of this concentration in different human cells. Subsequently, we induced inflammation in HGFs by *PgPE* to discover whether the FOLRs expression can occur in these cells. Firstly, a range of doses of *PgPE* (0 to 100 $\mu\text{g/mL}$) was prepared and protein integrity was determined by SDS analysis (Figure 4C). Surprisingly, *PgPE* had a slight effect on HGF cell viability after 1 day (Figure 4D) and 3 days (Figure 4E) of exposure. It can be speculated that cells respond to *PgPE* and produce inflammatory responses; however; the death of cells (i.e.; minor metabolism) is not achieved *in vitro*. The leading signaling pathway activated by *PgPE* is controversial, as recently reviewed (47). With relation to the time course experiment, overexpression of pró-inflammatory cytokines (such as IL6, IL-1 β , COX-2, and TNF- α) in inflamed HFGs was verified by RT-PCR analysis, confirming the inflammatory reaction induced by *PgPE* (data not shown). Furthermore, it is important to highlight that 3h exposure of HGF with 1 $\mu\text{g/mL}$ promoted the up-regulation of FOLR-1 and FOLR-3 expression. On the other hand, FOLR-2 did not have a strong expression in HGF compared to the control (data not shown).

After discovering the expression of FOLR-1 and FOLR-3 in HGF, we validated this finding in 3 different populations. For all populations (NL, RG, and TB), the exposure with 1 $\mu\text{g/ml}$ of *PgPE* for 3 h increased the expression of FOLR-1 (Figure 4F) and FOLR-2 (Figure 4G) compared to the control (i.e.; without *PgPE* exposure). The biological function of FRs is to internalize folates into the cells, where the vitamin is of crucial importance to DNA

synthesis and repair(15). However, other important functions have recently been assigned to the receptor such as modulating the pro-inflammatory cytokines synthesis via some intracellular pathways(16). Altogether, these findings not only increase the comprehension of the processes governing peri-implant inflammation but also give insight into new pathways that are of value to modulate, such as folate-target receptors describes herein.

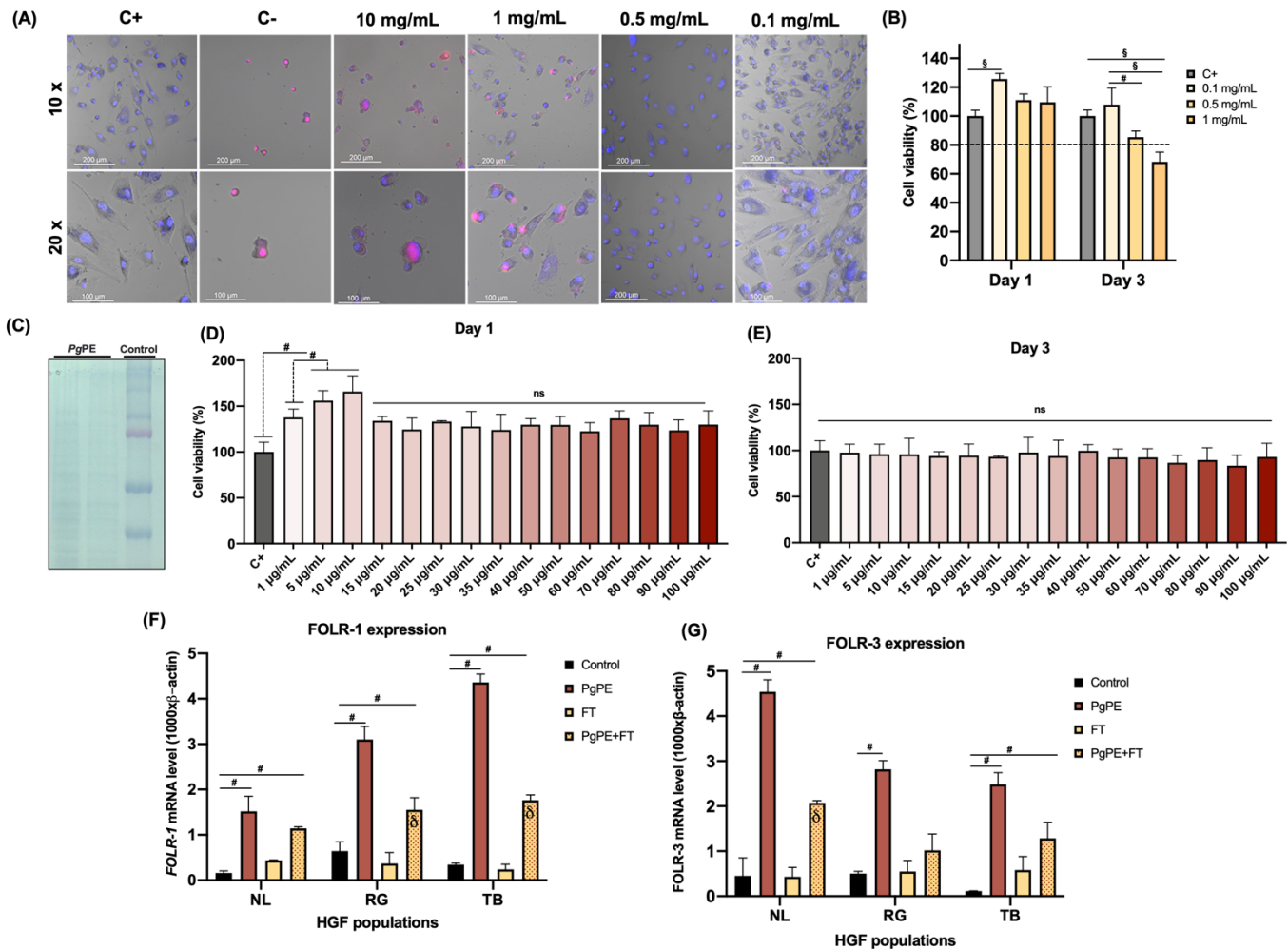


Figure 4. *In vitro* inflammatory response modulated via topically folate administration and FOLRs expression. (A) HGF cell viability and morphology ($n = 1$). Cells were stained with Hoescht 33342 (blue) and PI solution (red) to show live and dead cells, respectively. **(B)** HGF metabolic activity (%) by MTT assay at 1 and 3 days under FT exposure ($n = 3$; 2 independent experiments). **(C)** Electrophoresis analysis confirming the protein integrity ($n = 1$). The effect of PgPE on HGF cell metabolism was evaluated by MTT assay at 1 **(D)** and 3 **(E)** days. Cellular expression of FOLR-1 **(F)** and FOLR-3 **(G)** after 3 h of inflammation challenges with 1 µg/mL of PgPE. Bars indicate mean \pm

SD. Statistically significant differences between groups are indicated by symbols: # $p < 0.05$, § $p < 0.01$.

3.5. The newly developed PCL-MIP@FT did not have systemic toxicity

Toxicological assessment of an experimental healthcare biomaterial is an important step prior to its clinical translatability(48). Based on this, we determine the *in vivo* toxicity of the polymers using the *G. mellonella* model (Figure 5A and 5B), which is a widely accepted and validated model for the toxicological screening of drugs (39). This approach has a low cost, generates rapid results and, most importantly, reduces the number of animals for experimentation as its results correlate with those observed in mammals (vertebrates)(40,48). In our study, we did not find the lethal dose (LD₅₀) in the larvae in none of the samples tested (Figure 5C). For PCL-MIP@FT, its eluate did not have any toxic effects on larvae at doses up to 1,3 mg/kg with 100% survival of the treated larvae. We believed that the presence of FT in the eluate could exert some protective (antioxidant) effects on the larvae and this finding needs further investigation.

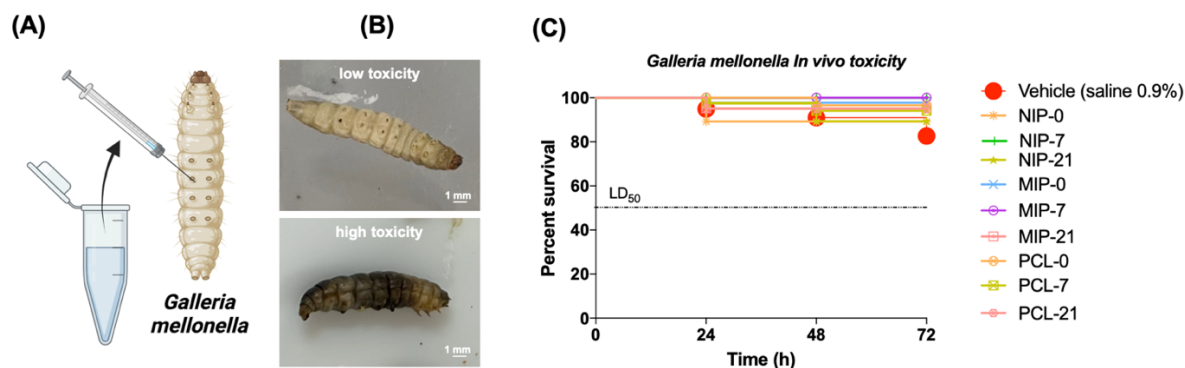


Figure 5. The effects of FT-MIP@FT on the systemic toxicity of *Galleria mellonella* larvae. (A) Larvae were treated with eluates from the release of PCL-NIP, PCL-MIP@FT, and PBS (control) at 0,7, and 21 days. (B) Viability of larvae was monitored by visual inspection of the body appearance (brown-dark brown colour) and by lack of body movement. (C) Survival rate of *G. mellonella* larvae after administration of polymers eluates over 3 days experiment period. Control curve was obtained by administrating sterile phosphate-buffered saline (PBS) into larvae. The results were expressed as mean \pm SD ($n = 15$; 2 independent experiments). LD₅₀ = Lethal Dose. No statistically significant differences between groups were founded.

3.6. pH-responsive imprinted polymer delivering folate promotes an alleviating in inflammatory reaction

Encouraged by the possible inflammation modulation provides due to folate-FOLR interactions, we further validated this promising effect using a rat model. As this is an initial study, we use the well-established and accepted model for the biocompatibility testing of materials via subcutaneous implantation of the polymer (Figure 6A). Our results showed that PCL-MIP@FT can decrease the inflammatory infiltrate and it is able to stimulate the repair (Figure 6B). At 3 days postoperative time, the control group showed the highest number of inflammatory cells, followed by PCL-NIP, and PCL-MIP@FT groups ($p < 0.05$; Figure 6C). Thus, local treatment with the newly imprinted polymer modulated the inflammatory process in a folate-dependent manner, reinforcing the folate-targeted immunotherapy for inflamed tissues *in vivo*. This significant reduction of local inflammation can be partially explained by the pH mechanism of PCL-MIP@FT to drive folate release. In inflamed tissues, pH decreases occur due to lactic acid production and oxygen, consequently, using a topical PCL-MIP@FT, a more substantial release of folate can be obtained in this acidic environment. As a result, the linkage between FT and FOLRs-1 and FOLRs-2 (overexpression during inflammation) induces the down-regulated of intracellular mediators such as pro-inflammatory cytokines and cytotoxic molecules (e.g: reactive oxygen species; ROS), decreasing the risk of tissue damage(13,15). Moreover, FT can act in the switching of macrophage phenotype (from M1 to M2), contributing to attenuating inflammation and promoting the tissue repair process(17), which warrants further studies. Importantly, the intracellular signaling pathways underlying this anti-inflammatory molecular event caused by the PCL-MIP@FT treatment need to be fully investigated.

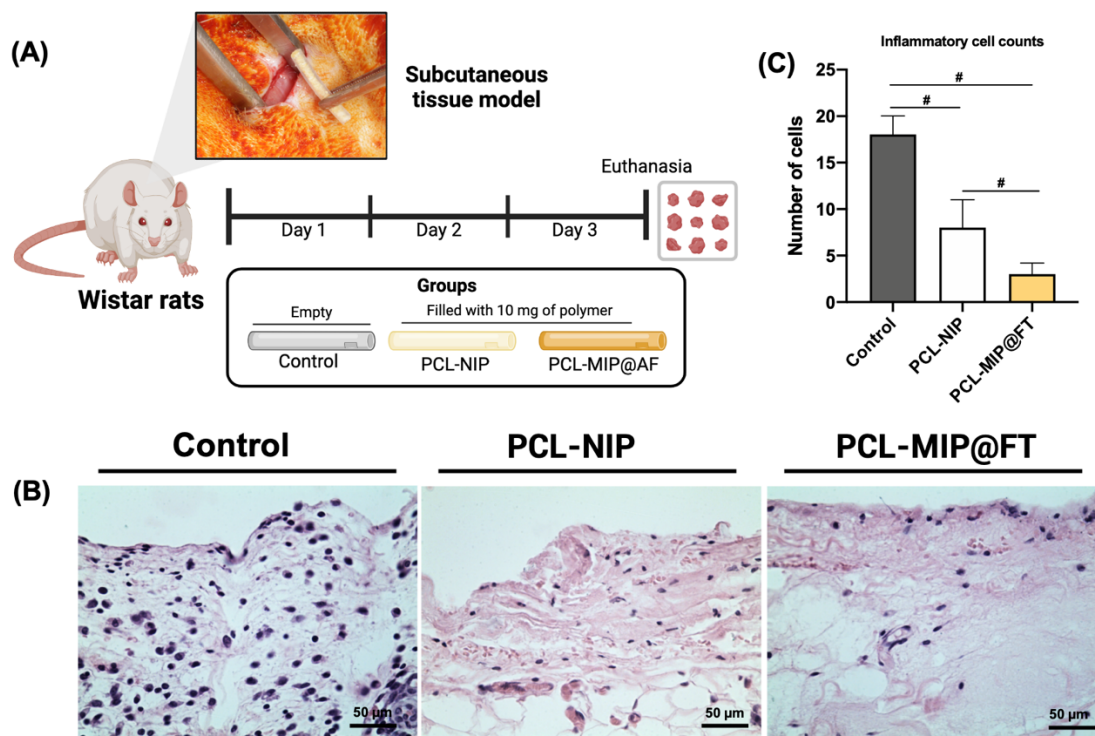


Figure 6. *In vivo* biocompatibility of PCL-MIP@FT. (A) Experimental design of the subcutaneous model adopted. (B) Representative images from the subcutaneous tissue reactions for PCL-NIP, PCL-MIP@FT, and the control tube at 3 days postoperative (Hematoxylin- eosin staining, $\times 400$). (C) Inflammatory profile determined from cell counts by ImageJ software. The results were expressed as mean \pm SD. Statistically significant differences between groups are indicated by symbols: # $p < 0.001$.

Collectively, the above *in vitro* and *in vivo* results proven that PCL-MIP@FT holds a therapeutic function to moderate inflammation, mainly by regulating the FT-FOLRs interaction. This study lays the groundwork for further investigation of folate-target immunotherapy as a drug-free platform to treat implant infections in the near future. From a clinical standpoint, PCL-MIP@FT therapy can be combined with additional mechanical decontamination and antimicrobial approaches, aiming to mitigate or compensate for the absence of direct antimicrobial effect, leading to new paths for improved implant survival. Finally, clinical trials should be performed to better elucidate the effects of PCL-MIP@FT therapy in humans.

4. Conclusion

In summary, we here successfully synthesized a biodegradable pH-responsive polymer co-delivering folate in a facile manner using the molecularly imprinted technique. We systematically demonstrated the therapeutic effect of the newly developed PCL-MIP@FT under in vitro and in vivo conditions. Interestingly, for the first time, folate receptors were described in the fibroblast cells, thus being a promising target for immunotherapy in inflammatory disorders. Although further studies are required to optimize the imprinted polymer and to confirm its extensive applicability, the current findings suggest the possible use of pH-responsive imprinted polymer with folate in moderating inflammatory events as a novel drug-free therapeutic platform for dental implant infections.

ACKNOWLEDGMENTS

This study was funded by The São Paulo Research Foundation (FAPESP), Grant/Award numbers: 2020/10436-4 to R.C.C, and 2020/05231-4 to V.A.R.B.; Conselho Nacional de Desenvolvimento Científico e Tecnológico (CNPq), Grant/Award number: #307471/2021-7 to V.A.R.B; and Coordenação de Aperfeiçoamento de Pessoal de Nível Superior (CAPES), Finance code 001.

DATA AVAILABILITY STATEMENT

The data that support the findings of this study are available from the corresponding author upon reasonable request.

EXPERIMENTOS À SEREM INCORPORADOS NESTE ARTIGO:

- Resultados do experimento “*time course*” (Dosagem de citocinas e receptores de folato - RT-PCR);
- Dosagem de citocinas pró-inflamatória (IL-6; IL-1 β ; TNF- α , COX-2) via RT-PCR
- Histologia via picrosirius red

REFERENCES

1. Berglundh T, Armitage G, Araujo MG, Avila-Ortiz G, Blanco J, Camargo PM, et al. Peri-implant diseases and conditions: Consensus report of workgroup 4 of the 2017 World Workshop on the Classification of Periodontal and Peri-Implant Diseases and Conditions. *J Clin Periodontol*. 2018;45 Suppl 20:S286–91.
2. Araujo MG, Lindhe J. Peri-implant health. *Journal of Clinical Periodontology*. 2018;45(S20):S230–6.
3. Corrêa MG, Pimentel SP, Ribeiro FV, Cirano FR, Casati MZ. Host response and peri-implantitis. *Braz Oral Res*. 2019;33(suppl 1):e066.
4. Dyke TEV, Sima C. Understanding resolution of inflammation in periodontal diseases: Is chronic inflammatory periodontitis a failure to resolve? *Periodontology 2000*. 2020;82(1):205–13.
5. Hajishengallis G, Darveau RP, Curtis MA. The keystone-pathogen hypothesis. *Nat Rev Microbiol*. 2012 Oct;10(10):717–25.
6. Schwarz F, Derks J, Monje A, Wang HL. Peri-implantitis. *J Clin Periodontol*. 2018 Jun;45 Suppl 20:S246–66.
7. Heitz-Mayfield LJA, Mombelli A. The therapy of peri-implantitis: a systematic review. *Int J Oral Maxillofac Implants*. 2014;29 Suppl:325–45.
8. Schwarz F, Alcoforado G, Guerrero A, Jönsson D, Klinge B, Lang N, et al. Peri-implantitis: Summary and consensus statements of group 3. The 6th EAO Consensus Conference 2021. *Clinical Oral Implants Research*. 2021;32(S21):245–53.
9. Pack AR. Effects of folate mouthwash on experimental gingivitis in man. *J Clin Periodontol*. 1986 Aug;13(7):671–6.
10. Thomson ME, Pack AR. Effects of extended systemic and topical folate supplementation on gingivitis of pregnancy. *J Clin Periodontol*. 1982 May;9(3):275–80.
11. Khan S, Rahman SZ, Ahad A. Local drug delivery of folic acid promotes oral mucosal wound healing. *J Dent Sci*. 2021 Jan;16(1):532–3.
12. Low PS, Kularatne SA. Folate-targeted therapeutic and imaging agents for cancer. *Current Opinion in Chemical Biology*. 2009 Jun 1;13(3):256–62.
13. Low PS, Henne WA, Doorneweerd DD. Discovery and development of folic-acid-based receptor targeting for imaging and therapy of cancer and inflammatory diseases. *Acc Chem Res*. 2008 Jan;41(1):120–9.
14. Erdemir EO, Bergstrom J. Relationship between smoking and folic acid, vitamin B12 and some haematological variables in patients with chronic periodontal disease. *Journal of Clinical Periodontology*. 2006;33(12):878–84.
15. Chen C, Ke J, Zhou XE, Yi W, Brunzelle JS, Li J, et al. Structural basis for molecular recognition of folic acid by folate receptors. *Nature*. 2013 Aug;500(7463):486–9.
16. Ebrahimnejad P, Sodagar Taleghani A, Asare-Addo K, Nokhodchi A. An updated review of folate-functionalized nanocarriers: A promising ligand in cancer. *Drug Discovery Today*. 2022 Feb 1;27(2):471–89.

17. Kim TH, Kang MS, Mandakhbayar N, El-Fiqi A, Kim HW. Anti-inflammatory actions of folate-functionalized bioactive ion-releasing nanoparticles imply drug-free nanotherapy of inflamed tissues. *Biomaterials*. 2019;207:23–38.
18. Alkan D, Guven B, Turer CC, Balli U, Can M. Folate-receptor 1 level in periodontal disease: a pilot study. *BMC Oral Health*. 2019 Oct 11;19(1):218.
19. Liu R, Poma A. Advances in Molecularly Imprinted Polymers as Drug Delivery Systems. *Molecules*. 2021 Jun 11;26(12):3589.
20. Alqahtani MS, Kazi M, Alsenaidy MA, Ahmad MZ. Advances in Oral Drug Delivery. *Front Pharmacol*. 2021;12:618411.
21. Villa JEL, Khan S, Neres LCS, Sotomayor MDPT. Preparation of a magnetic molecularly imprinted polymer for non-invasive determination of cortisol. *J Polym Res*. 2021 Jul 14;28(8):298.
22. Pupin RR, Foguel MV, Gonçalves LM, Sotomayor M del PT. Magnetic molecularly imprinted polymers obtained by photopolymerization for selective recognition of penicillin G. *Journal of Applied Polymer Science*. 2020;137(13):48496.
23. Neres LCS, Feliciano GT, Dutra RF, Sotomayor MDPT. Development of a selective molecularly imprinted polymer for troponin T detection: a theoretical-experimental approach. *Materials Today Communications*. 2022 Mar 1;30:102996.
24. Zhang H. Molecularly Imprinted Nanoparticles for Biomedical Applications. *Advanced Materials*. 2020;32(3):1806328.
25. Lee KS, Kim DS, Kim BS. Biodegradable molecularly imprinted polymers based on poly(ϵ -caprolactone). *Biotechnol Bioprocess Eng*. 2007 Apr 1;12(2):152–6.
26. Neese F. The ORCA program system. *WIREs Computational Molecular Science*. 2012;2(1):73–8.
27. Lee C, Yang W, Parr RG. Development of the Colle-Salvetti correlation-energy formula into a functional of the electron density. *Phys Rev B*. 1988 Jan 15;37(2):785–9.
28. Weigend F, Ahlrichs R. Balanced basis sets of split valence, triple zeta valence and quadruple zeta valence quality for H to Rn: Design and assessment of accuracy. *Phys Chem Chem Phys*. 2005 Aug 30;7(18):3297–305.
29. Hanwell MD, Curtis DE, Lonie DC, Vandermeersch T, Zurek E, Hutchison GR. Avogadro: an advanced semantic chemical editor, visualization, and analysis platform. *Journal of Cheminformatics*. 2012 Aug 13;4(1):17.
30. Humphrey W, Dalke A, Schulten K. VMD: visual molecular dynamics. *J Mol Graph*. 1996 Feb;14(1):33–8, 27–8.
31. Costa RC, Souza JGS, Cordeiro JM, Bertolini M, de Avila ED, Landers R, et al. Synthesis of bioactive glass-based coating by plasma electrolytic oxidation: Untangling a new deposition pathway toward titanium implant surfaces. *Journal of Colloid and Interface Science*. 2020 Nov 1;579:680–98.
32. Cordeiro JM, Barão VAR, de Avila ED, Husch JFA, Yang F, van den Beucken JJJP. Tailoring Cu²⁺-loaded electrospun membranes with antibacterial ability for guided bone regeneration. *Biomaterials Advances*. 2022 Aug 1;139:212976.

33. Schuh CMAP, Benso B, Naulin PA, Barrera NP, Bozec L, Aguayo S. Modulatory Effect of Glycated Collagen on Oral Streptococcal Nanoadhesion. *J Dent Res*. 2021 Jan 1;100(1):82–9.
34. Leiva-Sabadini C, Alvarez S, Barrera NP, Schuh CMAP, Aguayo S. Antibacterial Effect of Honey-Derived Exosomes Containing Antimicrobial Peptides Against Oral Streptococci. *International Journal of Nanomedicine*. 2021 Dec 31;16:4891–900.
35. Stolf CS, Sacramento CM, Paz HES, Machado RA, Ramos LP, de Oliveira LD, et al. IL10 promoter rs6667202 polymorphism is functional in health but not in grade c periodontitis patients: A pilot study. *Journal of Periodontal Research*. 2022;57(1):85–93.
36. Borges MHR, Nagay BE, Costa RC, Sacramento CM, Ruiz KG, Landers R, et al. A tattoo-inspired electrosynthesized polypyrrole film: crossing the line toward a highly adherent film for biomedical implant applications. *Materials Today Chemistry*. 2022 Dec 1;26:101095.
37. Albiero ML, Stipp RN, Saito MT, Casati MZ, Sallum EA, Nociti FH, et al. Viability and Osteogenic Differentiation of Human Periodontal Ligament Progenitor Cells Are Maintained After Incubation With *Porphyromonas gingivalis* Protein Extract. *J Periodontol*. 2017;88(11):e188–99.
38. Sacramento CM, Assis RIF, Saito MT, Coletta RD, da Rocha Dourado M, Sallum EA, et al. BMP-2 and asporin expression regulate 5-aza-dC-mediated osteoblast/cementoblast differentiation of periodontal dental ligament mesenchymal progenitor cells. *Differentiation*. 2022 Mar 1;124:17–27.
39. Lazarini JG, Massarioli AP, Soares JC, Nani BD, Charo N, Oliveira DS, et al. The phytoactive constituents of *Eugenia selloi* B.D. Jacks (pitangatuba): Toxicity and elucidation of their anti-inflammatory mechanism(s) of action. *Food Chemistry: Molecular Sciences*. 2022 Jul 30;4:100093.
40. Lazarini JG, Franchin M, Soares JC, Nani BD, Massarioli AP, Alencar SM de, et al. Anti-inflammatory and antioxidant potential, in vivo toxicity, and polyphenolic composition of *Eugenia selloi* B.D.Jacks. (pitangatuba), a Brazilian native fruit. *PLOS ONE*. 2020 Jun 9;15(6):e0234157.
41. Percie du Sert N, Hurst V, Ahluwalia A, Alam S, Avey MT, Baker M, et al. The ARRIVE guidelines 2.0: Updated guidelines for reporting animal research. *BMC Veterinary Research*. 2020 Jul 14;16(1):242.
42. de Oliveira PHC, Gomes Filho JE, Rodrigues MJ da S, da Silva CC, Cardoso C da BM, Cosme daSilva L, et al. Influence of supplement administration of omega-3 on the subcutaneous tissue response of endodontic sealers in Wistar rats. *International Endodontic Journal*. 2022;55(10):1026–41.
43. Gagliardi M, Bertero A, Bifone A. Molecularly Imprinted Biodegradable Nanoparticles. *Scientific Reports*. 2017 Jan 10;7(1):40046.
44. BelBruno JJ. Molecularly Imprinted Polymers. *Chem Rev*. 2019 Jan 9;119(1):94–119.
45. Mirzaei Z, S. Kordestani S, Kuth S, Schubert DW, Detsch R, Roether JA, et al. Preparation and Characterization of Electrospun Blend Fibrous Polyethylene Oxide:Polycaprolactone Scaffolds to Promote Cartilage Regeneration. *Advanced Engineering Materials*. 2020;22(9):2000131.
46. Kanamala M, Wilson WR, Yang M, Palmer BD, Wu Z. Mechanisms and biomaterials in pH-responsive tumour targeted drug delivery: A review. *Biomaterials*. 2016 Apr;85:152–67.
47. Xu W, Zhou W, Wang H, Liang S. Chapter Two - Roles of *Porphyromonas gingivalis* and its virulence factors in periodontitis. In: Donev R, editor. *Advances in Protein Chemistry and Structural Biology* [Internet]. Academic Press; 2020 [cited 2023 Jun 4]. p. 45–84. (Inflammatory Disorders - Part B; vol. 120). Available from: <https://www.sciencedirect.com/science/article/pii/S1876162319300963>

48. Freires IA, Sardi J de CO, de Castro RD, Rosalen PL. Alternative Animal and Non-Animal Models for Drug Discovery and Development: Bonus or Burden? *Pharm Res.* 2017 Apr 1;34(4):681–6.

3 DISCUSSÃO

Os biomateriais são cada vez mais utilizados na implantodontia como uma abordagem preventiva/terapêutica para as infecções (Castagnola et al., 2021). Neste contexto, superfícies multi-funcionais, “*scaffolds*”, materiais para regeneração tecidual, sistemas de entrega de medicamentos e biopolímeros são materiais versáteis que podem ser adaptados para condições clínicas desafiadoras, incluindo as infecções peri-implantares (Costa et al., 2021). O projeto de novos biomateriais envolve a fusão de diversas áreas do conhecimento, com etapas rigorosas de pesquisa laboratorial e clínica, visando o desenvolvimento de materiais estáveis, seguros e biocompatíveis (Kohn, 2019). Diante desses desafios, apesar dos avanços recentes, apenas algumas formulações tiveram tradução clínica bem-sucedida (Ananth et al., 2015). Além disso, ressaltamos a importância de entender a etiopatogênese das infecções peri-implantares com conhecimento de biofilmes e de resposta imune-inflamatória para direcionar novos biomateriais para aplicação odontológica (Bertolini et al., 2022).

Em relação à ciência de superfícies para implantes de Ti, demonstrou-se no Estudo 1 (Costa et al., 2021) que não existe consenso sobre a melhor superfície disponível para reduzir o acúmulo microbiano e prevenir as infecções peri-implantares. Essa condição foi reforçada posteriormente pelo nosso grupo (Malheiros et al., 2023) e por outros (Alipal et al., 2021; Sahoo et al., 2022). Notavelmente, muitas superfícies com propriedades antimicrobianas geralmente têm seu efeito bem promissor em estudos pré-clínicos e limitados em cenários clínicos. Os achados dessa revisão demonstram que a verdadeira fraqueza do processo encontra-se nas questões metodológicas, que são cruciais para a tradução clínica (Castagnola et al., 2021). Por exemplo, ensaios microbiológicos com bactérias orais relevantes e modelos animais com condições mais próximas do ambiente oral são escassos. Desta forma, estudo confirmatórios são necessários aumentando o tempo para o desenvolvimento e o desperdício de recursos na pesquisa (Pandis et al., 2021). Com base no conhecimento etiológico da infecção peri-implantar, superfícies de implantes com revestimentos de liberação inteligente ou ativação sob demanda são promissoras para aplicações odontológicas. Em resumo, essas superfícies inteligentes são ativadas apenas durante um período de infecção para controlar a liberação de drogas antimicrobianas com concentrações adequadas para combater a doença sem causar toxicidade tecidual ou

resistência bacteriana. Atualmente, todas as superfícies dessa nova geração encontram-se em fase de validação *in vitro*.

Com base em terapias voltadas para patogênese, o estudo 2 (Costa et al., 2022) sumariza, pela primeira vez, os achados da literatura sobre o papel da matriz extracelular do biofilme com foco nas superfícies de implante e sugere esse fator de virulência como um possível alvo para aprimorar terapias antimicrobianas. Com base na teoria da plausibilidade biológica (Whaley et al., 2022), a matriz extracelular contempla os seguintes postulados: (1) a matriz EPS promove adesão microbiana, crescimento de biofilme e acúmulo de biomassa e, conseqüentemente, exacerba o papel do biofilme para induzir as infecções peri-implantares; (2) maior biomassa e mudanças estruturais/funcionais devido ao ambiente enriquecido com polissacarídeos extracelulares levam a uma mudança microbiológica nos biofilmes relacionados ao implante, promovendo o crescimento microbiano anaeróbico; (3) a matriz também favorece a interação cross-kingdom com *C. albicans* que promove a expressão de enzimas bacterianas, síntese de exopolissacarídeos e crescimento fúngico em biofilmes associados com implantes; (4) a matriz de EPS reduz a suscetibilidade antimicrobiana dos biofilmes criando uma camada protetora e dificultando a difusão de medicamentos; (5) a mudança microbiológica encontrada em biofilmes com matriz abundante aumenta o dano às células hospedeiras nas superfícies dos implantes. Sendo assim, foi confirmado o papel da matriz na patogênese das infecções relacionadas à implantes dentários.

Atualmente, não há clinicamente nenhum protocolo previsível de descontaminação para a remoção efetiva de biofilmes patogênicos aderidos em superfícies de implantes, assim como, o papel da matriz extracelular tem sido negligenciado nos protocolos de tratamento. Com base nisto, propomos um protocolo inovador de descontaminação em 3 etapas para superfícies ásperas de implantes de titânio, que é uma prova de conceito para nossa terapia de degradação de matriz de biofilme para descontaminação eficaz (Estudo 3). O iodopovidine (PVPI) 0,2% não foi usado como um antimicrobiano, mas como um agente de degradação da matriz em baixas concentrações para ser aplicado subgingivalmente antes de um antimicrobiano para aumentar ainda mais a morte bacteriana. O PVPI tem se mostrado eficaz como agente degradante de matriz de bactérias e fungos em superfícies dentárias (KIM et al., 2018) e superfícies lisa de Ti (Costa et al., 2020). O seguinte protocolo de 3 etapas foi estabelecido: Laser Er:YAG [Etapa 1: para remoção

mecânica de biofilmes e possíveis depósitos de cálculo] + PVPI 0,2% [Etapa 2: para degradar a matriz do biofilme presente na estrutura complexa da superfície dos implantes] + NaCl 0,95% [Etapa 3: para erradicar bactérias vivas remanescentes]. Este protocolo mostrou-se superior a outras estratégias *in vitro* previamente publicados (~99% redução) (Ichioka et al., 2021) e foi capaz de modular a comunidade polimicrobiana favorecendo um perfil microbiano compatível com o hospedeiro no Ti. Entretanto, considerando os fatores moduladores presente na cavidade oral e as limitações dos modelos *in vitro* e *in situ* adotado, esse protocolo deve ser testado em futuros ensaios clínicos.

Visando aprimorar ainda mais estratégias antimicrobianas para o controle das doenças peri-implantares, terapias baseada na modulação da resposta inflamamtória tem sido propostas (Corrêa et al., 2019). Com base nesta perspectiva, desenvolvemos o Estudo 4 pautado na síntese de um novo polímero, biodegradável por demanda de pH e carregado com folato. Diante dos benefícios modulatórios da terapia à base de folato, mostra-se estratégico testar essa abordagem também para doenças peri-implantares. Pela primeira vez, revelamos que FOLRs podem ser expressos em fibroblastos gengivais e que sua interação com folato reduz o processo inflamatório *in vitro* e *in vivo*. Estudos futuros devem considerar essa terapia nos protocolos de tratamento das doenças peri-implantares

O impacto deste trabalho se dar inicialmente no entendimento generalista da etiopatogenia e dos fatores moduladores dependentes do material e do hospedeiro e na doença peri-implantar. Para isso, uma discussão crítica com base na literatura disponível sobre superfícies antimicrobianas e matriz extracelular do biofilme foi desenvolvida como um preambulo. Por fim, o desenvolvimento de um novo protocolo de descontaminação para implantes baseado na degradação da matriz do biofilme foi descrito pela primeira vez. Estudo *in vitro* e *in situ*, como os apresentados aqui, são indispensáveis para compreender as terapias experimentais e verificar se estas alcançaram os requisitos mínimos para a sua aplicação. Espera-se que o protocolo pode ser aliado com a terapia de modulação da inflamação também desenvolvida neste estudo para proporcionar maior longevidade as reabilitações implanto-suportadas a longo prazo e qualidade de vida ao paciente.

4 CONCLUSÃO

As modificações antimicrobianas da superfície demonstraram resultados promissores para o controle do biofilme. Contudo, não há consenso sobre a melhor estratégia de modificação e informações aprofundadas sobre a segurança e longevidade do efeito antimicrobiano devem ser verificados em estudos clínicos bem delineados.

Há evidências emergentes sugerindo que a matriz EPS pode ser um fator crítico de virulência no biofilme oral relacionado a implantes dentários. Desta forma, a matriz de EPS parece ser um alvo potencial para desenvolver estratégias de controle de biofilme e promover o estado de saúde peri-implantar e mais estudos mecanísticos são necessários.

A terapia de degradação da matriz extracelular do biofilme potencializou o protocolo mecânico (laser Er:YAG) e químico (NaOCl 0,95%) de descontaminação de superfícies de implantes. Este protocolo de descontaminação pode ser considerado confiável, fornecendo plausibilidade biológica e evidências teóricas suficientes para uma tradução clínica bem-sucedida e abrindo novas perspectivas para melhorar as terapias não cirúrgicas de infecções relacionadas a implantes.

O processo inflamatório induz a superexpressão de receptores de folato em fibroblastos gengivais humanos, sendo um importante alvo para terapia de direcionamento de folato. Baseados neste mecanismo, um polímero biodegradável por demanda de pH para liberação tópica de folato em sítios peri-implantares doentes foi desenvolvido com sucesso pela técnica de impressão molecular e validade *in vitro* e *in vivo*.

REFERENCIAS

ADELL, R. et al. A 15-year study of osseointegrated implants in the treatment of the edentulous jaw. **International Journal of Oral Surgery**, v. 10, n. 6, p. 387–416, dez. 1981.

AIRES, C. P. et al. Structural characterization of exopolysaccharides from biofilm of a cariogenic streptococci. **Carbohydrate Polymers**, v. 84, n. 4, p. 1215–1220, 2 abr. 2011.

ALIPAL, J. et al. An updated review on surface functionalisation of titanium and its alloys for implants applications. **Materials Today: Proceedings**, 24 fev. 2021.

ANANTH, H. et al. A Review on Biomaterials in Dental Implantology. **International Journal of Biomedical Science : IJBS**, v. 11, n. 3, p. 113–120, set. 2015.

ARAUJO, M. G.; LINDHE, J. Peri-implant health. **Journal of Clinical Periodontology**, v. 45, n. S20, p. S230–S236, 2018.

BARÃO, V. A. R. et al. Emerging titanium surface modifications: The war against polymicrobial infections on dental implants. **Brazilian Dental Journal**, v. 33, p. 1–12, 7 mar. 2022.

BERGLUNDH, T. et al. Peri-implant diseases and conditions: Consensus report of workgroup 4 of the 2017 World Workshop on the Classification of Periodontal and Peri-Implant Diseases and Conditions. **Journal of Clinical Periodontology**, v. 45, n. S20, p. S286–S291, 2018.

BERTOLINI, M. et al. Oral Microorganisms and Biofilms: New Insights to Defeat the Main Etiologic Factor of Oral Diseases. **Microorganisms**, v. 10, n. 12, p. 2413, dez. 2022.

BRANDA, S. S. et al. Biofilms: the matrix revisited. **Trends in Microbiology**, v. 13, n. 1, p. 20–26, jan. 2005.

BRÅNEMARK, P. I. et al. Osseointegrated implants in the treatment of the edentulous jaw. Experience from a 10-year period. **Scandinavian Journal of Plastic and Reconstructive Surgery. Supplementum**, v. 16, p. 1–132, 1977.

CARDOSO, R. G. et al. Impact of mandibular conventional denture and overdenture on quality of life and masticatory efficiency. **Brazilian Oral Research**, v. 30, n. 1, p. e102, 10 out. 2016.

CASTAGNOLA, V. et al. Editorial: Short-Term Versus Long-Term Challenges in Functional Biomaterials Interfacing Living Systems: Two Sides of the Coin. **Frontiers in Bioengineering and Biotechnology**, v. 9, 2021.

CHEN, J. et al. Immediate versus early or conventional loading dental implants with fixed prostheses: A systematic review and meta-analysis of randomized controlled clinical trials. **The Journal of Prosthetic Dentistry**, v. 122, n. 6, p. 516–536, dez. 2019.

CHIAPASCO, M.; GATTI, C. Implant-retained mandibular overdentures with immediate loading: a 3- to 8-year prospective study on 328 implants. **Clinical Implant Dentistry and Related Research**, v. 5, n. 1, p. 29–38, 2003.

CHOCHLIDAKIS, K. et al. Survival rates and prosthetic complications of implant fixed complete dental prostheses: An up to 5-year retrospective study. **The Journal of Prosthetic Dentistry**, 22 jan. 2020.

COSTA, R. C. et al. Extracellular biofilm matrix leads to microbial dysbiosis and reduces biofilm susceptibility to antimicrobials on titanium biomaterial: An in vitro and in situ study. **Clinical Oral Implants Research**, v. 31, n. 12, p. 1173–1186, 2020.

COSTA, R. C. et al. Fitting pieces into the puzzle: The impact of titanium-based dental implant surface modifications on bacterial accumulation and polymicrobial infections. **Advances in Colloid and Interface Science**, v. 298, p. 102551, 1 dez. 2021.

COSTA, R. C. et al. Polymicrobial biofilms related to dental implant diseases: unravelling the critical role of extracellular biofilm matrix. **Critical Reviews in Microbiology**, v. 0, n. 0, p. 1–21, 18 maio 2022.

DAUBERT, D. M.; WEINSTEIN, B. F. Biofilm as a risk factor in implant treatment. **Periodontology 2000**, v. 81, n. 1, p. 29–40, 2019.

DERKS, J.; TOMASI, C. Peri-implant health and disease. A systematic review of current epidemiology. **Journal of Clinical Periodontology**, v. 42 Suppl 16, p. S158-171, abr. 2015.

DOSTIE, S. et al. Chemotherapeutic decontamination of dental implants colonized by mature multispecies oral biofilm. **Journal of Clinical Periodontology**, v. 44, n. 4, p. 403–409, abr. 2017.

FERRARIS, S. et al. Antibacterial and bioactive nanostructured titanium surfaces for bone integration. **Applied Surface Science**, v. 311, p. 279–291, 30 ago. 2014.

FLEMMING, H.-C.; WINGENDER, J. The biofilm matrix. **Nature Reviews. Microbiology**, v. 8, n. 9, p. 623–633, set. 2010.

GALLARDO, Y. N. R. et al. A Systematic Review of Clinical Outcomes on Patients Rehabilitated with Complete-Arch Fixed Implant-Supported Prostheses According to the Time of Loading. **Journal of Prosthodontics: Official Journal of the American College of Prosthodontists**, 21 ago. 2019.

GUGGENHEIM, B. Extracellular polysaccharides and microbial plaque. **International Dental Journal**, v. 20, n. 4, p. 657–678, dez. 1970.

HEITZ-MAYFIELD, L. J. A.; MOMBELLI, A. The therapy of peri-implantitis: a systematic review. **The International Journal of Oral & Maxillofacial Implants**, v. 29 Suppl, p. 325–345, 2014.

HEITZ-MAYFIELD, L. J. A.; SALVI, G. E. Peri-implant mucositis. **Journal of Clinical Periodontology**, v. 45, n. S20, p. S237–S245, 2018.

HOWE, M.-S.; KEYS, W.; RICHARDS, D. Long-term (10-year) dental implant survival: A systematic review and sensitivity meta-analysis. **Journal of Dentistry**, v. 84, p. 9–21, maio 2019.

HU, M.-L. et al. Comparison of technical, biological, and esthetic parameters of ceramic and metal-ceramic implant-supported fixed dental prostheses: A systematic review and meta-analysis. **The Journal of Prosthetic Dentistry**, 18 nov. 2019.

ICHIOKA, Y. et al. In vitro evaluation of chemical decontamination of titanium discs. **Scientific Reports**, v. 11, n. 1, p. 22753, 23 nov. 2021.

KARYGIANNI, L. et al. Biofilm Matrixome: Extracellular Components in Structured Microbial Communities. **Trends in Microbiology**, v. 28, n. 8, p. 668–681, ago. 2020.

KIM, D. et al. Bacterial-derived exopolysaccharides enhance antifungal drug tolerance in a cross-kingdom oral biofilm. **The ISME journal**, v. 12, n. 6, p. 1427–1442, 2018.

KLEIN, M. I. et al. Streptococcus mutans-derived extracellular matrix in cariogenic oral biofilms. **Frontiers in Cellular and Infection Microbiology**, v. 5, p. 10, 2015.

KOHN, D. H. Multi-functional Biomaterials with Clinical Utility. **Matter**, v. 1, n. 5, p. 1114–1115, 6 nov. 2019.

KOO, H.; FALSETTA, M. L.; KLEIN, M. I. The Exopolysaccharide Matrix. **Journal of Dental Research**, v. 92, n. 12, p. 1065–1073, dez. 2013.

KOTSAKIS, G. A.; OLMEDO, D. G. Peri-implantitis is not periodontitis: Scientific discoveries shed light on microbiome-biomaterial interactions that may determine disease phenotype. **Periodontology 2000**, 10 mar. 2021.

LAFURIE, G. I. et al. Microbiome and Microbial Biofilm Profiles of Peri-Implantitis: A Systematic Review. **Journal of Periodontology**, v. 88, n. 10, p. 1066–1089, 2017.

LAM VO, T. et al. Masticatory function and bite force of mandibular single-implant overdentures and complete dentures: a randomized crossover control study. **Journal of Prosthodontic Research**, v. 63, n. 4, p. 428–433, out. 2019.

LEE, C.-T. et al. Prevalences of peri-implantitis and peri-implant mucositis: systematic review and meta-analysis. **Journal of Dentistry**, v. 62, p. 1–12, jul. 2017.

LEE, J. et al. The impact of surface treatment in 3-dimensional printed implants for early osseointegration: a comparison study of three different surfaces. **Scientific Reports**, v. 11, n. 1, p. 10453, 17 maio 2021.

LOUROPOULOU, A.; SLOT, D. E.; VAN DER WEIJDEN, F. The effects of mechanical instruments on contaminated titanium dental implant surfaces: a systematic review. **Clinical Oral Implants Research**, v. 25, n. 10, p. 1149–1160, out. 2014.

LOUROPOULOU, A.; SLOT, D. E.; VAN DER WEIJDEN, F. A. Titanium surface alterations following the use of different mechanical instruments: a systematic review. **Clinical Oral Implants Research**, v. 23, n. 6, p. 643–658, jun. 2012.

MALHEIROS, S. S. et al. Biomaterial engineering surface to control polymicrobial dental implant-related infections: focusing on disease modulating factors and coatings development. **Expert Review of Medical Devices**, p. 1–17, 29 maio 2023.

MOMBELLI, A.; DÉCAILLET, F. The characteristics of biofilms in peri-implant disease. **Journal of Clinical Periodontology**, v. 38 Suppl 11, p. 203–213, mar. 2011.

OLIVEIRA, B. E. C.; CURY, J. A.; FILHO, A. P. R. Biofilm extracellular polysaccharides degradation during starvation and enamel demineralization. **PLOS ONE**, v. 12, n. 7, p. e0181168, 17 jul. 2017.

PANDIS, N. et al. Dental Research Waste in Design, Analysis, and Reporting: A Scoping Review. **Journal of Dental Research**, v. 100, n. 3, p. 245–252, mar. 2021.

SAHOO, J. et al. Nanomaterial-Based Antimicrobial Coating for Biomedical Implants: New Age Solution for Biofilm-Associated Infections. **ACS omega**, v. 7, n. 50, p. 45962–45980, 20 dez. 2022.

SCHWARZ, F. et al. Peri-implantitis: Summary and consensus statements of group 3. The 6th EAO Consensus Conference 2021. **Clinical Oral Implants Research**, v. 32, n. S21, p. 245–253, 2021.

SOUZA, J. G. S. et al. Role of glucosyltransferase R in biofilm interactions between *Streptococcus oralis* and *Candida albicans*. **The ISME journal**, v. 14, n. 5, p. 1207–1222, maio 2020.

SOUZA, J. G. S. et al. Targeting implant-associated infections: titanium surface loaded with antimicrobial. **iScience**, v. 24, n. 1, p. 102008, 22 jan. 2021.

SOUZA, J. G. S. et al. Bacterial-derived extracellular polysaccharides reduce antimicrobial susceptibility on biotic and abiotic surfaces. **Archives of Oral Biology**, v. 142, p. 105521, 1 out. 2022.

WHALEY, P. et al. Biological plausibility in environmental health systematic reviews: a GRADE concept paper. **Journal of Clinical Epidemiology**, v. 146, p. 32–46, jun. 2022.

XIAO, J. et al. The exopolysaccharide matrix modulates the interaction between 3D architecture and virulence of a mixed-species oral biofilm. **PLoS pathogens**, v. 8, n. 4, p. e1002623, 2012.

YANG, T. et al. Residual extracellular polymeric substances (EPS) detected by fluorescence microscopy on dental implants after different decontamination. **Materials Chemistry and Physics**, v. 296, p. 127242, 15 fev. 2023.

ANEXO

Anexo 1. Certificado de aprovação no Comitê de Ética em Pesquisa da FOP/UNICAMP 1

CERTIFICADO CEP nº 2/2023



COMITÊ DE ÉTICA EM PESQUISA
FACULDADE DE ODONTOLOGIA DE PIRACICABA
UNIVERSIDADE ESTADUAL DE CAMPINAS



CERTIFICADO

O Comitê de Ética em Pesquisa da FOP-UNICAMP certifica que o projeto de pesquisa "**Influência dos métodos físicos de descontaminação na degradação das superfícies dos implantes dentários**", CAAE **53844321.2.0000.5418**, dos pesquisadores **Raphael Cavalcante Costa, Thais Terumi Sadamitu Takeda, João Gabriel Silva Souza e Valentim Adelino Ricardo Barão**, satisfaz as exigências das resoluções específicas sobre ética em pesquisa com seres humanos do Conselho Nacional de Saúde – Ministério da Saúde e foi aprovado por este comitê em 02/03/2022.

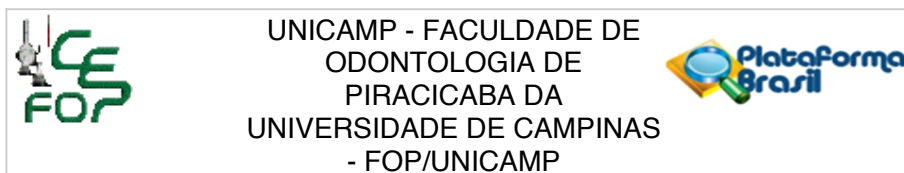
The Research Ethics Committee of the Piracicaba Dental School of the University of Campinas (FOP-UNICAMP) certifies that research project "**Influence of physical decontamination methods on the degradation of dental implants surfaces**", CAAE **53844321.2.0000.5418**, of the researcher's **Raphael Cavalcante Costa, Thais Terumi Sadamitu Takeda, João Gabriel Silva Souza** and **Valentim Adelino Ricardo Barão**, meets the requirements of the specific resolutions on ethics in research with human beings of the National Health Council - Ministry of Health, and was approved by this committee on March, 2, 2022.

Prof. Jacks Jorge Junior
 Coordenador
 CEP/FOP/UNICAMP

Nota: O título do protocolo e a lista de autores aparecem como fornecidos pelos pesquisadores, sem qualquer edição.
 Notice: The title and the list of researchers of the project appears as provided by the authors, without editing.

Documento assinado. Verificar autenticidade em sigad.unicamp.br/verifica
 Informar código A29A6A4D 708D4E48 A092F683 6EDEFBB3

Anexo 2. Certificado de aprovação no Comitê de Ética em Pesquisa da FOP/UNICAMP 2



PARECER CONSUBSTANCIADO DO CEP

DADOS DO PROJETO DE PESQUISA

Título da Pesquisa: Síntese, caracterização e desempenho biológico de nanopolímeros pH-sensitivos produzidos por impressão molecular para o tratamento das infecções peri-implantares: estudo in vitro e in situ

Pesquisador: Raphael Cavalcante Costa

Área Temática:

Versão: 2

CAAE: 43482721.9.0000.5418

Instituição Proponente: Faculdade de Odontologia de Piracicaba - Unicamp

Patrocinador Principal: Financiamento Próprio

DADOS DO PARECER

Número do Parecer: 4.614.774

Apresentação do Projeto:

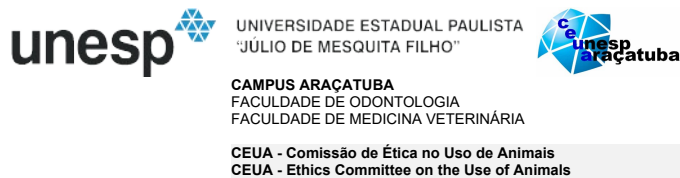
O parecer inicial é elaborado com base na transcrição editada do conteúdo do registro do protocolo na Plataforma Brasil e dos arquivos anexados à Plataforma Brasil. Os pareceres de retorno, emendas e notificações são elaborados a partir dos dados e arquivos da última versão apresentada.

A EQUIPE DE PESQUISA citada na capa do projeto de pesquisa inclui RAPHAEL CAVALCANTE COSTA (Cirurgião Dentista, Doutorando no PPG em Clínica Odontológica da FOP-UNICAMP, Pesquisador responsável, Orientando), VALENTIM ADELINO RICARDO BARO (Cirurgião Dentista, Docente do Departamento de Prótese e Periodontia, Orientador), o que é confirmado na declaração dos pesquisadores e na PB.

Delineamento da pesquisa: Trata-se de estudo clínico-laboratorial, experimental, comparativo, em duas fases (in vitro e in situ) que envolverá 15 alunos de Graduação e de Pós-Graduação da FOP-UNICAMP, com idade de 18 anos ou mais, sem distinção de sexo. Na fase in vitro serão envolvidos com 3 voluntários, dos quais serão coletadas amostras de 10 mls de saliva total não estimulada em 3 ocasiões. As amostras serão utilizadas como insumo na pesquisa. O estudo in situ, será duplo-cego, cruzado, de 3 fases (7 dias) e período de wash-out (7 dias) e serão envolvidos 12

Endereço: Av. Limeira 901 Caixa Postal 52
Bairro: Areião **CEP:** 13.414-903
UF: SP **Município:** PIRACICABA
Telefone: (19)2106-5349 **Fax:** (19)2106-5349 **E-mail:** cep@fop.unicamp.br

Anexo 3. Certificado de aprovação no Comitê de Ética no Uso de Animais (CEUA)



CERTIFICADO

Certificamos que o Projeto de Pesquisa intitulado "**Síntese, caracterização e desempenho biológico de polímeros pH-sensitivos produzidos por impressão molecular para o tratamento de infecções peri-implantares**", Processo FOA nº 433-2023, sob responsabilidade de Leonardo Perez Faverani apresenta um protocolo experimental de acordo com os Princípios Éticos da Experimentação Animal e sua execução foi aprovada pela CEUA em 23 de Maio de 2023.

VALIDADE DESTE CERTIFICADO: 23 de Outubro de 2023.

DATA DA SUBMISSÃO DO RELATÓRIO FINAL: até 23 de Novembro de 2023.

CERTIFICATE

We certify that the study entitled "**Synthesis, characterization and biological performance of pH-sensitive polymers produced by molecular printing for the treatment of peri-implant infections**", Protocol FOA nº 433-2023, under the supervision of Idelmo Rangel Garcia Júnior presents an experimental protocol in accordance with the Ethical Principles of Animal Experimentation and its implementation was approved by CEUA on May 23, 2023.

VALIDITY OF THIS CERTIFICATE: October 23, 2023.

DATE OF SUBMISSION OF THE FINAL REPORT: November 23, 2023.

Prof. Dr. Fellippo Ramos Verri
Coordenador da CEUA
CEUA Coordinator

CEUA - Comissão de Ética no Uso de Animais
Faculdade de Odontologia de Araçatuba
Faculdade de Medicina Veterinária de Araçatuba
Rua José Bonifácio, 1193 – Vila Mendonça - CEP: 16015-050 – ARAÇATUBA – SP
Fone (18) 3636-3234 Email CEUA: ceua.foa@unesp.br

Anexo 4. Autorização de re-utilização na Tese (Artigo 1)



Home
Help ▾
Live Chat
Sign in
Create Account



Fitting pieces into the puzzle: The impact of titanium-based dental implant surface modifications on bacterial accumulation and polymicrobial infections

Author:
Raphael C. Costa, Bruna E. Nagay, Martinna Bertolini, Bárbara E. Costa-Oliveira, Aline A. Sampaio, Belén Retamal-Valdes, Jamil A. Shibli, Magda Feres, Valentin A.R. Barão, João Gabriel S. Souza

Publication: Advances in Colloid and Interface Science

Publisher: Elsevier

Date: December 2021

© 2021 Elsevier B.V. All rights reserved.

Journal Author Rights

Please note that, as the author of this Elsevier article, you retain the right to include it in a thesis or dissertation, provided it is not published commercially. Permission is not required, but please ensure that you reference the journal as the original source. For more information on this and on your other retained rights, please visit: <https://www.elsevier.com/about/our-business/policies/copyright#Author-rights>

BACK
CLOSE WINDOW

© 2023 Copyright - All Rights Reserved | [Copyright Clearance Center, Inc.](#) | [Privacy statement](#) | [Data Security and Privacy](#) | [For California Residents](#) | [Terms and Conditions](#)
Comments? We would like to hear from you. E-mail us at customer-care@copyright.com

Anexo 5. Autorização de re-utilização na Tese (Artigo 2)

Home Help Live Chat Sign in Create Account



Polymicrobial biofilms related to dental implant diseases: unravelling the critical role of extracellular biofilm matrix
Author: Raphael C. Costa, , Martina Bertolini, et al
Publication: Critical Reviews in Microbiology
Publisher: Taylor & Francis
Date: May 4, 2023
Rights managed by Taylor & Francis

Thesis/Dissertation Reuse Request

Taylor & Francis is pleased to offer reuses of its content for a thesis or dissertation free of charge contingent on resubmission of permission request if work is published.

[BACK](#) [CLOSE](#)

© 2023 Copyright - All Rights Reserved | [Copyright Clearance Center, Inc.](#) | [Privacy statement](#) | [Data Security and Privacy](#) | [For California Residents](#) | [Terms and Conditions](#)
Comments? We would like to hear from you. E-mail us at customercare@copyright.com

Anexo 6. Relatório de similaridade

